Shining a Light on Dense Granules – A Biochemical, Genetic and Cell Biological Investigation of an Essential but Understudied Compartment of the Malaria Parasite

Tansy M. R. Vallintine

Thesis submitted in accordance with the requirements

for the degree of Doctor of Philosophy

University of London

January 2024

Department of Infection Biology

Faculty of Infectious Tropical Disease

London School of Hygiene and Tropical Medicine

Primary Supervisor: Christiaan van Ooij

Secondary Supervisor: Henry Staines

Funded by the MRC

Declaration

I, Tansy Vallintine, confirm that the work presented in this thesis is my own. Where information has been derived from other sources it has been indicated within the thesis.

Abstract

Malaria is a significant infectious disease of tropical and sub-tropical regions that is caused by six species of Apicomplexan parasites of the genus *Plasmodium.* With 228 million cases and an estimated 619,000 mortalities worldwide in 2021 (1), this disease is endemic in developing countries in which the transmission vector, species of the *Anopheles* mosquito, most commonly *A. gambiae*, is found. Further, malaria is a major cause of mortality in children, with 65% of cases occurring in those under the age of 5 (2). Between 2000 and 2019 rates of malaria fatality decreased steadily, with a 10% increase in mortality in 2020 followed by a slight decline in 2021 (1). However, the disease remains a major global health burden and new insights into the pathogenesis of the disease are needed if new interventions are to be developed.

The clinical symptoms of malaria are caused by invasion, replication within, and destruction of host red blood cells by the *Plasmodium* parasite. Invasion of the host cell by the parasite requires the highly regulated secretion of proteins from three specialised secretory organelles: micronemes, rhoptries, and dense granules (DGs). Microneme and rhoptry proteins function in host cell recognition attachment and invasion and establishment of the parasitophorous vacuole (PV), respectively, in *Plasmodium* spp. (3,4). DGs are speculated to be required for the erythrocyte remodelling that enables parasite survival and replication within the host cell post invasion, with known proteins functioning in transport of parasite effector proteins into the erythrocyte (5) and alteration of host cell mechanical properties (6).

Host erythrocyte remodelling by the parasite is a process that may be exploited for development of drugs capable of inhibiting parasite growth and replication, blocking further cycles of infection. Very little is known about *Plasmodium* DGs, therefore shedding light on the biogenesis, protein composition and function of DGs in *Plasmodium* may aid drug development efforts. This project aims to address these questions in *Plasmodium falciparum* using molecular biological and bioinformatics techniques.

Acknowledgements

This PhD is dedicated to my Mum, my first and best teacher, without whom I never would have become a scientist. My first memories are of walks in the Warren, looking under rocks with you. You taught me how to really look and wonder at the world. Everything was built on that, not just my development into a scientist but also my ability to see how amazing our world and all the life in it is, and how lucky I am to witness it. You also taught me how to read when everyone else had given up, that probably helped too. For the past four years you have been on the other end of the phone with sympathy and support whenever "parasites said no", which was an awful lot. Thank you always, for everything.

Thank you Pup, even though you could never stay awake through an explanation of my PhD project, you were always on the end of the phone to support me. You said that if the PhD was making me too miserable I could just quit and come home, and that you would support me in that decision. Sometimes just knowing that made all the difference. You can keep telling people I am a medical doctor if you want.

Julian, I know that in a crisis you will be there to help me, and that makes me feel safe and able to pursue my dreams, in this PhD and in life. Thank you, always.

Thank you, my dear friend and colleague Aline, who always listens and has all the best advice, I would have gone crazy without you. To Penny and Giulia also, for supportive rant sessions after work at the bar, a girl couldn't ask for three better friends.

Thank you to the many lovely inhabitants of office 390, for lunchtime coffees and walks in Russel Square to see some daylight and get some headspace, and for always being sympathetic to complaints of awful westerns and culture failures. Thank you also to my friends and housemates Ashley and Becca, for listening to all my PhD ups and downs and escaping reality with me regularly with every trashy reality tv show and crime documentary we could find.

I am also owe this PhD to the MFM ladies. During the darkest months when I couldn't listen to my own thoughts, your voices got me through. SSDGM. And to Rachel and Bobbie, who will never read this thesis but to whom I am sure I owe my sanity and this PhD, thank you.

Finally, I would like to thank my supervisor Dr Christiaan van Ooij, for welcoming me into his lab with genuine enthusiasm. I do not think I would have completed this endeavour without your endless support and patience. I would also like to thank the MRC, who's funding has made this project possible.

Nolite te bastardes carborundorum

Thesis publications and manuscripts

Vallintine T, van Ooij C. Timing of dense granule biogenesis in asexual malaria parasites. Microbiology. 2023;169(8).

Additional Publications

Vallintine T, van Ooij C. Distribution of malaria parasite-derived phosphatidylcholine in the infected erythrocyte. mSphere. 2022;e0013123.

Table of Contents

List of Figures

List of Tables

Abbreviations

ACT	Artemisinin combination therapy
AMA1	Apical membrane antigen 1
Cas9	CRISPR associated protein 9
CRISPR	Clustered regularly interspaced short palindromic repeats
CSP	Circumsporozoite protein
DIC	Differential interference contrast
DG	Dense granule
DNA	Deoxyribonucleic acid
DV	Digestive vacuole
EBA	Erythrocyte binding antigen
EMP	Erythrocyte membrane protein
EXP	Exported protein
gDNA	Genomic deoxyribonucleic acid
GIG	Gametogenesis implicated protein
HSP	Heat shock protein
IFA	Indirect immunofluorescence assay
iGP	Inducible gametocyte producer
kb	Kilobase
kDa	Kilo daltons
KO	Knock out
LSA	Liver stage antigen
mg	Milligrams
MJ	Moving junction

mL	Millilitre
mM	Millimolar
mNG	mNeonGreen
nM	Nanomolar
PBS	Phosphate-buffered saline
PEXEL	*Plasmodium* export element
PFA	Paraformaldehyde
PMV	Plasmepsin V
PPM	Parasite plasma membrane
PTP	Protein tyrosine phosphatase
PV	Parasitophorous vacuole
PVM	Parasitophorous vacuole membrane
PV1	Parasitophorous vacuolar protein 1
RESA	Ring-infected erythrocyte surface antigen
REX1	Ring exported protein 1
RON	Rhoptry neck protein
SBP1	Skeleton-binding protein 1
SERA	Serine repeat antigen
SLI	Selection-Linked Integration
TM	Trans membrane
µg	Microgram
µl	Microlitre
µM	Micromolar
µm	Micrometre

VSA Variable surface antigen

WHO World Health Organization

Chapter 1: General Introduction

1.1 **Malaria**

Malaria is endemic in equatorial regions including much of Africa and areas of South America and Asia, with Nigeria, the Democratic Republic of the Congo, Uganda and Mozambique accounting for almost half of all cases globally, and with 95% of all cases in 2021 occurring in the WHO African Region (1). In humans, malaria is caused by six species of the single celled Apicomplexan parasite of the genus *Plasmodium: Plasmodium malariae*, *Plasmodium knowlesi*, *Plasmodium falciparum*, *P. vivax, Plasmodium ovale wallikeri* and *Plasmodium ovale curtisi* (8–10). *P. falciparum* is the predominant species in sub-Saharan Africa and causes the most severe form of the disease and the greatest number of fatalities globally (2,3). Malaria is often characterised by symptoms including, but not limited to fever, fatigue, vomiting, and headache. More severe disease can lead to jaundice, coma, seizures and death (4).

The WHO currently recommends artemisinin-based combination therapy (ACT) as treatment for infected individuals (5), however drug resistance against all classes of antimalarials is now common and represents a significant threat to global malaria control efforts, with cases of resistance to many ACT therapies occurring in the Greater Mekong area (6). Most *P. falciparum* endemic countries are found in the WHO Africa region, in which parasite resistance to artemisinin is an emerging threat, with independently evolved partial resistance verified in Uganda, Eritrea and Rwanda (7–10). Until recently the only vaccine approved for use was the RTS,S/AS01 vaccine which targets the sporozoite, however this vaccine has low efficacy (11,12). Preliminary results indicate that a new vaccine R21/Matrix-M which also targets the sporozoite is more effective than the previous RTS/S vaccine (13), although it has yet to be cleared for use by the WHO.

1.2 **Apicomplexa**

The genus *Plasmodium* belongs to the phylum Apicomplexa, which comprises single-cell eukaryotic alveolates such as *Toxoplasma gondii, Cryptosporidium* spp., and *Eimeria* spp. (14), and the class Aconoidasidia which lack a conoid (except for in the ookinete stage) (15), unlike *Toxoplasma* spp., *Cryptosporidium* spp. and *Eimeria* spp. of the class Conoidasidia (16). Although Apicomplexan parasites display great diversity in host-cell types and methods of

parasite-host interaction, each species contain a set of secretory organelles located to the apical pole of the parasite, an 'apical complex', which in intracellular parasites like those of the genera *Plasmodium* and *Toxoplasma* facilitate host cell invasion and remodelling (17,18).

1.3 ***Plasmodium*** **life cycle**

Throughout the life cycle of *Plasmodium* parasites, the parasite migrates through multiple intracellular and extracellular environments in both vertebrate and invertebrate hosts. Three environmentally distinct cycles are completed by *Plasmodium* parasites: the mosquito or 'sporogonic' cycle, the human liver stage or 'exoerythrocytic' cycle, and the human blood or 'erythrocytic' cycle, the pathogenic phase of the parasite life cycle (figure 1).

When an infected mosquito bites a human, motile sporozoites are transferred from the mosquito salivary glands into the human bloodstream from which they infect hepatocytes of the liver (the exo-erythrocytic cycle). Here they develop into invasive merozoites which, once in the bloodstream, infect erythrocytes and initiate the erythrocytic cycle – the part of the lifecycle that is responsible for the clinical symptoms of malaria. After invasion, the merozoite exists in a juvenile trophozoite ring form that displays little metabolic activity and eventually transitions into a trophozoite (feeding and growth) stage, before becoming a multi-nucleated schizont. Finally, cytokinesis forms 8-32 (depending on species) daughter merozoites (19). More rarely gametocytes are also produced at this stage (20). Importantly, rupture of the erythrocyte and release of the daughter merozoites (a process called egress) releases glycosylphosphatidylinositol (putative malaria toxin) and parasite and erythrocyte debris, activating mononuclear cells and cytokine release (21,22). Increased cytoadherence of infected erythrocytes causes vascular damage and further inflammatory response (19,23). Upon egress daughter merozoites can initiate new rounds of erythrocytic infection, whereas gametocytes can initiate a new sporogonic cycle and allow vector transmission when taken up in a blood meal by a female *Anopheles* mosquito (24).

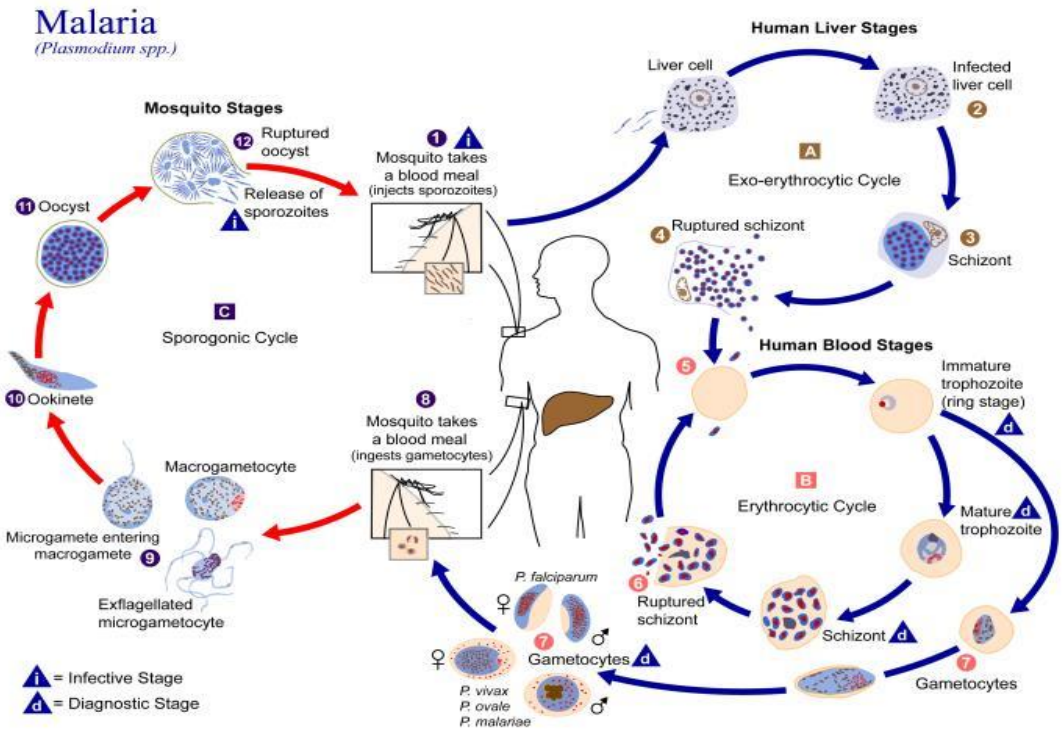

Figure 1. *Plasmodium falciparum* life cycle. The *P. falciparum* life cycle involves both a human host and mosquito vector. An infected mosquito infects the human host with sporozoites during a blood meal. Parasites enter the bloodstream and subsequently infect hepatocytes (the exoerythrocytic cycle). (A). The parasites develop and replicate in the liver over the course of 10 days, after which they are released from the host cell in the form of merozoites. Following rupture of the hepatocyte, merozoites enter the bloodstream and initiate rounds of asexual erythrocytic infection (B). A subset of parasites develop into gametocytes, which when taken up by a mosquito in a blood meal, develop into gametes that can fuse to form ookinetes and begin the sporogonic cycle (C). Image from Riglar *et al.* (25).

1.4 **Parasite invasion and remodelling of the host erythrocyte – the key to pathogenesis**

Prior to invasion the parasite secretes the components of the micronemes which allow host cell binding and invasion. Initial contact and attachment can occur between any points of the merozoite and erythrocyte surface and is followed by reorientation of the merozoite. This reorientation brings the apical pole of the merozoite into position directly adjacent to the erythrocyte membrane where an irreversible high affinity attachment occurs, and a connection termed the moving junction is formed with the erythrocyte membrane. The merozoite then initiates discharge of the contents of the rhoptries and DGs into the erythrocyte via the point of contact. Rapid deformation of the erythrocyte with invagination of the erythrocyte membrane at the point of contact initiates the envelopment of the merozoite in a process that resembles

endocytosis (23,26,27). As the parasite pushes into the cell, it is surrounded by a membrane, which pinches off to form a compartment encasing the parasite called the parasitophorous vacuole (PV). There is some dispute over whether the PV membrane (PVM) is derived from the parasite or the host cell, and how the isolated PV accesses the phospholipids necessary for membrane expansion to accommodate the growing parasite (28). The PVM forms a barrier around the parasite that inhibits access to nutrients in the erythrocyte, the fact that breakdown of the PV does not occur after invasion as it does in other Apicomplexans, such as *Babesia* spp. and *Theileria* spp. (24,29–31), suggests an important function for the PV, although what that is is currently unknown (32,33). The stages of merozoite invasion of the host erythrocyte are depicted in figure 2.

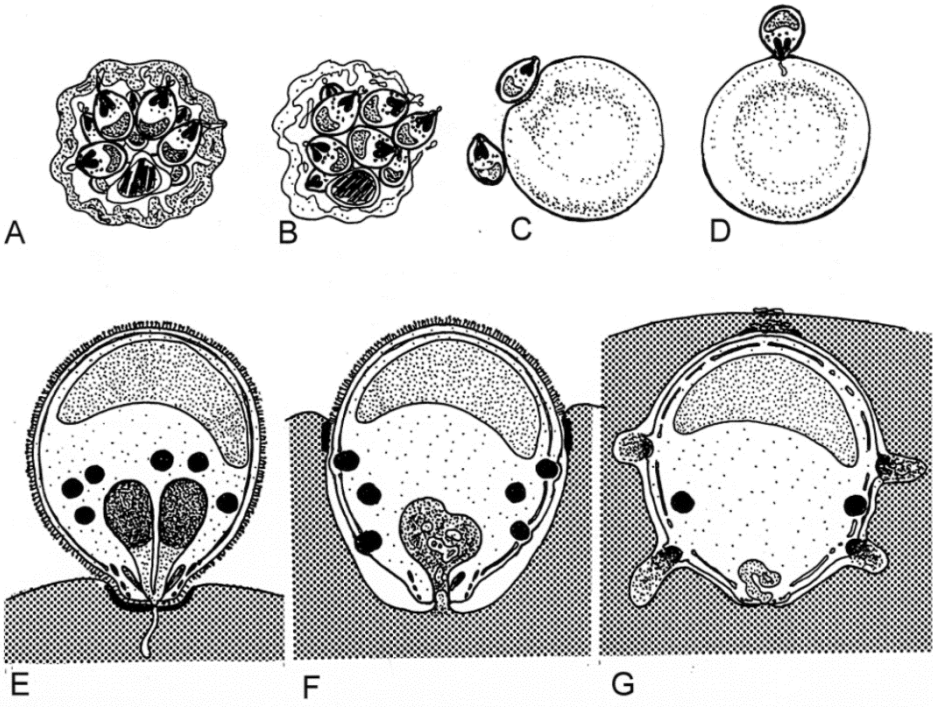

Figure 2. Stages of egress and invasion of the *Plasmodium* spp. intraerythrocytic life cycle. A: Late stage schizont just prior to egress. B: Merozoite egress from the host erythrocyte. C: Merozoite attachment and reorientation at the erythrocyte membrane. D: Invasion is initiates. E: Rhoptry proteins are secreted into the host cell and the MJ is formed. F: Bounded by the PVM the parasite moves into the host cell via the MJ. G: Inside the host cell the DGs are secreted. Image from Preiser *et al.* (34).

1.4.1 Apical secretory organelles and proteins

Unlike members of the Euglenozoa phylum like *Leishmania* spp. and *T. cruzi,* which use the host endocytic system to enter the host cell (35,36) most Apicomplexans have developed an

advanced system involving specialised secretory organelles called the apical organelles. In *Plasmodium* spp. merozoites, these are contained within an 'apical complex' which is located in an attenuated apical prominence of the merozoite. The apical complex comprises three specialised secretory organelles termed micronemes, rhoptries and DGs (figure 3), linked with components of the parasite cytoskeleton. Initial interaction with the host cell, attachment, invasion, and erythrocyte remodelling is facilitated by secretion of the protein contents of these three apical organelles (34,37).

The presence of three distinct apical organelles allows compartmentalisation of proteins with specific functions and temporal regulation of protein discharge for rapid and efficient invasion and modification of the host cell (34,37). Micronemes secrete their contents prior to invasion and primarily control host cell recognition, attachment, and invasion through release of proteins such as erythrocyte binding antigen 175 (EBA-175) (38,39) and AMA1 (40–42). The micronemes are described as flask-shaped or cigar-shaped, varying in number and shape between species. In *P. falciparum*, micronemes are roughly 120nm long and connected to the rhoptry neck near the apical pole of the merozoite (43,44). The rhoptries are second to discharge their contents. Conserved among the Apicomplexa, rhoptries function in attachment, invasion and establishment of the PV. The largest of the apical organelles, they are an elongated club-shaped organelle that vary in number depending upon species. *Plasmodium* spp. have two elongated rhoptries, whereas *Cryptosporidium* parasites have only one rhoptry per zoite (45), and *Toxoplasma gondii* has around eight (46). Apicomplexan rhoptries are separated into two regions: the electron translucent rhoptry neck, a narrow-elongated region terminating at the apical pole of the parasite, and a rounded electron dense body called the rhoptry bulb (47). This compartmentalisation allows segregation of proteins by function and temporal regulation of protein release. Rhoptry neck proteins are thought to primarily function in host cell recognition, attachment and invasion, whereas rhoptry bulb proteins and lipids are primarily involved in invasion and initiation of the PVM (48–51).

Although most apical organelle proteins appear to be segregated along functional lines, studies in *Plasmodium* spp. and *T. gondii* have revealed cooperation between rhoptry and microneme proteins that allows parasite invasion of the host erythrocyte (52). For example, microneme protein AMA1 at the merozoite surface binds the exported rhoptry neck protein RON2 in the erythrocyte membrane to form the highly conserved RON complex (53) an essential interaction for the formation of the moving junction (MJ), the step that commits parasites to the invasion process (54).

Another secretory organelle, the exoneme, has been described in *P. falciparum,* although this is not commonly described as a part of the apical complex (55). The exoneme is thought to function in the initiation of parasite egress from the host cell. Yeoh *et al.* (2007) found that an HA-tagged version of SUB1, a conserved subtilisin-like serine protease that is refractory to disruption in blood stages, exhibited patterning like that of DGs but did not co-localise with the DG marker ring infected erythrocyte surface antigen (RESA). SUB1 expression peaks in late-stage schizonts (56), and exonemes are not present in newly invaded erythrocytes, SUB1 is only detectible in the supernatant of egressed schizonts. Taken together these results indicated the presence of a new secretory organelle which is released just prior to schizont egress. Inhibition of SUB1 function blocked egress *in vitro,* indicating that SUB1 is essential to schizont egress and reinvasion, likely functioning through proteolytic maturation of two members of the SERA protein family, SERA4 and SERA5, which regulate merozoite egress (55,57).

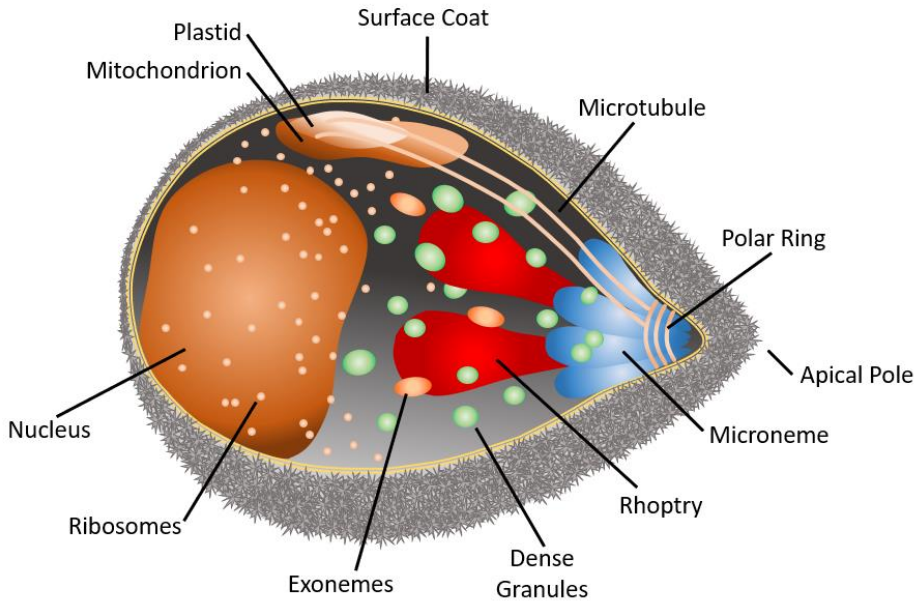

Figure 3. The morphology of *Plasmodium* merozoite.

The *Plasmodium* merozoite has a distinctive polar shape with the secretory organelles - the rhoptries, micronemes and DGs - at the apical pole of the parasite.

1.4.2 ***Dense granules***

Plasmodium DGs are the last organelle to secrete their contents. Immediately following invasion, the DGs move to the merozoite surface where they release their protein cargo into the PV by exocytosis (58), where they act to modify the PV and host cell. DGs are the smallest of the apical organelles, measuring only 100-120nm in diameter in *P. falciparum* and *P. knowlesi* (59–61). Viewed by TEM they are spherical electron dense structures (from which they get their name), with a narrow electron-lucent band just below the bounding membrane (44,59,62), situated free in the apical portion of the merozoite cytoplasm. Present in invasive stages of Apicomplexa, the DGs were first described in *Sarcocystis tenella*, in which DGs are larger, at approximately 200 nm in diameter, and considerably more abundant than in other Apicomplexa. This abundance allowed for purification of DGs by sucrose gradient (63). Trager *et al.* described successful isolation of *P. falciparum* DGs by cell fractionation on a sucrose gradient, although DGs sedimented with a peak density of 1.17 g/ml close to that of rhoptries, which causes DGs and rhoptries to precipitate together (64,65). Unlike in other Apicomplexa where DGs are formed continually through the intracellular stage (66,67), DGs in *Plasmodium* spp. are only present for a short portion of the parasite life cycle as they disappear when discharged upon invasion and not formed again until replication has commenced and merozoites are produced.

Whereas over 60 DG proteins have been described in *T. gondii,* relatively few DG proteins have been identified in *Plasmodium* spp. (52,66,68–70). The known DG proteins include the components of the *Plasmodium* translocon of exported proteins (PTEX), which is a translocon complex that exports parasite proteins across the PVM into the host erythrocyte (71–73), RESA, which binds spectrin tetramers at the host cell periphery (60), exported protein 2 (EXP2) that has a dual function, acting as both a nutrient pore that allows nutrient passage across the PVM and as the core component of the PTEX (74,75), exported protein 1 (EXP1), which is a membrane protein in the PVM and necessary for correct localisation of nutrient pore forming EXP2 to the PVM (76–80), parasitophorous vacuolar protein 1 (PV1), which interacts with exported proteins at the PTEX (81), liver stage antigen 3 (LSA3) (79), and Pf113, a PTEX accessory molecule of unknown function (82). The components of the PTEX include EXP2, heat shock protein 101 (HSP101), PTEX-150, thioredoxin 2 (TRX2), and PTEX88 (72). Knockdown of PTEX components greatly reduces transport of all classes of exported proteins across the PVM and blocks parasite development (73,75,80,83–85). EXP1 affects the function of the pore protein of the PTEX, EXP2, with loss of EXP1 causing mislocalisation of EXP2

and subsequent hypersensitivity to nutrient deficiency (80). RESA binds to spectrin below the erythrocyte surface where it stabilises spectrin tetramers, reducing host cell deformability and microcirculation (circulation in the smallest blood vessels) (86,87). It is possible that that reduced deformability inhibits invasion of the host cell by other merozoites and/or confers heat shock resistance from the elevated body temperatures of malaria paroxysm (88,89).

The components of the PTEX are conserved between *P. malariae*, *P. knowlesi, P. vivax, P. ovale*, and the model rodent malaria parasite species *P. berghei,* which encode homologues or putative homologues for all of the known DG proteins except for RESA and LSA3 (90). PTEX150, HSP101 and EXP2 are refractory to disruption in *P. berghei*, indicating a similarly essential function of the core PTEX components in protein export as demonstrated in *P. falciparum* (72,91–93). TRX2 and PTEX88, however, were successfully deleted in *P. berghei* (91,92), with deletion causing a moderate growth defect, decreased virulence, and lower levels of protein export in the case of TRX2, indicating an auxiliary role in protein export across the PTEX (85,91,92,94).

The DG proteome of the related Apicomplexan parasite *T. gondii* has been more thoroughly described, with over 60 proteins identified. These proteins have diverse functions in mediating host-parasite interactions and localise to the PV, the intravacuolar network (IVN), the PVM, and the host cell (66). The IVN consists of a complex network of membrane-limited tubules within the PV of the parasite, the function of which remains uncertain, although it has been implicated in nutrient acquisition (95,96). The IVN-associated GRAs - GRA2, GRA4, GRA6, GRA9 and GRA12 - have been demonstrated to regulate development of the chronic *T. gondii* cyst matrix and wall, with deletion of GRA2 resulting in an inability to develop a normal cyst matrix and deletion of GRA2 and GRA6 resulting in abnormal cyst morphology, and deletion of the other IVN associated GRAs decreasing the rate at which cyst wall proteins accumulate at the cyst surface (96–101). *T. gondii* uses the host cell as a source of lipids. GRA2 and GRA6 double knockout parasites also display decreased uptake of host sphingolipid - containing vesicles into the IVN, and along with knockout of the DG protein LCAT, decreased uptake of neutral lipid droplets which are required for parasite organellar membrane growth (102,103).

Implicating the IVN in uptake of soluble proteins as a source of nutrients from the host, deletion of GRA2 and GRA6 resulted in decreased rates of host protein uptake (95,96). GRA17 and GRA23 are orthologs *Plasmodium* EXP2 and perform a similar function in the passive

transport of small molecules across the PVM (104,105), with deletion of GRA17 leading to decreased parasite growth rates and swelling of the PV (104).

Many *T. gondii* GRA proteins are exported across the PVM, including GRA16 (106), GRA18 (107), GRA24 (108), TEEGR/HCEI (109,110), and IST1 (111), where they function in regulating host cell gene expression and immune response. The translocon complex that controls export of GRA proteins into the host cell cytosol is comprised of MYR1, MYR2 and MYR3, MYR4, GRA44, GRA45, PPM3C, and ROP17 (110,112–116). Deletion all of the MYR components blocked effector protein export to the host cell and caused a reduction in parasite replication (112,114), whereas deletion of the putative chaperone GRA45 causes failure of the MYR proteins to associate with PVM (116).

The GRA proteins HCE1/TEERG and GRA16 have also been implicated in controlling the host cell cycle signalling pathways which lead to cell cycle arrest in G2 upon infection with *T. gondii*. After export across the PVM GRA16 and TEEGR/HCE1 localise to the host cell nucleus. Gra16 interacts with host cell proteins HAUSP (106), and HAUSP interacts with transcription factor p53 (Li 2002). When GRA16 interacts with HAUSP, p53 is stabilised which in turn causes reduced levels of Cyclin B which controls the G2/M transition (106). TEEGR/HCE1 interacts with the host transcription factor E2F-DP1, increasing expression of cyclin E and initiating G1/S cycle transition (109,110).

GRA proteins also function to influence host immune signalling pathways, for example GRA15 causes nuclear translocation of NF-kB which causes upregulation of pro-inflammatory cytokines IL-12 and IL-1β (117). Conversely, TEEGR/HCE1 binding of E2F-DP1 represses expression of some NF-kB effectors (109,110).

The great number and diversity of functions of the GRA proteins described in *T. gondii* indicates that *Plasmodium* spp. DGs may contain many more yet unidentified DG proteins.

1.4.3 ***Protein export***

The mammalian erythrocyte has restricted functionality as it loses all organelles and endomembrane systems during development and is less metabolically active than the *Plasmodium* parasite (118). To obtain metabolites essential for parasite development and evade host defences, the intraerythrocytic *Plasmodium* parasite exports hundreds of proteins into the host cell, by some estimates, 10% of the proteome (119–125).

For proteins to be exported from the parasite into the host erythrocyte they must be inserted into the endoplasmic reticulum (ER) for entrance into the secretory system, and then cross two membranes: the parasite plasma membrane (PPM) and the PVM (126). Exported transmembrane proteins then require additional transport across the host cell cytosol to their target locations in Maurer's clefts (MCs) and at the erythrocyte membrane as nutrient channels and as erythrocyte surface antigens functioning in erythrocyte – endothelial cytoadhesion. To allow this, specialised mechanisms such as the MCs and J-dots have evolved to meet the different transport needs required for correct localisation of soluble and membrane-bound proteins within the host erythrocyte (127–133).

Exported proteins contain a signal sequence for entrance into the secretory pathway through which they are secreted across the PM into the PV. A signal sequence alone is enough to target transport of a reporter protein into the ER and past the PPM into the PV (134,135). Once released into the PV, proteins must cross a second membrane, the PVM, to access the host erythrocyte. The great majority of characterised exported proteins contain a further sequence motif which targets many proteins for export across the PVM into the host cell. This pentapeptide motif, the *Plasmodium* export element (PEXEL), is located 25-30 amino acids downstream of the signal sequence (120,121). This motif, with the sequence RXLX(E/Q/D), where X signifies any amino acid, was identified by Marti *et al.* and Hiller *et al.* (2004) using sequence alignments of known exported proteins (120,121).

The PEXEL motif is cleaved by the essential aspartic protease Plasmepsin V (PM V) (136–138). PM V cleaves the PEXEL after the conserved leucine residue, which removes the N-terminal signal sequence and allows acetylation of the newly formed N terminus by an unknown acetyl transferase (124,138,139). Similarly, the *Toxoplasma* TEXEL is cleaved in the Golgi by aspartyl protease 5 (Asp5) before mature TEXEL-containing proteins are transported to the DGs (140). PEXEL cleavage by PM V releases the N-terminal region that contains the signal sequence from the ER membrane (141). Work by Boddey *et al.* demonstrated that the arginine and leucine residues are essential for correct cleavage of the PEXEL motif, but that export is dependent on the fourth residue (141). Experiments using a PfEMP3 mutant that lacks a PEXEL but possesses an identical N terminus when processed by signal peptidase was not exported but was instead retained in the PV (137). However, Tarr *et al*. showed that a correct mature N terminus, regardless of cleavage enzyme, is sufficient for protein export to the host cell (142–144). PM V has been shown to associate with chaperones that function in protein (124)the PVM for export (138).

The RESA protein family contain a noncanonical 'relaxed' PEXEL motif (RxLxxE) (122), which is processed by PM V after the conserved leucine (124). Mutation of the 6th residue of the relaxed PEXEL (E>A) when expressed from the *resa* promoter, preserves processing by PM V but results in ≈20% reduction in export (124). As RESA export is dependent upon correct expression timing in the late schizont stage (145), it is hypothesised that the relaxed PEXEL is required for correct trafficking during schizogony, with the N terminus produced by PM V cleavage (xxE) functioning in transport to the DGs or DG protein secretion, perhaps due to recognition by transport mechanisms only expressed during schizogony.

It is important to note that not all PEXEL-containing proteins are exported. Fierro *et al.* report that the PEXEL-containing PV protein UIS2 is processed by PMV but is not exported into the host erythrocyte. They identify an unusual aspartic acid residue at the N terminus of the processed peptide that blocked export in chimeric reporter fusions, with replacement of the aspartic acid with an alanine restoring reporter export. They also identify RON11 and PMIX as additional PEXEL-containing non-exported proteins (146). Ressurreição *et al.* similarly determine that the PEXEL-containing protein PV6 is not exported, instead localising to the PV (147). These findings further support the hypothesis that the presence of a correct mature N-terminus, and not PEXEL cleavage by PMV alone, is the factor that targets proteins for export. Furthermore, not all exported proteins contain a PEXEL sequence, these proteins are termed PEXEL negative exported proteins (PNEPs). PNEPs are transported to the ER by the conventional Sec61 channel (without associated Sec62/63), usually mediated by a hydrophobic sequence. The PNEP N-terminus functions similarly to the mature PEXEL N-terminus in export targeting (144).

The complex responsible for protein unfolding and export across the PVM, the PTEX, was identified through proteomic analysis of detergent-resistant membrane fractions. For consideration candidate proteins found within the fractions had to demonstrate interaction with PEXEL proteins, be expressed during the intraerythrocytic cycle, be conserved across *Plasmodium* species, and contain an ATPase to drive active transport, amongst other criteria (72). Five components of the PTEX have been identified, EXP2, HSP101, PTEX150, TRX2 and PTEX88 (72,83,148) and PV1 and Pf113 have been identified as PTEX accessory factors (81,149–152).

The PTEX components localise to the DGs in the merozoite, where they are released into the PV immediately following invasion, after which the pore component of the PTEX, EXP2, is

inserted into the membrane where it associates with the protein unfoldase HSP101 and the structural component PTEX150 (72,153). These three components were confirmed to act as the core complex of a translocon by near-atomic resolution cryoEM, which demonstrated that EXP2 and PTEX150 interlink to form a symmetric funnel-shaped protein conducting pore that spans the vacuolar membrane. Above this pore, a coiled HSP101 hexamer undergoes formational compression, causing three tyrosine-bearing pore loops margining the HSP101 hexamer to dissociate from the cargo and allowing the translocon core complex to reset (73). Recent work by Gabriella *et al.*, has demonstrated that in addition to localising to the PV, HSP101 also localises to the ER throughout the ring and trophozoite stage when protein export is at its highest, and that EXP2-PTEX150 association forms a stable subcomplex which allows docking of HSP101 for cargo export (128). These findings suggest that HSP101 recognises PEXEL proteins in the ER and chaperones them into the PV, where HSP101 associates with the EXP2-PTEX150 subcomplex targets PEXEL proteins directly to the PTEX where ATP hydrolysis by HSP101 is thought to power protein unfolding and threading into the EXP2 channel (71–73,84) for export across the PVM. The protein-disulphide isomerase TRX2 assists HSP101 in unfolding exported proteins by reducing disulphide bonds (153,154). Immunoprecipitation studies have shown that PV1 co-precipitates with the exported protein PTP5 and that a PfPV1 High Affinity Region (PHR) at the C-terminal region of PTP5 is required for export of PTP5 to the host cell, indicating that PV1 has an important role in protein export at the PVM (81,149). P113 has been demonstrated to form a stable translocation intermediate complex with mini-SURFIN$_{4.1}$ and therefore is likely to function in integral membrane protein translocation to the PTEX (82).

Inducible knockdown of expression of EXP2, the pore component of the PTEX and nutrient pore, caused reduced parasite growth proportional to the level of reduced expression, and lead to halted development midway through the asexual cycle (75). Parasite lines defective in HSP101 or PTEX150 display almost blocked protein export of both PEXEL-positive proteins and PNEPs, with greatly reduced export of the malarial virulence factor PfEMP1 to the infected erythrocyte surface and significant impact on the parasites ability to successfully complete the intraerythrocytic cycle *in vivo* and *in vitro* (83,84). Complete knockout of TRX2 and PTEX88 is possible, which given the essential nature of the PTEX, indicates that these proteins fulfil auxiliary roles in protein export. TRX2 knockout in blood stage asexual parasites leads to reduced expression of parasite surface antigens, reduced growth rates *in vivo* and *in vitro*, and a reduction in cases of severe cerebral malaria in mouse models (83,91,92). Deletion of

PTEX88 results in a stronger multiplication rate deficiency than seen in TRX2 deletion lines, and reduced erythrocyte binding of the endothelial receptor CD36 (85,92). PTEX88 has been demonstrated to interact with the exported protein interacting complex (EPIC), of which PV1 is a component along with PV2 and EXP3 (81,149,155). EPIC interacts with PfEMP1 and contributes to host erythrocyte knob formation, cytoadherence properties, and rigidification of the host cell by auxiliary action with the PTEX (149,150). The DG protein P113 (152) has been demonstrated to interact with both the PTEX and EPIC (149,150), co-immunoprecipitating with the PTEX complex (150) and has recently been demonstrated to bind SURFIN4.1 mini proteins prior to their export through the PTEX (82). Combined, these results support the role of the PTEX and its auxiliary molecules as the primary mechanism in malarial effector protein export into the host cell. The components and structure of the PTEX are shown in figure 4.

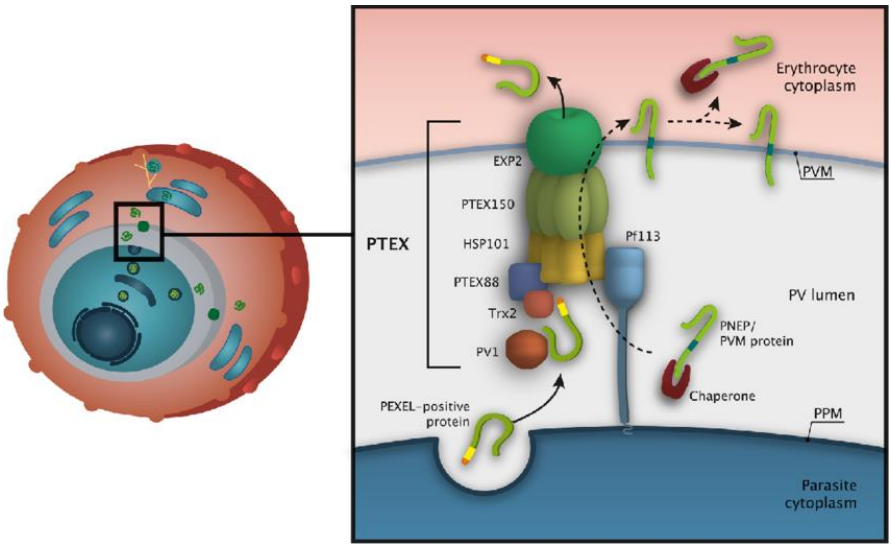

Figure 4. The components and structure of the PTEX translocon. EXP2 is the pore component of the PTEX translocon, it interacts with the protein unfoldase HSP101 and the structural component PTEX150. TRX2 assists HSP101 in unfolding of exported proteins, and PTEX88 interacts with PV1 as part of the EPIC complex which in turn interacts with PfEMP1. Pf113 is a PTEX accessory molecule of unknown function which has also been shown to interact with EPIC. Image taken from Przyborski *et al.* (156).

1.5 **Erythrocyte remodelling**

As stated above, mature mammalian erythrocytes have low levels of metabolic activity and are terminally differentiated, lacking a nucleus, RNA, transcription, or protein trafficking. The

Plasmodium parasite exports proteins broadly termed variant surface antigens (VSAs) to the host cell surface, where they modify host cell cytoadherence properties. The virulence protein *P. falciparum* erythrocyte membrane protein 1 (PfEMP1), localises to the erythrocyte membrane where it modifies the adherence properties of the erythrocyte, causing infected erythrocytes to adhere to endothelial cell receptors and other infected erythrocytes (157–159). This increased adhesiveness leads to sequestration of infected erythrocytes in the microvasculature where they can avoid filtration and destruction by the spleen and the reticuloendothelial system (160). The PfEMP1 family are encoded by ≈60 *var* genes which are expressed in a mutually exclusive way (161,162), with gene switching enabling host immune evasion (163). PfEMP1 receptor binding is enhanced by the function of knob-associated histidine-rich protein (KAHRP) binds to the erythrocyte cytoskeleton to form knob-like structures that protrude outward from the erythrocyte surface extending PfEMP1 into the external environment and causes increased rigidification of the host erythrocyte membrane (164–166). Another exported protein that localises to the host erythrocyte surface is PfEMP3 (167,168), which associates with the host cell surface cytoskeleton via its N-terminal domain (169) where it is thought to contribute to a decrease in host cell deformability (164). The *P. falciparum* skeleton binding protein 1 (PfSBP1) is an integral membrane protein that localises to the MCs, with its C-terminal domain facing the erythrocyte cytoplasm (170–173). It is thought that PfSBP1 may function in linking the MCs to the host cell cytoskeleton and has an important function in parasite virulence as knockdown of PfSBP1 blocks PfEMP1 presentation at the host cell surface (172,173). Another MC resident transmembrane protein is the membrane-associated Hs-rich protein 1 (MAHRP1), which is similarly positioned with its His-rich C-terminal domain exposed to the erythrocyte cytoplasm (132,174). Knock down of MAHRP causes PfEMP1 to accumulate at the PV membrane, indicating a function in PfEMP1 transfer from the PV into the MCs for transport to the erythrocyte surface (132,174,175). Ring exported protein 1 (REX1) is a MC peripheral membrane protein and PNEP that associates with the cytoplasmic surface of the MCs via a predicted coiled coil domain, (176–178). REX1 binding of the MC membrane is required for correct morphology of these organelles, with disruption of REX1 causing MCs to form stacked or whorled cisternae (179).

Other families of exported VSA proteins in *P. falciparum* include the repetitive interspersed (RIFINs) and the subtelomeric variable open reading frame (STEVOR) families. RIFINs represent the largest family of VSAs, encoded by the *rif*-gene family of which there are ≈150 members associated with *var* subtelomeric sites on genome (180). RIFINS are divided into

types A and B. The majority of RIFINS, (70%), are type A, and are characterised by a series of 25 amino acids downstream of the PEXEL sequence at the N terminus which are absent in type B (181). A-type RIFINs localise to the host cell surface, whereas the majority of B-type RIFINS localise to the parasite cytosol (181–183). In addition to modifying the adhesion properties of the host cell, a subset of exported RIFINS also act as immune inhibitors, binding to inhibitory receptors of host immune cells leukocyte immunoglobulin-like receptor B1 and leukocyte-associated immunoglobulin-like receptor 1, down regulating the host immune response (184,185). Due to the high levels of polymorphism in the *rif* family, RIFINS themselves avoid recognition by the host immune system (185,186). STEVOR proteins, encoded by ≈40 *stevor* genes, have diverse functions in mediating invasion of the host cell, binding of uninfected erythrocytes, and decreasing host cell deformability (187–189).

Erythrocytic mechanical properties are altered through the function of exported proteins which variably bind, phosphorylate, and cleave erythrocyte cytoskeletal proteins. The *Plasmodium* helical interspersed subtelomeric (PHIST) proteins are a family of 89 proteins (122,190) which are divided into three subgroups a-c and are characterised by a conserved domain of around 150 amino acids which are predicted to form four alpha helices (191). Of the known PHIST proteins, 64 contain a PEXEL sequence and are therefore likely to be exported (122,124). PHIST proteins have diverse functions, including mediating correct localisation of PfEMP1, and reducing host cell deformability, as is the case for the DG protein RESA, which is a PHIST protein that binds to and stabilises host cell actin tetramers below the erythrocyte surface (192–194). PHIST proteins have also been implicated in gametocytogenesis (195,196).

Similarly, FIKK kinases of the Laverania subgroup of the genus *Plasmodium* affect the host cell cytoskeleton. FIKK kinases are Apicomplexan-specific serine/threonine kinases, which in nearly all species are present in a single copy. However, in the Laverania lineage, the family has expanded and most members of the expanded family have acquired an export signal that allows them to be exported into the host cell cytoplasm. These exported FIKK serine/threonine kinases are hypothesised to enable survival of parasites by regulating modification of the host cell through phosphorylation of host cell proteins (197,198). FIKK4.1 has been demonstrated to influence host cell rigidification and is required for correct trafficking of the malarial virulence protein PfEMP1, a parasite effector protein that increases the cytoadhesion properties of infected cells, to the erythrocyte surface (197). Disruption of *fikk7.1* and *fikk12* caused no change in host cell binding to the endothelial receptors' chondroitin sulphate or CD36 in vitro but exhibited a reduction in rigidity of the host cell (198). Together, these results indicate that

the exported FIKK kinases function to increase infected erythrocyte cytoadhesion and rigidity, leading to increased heat shock resistance, avoidance of splenic clearance through sequestration in the microvasculature and protection of erythrocytes from further merozoite invasion.

Interestingly, many of the genes encoding PEXEL-containing proteins are located in subtelomeric regions, where increased mutation rates (122) may have contributed to the large size of some families of exported proteins such as the PHIST proteins and FIKK kinases (199). Silvestrini *et al.* demonstrated that a PEXEL-based export pathway is also used in early-stage gametocytes, with PfGEXP10, Pfg14.774 and PgRex-3 all being cleaved before the conserved leucine residue, N-terminally acetylated and exported (195). The PEXEL motif, is conserved across *Plasmodium* species (122), and the closely related Apicomplexan species *Toxoplasma* contain a similar *Toxoplasma* export element or TEXEL sequence (140,200).

PEXEL containing proteins are translocated into the ER by the Sec61 translocon channel associated with Sec62 and Sec63 on the ER membrane.

1.5.1 ***NPPs***

Inside the host erythrocyte, the parasite digests host haemoglobin, possibly to gain the amino acids they require for protein production. It is important to note that work by Lin *et al.* demonstrated that haemoglobin digestion is not required for replication of *Plasmodium* parasites in the intraerythrocytic stages (201,202), and that haemoglobin digestion may instead function to free space inside the erythrocyte, allowing the parasite to grow, and allows the regulation of host cell osmotic pressure (203,204). Haemoglobin contains low levels of methionine and does not contain isoleucine, which is essential for parasite development, and the parasite cannot synthesise either *de novo.* Erythrocytes take up many nutrients from ist surroundings using nutrient transporters, which include urea transporters, aquaporins, organic anion and cation channels, ATP-powered transporters, P-type ATPases, monocarboxylate transporter1 (MCP1), equilibrative nucleoside transporter 1 and anion exchanger 1 (205). The increased metabolic activity in the infected erythrocyte owing to the added metabolism of the parasite means that the rate at which erythrocyte transporters take up nutrients is exceeded by the rate that they are consumed. To alleviate this deficit and allow nutrient uptake from the host serum, the parasite exports proteins that form pores in the host cell membrane, increasing selective permeability to low molecular weight solutes, including sugars, amino acids, ions, purines and vitamins (206). These pores are termed the new permeability pathways (NPPs) and

are also referred to as the *Plasmodium* surface anion channel (PSAC) as they behave similarly to anion-selective channels (207–209). It has not been determined whether the PSAC is the only NPP or whether it is entirely parasite derived.

Some proteins which have been linked to NPPs include the products of the *clag3.1* and *clag3.2* genes. These were first linked to the NPPs through use of NPP inhibitors, nutrient restriction and genetic approaches (210–213). Whilst knockout of the *clag3* genes is not lethal (with some nutrient transport remaining), delayed growth and altered NPP activity is observed in parasites in which in vitro selection and epigenetic silencing are used (214–216). Mira-Ramirez *et al*. demonstrated that parasite resistance to the antibiotic blasticidin is linked to altered solute uptake through epigenetic gene switching between the *clag3.1* and *clag 3.2* genes. Low-level selection with blasticidin caused expression switching from *clag3.2* to *clag 3.1*, implying that each gene confers different solute transport properties to the PSAC (215). High levels of blasticidin selection caused silencing of both genes and blocked uptake of many PSAC substrates, indicating that silencing of the *clag3* paralogs causes deformation of the PSAC. Similarly, the work of Sharma *et al*. demonstrated that a *clag3* mutation to an alpha-helical transmembrane domain predicted to form a water-filled pore (A1210T) alters PSAC activity and confers resistance to the protease inhibitor leupeptin (216). Comeaux *et al.* demonstrated that switching between the two paralogous *clag3* genes is epigenetically regulated. Additionally, disruption of the *clag3.2* gene resulted in *clag3.1* gene silencing and production of shortened *clag3.1* and *3.2* transcripts, these *clag3* null parasites exhibited significant growth defects (214).

The non-lethal effect of *clag3.1* and *clag3.2* knockout is surprising given the essential nature of nutrient uptake to parasite survival. The two paralogous *clag3* genes however belong to a larger multigene family called RhopH1, which in *P. falciparum* contains 3 additional clag genes, *clag2*, *clag8* and *clag9* (217). There is high conservation between the 5 genes in *P. falciparum* isolates, with each paralog retaining 90% sequence identity between isolates from geographically distant locations (218). This conservation suggests either that loss of *clag3* genes is complemented by the other paralogs or that all 5 genes could encode distinct channels which transport different solutes.

1.5.2 ***RhopH2, RhopH3 and the NPP***

The CLAG3 proteins are synthesised in the schizont stage of the intraerythrocytic cycle and stored within the rhoptry as part of the RhopH complex, which comprises the RhopH2, RhopH3

and CLAG3 proteins in a 1:1:1 stoichiometry (219,220) and is highly conserved among *Plasmodium* species. During merozoite invasion the RhopH complex is conveyed to the erythrocyte membrane (221) and associate with the host cytoskeleton (222). The RhopH3 subunit of the RhopH complex is the only one which functions in the invasion process (219,223). An inability to successfully knockout either *RhopH2* or *RhopH3* genes indicates that they are essential to parasite survival (224–226). More recently, use of inducible knockdown methods has demonstrated that reduction of RhopH2 and RhopH3 causes reduced NPP activity with significant parasite growth defects (219,222,223). Parasite development was observed to stall midway through the intraerythrocytic cycle, which is consistent with the timing of RhopH2 and RhopH3 activity, and the time at which protein export becomes essential (84). The growth defects observed may be attributed to the decreased levels of essential solutes seen in response to depletion of RhopH3 (222). Around 18 hours post invasion the CLAG3 subunit is inserted into the host cell membrane where it functions as a PSAC (210,212).

1.5.3 ***PVM nutrient permeability***

Once nutrients have crossed the erythrocyte membrane via the NPP they need to cross the PVM. Studies using patch clamp techniques have indicated the PVM contains a nutrient pore with a size exclusion limit of 1.4kDa and diameter of 23Å (208,227), which allows passage of amino acids and monosaccharides. As described above, a similar pore is present within the PVM of *T. gondii*, in which passive transport of small molecules across the PVM is mediated by the DG protein GRA17 working synergistically with GRA23 (104). GRA17 and GRA23 are orthologs of EXP2, which is conserved across PV-residing Apicomplexa (104). Reduced PVM permeability, aberrant PV morphology and structural instability are seen in cells infected with GRA17-deficient parasites, phenotypes which are reversed by complementation with *P. falciparum* EXP2. This work led to further investigation of EXP2 function in *P. falciparum*, where patch-clamp measurements, mutagenesis and regulation of gene expression were used to demonstrate a tight association between levels of EXP2 and the density of PVM channels (74). Truncation of EXP2 altered the channels voltage response, further indicating that EXP2 fulfils dual roles in protein export and translocon independent small molecule permeability in the PVM (74). This remains the only channel activity demonstrated to be present in the PMV to date, despite multiple independent studies using varied patch-clamping techniques, indicating that EXP2 may represent the only solute transport mechanism at the PVM (74,227).

1.5.4 ***The cytostome***

As described above, it is theorised that *Plasmodium* spp. source many amino acids required for growth from host cell haemoglobin. To access the haemoglobin from within the PVM the parasite endocytoses more than two thirds of the soluble host cell content through an invagination of both the PVM and PPM membranes to form a 'flask-shaped' organelle with a narrow neck (≈100 nm) and an electron-dense collar termed the cytostome (228,229). A structure termed the phagotroph may also be responsible by host cell cytosol uptake, but evidence indicating that protease plasmepsin II is transported to the DV via the cytostome (230), and localisation of proteins involved in endocytosis to components of the cytostome (231), indicate that the cytostome is the organelle responsible for host cell cytoplasm uptake. The pathways underlying nutrient transport from the cytostome to the lysosome-like organelle the digestive vacuole (DV), where haemoglobin digestion occurs have yet to be elucidated. Two potential processes for endosomal structure formation have been suggested. Either the entire cytostome periodically buds off from the PVM and PPM, is transported to the DV, and a new cytostome is formed (the 'cytostome maturation model'), or smaller vesicles are continually pinched off from the cytostome and transported to the DV whilst the cytostome remains intact (the 'cytostome hub model') (232). Abu Baker *et al*. demonstrated that haemoglobin digestion begins during transport to the DV, where digestion is completed (233). During digestion, cysteine endoproteases and aspartic proteases first remove polypeptide globin chains which are further cleaved by metalloproteases and aminopeptidases into oligopeptides and dipeptides, a form from which the parasite can access the amino acids it requires for growth (234). Haemoglobin digestion also produces toxic haem which the parasite converts into nontoxic haemozoin, which can be seen as a dark pigment within the DV.

The parasite uses less than 20% of the amino acids derived from the digestion of haemoglobin, indicating an additional purpose to parasite uptake of host cell cytosol (203,235). It is possible that one of these functions is to reduce the host cell content volume in order to provide the parasite room to grow and to maintain osmotic equilibria (204,236).

To date the molecular mechanisms underlying the endocytosis of cytostome formation are unknown. Potential candidates include actin, dynamin, adaptor protein 2, Rab proteins and soluble N-ethylmaleimide sensitive factor attachment proteins (SNAP) receptor proteins (SNAREs) among many others (232). Host cell cytosol uptake and haemoglobin digestion are important processes, as demonstrated by the role of host cell cytosol uptake in artemisinin

resistance. The *P. falciparum* Kelch-13 endocytosis pathway has been linked to artemisinin resistance as inactivation of proteins associated with the Kelch-13 defined compartment (including Kelch-13) causes decreased haemoglobin endocytosis. As artemisinins are activated by the degradation products of haemoglobin digestion, reduced haemoglobin endocytosis from the host cell cytosol leads to reduced levels of haem and therefore decreased artemisinin activation and artemisinin resistance (231). Therefore, more research is required to uncover the mechanisms underlying cytostome formation and nutrient transport to the DV.

1.5.5 ***The PVM and the tubovesicular network***

As described above, during erythrocyte invasion the parasite sets up a vacuolar compartment termed the parasitophorous vacuole (PV) within which it resides throughout the intraerythrocytic cycle. This membranous shelter serves as an interface for host-pathogen interactions, functioning in protein export and nutrient import. The source of the PVM has to date not been sufficiently demonstrated, with studies reporting conflicting results. Transmission electron microscopy (TEM) analysis has revealed that upon merozoite invasion the PVM and erythrocyte membrane form a continuous uninterrupted structure (237), indicating that the PVM may originate from the host cell membrane. Further, studies introducing fluorescent lipophilic probes into the erythrocyte membrane observe equivalent concentration of probes in the PVM as in the erythrocyte membrane (238–240). However, erythrocyte membrane surface area is not reduced following parasite invasion, indicating that the majority of PVM lipids are parasite derived (241). Also, parasite-derived metabolically labelled lipids are observed to localise to the PMV, indicating that parasite-derived lipids at least partially contribute to PVM biogenesis (242,243). As the PVM and PPM come into close proximity during merozoite invasion, the ability of labelled lipid probes to move across aqueous solutions should be considered in evaluating the strength of this evidence. Some studies have indicated that the rhoptries may be the source of the parasite derived lipid content of the PVM. Upon invasion, the membranous whirls contained within the rhoptries are observed to shrink (44,244,245). This coincides with the release of multilamellar membrane aggregates into the host cell from the apical pole of the parasite (44,244,246) and visualisation of tubular extensions and vesicles near the site of invasion (25,247,248). Freeze fracture electron microscopy has determined that similarly to the PVM, these membranes are devoid of membrane-bound particles, which only appear after DG protein secretion into the PVM (246,249,250).

As the parasite matures, the PVM develops membranous extensions that exptend into the erythrocyte cytoplasm. This membranous complex, termed the tubovesicular network (TVN), functions as an exported parasite organelle (251), which has been demonstrated to contain PV markers including EXP1 and EXP2, as well as soluble PV markers, indicating a direct connection between the lumen of the PV and the TVN (80,252,253). To date the TVN has been best described in *P. falciparum*, although similar structures have also been described in rodent malaria species (254). The function of the TVN remains uncertain as the appearance of the TVN is highly variable and it is sometimes absent. Early imaging studies utilised fluorescent lipid dyes (238,255,256), whilst more recent work using serial sectioning and immunogold labelling has revealed that the TVN comprises double membrane whorls encompassing host cell cytoplasm (257), the whorls are connected by membranous tubules and vesicular structures originating from the PV. (94,255,257). It is theorised that the TVN could function as a storage site for incorrectly folded exported proteins, which could account for the apparent variation in TVN presence and morphology. In this model the TVN would have a role equivalent to that of the ER stress response (258). In support of this hypothesis, work by Charnaud *et al.*, found that exported proteins induced into a tightly folded conformation aggregated in the loops of the TVN and initiated further loop formation. Sequestration of misfolded proteins in this way may serve to protect the parasite protein transport machinery from blockage (75). This theory is supported further by a marked absence of an exported reporter protein from the TVN loops in comparison to the PVM during trafficking, indicating that loop regions do not contribute to protein export (259), and by a lack of translocon PTEX components from the TVN (71,72,75,260).

1.6 **Why a PV?**

The function of the PV remains unknown. PV assembly and maintenance requires considerable resources, whilst presenting a barrier to nutrient access and host egress which require complex molecular mechanisms to overcome. In many intracellular pathogens, such as *T. gondii*, a vacuolar compartment can serve as a protective barrier between the parasite and host cell-autonomous resistance mechanisms, such as host immunity-related GTPases and guanylate-binding proteins (261–263). For example, degradation of the *T. gondii* PVM quickly results in parasite death (264). Given the terminally differentiated nature of the human erythrocyte, which lacks organelles, pathogen-recognition and cell-autonomous defence mechanisms, the benefits of a PV remain unknown. Closely related Apicomplexan parasites of the order piroplasmida *Babesia* spp. and *Theileria* spp., rapidly degrade their PVM after invasion so that the parasites

are free in the host cell cytosol (29,265), whilst other aspects of host cell remodelling closely mirror those seen in *Plasmodium* parasites (266,267), indicating that a PVM is not required for effective remodelling of the host cell by these organisms or that haemoglobin has a toxic effect on the parasites. It is possible that export across the PTEX is essential for remodelling as exported proteins are folded in the erythrocyte cytosol by PTEX associated complexes post translocation (268). Without correct folding exported proteins would not be able to function, so the presence of the PVM containing the PTEX may be necessary to act as final processing step in the production of functional exported proteins.

Despite the lack of immune surveillance and the low metabolism of the erythrocyte, it is possible that the PVM serves as a protective shield, not from host cell defence mechanisms but from reactive oxygen species such as free haem that are a product of the erythrocyte's role in oxygen transport (269). Within the erythrocyte free haem can reach concentrations of up to ≈20 μM (270). The erythrocyte protects itself from damage from free haem and radical oxygen species using redox regulators (271), however the rapidly growing parasite may require further protection in the form of a shielding PVM. Initial evidence suggested that EXP1 acts as a membrane glutathione S-transferase, functioning to degrade cytotoxic haem in vitro (272), potentially supporting the role of the PVM in redox protection. However, these results were not proven in in vitro studies, where EXP1 enzymatic activity was not found to aid intraerythrocytic survival and replication (80).

As hepatocytes possess adaptive defence mechanisms, the parasite may require the PV as a protective niche during the intra-hepatocytic stage. This has been demonstrated in mouse models lacking expression of 6/Cys family related proteins. At the hepatocytic stage these cells lose their PVM, parasite development stalls, host defences are triggered and the host cell undergoes apoptosis (273). It is therefore possible that the parasite adheres to this mechanism during the blood stage because it is already established and encoded in the genome, however this seems inefficient as the cost of PVM construction and development of new pathways for nutrient uptake and egress would likely outweigh the cost of PVM degradation.

1.7 **Protein transport across the cytoplasm, Maurer's clefts, J-dots, chaperones**

Following transport across the PVM, exported proteins are re-folded and targeted to specific locations within the host cell through specialised mechanisms of extraparasite trafficking. Two structures that have been implicated in this process in *P. falciparum* are the MCs, and J-dots.

MCs are membrane-bound compartments within the host cytoplasm that become tethered to the erythrocyte membrane upon parasite maturation (171,274). From here they transfer parasite exported proteins, such as PfEMP1, into the erythrocyte membrane. J-dots are large protein complexes that are mobile within the host cytoplasm (28). It has been suggested that J-dots may function in transport of effector proteins from the PVM to the MCs (275). In addition to these structures, the parasite exports many molecular chaperones that have essential roles in many aspects of effector protein trafficking into both the PV and the host cell. J-dots are comprised of exported HSP70x and HSP40 co-chaperones (276–278), and associate with PfEMP1 and other effector proteins (277,279,280). HSP70x has been determined to be dispensable in vitro although deletion does have a minor negative effect during the ring stages (281–283), whereas some of the HSP40 co-chaperones which are shown to associate with HSP70x in J-dots (173,277,280,284), indicating that they are essential for host cell remodelling. The non-essential nature of HSP70x brings the potential role of the J-dots in effector protein trafficking across the host cytosol into question, although it is possible that HSP70x depletion may have a negative effect under in vivo conditions. It has been suggested that PfHSP70 may have a redundant function with host HSP70 present within the human erythrocyte, which may fulfil this function in parasites in which PfHSP70x has been disrupted. Work showing that host HSP70 localisation changes from a soluble fraction to a detergent-resistant fraction upon infection with *P. falciparum* supports this theory and indicates that transport of effector proteins in the erythrocyte cytosol may be mediated by chaperones originating from both the parasite and the host cell (285).

The cargo of the MCs includes the adhesin *Pf*EMP1 (286), with other proteins having been identified associated with the MCs having roles in MC morphology, transfer of protein cargo to the MCs and from the MCs to the erythrocyte membrane and visa-versa (130).

The origin of the J-dots and MCs is unknown (251), although work that has localised MC's adjacent to the PVM indicates that they may originate from the PVM, other studies which utilise fluorescently labelled parasite phosphatidylcholine to investigate the origins of lipids of the exomembrane system indicate that there is no parasite-derived phosphatidylcholine within the MCs and that they are therefore unlikely to contain any parasite derived lipid content (287).

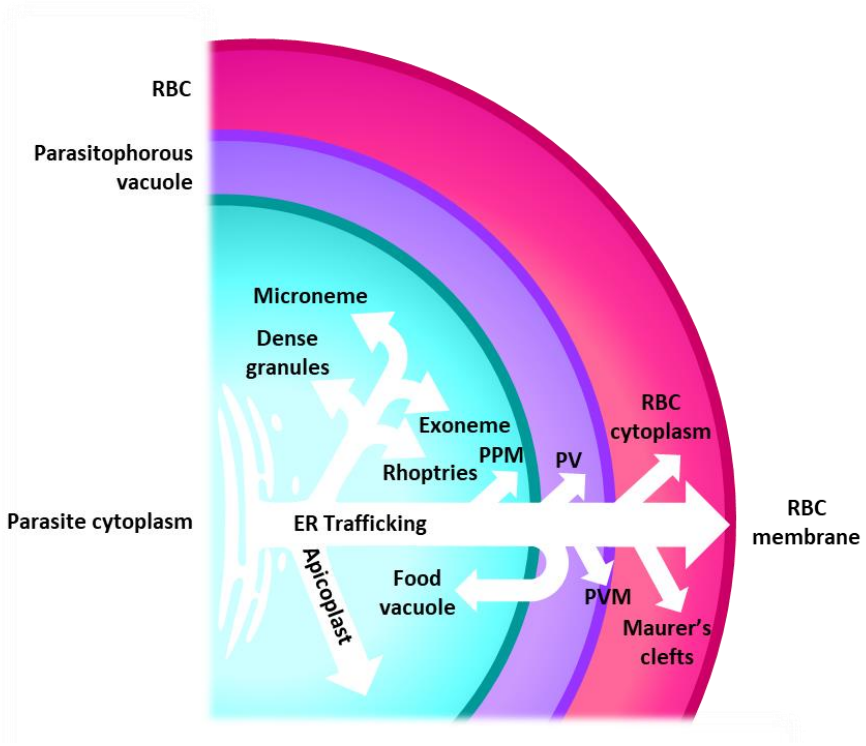

Figure 5. Pathways of protein trafficking from the ER. Pathways of protein trafficking from the ER to locations within the parasite cell, the PV and the host cell.

1.8 **Summary**

The timing of DG protein secretion immediately following invasion, the extensive nature of erythrocyte remodelling, and the greater number of DG proteins found in other Apicomplexan parasites all suggest that *Plasmodium* DGs likely contain many more essential exported proteins than those currently identified. Most of the known DG proteins localise to the PV and PVM, the PTEX exports effector proteins across the PVM and RESA is one such exported protein which functions in erythrocyte protection against fever, it is possible that the DG may contain many more exported proteins which function to modify the erythrocyte to facilitate parasite passage through the erythrocytic phase. This theory is supported by the transcriptional expression profiles of 90 genes that encode proteins that contain a *Plasmodium* Export Element (PEXEL) demonstrating that *P. falciparum* exported proteins are synthesised very late in the life cycle, close to the time of DG biogenesis.

For gains in the fight against malaria to increase, new light must be shed on the pathogenesis of the *Plasmodium* parasite. As DG function is essential for parasite survival within the host

erythrocyte, discovery of the mechanisms underlying DG biogenesis, protein composition and function in *Plasmodium* parasites may inform vital drug discovery efforts against this significant disease.

1.9 **Project Aims**

This project aims to address three key aspects of DG biology: DG biogenesis timing, the mechanism of protein targeting to the DGs and the DG proteome.

1.9.1 Aim 1: Timing of DG biogenesis. I aim to identify when DGs are produced using live fluorescence microscopy of *P. falciparum* parasites that produce a fluorescent fusion of a DG protein (61) to allow visualisation of the biogenesis of the DGs in relation to egress.

1.9.2 Aim 2: Identification of new DG proteins. I will utilize two methods to identify potential DG proteins. First, I will use bioinformatics to identify proteins with a transcriptional profile similar to known DG proteins. Second, I aim to produce a fusion of a DG protein with the APEX protein and then perform proximity biotinylation.

1.9.3 Aim 3: Identify the information that targets proteins to the DGs. In particular I will test whether timing or sequence information within the protein is required for proper targeting to the DGs using the appropriate gene and promoter fusions.

Bibliography

1. By-Nc-Sa C. World malaria report 2022. 2022;

2. World Health Organization. World malaria report 2019. Geneva, Switzerland: World Health Organization; 2019.

3. Richard D, Kats LM, Langer C, Black CG, Mitri K, Boddey JA, et al. Identification of Rhoptry Trafficking Determinants and Evidence for a Novel Sorting Mechanism in the Malaria Parasite *Plasmodium falciparum*. Striepen B, editor. PLoS Pathog. 2009 Mar 6;5(3):e1000328.

4. Bartoloni A, Zammarchi L. Clinical aspects of uncomplicated and severe malaria. Mediterr J Hematol Infect Dis. 2012;4(1).

5. World Health Organization. Guidelines for the treatment of malaria - 3rd edition. 2015 p. 31–41.

6. World Health Organization. Artemisinin and artemisinin-based combination therapy resistance. Geneva, Switzerland; 2017.

7. Mihreteab S, Platon L, Berhane A, Stokes BH, Warsame M, Campagne P, *et al*. Increasing Prevalence of Artemisinin-Resistant HRP2-Negative Malaria in Eritrea. N Engl J Med. 2023 Sep 28;389(13):1191–202.

8. Conrad MD, Asua V, Garg S, Giesbrecht D, Niaré K, Smith S, *et al*. Evolution of Partial Resistance to Artemisinins in Malaria Parasites in Uganda. N Engl J Med. 2023 Aug 24;389(8):722–32.

9. Uwimana A, Legrand E, Stokes BH, Ndikumana JLM, Warsame M, Umulisa N, *et al*. Emergence and clonal expansion of in vitro artemisinin-resistant *Plasmodium falciparum* kelch13 R561H mutant parasites in Rwanda. Nat Med. 2020 Oct 1;26(10):1602–8.

10. Van Loon W, Oliveira R, Bergmann C, Habarugira F, Ndoli J, Sendegeya A, *et al*. In Vitro Confirmation of Artemisinin Resistance in *Plasmodium falciparum* from Patient Isolates, Southern Rwanda, 2019. Emerg Infect Dis. 2022 Apr;28(4):852–5.

11. Regules JA, Cummings JF, Ockenhouse CF. The RTS,S vaccine candidate for malaria. Expert Rev Vaccines. 2011 May;10(5):589–99.

12. Asante P, Owusu R, Osei-Kwakye K, Apanga S, Kwara E, Dip K, *et al*. Safety and efficacy of the RTS,S/AS01 E candidate malaria vaccine given with expanded-programme-on-immunisation vaccines: 19 month follow-up of a randomised, open-label, phase 2 trial. Lancet Infect Dis. 2011;11:741–9.

13. Datoo MS, Natama HM, Somé A, Bellamy D, Traoré O, Rouamba T, *et al*. Efficacy and immunogenicity of R21/Matrix-M vaccine against clinical malaria after 2 years' follow-up in children in Burkina Faso: a phase 1/2b randomised controlled trial. Lancet Infect Dis. 2022 Dec;22(12):1728–36.

14. Archibald JM, Simpson AGB, Slamovits CH. Handbook of the Protists Second Edition. Boston: Springer International Publishing; 1990.

15. Melhorn H, Peters W, Haberkorn A. The formation of kinetes and oocysts in Plasmodium gallinaceum and considerations on phylogenetic relationships between Haemosporidia, Piroplasmida, and other Coccidia. Protistologica. 1980;16:135–54.

16. Levine ND. The protozoan phylum Apicomplexa. 1st ed. Vol. 1. Boca Raton: CRC Press; 1988.

17. Morrison DA. Evolution of the Apicomplexa: where are we now? Trends Parasitol. 2009 Aug;25(8):375–82.

18. Katris NJ, van Dooren GG, McMillan PJ, Hanssen E, Tilley L, Waller RF. The Apical Complex Provides a Regulated Gateway for Secretion of Invasion Factors in *Toxoplasma*. PLoS Pathog. 2014;10(4).

19. Autino B, Corbett Y, Castelli F, Taramelli D. Pathogenesis of malaria in tissues and blood. Mediterr J Hematol Infect Dis. 2012;4(1).

20. Crutcher JM, Hoffman SL. Medical Microbiology. 4th ed. Galveston (TX): University of Texas Medical Branch at Galveston; 1996.

21. Boutlis C, Riley E, Anstey N, de Souza J. Glycosylphosphatidylinositols in malaria pathogenesis and immunity: potential for therapeutic inhibition and vaccination. In: Immunology and Immunopathogenesis of Malaria. Berlin/Heidelberg: Springer; 2005. p. 145–85. (CT Microbiology; vol. 297).

22. Brattig NW, Kowalsky K, Liu X, Burchard GD, Kamena F, Seeberger PH. *Plasmodium falciparum* glycosylphosphatidylinositol toxin interacts with the membrane of non-parasitized red blood cells: a putative mechanism contributing to malaria anemia. Microbes Infect. 2008 Jul;10(8):885–91.

23. Cowman AF, Crabb BS. Invasion of red blood cells by malaria parasites. Cell. 2006 Feb 24;124(4):755–66.

24. Blackman MJ, Carruthers VB. Recent insights into apicomplexan parasite egress provide new views to a kill. Curr Opin Microbiol. 2013;16(4):459–64.

25. Riglar DT, Richard D, Wilson DW, Boyle MJ, Dekiwadia C, Turnbull L, et al. Super-resolution dissection of coordinated events during malaria parasite invasion of the human erythrocyte. Cell Host Microbe. 2011 Jan 20;9(1):9–20.

26. Dvorak JA, Miller LH, Whitehouse WC, Shiroishi T. Invasion of erythrocytes by malaria merozoites. Science. 1975 Feb 28;187(4178):748–50.

27. Gilson PR, Crabb BS. Morphology and kinetics of the three distinct phases of red blood cell invasion by *Plasmodium falciparum* merozoites. Int J Parasitol. 2009 Jan;39(1):91–6.

28. Sherling ES, Van Ooij C. Host cell remodeling by pathogens: the exomembrane system in *Plasmodium*-infected erythrocytes. FEMS Microbiol Rev. 2016;016:701–21.

29. Asada M, Goto Y, Yahata K, Yokoyama N, Kawai S, Inoue N, *et al*. Gliding Motility of *Babesia bovis* Merozoites Visualized by Time-Lapse Video Microscopy. Templeton TJ, editor. PLoS ONE. 2012 Apr 10;7(4):e35227.

30. Rudzinska MA, Trager W, Lewengrub SJ, Gubert E. An electron microscopic study of *Babesia microti* invading erythrocytes. Cell Tissue Res. 1976 Jun;169(3):323–34.

31. Repnik U, Gangopadhyay P, Bietz S, Przyborski JM, Griffiths G, Lingelbach K. The apicomplexan parasite *Babesia divergens* internalizes band 3, glycophorin A and spectrin during invasion of human red blood cells. Cell Microbiol. 2015 Jul 1;17(7):1052–68.

32. De Koning-Ward TF, Dixon MWA, Tilley L, Gilson PR. *Plasmodium* species: Master renovators of their host cells. Nat Rev Microbiol. 2016 Aug 1;14(8):494–507.

33. Proellocks NI, Coppel RL, Mohandas N, Cooke BM. Malaria Parasite Proteins and Their Role in Alteration of the Structure and Function of Red Blood Cells. Adv Parasitol. 2016;91:1–86.

34. Preiser P, Kaviratne M, Khan S, Bannister L, Jarra W. The apical organelles of malaria merozoites: host cell selection, invasion, host immunity and immune evasion. Microbes Infect. 2000 Oct;2(12):1461–77.

35. Horta MF, Andrade LO, Martins-Duarte ÉS, Castro-Gomes T. Cell invasion by intracellular parasites - the many roads to infection. J Cell Sci. 2020 Feb 1;133(4).

36. David Sibley L. Invasion and intracellular survival by protozoan parasites: Parasite invasion strategies. Immunol Rev. 2011 Mar;240(1):72–91.

37. Carruthers VB, Sibley LD. Sequential protein secretion from three distinct organelles of *Toxoplasma gondii* accompanies invasion of human fibroblasts. Eur J Cell Biol. 1997;73(2):114–23.

38. Camus D, Hadley TJ. A *Plasmodium falciparum* Antigen That Binds to Host Erythrocytes and Merozoites. Science. 1985;230(4725):553–6.

39. Adams JH, Sim BKL, Dolan SA, Fang X, Kaslow DC, Miller LH. A family of erythrocyte binding proteins of malaria parasites. Proc Natl Acad Sci U S A. 1992;89(15):7085–9.

40. Triglia T, Healer J, Caruana SR, Hodder AN, Anders RF, Crabb BS, *et al*. Apical membrane antigen 1 plays a central role inerythrocyte invasion by *Plasmodium* species. Mol Microbiol. 2000;38(4):706–18.

41. Deans JA, Thomas AW, Alderson T, Cohen S. Biosynthesis of a putative protective *Plasmodium knowlesi* merozoite antigen. Mol Biochem Parasitol. 1984;11(C):189–204.

42. Peterson MG, Marshall VM, Smythe JA, Crewther PE, Lew A, Silva A, *et al*. Integral Membrane Protein Located in the Apical Complex of *Plasmodium falciparum*. Vol. 9, Molecular and Cellular Biology. 1989 p. 3151–4.

43. Ladda R, Aikawa M, Sprinz H. Penetration of Erythrocytes by Merozoites of Mammalian and Avian Malarial Parasites *. J Parasitol. 2001 Jun;87(3):470–8.

44. Bannister LH, Mitchell GH. The Fine Structure of Secretion by *Plasmodium knowlesi* Merozoites during Red Cell Invasion. J Protozool. 1989;36(4):362–7.

45. Tetley L, Brown SMA, McDonald V, Coombs GH. Ultrastructural analysis of the sporozoite of *Cryptosporidium parvum*. Microbiology. 1998;12:3249–55.

46. Blackman MJ, Bannister LH. Apical organelles of Apicomplexa: biology and isolation by subcellular fractionation. Vol. 117, Molecular & Biochemical Parasitology. 2001 p. 11–25.

47. Bannister LH, Hopkins JM, Fowler RE, Krishna S, Mitchell GH. Ultrastructure of rhoptry development in *Plasmodium falciparum* erythrocytic schizonts. Parasitology. 2000;121:273–87.

48. Alexander DL, Mital J, Ward GE, Bradley P, Boothroyd JC. Identification of the moving junction complex of *Toxoplasma gondii*: A collaboration between distinct secretory organelles. PLoS Pathog. 2005;1(2):0137–49.

49. Besteiro S, Michelin A, Poncet J, Dubremetz JF, Lebrun M. Export of a *Toxoplasma gondii* Rhoptry Neck Protein Complex at the Host Cell Membrane to Form the Moving Junction during Invasion. PLoS Pathog. 2009;5(2):1000309.

50. Topolska AE, Richie TL, Nhan DH, Coppel RL. Associations between responses to the rhoptry-associated membrane antigen of *Plasmodium falciparum* and immunity to malaria infection. Infect Immun. 2004 Jun;72(6):3325–30.

51. Cao J, Kaneko O, Thongkukiatkul A, Tachibana M, Otsuki H, Gao Q, *et al*. Rhoptry neck protein RON2 forms a complex with microneme protein AMA1 in *Plasmodium falciparum* merozoites. Parasitol Int. 2009 Mar;58(1):29–35.

52. Bai MJ, Wang JL, Elsheikha HM, Liang QL, Chen K, Nie LB, *et al*. Functional Characterization of Dense Granule Proteins in *Toxoplasma gondii* RH Strain Using CRISPR-Cas9 System. Front Cell Infect Microbiol. 2018 Aug 28;8(AUG):300.

53. Proellocks NI, Coppel RL, Waller KL. Dissecting the apicomplexan rhoptry neck proteins. Trends Parasitol. 2010 Jun;26(6):297–304.

54. Srinivasan P, Beatty WL, Diouf A, Herrera R, Ambroggio X, Moch JK, *et al*. Binding of *Plasmodium* merozoite proteins RON2 and AMA1 triggers commitment to invasion. Proc Natl Acad Sci U S A. 2011 Aug 9;108(32):13275–80.

55. Yeoh S, O'Donnell RA, Koussis K, Dluzewski AR, Ansell KH, Osborne SA, *et al*. Subcellular Discharge of a Serine Protease Mediates Release of Invasive Malaria Parasites from Host Erythrocytes. Cell. 2007 Dec 14;131(6):1072–83.

56. Blackman MJ, Fujioka H, Stafford WHL, Sajid M, Clough B, Fleck SL, *et al*. A Subtilisin-like Protein in Secretory Organelles of *Plasmodium falciparum* Merozoites. J Biol Chem. 1998 Sep;273(36):23398–409.

57. Collins CR, Hackett F, Atid J, Tan MSY, Blackman MJ. The *Plasmodium falciparum* pseudoprotease SERA5 regulates the kinetics and efficiency of malaria parasite egress from host erythrocytes. Billker O, editor. PLOS Pathog. 2017 Jul 6;13(7):e1006453.

58. Mercier C, Adjogble KDZ, Däubener W, Delauw MFC. Dense granules: Are they key organelles to help understand the parasitophorous vacuole of all apicomplexa parasites? Int J Parasitol. 2005;35(8):829–49.

59. Torii M, Adams JH, Miller LH, Aikawa M. Release of Merozoite Dense Granules during Erythrocyte Invasion by *Plasmodium knowlesi*. Infect Immun. 1989;57(10):3230–3.

60. Aikawa M, Torii M, Sjolander A, Berzins K, Louis Millers AH. Pf155/RESA Antigen Is Localized in Dense Granules of *Plasmodium falciparum* Merozoites. Exp Parasitol. 1990;71(3):326–9.

61. Culvenor JG, Day KP, Anders RF, Mr E. *Plasmodium falciparum* Ring-Infected Erythrocyte Surface Antigen Is Released from Merozoite Dense Granules after Erythrocyte Invasion. Infection and Immunity. 1991 p. 1183–7.

62. Bannister LH, Butcher GA, Dennisf ED, Mitchellf GH. Structure and invasive behaviour of *Plasmodium knowlesi* merozoites in vitro. Parasitology. 1975;71:483–91.

63. Dubremetz JF, Dissous C. Characteristic Proteins of Micronemes and Dense Granules from *Sarcocystis tenella* Zoites (Protozoa, Coccidia). Mol Biochem Parasitol. 1980;1(5):279–89.

64. Trager W, Rozario C, Shio H, Williams J, Perkins ME. Transfer of a dense granule protein of *Plasmodium falciparum* to the membrane of ring stages and isolation of dense granules. Infect Immun. 1992 Nov;60(11):4656–61.

65. Etzion Z, Murray MC, Perkins ME. Isolation and characterization of rhoptries of *Plasmodium falciparum*. Mol Biochem Parasitol. 1991 Jul;47(1):51–61.

66. Griffith MB, Pearce CS, Heaslip AT. Dense granule biogenesis, secretion, and function in *Toxoplasma gondii*. J Eukaryot Microbiol. 69(6):e12904.

67. Sheffield HG, Melton LM. The Fine Structure and Reproduction of *Toxoplasma Gondii*. J Parasitol. 1968;54(2):209–26.

68. Carey KL, Donahue CG, Ward GE. Identification and molecular characterization of GRA8, a novel, proline-rich, dense granule protein of *Toxoplasma gondii*. Mol Biochem Parasitol. 2000 Jan 5;105(1):25–37.

69. Cesbron-Delauw MF, Guy B, Torpier G, Pierce RJ, Lenzen G, Cesbron JY, *et al*. Molecular characterization of a 23-kilodalton major antigen secreted by *Toxoplasma gondii*. Proc Natl Acad Sci. 1989 Oct;86(19):7537–41.

70. Leriche MA, Dubremetz JF. Characterization of the protein contents of rhoptries and dense granules of *Toxoplasma gondii* tachyzoites by subcellular fractionation and monoclonal antibodies. Mol Biochem Parasitol. 1991 Apr;45(2):249–59.

71. Bullen HE, Charnaud SC, Kalanon M, Riglar DT, Dekiwadia C, Kangwanrangsan N, *et al*. Biosynthesis, localization, and macromolecular arrangement of the *Plasmodium falciparum* translocon of exported proteins (PTEX). J Biol Chem. 2012 Mar 9;287(11):7871–84.

72. De Koning-Ward TF, Gilson PR, Boddey JA, Rug M, Smith BJ, Papenfuss AT, *et al*. A newly discovered protein export machine in malaria parasites. Nature. 2009 Jun 18;459(7249):945–9.

73. Ho CM, Beck JR, Lai M, Cui Y, Goldberg DE, Egea PF, *et al*. Malaria parasite translocon structure and mechanism of effector export. Nature. 2018 Sep 6;561(7721):70–5.

74. Garten M, Nasamu AS, Niles JC, Zimmerberg J, Goldberg DE, Beck JR. EXP2 is a nutrient-permeable channel in the vacuolar membrane of *Plasmodium* and is essential for protein export via PTEX. Nat Microbiol. 2018 Oct 1;3(10):1090–8.

75. Charnaud SC, Kumarasingha R, Bullen HE, Crabb BS, Gilsonid PR. Knockdown of the translocon protein EXP2 in *Plasmodium falciparum* reduces growth and protein export. 2018 Nov; 13(11):e0204785.

76. Iriko H, Ishino T, Otsuki H, Ito D, Tachibana M, Torii M, *et al*. *Plasmodium falciparum* Exported Protein 1 is localized to dense granules in merozoites. Parasitol Int. 2018 Oct 1;67(5):637–9.

77. Gunther K, Tijmmler M, Arnold HH, Ridley R, Goman M, Scaife JG, et al. An exported protein of *Plasmodium falciparum* is synthesized as an integral membrane protein. Mol Biochem Parasitol. 1991;46:149–58.

78. Simmons D, Woollett G, Bergin-Cartwright' M, Kay' D, Scaife J, Dunn W. A malaria protein exported into a new compartment within the host erythrocyte. Vol. 6, The EMBO Journal. 1987 p. 485–91.

79. Morita M, Takashima E, Ito D, Miura K, Thongkukiatkul A, Diouf A, *et al*. Immunoscreening of *Plasmodium falciparum* proteins expressed in a wheat germ cell-free system reveals a novel malaria vaccine candidate. Sci Rep. 2017 Apr 5;7.

80. Mesén-Ramírez P, Bergmann B, Tran TT, Garten M, Stäcker J, Naranjo-Prado I, *et al*. EXP1 is critical for nutrient uptake across the parasitophorous vacuole membrane of malaria parasites. PLoS Biol. 2019;17(9).

81. Morita M, Nagaoka H, Ntege EH, Kanoi BN, Ito D, Nakata T, *et al*. PV1, a novel *Plasmodium falciparum* merozoite dense granule protein, interacts with exported protein in infected erythrocytes. Sci Rep. 2018 Dec 1;8(1):1–11.

82. Miyazaki S, Chitama BYA, Kagaya W, Lucky AB, Zhu X, Yahata K, *et al*. *Plasmodium falciparum* SURFIN4.1 forms an intermediate complex with PTEX components and Pf113 during export to the red blood cell. Parasitol Int. 2021 Aug;83:102358.

83. Elsworth B, Matthews K, Nie CQ, Kalanon M, Charnaud SC, Sanders PR, *et al*. PTEX is an essential nexus for protein export in malaria parasites. Nature. 2014;511(7511):587–91.

84. Beck JR, Muralidharan V, Oksman A, Goldberg DE. PTEX component HSP101 mediates export of diverse malaria effectors into host erythrocytes. Nature. 2014;511(7511):592–5.

85. Chisholm SA, McHugh E, Lundie R, Dixon MWA, Ghosh S, O'Keefe M, *et al*. Contrasting inducible knockdown of the auxiliary PTEX component PTEX88 in *P. falciparum* and *P. berghei* unmasks a role in parasite virulence. PLoS ONE. 2016 Feb 1;11(2).

86. Diez-Silva M, Park Y, Huang S, Bow H, Mercereau-Puijalon O, Deplaine G, *et al*. Pf155/RESA protein influences the dynamic microcirculatory behaviour of ring-stage *Plasmodium falciparum* infected red blood cells. Sci Rep. 2012;2.

87. Pei X, Guo X, Coppel R, Bhattacharjee S, Haldar K, Gratzer W, *et al*. The ring-infected erythrocyte surface antigen (RESA) of *Plasmodium falciparum* stabilizes spectrin tetramers and suppresses further invasion. Blood. 2007 Aug 1;110(3):1036–42.

88. Silva MD, Cooke BM, Guillotte M, Buckingham DW, Sauzet JP, Le Scanf C, *et al*. A role for the *Plasmodium falciparum* RESA protein in resistance against heat shock demonstrated using gene disruption. Mol Microbiol. 2005 May;56(4):990–1003.

89. Da Silva E, Foley M, Dluzewski AR, Murray LJ, Anders RF, Tilley L. The *Plasmodium falciparum* protein RESA interacts with the erythrocyte cytoskeleton and modifies erythrocyte thermal stability. Mol Biochem Parasitol. 1994 Jul 1;66(1):59–69.

90. Aurrecoechea C, Brestelli J, Brunk BP, Dommer J, Fischer S, Gajria B. PlasmoDB: a functional genomic database for malaria parasites. Nucleai Acids Res. 2009;37:D539–43.

91. Matthews K, Kalanon M, Chisholm SA, Sturm A, Goodman CD, Dixon MWA, *et al*. The *Plasmodium* translocon of exported proteins (PTEX) component thioredoxin-2 is important for maintaining normal blood-stage growth: Characterization of PTEX in *P. berghei*. Mol Microbiol. 2013 Sep;89(6):1167–86.

92. Matz JM, Matuschewski K, Kooij TWA. Two putative protein export regulators promote *Plasmodium* blood stage development in vivo. Mol Biochem Parasitol. 2013 Sep;191(1):44–52.

93. Sanderson T. PhenoPlasm data dump: 2017-06-16. figshare; 2017 [cited 2023 Aug 29]. p. 578528 Bytes. Available from: https://figshare.com/articles/dataset/PhenoPlasm_All_Phenotypes_2017-06-16/5114017

94. Matz JM, Goosmann C, Brinkmann V, Grützke J, Ingmundson A, Matuschewski K, *et al*. The *Plasmodium berghei* translocon of exported proteins reveals spatiotemporal dynamics of tubular extensions. Sci Rep. 2015 Jul 29;5(1):12532.

95. Dou Z, McGovern OL, Di Cristina M, Carruthers VB. *Toxoplasma gondii* Ingests and Digests Host Cytosolic Proteins. Weiss LM, editor. mBio. 2014 Aug 29;5(4):e01188-14.

96. Rommereim LM, Bellini V, Fox BA, Pètre G, Rak C, Touquet B, *et al*. Phenotypes Associated with Knockouts of Eight Dense Granule Gene Loci (GRA2-9) in Virulent *Toxoplasma gondii*. Blader IJ, editor. PloS One. 2016 Jul 26;11(7):e0159306.

97. Guevara RB, Fox BA, Falla A, Bzik DJ. *Toxoplasma gondii* Intravacuolar-Network-Associated Dense Granule Proteins Regulate Maturation of the Cyst Matrix and Cyst Wall. Moreno SNJ, editor. mSphere. 2019 Oct 30;4(5):e00487-19.

98. Cesbron-Delauw MF, Gendrin G, Travier L, Ruffiot P, Mercier C. Apicomplexa in Mammalian Cells: Trafficking to the Parasitophorous Vacuole. Traffic. 2008;9(5):657–64.

99. Mercier C, Dubremetz JF, Rauscher B, Lecordier L, Sibley LD, Cesbron-Delauw MF. Biogenesis of Nanotubular Network in *Toxoplasma* Parasitophorous Vacuole Induced by Parasite Proteins. Lippincott-Schwartz J, editor. Mol Biol Cell. 2002 Jul;13(7):2397–409.

100. Travier L, Mondragon R, Dubremetz JF, Musset K, Mondragon M, Gonzalez S, *et al*. Functional domains of the *Toxoplasma* GRA2 protein in the formation of the membranous nanotubular network of the parasitophorous vacuole. Int J Parasitol. 2008 Jun;38(7):757–73.

101. Michelin A, Bittame A, Bordat Y, Travier L, Mercier C, Dubremetz JF, *et al*. GRA12, a *Toxoplasma* dense granule protein associated with the intravacuolar membranous nanotubular network. Int J Parasitol. 2009 Feb;39(3):299–306.

102. Nolan SJ, Romano JD, Coppens I. Host lipid droplets: An important source of lipids salvaged by the intracellular parasite *Toxoplasma gondii*. Billker O, editor. PLOS Pathog. 2017 Jun 1;13(6):e1006362.

103. Hu X, Binns D, Reese ML. The coccidian parasites *Toxoplasma* and *Neospora* dysregulate mammalian lipid droplet biogenesis. J Biol Chem. 2017 Jun;292(26):11009–20.

104. Gold DA, Kaplan AD, Lis A, Cl Bett G, Rosowski EE, Cirelli KM, *et al*. The *Toxoplasma* dense granule proteins GRA17 and GRA23 mediate the movement of small molecules between the host and the parasitophorous vacuole HHS Public Access. Cell Host Microbe. 2015;17(5):642–52.

105. Schwab JC, Beckers CJ, Joiner KA. The parasitophorous vacuole membrane surrounding intracellular *Toxoplasma gondii* functions as a molecular sieve. Proc Natl Acad Sci. 1994 Jan 18;91(2):509–13.

106. Bougdour A, Durandau E, Brenier-Pinchart MP, Ortet P, Barakat M, Kieffer S, *et al*. Host Cell Subversion by *Toxoplasma* GRA16, an Exported Dense Granule Protein that Targets the Host Cell Nucleus and Alters Gene Expression. Cell Host Microbe. 2013 Apr;13(4):489–500.

107. He H, Brenier-Pinchart MP, Braun L, Kraut A, Touquet B, Couté Y, *et al*. Characterization of a *Toxoplasma* effector uncovers an alternative GSK3/β-catenin-regulatory pathway of inflammation. eLife. 2018 Oct 15;7:e39887.

108. Braun L, Brenier-Pinchart MP, Yogavel M, Curt-Varesano A, Curt-Bertini RL, Hussain T, *et al*. A *Toxoplasma* dense granule protein, GRA24, modulates the early immune response to infection by promoting a direct and sustained host p38 MAPK activation. J Exp Med. 2013 Sep 23;210(10):2071–86.

109. Braun L, Brenier-Pinchart MP, Hammoudi PM, Cannella D, Kieffer-Jaquinod S, Vollaire J, *et al*. The *Toxoplasma* effector TEEGR promotes parasite persistence by modulating NF-κB signalling via EZH2. Nat Microbiol. 2019 Apr 29;4(7):1208–20.

110. Panas MW, Ferrel A, Naor A, Tenborg E, Lorenzi HA, Boothroyd JC. Translocation of Dense Granule Effectors across the Parasitophorous Vacuole Membrane in *Toxoplasma*-Infected Cells Requires the Activity of ROP17, a Rhoptry Protein Kinase. Sullivan WJ, editor. mSphere. 2019 Aug 28;4(4):e00276-19.

111. Gay G, Braun L, Brenier-Pinchart MP, Vollaire J, Josserand V, Bertini RL, *et al*. *Toxoplasma gondii* TgIST co-opts host chromatin repressors dampening STAT1-dependent gene regulation and IFN-γ–mediated host defenses. J Exp Med. 2016 Aug 22;213(9):1779–98.

112. Marino ND, Panas MW, Franco M, Theisen TC, Naor A, Rastogi S, *et al*. Identification of a novel protein complex essential for effector translocation across the parasitophorous vacuole membrane of *Toxoplasma gondii*. Coppens I, editor. PLOS Pathog. 2018 Jan 22;14(1):e1006828.

113. Blakely WJ, Holmes MJ, Arrizabalaga G. The Secreted Acid Phosphatase Domain-Containing GRA44 from *Toxoplasma gondii* Is Required for c-Myc Induction in Infected Cells. 2020;5(1).

114. Cygan AM, Theisen TC, Mendoza AG, Marino ND, Panas MW, Boothroyd JC. Coimmunoprecipitation with MYR1 Identifies Three Additional Proteins within the *Toxoplasma gondii* Parasitophorous Vacuole Required for Translocation of Dense Granule Effectors into Host Cells. Mitchell AP, editor. mSphere. 2020 Feb 26;5(1):e00858-19.

115. Mayoral J, Shamamian P, Weiss LM. *In Vitro* Characterization of Protein Effector Export in the Bradyzoite Stage of *Toxoplasma gondii*. Boothroyd JC, editor. mBio. 2020 Apr 28;11(2):e00046-20.

116. Wang Y, Sangaré LO, Paredes-Santos TC, Saeij JPJ. *Toxoplasma* Mechanisms for Delivery of Proteins and Uptake of Nutrients Across the Host-Pathogen Interface. Annu Rev Microbiol. 2020;74:567–86.

117. Rosowski EE, Lu D, Julien L, Rodda L, Gaiser RA, Jensen KDC, *et al*. Strain-specific activation of the NF-κB pathway by GRA15, a novel *Toxoplasma gondii* dense granule protein. J Exp Med. 2011 Jan 17;208(1):195–212.

118. Joshi A, Palsson BO. Metabolic dynamics in the human red cell: Part I—A comprehensive kinetic model. J Theor Biol. 1989;141(4):515–28.

119. Heiber A, Kruse F, Pick C, Grüring C, Flemming S, Oberli A, *et al*. Identification of New PNEPs Indicates a Substantial Non-PEXEL Exportome and Underpins Common Features in *Plasmodium falciparum* Protein Export. Przyborski JM, editor. PLoS Pathog. 2013 Aug 8;9(8):e1003546.

120. Hiller NL, Bhattacharjee S, Van Ooij C, Liolios K, Harrison T, Lopez-Estraño C, *et al*. A Host-Targeting Signal in Virulence Proteins Reveals a Secretome in Malarial Infection. Science. 2004 Dec 10;306(5703):1934–7.

121. Marti M, Good RT, Rug M, Knuepfer E, Cowman AF. Targeting Malaria Virulence and Remodelling Proteins to the Host Erythrocyte. Science. 2004 Dec 10;306(5703):1930–3.

122. Sargeant TJ, Marti M, Caler E, Carlton JM, Simpson K, Speed TP, *et al*. Lineage-specific expansion of proteins exported to erythrocytes in malaria parasites. Genome Biol. 2006 Feb 20;7(2).

123. Van Ooij C, Tamez P, Bhattacharjee S, Hiller NL, Harrison T, Liolios K, *et al*. The Malaria Secretome: From Algorithms to Essential Function in Blood Stage Infection. PLoS Pathog. 2008;4(6):e1000084.

124. Boddey JA, Carvalho TG, Hodder AN, Sargeant TJ, Sleebs BE, Marapana D, *et al*. Role of Plasmepsin V in Export of Diverse Protein Families from the *Plasmodium falciparum* Exportome. Traffic. 2013 May;14(5):532–50.

125. Schulze J, Kwiatkowski M, Borner J, Schlüter H, Bruchhaus I, Burmester T, *et al*. The *Plasmodium falciparum* exportome contains non-canonical PEXEL/HT proteins: PEXEL/HT plasticity. Mol Microbiol. 2015 Jul;97(2):301–14.

126. Matthews KM, Pitman EL, Koning-Ward TF. Illuminating how malaria parasites export proteins into host erythrocytes. Cell Microbiol. 2019 Apr [cited 2023 Aug 25];21(4). Available from: https://onlinelibrary.wiley.com/doi/10.1111/cmi.13009

127. Behl A, Kumar V, Bisht A, Panda JJ, Hora R, Mishra PC. Cholesterol bound *Plasmodium falciparum* co-chaperone 'PFA0660w' complexes with major virulence factor 'PfEMP1' via chaperone 'PfHsp70-x.' Sci Rep. 2019 Dec 1;9(1).

128. Gabriela M, Matthews KM, Boshoven C, Kouskousis B, Jonsdottir TK, Bullen HE, *et al*. A revised mechanism for how *Plasmodium falciparum* recruits and exports proteins into its erythrocytic host cell. Blackman MJ, editor. PLOS Pathog. 2022 Feb 22;18(2):e1009977.

129. Almaazmi SY, Kaur RP, Singh H, Blatch GL. The *Plasmodium falciparum* exported J domain proteins fine-tune human and malarial Hsp70s: pathological exploitation of proteostasis machinery. Front Mol Biosci. 2023 Jun 30;10:1216192.

130. Bhattacharjee S, Van Ooij C, Balu B, Adams JH, Haldar K. Maurer's clefts of *Plasmodium falciparum* are secretory organelles that concentrate virulence protein reporters for delivery to the host erythrocyte. Blood. 2008 Feb 15;111(4):2418–26.

131. Lanzer M, Wickert H, Krohne G, Vincensini L, Braun Breton C. Maurer's clefts: A novel multi-functional organelle in the cytoplasm of *Plasmodium falciparum*-infected erythrocytes. Int J Parasitol. 2006 Jan 1;36(1):23–36.

132. Spycher C, Rug M, Klonis N, Ferguson DJP, Cowman AF, Beck HP, *et al*. Genesis of and Trafficking to the Maurer's Clefts of *Plasmodium falciparum*-Infected Erythrocytes †. Mol Cell Biol. 2006;26(11):4074–85.

133. Cooke M, Lingelbach K, Bannister LH, Tilley L. Protein trafficking in *Plasmodium falciparum*-infected red blood cells. Trends Parasitol. 2004;20(12):581–9.

134. Tonkin CJ, Pearce JA, McFadden GI, Cowman AF. Protein targeting to destinations of the secretory pathway in the malaria parasite *Plasmodium falciparum*. Curr Opin Microbiol. 2006 Aug;9(4):381–7.

135. Adisa A, Rug M, Klonis N, Foley M, Cowman AF, Tilley L. The Signal Sequence of Exported Protein-1 Directs the Green Fluorescent Protein to the Parasitophorous Vacuole of Transfected Malaria Parasites. J Biol Chem. 2003 Feb;278(8):6532–42.

136. Chang HH, Falick AM, Carlton PM, Sedat JW, Derisi JL, Marletta MA, *et al*. N-terminal processing of proteins exported by malaria parasites NIH Public Access Author Manuscript. Mol Biochem Parasitol. 2008;160(2):107–15.

137. Boddey JA, Hodder AN, Günther S, Gilson PR, Patsiouras H, Kapp EA, *et al*. An aspartyl protease directs malaria effector proteins to the host cell. Nature. 2010;463:pages627-631.

138. Russo I, Babbitt S, Muralidharan V, Butler T, Oksman A, Goldberg DE. Plasmepsin v licenses *Plasmodium* proteins for export into the host erythrocyte. Nature. 2010 Feb 4;463(7281):632–6.

139. Osborne AR, Speicher KD, Tamez PA, Bhattacharjee S, Speicher DW, Haldar K. The host targeting motif in exported *Plasmodium* proteins is cleaved in the parasite endoplasmic reticulum. Mol Biochem Parasitol. 2010 May;171(1):25–31.

140. Coffey MJ, Dagley LF, Seizova S, Kapp EA, Infusini G, Roos DS, *et al*. Aspartyl Protease 5 Matures Dense Granule Proteins That Reside at the Host-Parasite Interface in *Toxoplasma gondii*. Sibley LD, editor. mBio. 2018 Nov 7;9(5):e01796-18.

141. Boddey JA, Moritz RL, Simpson RJ, Cowman AF. Role of the *Plasmodium* export element in trafficking parasite proteins to the infected erythrocyte. Traffic. 2009;10(3):285–99.

142. Tarr SJ, Cryar A, Thalassinos K, Haldar K, Osborne AR. The C -terminal portion of the cleaved HT motif is necessary and sufficient to mediate export of proteins from the malaria parasite into its host cell. Mol Microbiol. 2013 Feb;87(4):835–50.

143. Hasan MM, Polino AJ, Mukherjee S, Vaupel B, Goldberg DE. The mature N-termini of *Plasmodium* effector proteins confer specificity of export. Miller LH, editor. mBio. 2023 Oct 31;14(5):e01215-23.

144. Grüring C, Heiber A, Kruse F, Flemming S, Franci G, Colombo SF, *et al*. Uncovering Common Principles in Protein Export of Malaria Parasites. Cell Host Microbe. 2012 Nov;12(5):717–29.

145. Rug M, Wickham ME, Foley M, Cowman AF, Tilley L. Correct promoter control is needed for trafficking of the ring-infected erythrocyte surface antigen to the host cytosol in transfected malaria parasites. Infect Immun. 2004 Oct;72(10):6095–105.

146. Fierro MA, Muheljic A, Sha J, Wohlschlegel JA, Beck JR. PEXEL is a proteolytic maturation site for both exported and non-exported *Plasmodium* proteins. Microbiology; 2023 Jul.

147. Ressurreição M, Fréville A, Van Ooij C. Identification of a non-exported Plasmepsin V substrate that functions in the parasitophorous vacuole of malaria parasites. Microbiology; 2023 May.

148. Peng M, Cascio D, Egea PF. Crystal structure and solution characterization of the thioredoxin-2 from Plasmodium falciparum, a constituent of an essential parasitic protein export complex. Biochem Biophys Res Commun. 2015 Jan 2;456(1):403–9.

149. Batinovic S, McHugh E, Chisholm SA, Matthews K, Liu B, Dumont L, *et al*. An exported protein-interacting complex involved in the trafficking of virulence determinants in *Plasmodium*-infected erythrocytes. Nat Commun. 2017 Jul 10;8(1):16044.

150. Elsworth B, Sanders PR, Nebl T, Batinovic S, Kalanon M, Nie CQ, *et al*. Proteomic analysis reveals novel proteins associated with the *Plasmodium* protein exporter PTEX and a loss of complex stability upon truncation of the core PTEX component, PTEX150: Proteomic analysis reveals novel PTEX proteins. Cell Microbiol. 2016 Nov;18(11):1551–69.

151. Mesén-Ramírez P, Reinsch F, Blancke Soares A, Bergmann B, Ullrich AK, Tenzer S, *et al*. Stable Translocation Intermediates Jam Global Protein Export in *Plasmodium falciparum* Parasites and Link the PTEX Component EXP2 with Translocation Activity. Soldati-Favre D, editor. PLOS Pathog. 2016 May 11;12(5):e1005618.

152. Bullen HE, Sanders PR, Dans MG, Jonsdottir TK, Riglar DT, Looker O, *et al*. The *Plasmodium falciparum* parasitophorous vacuole protein P113 interacts with the parasite protein export machinery and maintains normal vacuole architecture. Mol Microbiol. 2022 May;117(5):1245–62.

153. El Bakkouri M, Pow A, Mulichak A, Cheung KLY, Artz JD, Amani M, *et al*. The Clp chaperones and proteases of the human malaria parasite *Plasmodium falciparum*. J Mol Biol. 2010 Dec 3;404(3):456–77.

154. Crabb BS, De Koning-Ward TF, Gilson PR. Protein export in *Plasmodium* parasites: From the endoplasmic reticulum to the vacuolar export machine. Int J Parasitol. 2010 Apr;40(5):509–13.

155. Hakamada K, Nakamura M, Midorikawa R, Shinohara K, Noguchi K, Nagaoka H, *et al*. PV1 Protein from *Plasmodium falciparum* Exhibits Chaperone-Like Functions and Cooperates with Hsp100s. Int J Mol Sci. 2020 Nov 16;21(22):8616.

156. Przyborski JM, Nyboer B, Lanzer M. Ticket to ride: export of proteins to the *Plasmodium falciparum*-infected erythrocyte. Mol Microbiol. 2016 Jul 1;101(1):1–11.

157. Baruch DI, Pasloske L, Singh B, Ma XC, Taraschi F, Howard' J. Cloning the *P. falciparum* Gene Encoding PfEMPl, a Malarial Variant Antigen and Adherence Receptor on the Surface of Parasitized Human Erythrocytes. Cell. 1995;82(1):77–87.

158. Baruch DI, Ma XC, Singh HB, Bi X, Pasloske BL, Howard RJ. Identification of a Region of PfEMP1 That Mediates Adherence of *Plasmodium falciparum* Infected Erythrocytes to CD36: Conserved Function With Variant Sequence. Blood. 1997 Nov 1;90(9):3766–75.

159. Smith JD, Chitnis CE, Craig AG, Roberts DJ, Hudson-Taylor DE, Peterson DS, *et al*. Switches in expression of *Plasmodium falciparum* var genes correlate with changes in antigenic and cytoadherent phenotypes of infected erythrocytes. Cell. 1995 Jul;82(1):101–10.

160. Chen Q, Barragan A, Fernandez V, Sundström A, Schlichtherle M, Sahlén A, *et al*. Identification of *Plasmodium falciparum* Erythrocyte Membrane Protein 1 (PfEMP1) as the Rosetting Ligand of the Malaria Parasite *P. falciparum*. J Exp Med. 1998 Jan 5;187(1):15–23.

161. Guizetti J, Scherf A. Silence, activate, poise and switch! Mechanisms of antigenic variation in *P lasmodium falciparum* . Cell Microbiol. 2013 May;15(5):718–26.

162. Su X, Heatwoie M, Wertheimer P, Hertfeldt A, Peterson DS, Ravetch A. The Large Diverse Gene Family w Encodes Proteins Involved in Cytoadherence and Antigenic Variation of *Plasmodium falciparum*-Infected Erythrocytes. Cell. 1995;82(1):89–100.

163. Roberts DJ, Biggs BA, Brown G, Newbold CI. Protection, pathogenesis and phenotypic plasticity in *Plasmodium falciparum* malaria. Parasitol Today. 1993 Aug;9(8):281–6.

164. Glenister FK, Coppel RL, Cowman AF, Mohandas N, Cooke BM. Contribution of parasite proteins to altered mechanical properties of malaria-infected red blood cells. Blood. 2002 Feb 1;99(3):1060–3.

165. Rug M, Prescott SW, Fernandez KM, Cooke BM, Cowman AF. The role of KAHRP domains in knob formation and cytoadherence of *P falciparum*-infected human erythrocytes. Blood. 2006 Jul 1;108(1):370–8.

166. Looker O, Blanch AJ, Liu B, Nunez-Iglesias J, McMillan PJ, Tilley L, *et al*. The knob protein KAHRP assembles into a ring-shaped structure that underpins virulence complex assembly. Blackman MJ, editor. PLOS Pathog. 2019 May 9;15(5):e1007761.

167. Pasloske BL, Baruch DI, Van Schravendlijk MR, Handunnetti SM, Aikawa M, Fujioka H, *et al*. Cloning and characterization of a *Plasmodium falciparum* gene encoding a novel high-molecular weight host membrane-associated protein, PfEMP3. Mol Biochem Parasitol. 1993 May;59(1):59–72.

168. Waterkeyn JG. Targeted mutagenesis of *Plasmodium falciparum* erythrocyte membrane protein 3 (PfEMP3) disrupts cytoadherence of malaria-infected red blood cells. EMBO J. 2000 Jun 15;19(12):2813–23.

169. Waller KL, Stubberfield LM, Dubljevic V, Nunomura W, An X, Mason AJ, *et al*. Interactions of *Plasmodium falciparum* erythrocyte membrane protein 3 with the red blood cell membrane skeleton. Biochim Biophys Acta BBA - Biomembr. 2007 Sep;1768(9):2145–56.

170. Blisnick T, Morales Betoulle ME, Barale JC, Uzureau P, Berry L, Desroses S, *et al*. Pfsbp1, a Maurer's cleft *Plasmodium falciparum* protein, is associated with the erythrocyte skeleton. Mol Biochem Parasitol. 2000 Nov;111(1):107–21.

171. Blisnick T, Vincensini L, Barale JC, Namane A, Braun Breton C. LANCL1, an erythrocyte protein recruited to the Maurer's clefts during *Plasmodium falciparum* development. Mol Biochem Parasitol. 2005 May;141(1):39–47.

172. Cooke BM, Buckingham DW, Glenister FK, Fernandez KM, Bannister LH, Marti M, *et al.* A Maurer's cleft–associated protein is essential for expression of the major malaria virulence antigen on the surface of infected red blood cells. J Cell Biol. 2006 Mar 13;172(6):899–908.

173. Maier AG, Rug M, O'Neill MT, Brown M, Chakravorty S, Szestak T, *et al*. Exported Proteins Required for Virulence and Rigidity of *Plasmodium falciparum*-Infected Human Erythrocytes. Cell. 2008 Jul 11;134(1):48–61.

174. Spycher C, Klonis N, Spielmann T, Kump E, Steiger S, Tilley L, *et al*. MAHRP-1, a Novel *Plasmodium falciparum* Histidine-rich Protein, Binds Ferriprotoporphyrin IX and Localizes to the Maurer's Clefts. J Biol Chem. 2003 Sep;278(37):35373–83.

175. Spycher C, Rug M, Pachlatko E, Hanssen E, Ferguson D, Cowman AF, *et al*. The Maurer's cleft protein MAHRP1 is essential for trafficking of PfEMP1 to the surface of *Plasmodium falciparum*-infected erythrocytes. Mol Microbiol. 2008 Jun;68(5):1300–14.

176. Hawthorne PL, Trenholme KR, Skinner-Adams TS, Spielmann T, Fischer K, Dixon MWA, *et al*. A novel *Plasmodium falciparum* ring stage protein, REX, is located in Maurer's clefts. Mol Biochem Parasitol. 2004 Aug;136(2):181–9.

177. Spielmann T, Gardiner DL, Beck HP, Trenholme KR, Kemp DJ. Organization of ETRAMPs and EXP-1 at the parasite-host cell interface of malaria parasites. Mol Microbiol. 2006 Feb;59(3):779–94.

178. Dixon MWA, Hawthorne PL, Spielmann T, Anderson KL, Trenholme KR, Gardiner DL. Targeting of the Ring Exported Protein 1 to the Maurers Clefts is Mediated by a Two-Phase Process. Traffic. 2008 Aug;9(8):1316–26.

179. Hanssen E, Hawthorne P, Dixon MWA, Trenholme KR, McMillan PJ, Spielmann T, *et al.* Targeted mutagenesis of the ring-exported protein-1 of *Plasmodium falciparum* disrupts the architecture of Maurer's cleft organelles. Mol Microbiol. 2008 Aug;69(4):938–53.

180. Cheng Q, Cloonan N, Fischer K, Thompson J, Waine G, Lanzer M, *et al*. stevor and rif are *Plasmodium falciparum* multicopy gene families which potentially encode variant antigens. Mol Biochem Parasitol. 1998;

181. Joannin N, Abhiman S, Sonnhammer EL, Wahlgren M. Sub-grouping and sub-functionalization of the RIFIN multi-copy protein family. BMC Genomics. 2008 Dec;9(1):19.

182. Petter M, Haeggström M, Khattab A, Fernandez V, Klinkert MQ, Wahlgren M. Variant proteins of the *Plasmodium falciparum* RIFIN family show distinct subcellular localization and developmental expression patterns. Mol Biochem Parasitol. 2007 Nov;156(1):51–61.

183. Bachmann A, Petter M, Tilly AK, Biller L, Uliczka KA, Duffy MF, *et al*. Temporal Expression and Localization Patterns of Variant Surface Antigens in Clinical *Plasmodium falciparum* Isolates during Erythrocyte Schizogony. Hviid L, editor. PLoS ONE. 2012 Nov 15;7(11):e49540.

184. Sakoguchi A, Saito F, Hirayasu K, Shida K, Matsuoka S, Itagaki S, *et al*. *Plasmodium falciparum* RIFIN is a novel ligand for inhibitory immune receptor LILRB2. Biochem Biophys Res Commun. 2021 Apr;548:167–73.

185. Saito F, Hirayasu K, Satoh T, Wang CW, Lusingu J, Arimori T, *et al.* Immune evasion of *Plasmodium falciparum* by RIFIN via inhibitory receptors. Nature. 2017 Dec 7;552(7683):101–5.

186. Xie Y, Li X, Chai Y, Song H, Qi J, Gao GF. Structural basis of malarial parasite RIFIN-mediated immune escape against LAIR1. Cell Rep. 2021 Aug;36(8):109600.

187. Khattab A, Bonow I, Schreiber N, Petter M, Schmetz C, Klinkert MQ. *Plasmodium falciparum* variant STEVOR antigens are expressed in merozoites and possibly associated with erythrocyte invasion. Malar J. 2008 Dec;7(1):137.

188. Sanyal S, Egée S, Bouyer G, Perrot S, Safeukui I, Bischoff E, *et al. Plasmodium falciparum* STEVOR proteins impact erythrocyte mechanical properties. Blood. 2012 Jan 12;119(2):e1–8.

189. Niang M, Bei AK, Madnani KG, Pelly S, Dankwa S, Kanjee U, *et al*. STEVOR Is a *Plasmodium falciparum* Erythrocyte Binding Protein that Mediates Merozoite Invasion and Rosetting. Cell Host Microbe. 2014 Jul;16(1):81–93.

190. Frech C, Chen N. Variant surface antigens of malaria parasites: functional and evolutionary insights from comparative gene family classification and analysis. BMC Genomics. 2013;14(1):427.

191. Shi J, Blundell TL, Mizuguchi K. FUGUE: sequence-structure homology recognition using environment-specific substitution tables and structure-dependent gap penalties11Edited by B. Honig. J Mol Biol. 2001 Jun;310(1):243–57.

192. Oberli A, Slater LM, Cutts E, Brand F, Mundwiler-Pachlatko E, Rusch S, *et al*. A *Plasmodium falciparum* PHIST protein binds the virulence factor PfEMP1 and comigrates to knobs on the host cell surface. FASEB J. 2014 Oct;28(10):4420–33.

193. Yang B, Wang X, Jiang N, Sang X, Feng Y, Chen R, *et al*. Interaction Analysis of a *Plasmodium falciparum* PHISTa-like Protein and PfEMP1 Proteins. Front Microbiol. 2020 Nov 13;11:611190.

194. Tarr SJ, Moon RW, Hardege I, Osborne AR. A conserved domain targets exported PHISTb family proteins to the periphery of *Plasmodium* infected erythrocytes. Mol Biochem Parasitol. 2014;196(1):29–40.

195. Silvestrini F, Lasonder E, Olivieri A, Camarda G, Van Schaijk B, Sanchez M, *et al*. Protein export marks the early phase of gametocytogenesis of the human malaria parasite *Plasmodium falciparum*. Mol Cell Proteomics. 2010;9(7):1437–48.

196. Eksi S, Haile Y, Furuya T, Ma L, Su X, Williamson KC. Identification of a subtelomeric gene family expressed during the asexual–sexual stage transition in *Plasmodium falciparum*. Mol Biochem Parasitol. 2005 Sep;143(1):90–9.

197. Davies H, Belda H, Broncel M, Ye X, Bisson C, Introini V, *et al*. An exported kinase family mediates species-specific erythrocyte remodelling and virulence in human malaria. Nat Microbiol. 2020;

198. Nunes MC, Okada M, Scheidig-Benatar C, Cooke BM, Scherf A. *Plasmodium falciparum* FIKK Kinase Members Target Distinct Components of the Erythrocyte Membrane. Nielsen K, editor. PLoS ONE. 2010 Jul 23;5(7):e11747.

199. Schneider AG, Mercereau-Puijalon O. A new Apicomplexa-specific protein kinase family: Multiple members in *Plasmodium falciparum*, all with an export signature. BMC Genomics. 2005 Mar 7;6.

200. Coffey MJ, Sleebs BE, Uboldi AD, Garnham A, Franco M, Marino ND, *et al*. An aspartyl protease defines a novel pathway for export of *Toxoplasma* proteins into the host cell. eLife. 2015 Nov 18;4:e10809.

201. Lin J wen, Spaccapelo R, Schwarzer E, Sajid M, Annoura T, Deroost K, *et al.* Replication of *Plasmodium* in reticulocytes can occur without hemozoin formation, resulting in chloroquine resistance. J Exp Med. 2015 Jun 1;212(6):893–903.

202. Liu J, Istvan ES, Gluzman IY, Gross J, Goldberg DE. *Plasmodium falciparum* ensures its amino acid supply with multiple acquisition pathways and redundant proteolytic enzyme systems. Proc Natl Acad Sci. 2006 Jun 6;103(23):8840–5.

203. Krugliak M, Zhang J, Ginsburg H. Intraerythrocytic *Plasmodium falciparum* utilizes only a fraction of the amino acids derived from the digestion of host cell cytosol for the biosynthesis of its proteins. Mol Biochem Parasitol. 2002;119(2):249–56.

204. Lew VL, Macdonald L, Ginsburg H, Krugliak M, Tiffert T. Excess haemoglobin digestion by malaria parasites: a strategy to prevent premature host cell lysis. Blood Cells Mol Dis. 2004 May;32(3):353–9.

205. Pretini V, Koenen MH, Kaestner L, Fens MHAM, Schiffelers RM, Bartels M, *et al*. Red Blood Cells: Chasing Interactions. Front Physiol. 2019 Jul 31;10:945.

206. Martin RE. The transportome of the malaria parasite. Biol Rev. 2020 Apr;95(2):305–32.

207. Ginsburg H, Kutner S, Krugliak M, Ioav Cabantchik Z. Characterization of permeation pathways appearing in the host membrane of *Plasmodium falciparum* infected red blood cells. Mol Biochem Parasitol. 1985;14:313–22.

208. Desai SA, Krogstad DJ, McCleskey EW. A nutrient-permeable channel on the intraerythrocytic malaria parasite. Nature. 1993;362(6421):643–6.

209. Counihan NA, Modak JK, de Koning-Ward TF. How Malaria Parasites Acquire Nutrients From Their Host. Front Cell Dev Biol. 2021 Mar 25;9.

210. Nguitragool W, Bokhari AAB, Pillai AD, Rayavara K, Sharma P, Turpin B, *et al*. Malaria Parasite clag3 Genes Determine Channel-Mediated Nutrient Uptake by Infected Red Blood Cells. Cell. 2011 May;145(5):665–77.

211. Nguitragool W, Rayavara K, Desai SA. Proteolysis at a Specific Extracellular Residue Implicates Integral Membrane CLAG3 in Malaria Parasite Nutrient Channels. Snounou G, editor. PLoS One. 2014 Apr 3;9(4):e93759.

212. Pillai AD, Nguitragool W, Lyko B, Dolinta K, Butler MM, Nguyen ST, *et al*. Solute Restriction Reveals an Essential Role for *clag3* -Associated Channels in Malaria Parasite Nutrient Acquisition. Mol Pharmacol. 2012 Dec;82(6):1104–14.

213. Gupta A, Balabaskaran-Nina P, Nguitragool W, Saggu GS, Schureck MA, Desai SA. CLAG3 Self-Associates in Malaria Parasites and Quantitatively Determines Nutrient Uptake Channels at the Host Membrane. Sibley LD, editor. mBio. 2018 Jul 5;9(3):e02293-17.

214. Comeaux CA, Coleman BI, Bei AK, Whitehurst N, Duraisingh MT. Functional analysis of epigenetic regulation of tandem RhopH1/clag genes reveals a role in *Plasmodium falciparum* growth: P. falciparum RhopH1 paralogue expression. Mol Microbiol. 2011 Apr;80(2):378–90.

215. Mira-Martínez S, Rovira-Graells N, Crowley VM, Altenhofen LM, Llinás M, Cortés A. Epigenetic switches in *clag3* genes mediate blasticidin S resistance in malaria parasites: *P. falciparum* transcription and solute uptake. Cell Microbiol. 2013 Aug;n/a-n/a.

216. Sharma P, Rayavara K, Ito D, Basore K, Desai SA. A CLAG3 Mutation in an Amphipathic Transmembrane Domain Alters Malaria Parasite Nutrient Channels and Confers Leupeptin Resistance. Adams JH, editor. Infect Immun. 2015 Jun;83(6):2566–74.

217. Kaneko O, Lim BYSY, Iriko H, Ling IT, Otsuki H, Grainger M, *et al*. Apical expression of three RhopH1/Clag proteins as components of the *Plasmodium falciparum* RhopH complex. Mol Biochem Parasitol. 2005 Sep;143(1):20–8.

218. Gupta A, Thiruvengadam G, Desai SA. The conserved clag multigene family of malaria parasites: Essential roles in host–pathogen interaction. Drug Resist Updat. 2015 Jan;18:47–54.

219. Ito D, Schureck MA, Desai SA. An essential dual-function complex mediates erythrocyte invasion and channel-mediated nutrient uptake in malaria parasites. eLife. 2017 Feb 21;6:e23485.

220. Schureck MA, Darling JE, Merk A, Shao J, Daggupati G, Srinivasan P, *et al*. Malaria parasites use a soluble RhopH complex for erythrocyte invasion and an integral form for nutrient uptake. eLife. 2021 Jan 4;10:e65282.

221. Sam-Yellowe TY, Shio H, Perkins ME. Secretion of *Plasmodium falciparum* rhoptry protein into the plasma membrane of host erythrocytes. J Cell Biol. 1988 May 1;106(5):1507–13.

222. Counihan NA, Chisholm SA, Bullen HE, Srivastava A, Sanders PR, Jonsdottir TK, *et al*. *Plasmodium falciparum* parasites deploy RhopH2 into the host erythrocyte to obtain nutrients, grow and replicate. eLife. 2017 Mar 2;6.

223. Sherling ES, Knuepfer E, Brzostowski JA, Miller LH, Blackman MJ, Van Ooij C. The *Plasmodium falciparum* rhoptry protein RhopH3 plays essential roles in host cell invasion and nutrient uptake. eLife. 2017 Mar 2;6.

224. Cowman AF, Baldi DL, Healer J, Mills KE, O'Donnell RA, Reed MB, *et al*. Functional analysis of proteins involved in *Plasmodium falciparum* merozoite invasion of red blood cells. FEBS Lett. 2000 Jun 30;476(1–2):84–8.

225. Janse CJ, Kroeze H, van Wigcheren A, Franke-Fayard B, Waters A, M. Khan S. A genotype and phenotype database of genetically modified malaria-parasites. Trends Parasitol. 2011;27(1):31–9.

226. Zhang M, Wang C, Otto TD, Oberstaller J, Liao X, Adapa SR, *et al*. Uncovering the essential genes of the human malaria parasite *Plasmodium falciparum* by saturation mutagenesis. Science. 2018 May 4;360(6388):eaap7847.

227. Desai SA, Rosenberg RL. Pore size of the malaria parasite's nutrient channel. Proc Natl Acad Sci. 1997 Mar 4;94(5):2045–9.

228. Milani KJ, Schneider TG, Taraschi TF. Defining the morphology and mechanism of the hemoglobin transport pathway in *Plasmodium falciparum*-infected erythrocytes. Eukaryot Cell. 2015;14(4):415–26.

229. Liu B, Blanch AJ, Namvar A, Carmo O, Tiash S, Andrew D, *et al*. Multimodal analysis of *Plasmodium knowlesi*-infected erythrocytes reveals large invaginations, swelling of the host cell, and rheological defects. Cell Microbiol. 2019 May 1;21(5).

230. Klemba M, Beatty W, Gluzman I, Goldberg DE. Trafficking of plasmepsin II to the food vacuole of the malaria parasite *Plasmodium falciparum*. J Cell Biol. 2004 Jan;164(1):47–56.

231. Birnbaum J, Scharf S, Schmidt S, Jonscher E, Hoeijmakers WAM, Flemming S, *et al*. A Kelch13-defined endocytosis pathway mediates artemisinin resistance in malaria parasites. Science. 2020 Jan 3;367(6473):51–9.

232. Spielmann T, Gras S, Sabitzki R, Meissner M. Endocytosis in *Plasmodium* and *Toxoplasma Parasites*. Trends Parasitol. 2020 Jun 1;36(6):520–32.

233. Bakar NA, Klonis N, Hanssen E, Chan C, Tilley L. Digestive-vacuole genesis and endocytic processes in the early intraerythrocytic stages of *Plasmodium falciparum*. J Cell Sci. 2010 Feb 1;123(3):441–50.

234. Goldberg DE. Hemoglobin degradation. Curr Trop Microbiol Immunol. 2005;295:275–91.

235. Sherman IW. Amino acid metabolism and protein synthesis in malarial parasites. Vol. 55, Bulletin of the World Health Organization. 1977 p. 265–76.

236. Hanssen E, Knoechel C, Dearnley M, Dixon MWA, Le Gros M, Larabell C, *et al*. Soft X-ray microscopy analysis of cell volume and hemoglobin content in erythrocytes infected with asexual and sexual stages of *Plasmodium falciparum*. J Struct Biol. 2012 Feb;177(2):224–32.

237. Aikawa M, Miller LH, Johnson J, Rabbege J. Erythrocyte Entry by Malarial Parasites. A Moving Junction Between Erythrocyte and Parasite. J Cell Biol. 1978;77:72–82.

238. Pouvelle B, Gormley JA, Taraschi TF. Characterization of trafficking pathways and membrane genesis in malaria-infected erythrocytes. Mol Biochem Parasitol. 1994 Jul;66(1):83–96.

239. Haldar K, Uyetake L. The movement of fluorescent endocytic tracers in *Plasmodium falciparum* infected erythrocytes. Mol Biochem Parasitol. 1992 Jan;50(1):161–77.

240. Ward GE, Miller LH, Dvorak JA. The origin of parasitophorous vacuole membrane lipids in malaria-infected erythrocytes. J Cell Sci. 1993 Sep 1;106(1):237–48.

241. Dluzewski AR, Mitchell GH, Fryer PR, Griffiths S, Wilson RJM, Gratzer WB. Origins of the parasitophorous vacuole membrane of the malaria parasite, *Plasmodium falciparum* , in human red blood cells. J Cell Sci. 1992 Jul 1;102(3):527–32.

242. Mikkelsen RB, Kamber M, Wadwat KS, Lin PS, Schmidt-Ullrich R. The role of lipids in *Plasmodium falciparum* invasion of erythrocytes: A coordinated biochemical and microscopic analysis. PNAS. 1988;85(16):5956–60.

243. Vallintine T, Van Ooij C. Distribution of malaria parasite-derived phosphatidylcholine in the infected erythrocyte. mSphere. 2023 Aug 22;e0013123.

244. Bannister LH, Mitchell GH, Butcher GA, Dennis ED. Lamellar membranes associated with rhoptries in erythrocytic merozoites of *Plasmodium knowlesi* : a clue to the mechanism of invasion. Parasitology. 1986 Apr;92(2):291–303.

245. Hanssen E, Dekiwadia C, Riglar DT, Rug M, Lemgruber L, Cowman AF, *et al*. Electron tomography of *Plasmodium falciparum* merozoites reveals core cellular events that underpin erythrocyte invasion. Cell Microbiol. 2013 Sep;15(9):1457–72.

246. Dluzewski AR, Fryer PR, Griffiths S, Wilson RJM, Gratzer WB. Red cell membrane protein distribution during malarial invasion. J Cell Sci. 1989 Apr 1;92(4):691–9.

247. Miller LH, Aikawa M, Johnson JG, Shiroishi T. Interaction between cytochalasin B-treated malarial parasites and erythrocytes. Attachment and junction formation. J Exp Med. 1979 Jan 1;149(1):172–84.

248. Hakansson S. Toxoplasma evacuoles: a two-step process of secretion and fusion forms the parasitophorous vacuole. EMBO J. 2001 Jun 15;20(12):3132–44.

249. McLaren DJ, Bannister LH, Trigg PI, Butcher GA. Freeze fracture studies on the interaction between the malaria parasite and the host erythrocyte in *Plasmodium knowlesi infections*. Parasitology. 1979 Aug;79(1):125–39.

250. Waller RF, Reed MB, Cowman AF, McFadden GI. Protein trafficking to the plastid of *Plasmodium falciparum* is via the secretory pathway. EMBO J. 2000;19(8):1794–802.

251. Matz JM, Beck JR, Blackman MJ. The parasitophorous vacuole of the blood-stage malaria parasite. Nat Rev Microbiol. 2020 Jul;18(7):379–91.

252. Kara UA, Stenzel DJ, Ingram LT, Kidson C. The parasitophorous vacuole membrane of *Plasmodium falciparum*: demonstration of vesicle formation using an immunoprobe. Eur J Cell Biol. 1988;46(1):9–17.

253. Stenzel DJ, Kara UA. Sorting of malarial antigens into vesicular compartments within the host cell cytoplasm as demonstrated by immunoelectron microscopy. Eur J Cell Biol. 1989;49(2):311–8.

254. Lanners HN, Wiser MF, Bafford RA. Characterization of the parasitophorous vacuole membrane from *Plasmodium chabaudi* and implications about its role in the export of parasite proteins. Parasitol Res. 1999 Mar 19;85(5):349–55.

255. Elmendorf H, Haldar K. *Plasmodium falciparum* exports the Golgi marker sphingomyelin synthase into a tubovesicular network in the cytoplasm of mature erythrocytes. J Cell Biol. 1994 Feb 15;124(4):449–62.

256. Behari R, Haldar K. *Plasmodium falciparum*: Protein Localization along a Novel, Lipid-Rich Tubovesicular Membrane Network in Infected Erythrocytes. Exp Parasitol. 1994;79(3):250–9.

257. Hanssen E, Carlton P, Deed S, Klonis N, Sedat J, DeRisi J, *et al*. Whole cell imaging reveals novel modular features of the exomembrane system of the malaria parasite, *Plasmodium falciparum*. Int J Parasitol. 2010 Jan;40(1):123–34.

258. Peng M, Chen F, Wu Z, Shen J. Endoplasmic Reticulum Stress, a Target for Drug Design and Drug Resistance in Parasitosis. Front Microbiol. 2021 May 31;12:670874.

259. McMillan PJ, Millet C, Batinovic S, Maiorca M, Hanssen E, Kenny S, *et al*. Spatial and temporal mapping of the PfEMP1 export pathway in *Plasmodium falciparum*: PfEMP1 export via the exomembrane system. Cell Microbiol. 2013 Aug;15(8):1401–18.

260. Riglar DT, Rogers KL, Hanssen E, Turnbull L, Bullen HE, Charnaud SC, *et al*. Spatial association with PTEX complexes defines regions for effector export into *Plasmodium falciparum*-infected erythrocytes. Nat Commun. 2013;4.

261. Hunn JP, Feng CG, Sher A, Howard JC. The immunity-related GTPases in mammals: a fast-evolving cell-autonomous resistance system against intracellular pathogens. Mamm Genome. 2011 Feb;22(1–2):43–54.

262. Qin A, Lai DH, Liu Q, Huang W, Wu YP, Chen X, *et al*. Guanylate-binding protein 1 (GBP1) contributes to the immunity of human mesenchymal stromal cells against *Toxoplasma gondii*. Proc Natl Acad Sci. 2017 Feb 7;114(6):1365–70.

263. Kravets E, Degrandi D, Ma Q, Peulen TO, Klümpers V, Felekyan S, *et al*. Guanylate binding proteins directly attack *Toxoplasma gondii* via supramolecular complexes. eLife. 2016 Jan 27;5:e11479.

264. Martens S, Parvanova I, Zerrahn J, Griffiths G, Schell G, Reichmann G, *et al*. Disruption of *Toxoplasma gondii* Parasitophorous Vacuoles by the Mouse p47-Resistance GTPases. Boothroyd J, editor. PLoS Pathog. 2005 Nov 18;1(3):e24.

265. Shaw MK, Tilney LG. The entry of *Theileria parva* merozoites into bovine erythrocytes occurs by a process similar to sporozoite invasion of lymphocytes. Parasitology. 1995 Nov;111(4):455–61.

266. Gohil S, Kats LM, Sturm A, Cooke BM. Recent insights into alteration of red blood cells by *Babesia bovis*: moovin' forward. Trends Parasitol. 2010 Dec;26(12):591–9.

267. Pellé KG, Jiang RHY, Mantel PY, Xiao YP, Hjelmqvist D, Gallego-Lopez GM, *et al*. Shared elements of host-targeting pathways among apicomplexan parasites of differing lifestyles: Protein export in Apicomplexa. Cell Microbiol. 2015 Nov;17(11):1618–39.

268. Desai SA, Miller LH. Protein-export pathway illuminated. Nature. 2014 Jul 31;511(7511):541–2.

269. Edwards CJ, Fuller J. Oxidative Stress in Erythrocytes. Comp Haematol Int. 1996;6(1):24–31.

270. Aich A, Freundlich M, Vekilov PG. The free heme concentration in healthy human erythrocytes. Blood Cells Mol Dis. 2015 Dec;55(4):402–9.

271. Çimen MYB. Free radical metabolism in human erythrocytes. Clin Chim Acta. 2008 Apr;390(1–2):1–11.

272. Lisewski AM, Quiros JP, Ng CL, Karani Adikesavan A, Miura K, Putluri N, *et al*. Supergenomic network compression and the discovery of EXP1 as a glutathione transferase inhibited by artesunate HHS Public Access. Cell. 2014;158(4):916–28.

273. Annoura T, Schaijk BCL, Ploemen IHJ, Sajid M, Lin J, Vos MW, *et al*. Two *Plasmodium* 6-Cys family-related proteins have distinct and critical roles in liver-stage development. FASEB J. 2014 May;28(5):2158–70.

274. Kriek N, Tilley L, Horrocks P, Pinches R, Elford BC, Ferguson DJP, *et al*. Characterization of the pathway for transport of the cytoadherence-mediating protein, PfEMP1, to the host cell surface in malaria parasite-infected erythrocytes: Trafficking of PfEMP1 in P. falciparum. Mol Microbiol. 2003 Nov 7;50(4):1215–27.

275. Rug M, Cyrklaff M, Mikkonen A, Lemgruber L, Kuelzer S, Sanchez CP, *et al*. Export of virulence proteins by malaria-infected erythrocytes involves remodelling of host actin cytoskeleton. Blood. 2014 Aug 19;124(23):3459–68.

276. Wiser MF. Unique endomembrane systems and virulence in pathogenic protozoa. Life. 2021;11(8).

277. Külzer S, Rug M, Brinkmann K, Cannon P, Cowman A, Lingelbach K, *et al*. Parasite-encoded Hsp40 proteins define novel mobile structures in the cytosol of the *P. falciparum*-infected erythrocyte. Cell Microbiol. 2010 Oct 1;12(10):1398–420.

278. Külzer S, Charnaud S, Dagan T, Riedel J, Mandal P, Pesce ER, *et al*. *Plasmodium falciparum* -encoded exported hsp70/hsp40 chaperone/co-chaperone complexes within the host erythrocyte: Chaperones in the *P. falciparum* -infected host cell. Cell Microbiol. 2012 Nov;14(11):1784–95.

279. Jonsdottir TK, Counihan NA, Modak JK, Kouskousis B, Sanders PR, Gabriela M, *et al*. Characterisation of complexes formed by parasite proteins exported into the host cell compartment of *Plasmodium falciparum* infected red blood cells. Cell Microbiol. 2021 Aug;23(8).

280. Zhang Q, Ma C, Oberli A, Zinz A, Engels S, Przyborski JM. Proteomic analysis of exported chaperone/co-chaperone complexes of *P. falciparum* reveals an array of complex protein-protein interactions. Sci Rep. 2017 Feb 20;7(1):42188.

281. Charnaud SC, Dixon MWA, Nie CQ, Chappell L, Sanders PR, Nebl T, *et al*. The exported chaperone Hsp70-x supports virulence functions for *Plasmodium falciparum* blood stage parasites. PLoS ONE. 2017 Jul 1;12(7).

282. Cobb DW, Florentin A, Fierro MA, Krakowiak M, Moore JM, Muralidharan V. The Exported Chaperone PfHsp70x Is Dispensable for the *Plasmodium falciparum* Intraerythrocytic Life Cycle. Blader IJ, editor. mSphere. 2017 Oct 25;2(5):e00363-17.

283. Day J, Passecker A, Beck H, Vakonakis I. The *Plasmodium falciparum* Hsp70-x chaperone assists the heat stress response of the malaria parasite. FASEB J. 2019 Dec;33(12):14611–24.

284. Petersen W, Külzer S, Engels S, Zhang Q, Ingmundson A, Rug M, *et al*. J-dot targeting of an exported HSP40 in *Plasmodium falciparum*-infected erythrocytes. Int J Parasitol. 2016 Jul 1;46(8):519–25.

285. Banumathy G, Singh V, Tatu U. Host Chaperones Are Recruited in Membrane-bound Complexes by *Plasmodium falciparum*. J Biol Chem. 2002 Feb;277(6):3902–12.

286. Knuepfer E, Rug M, Klonis N, Tilley L, Cowman AF. Trafficking of the major virulence factor to the surface of transfected *P. falciparum*–infected erythrocytes. Blood. 2005 May 15;105(10):4078–87.

287. Vallintine T, Van Ooij C. Distribution of malaria parasite-derived phosphatidylcholine in the infected erythrocyte. mSphere. 2023;e0013123.

Chapter 2: Materials and Methods

2.1 ***P. falciparum*** **culture**

2.1.1 ***In vitro maintenance and synchronisation of P. falciparum parasites***

P. falciparum strain 3D7 and iGP parasites were cultured in human erythrocytes (UK National Blood Transfusion Service and Cambridge Bioscience, UK) at 3% haematocrit, 37°C, in an atmosphere of 5% CO_2 in RPMI-1640 medium (Life Technologies) supplemented with 2.3 g/L sodium bicarbonate, 4 g/L dextrose, 5.957 g/L HEPES, 50µM hypoxanthine, 0.5% AlbuMax type II (Gibco), and 2 mM L-glutamine (cRPMI) according to established procedures (1,2).

Parasites were synchronised by isolation of late stage schizonts from asynchronous cultures on a 70% Percoll cushion (GE Healthcare) (3). Isolated schizonts were incubated at 37°C in the presence of 25 nM of egress inhibitor ML10 (2) for 3.5 hours to maximise the number of late-stage schizonts and synchronicity of egress upon release from ML10. ML10 was removed by washing the erythrocytes with cRPMI and the schizonts were resuspended in 5 ml cRPMI and added to fresh blood (2 ml 50% RBC and 5 mL cRPMI per T75 culture) and allowed to invade in a shaking incubator. After 1 hour the cultures were pelleted by centrifugation at 1,500 x g for 5 minutes and trophozoites and non-egressed schizonts were lysed by incubation at 37°C in the presence of an 2.5 x volume of 5% D-Sorbitol (Sigma-Aldrich) for 20 minutes (4). Newly invaded rings were washed and re-suspended in 30 mL cRPMI for continued culture. This schizont isolation, invasion, and sorbitol lysis was repeated every 48 hours to maintain synchronicity.

Culturing using human erythrocytes does not require ethical approval as all blood is anonymised and whole blood is washed to remove all other blood components which are discarded and destroyed by adding 10% Chloros followed by autoclaving, therefore no human DNA is present in our samples. After use, all parasite material and erythrocytes are destroyed under category 3 regulations.

2.1.2 ***Transfection of P. falciparum parasites***

Parasites were transfected using the schizont method (5). DNA for the transfections was isolated using a Monarch Midiprep Kit (New England Biolabs). For each transfection, 20 µg of plasmid in 100 µl sterile water was precipitated by adding 10 µl 3M sodium acetate and 250

µl 100% ethanol. Samples were stored overnight at -80°C and centrifuged at 12,000 x g for 10 minutes. Precipitated DNA was washed with 70% ethanol, centrifuges again and air dried in a sterile environment before re-suspension in 10 µl sterile TE buffer. The DNA was resuspended in 10 µl TE and 100 µl AMAXA P3 buffer solution just prior to transfection. For transfection using the mCherry fusion plasmids used in the DG targeting mechanism study of chapter 4, 20 µg plasmid pDC287, which encodes the *pfs47* guide RNA and Cas9 (6), was included with the target plasmid DNA to allow for Cas9 mediated double crossover recombination into the *pfs47* locus. The pDC287 plasmid contains a human dihydrofolate resistance marker for selection of transfectants with 2.5 nM WR 99210 (a kind gift of Prof. David Baker, LSHTM).

To prepare the parasites for transfection, late-stage schizonts were isolated from synchronised cultures in two T-75 flasks on a 70% Percoll cushion (GE Healthcare) (3) and incubated at 37˚C in the presence of 25 nM of the parasite egress inhibitor ML10 for 1.5 hours (2) to maximise numbers of late-stage segmented schizonts. The parasites were then washed with cRPMI to remove ML10 and resuspended in 5 ml cRPMI, which was distributed over 5 microcentrifuge tubes (1 tube per transfection) and incubated at 37°C for 18 minutes. The cells were pelleted, re-suspended in the DNA/AMAXA buffer mixer and subsequently transferred to AMAXA transfection cuvettes and transfected in the using the LONZA Nucleofactor™ electroporation device using the P3 Primary Cell transfection reagent programme and setting FP-158. The electroporated parasite suspension was transferred to T-25 cell culture flasks containing 300 µl packed erythrocytes in 2 ml cRPMI and the released merozoites were allowed to invade in a shaking incubator. After 30 minutes 8 ml medium was added to each flask and the cultures were transferred to a non-shaking incubator at 37°C in an atmosphere of 5% CO_2. After 24 hours WR99210, was added to 2.5 nM to the parasites to select for transfectants. Transfected parasites were generally recovered after approximately 3 weeks. In the case where plasmids integrated through single-crossover integration, integrants were selected with treatment with G418 (Generon) at 600 µg/ml.

2.1.3 ***Isolation of parasites for genomic DNA extraction***

Parasite culture was pelleted by centrifugation at 2000 x g for 5 minutes. The pellet was washed with 1 ml RPMI and re-suspended in a 1.5x volume of 0.15% saponin in phosphate buffered saline (PBS) to release the parasites from the erythrocytes. Parasites were pelleted by centrifugation at 13,000 x g for 5 minutes and the parasite DNA was purified using the

Monarch® Genomic DNA Purification Kit (New England Biolabs) and eluted in 40 µl elution buffer.

2.1.4 *Isolation of parasite material for immunoblotting*

Late-stage segmented schizonts were isolated via density gradient centrifugation on a 70% Percoll cushion and treated with 25 nM ML10 for three hours to maximise the number of DG containing parasites within the parasite population. Schizonts were then isolated from erythrocyte membrane fractions by saponin lysis in 1.5 x volume 0.15% saponin and pelleted by centrifugation at 2000 x g for five minutes. Pellets were washed with PBS, re-suspended in SDS-PAGE loading dye and boiled for 20 minutes at 95°C for protein denaturation. A solution of SDS-PAGE loading dye comprises 50 mM Tris-Cl (pH 6.8), 2% SDS, 0.1% Bromophenol Blue, 10% glycerol and 100mM DTT.

2.2 **Molecular biology techniques**

2.2.1 *Polymerase chain reaction (PCR)*

All PCRs were set up using Q5 polymerase (New England Biolabs) according to the manufacturer's instructions. A typical PCR reaction consisted of 0.5 µl template DNA, 5 µl 10 mM dNTPs, 10 µl 5X Q5 reaction buffer, 2.5 µl 10 µM forward primer, 2.5 µl 10 µM reverse primer, 0.2 µl Q5 polymerase, and sterile water for a total reaction volume of 50 µl. For colony PCR, a reaction consisted of 1 bacterial colony, 7.5 µl One-Taq quick-load mix (NEB), 0.75 µl of each primer (10 µM) and 6 µl of water for a total reaction volume of 15 µl. The thermocycler parameters were set to the settings shown in table 1 Primer pairs for PCR detection of integration events are shown in tables 2A-C.

Table 1: Thermocycler parameters used or PCR reactions for this project.

Step	**Temperature**	**Duration**
Initial denaturation	95°C	3 minutes
Denaturation	94°C	15 seconds
Primer annealing	50°C	15 seconds
Extension	64°C	1 minute/kb
Final extension	65°C	1 minute

Table 2: Primer pairs used for PCR detection of integration events. (A) Primers used to detect integration of the gene encoding the RESA-mNG fusion into the native RESA locus, chapter 3. (B) Primers used to detect integration of the genes encoding the mCherry-truncation fusions into the *pfs47* locus, Chapter 4. (C) Primers used to detect integration of the gene encoding the RESA-APEX fusion into the native RESA locus, Chapter 5.

A

Primer pairs

5': CVO545 + CVO551

3': CVO600 + TMR066A

WT: CVO545 + TMRO66A

Name	Binding site	Primer sequence
CVO545	*resa* exon 2, 968 bp upstream of STOP	GTGAACAAATGAATTCAATAACATACAATTTCG
CVO551	mNG 3' end	ACGCGTTGC TTTATACAATTCATCCATTCCCATAACATCTGTAAATG
CVO600	5' end of pCAM promoter	CAAAATGGTTAACAAAGAAGAAGCTCAGAG
TMRO66A	*resa* gDNA 62 bp downstream of exon 1	CACATTTCTTTTTCATATATCTTGTTTTAAATATTTTATTTTCATAAAGAG

B

Primer pairs

5': CVO120 + CVO505 (pRESA), CVO120 + CVO694 (pCAM)

3': CVO119 + CVO070

WT: CVO119 + CVO120

Name	Binding site	Primer sequence
CVO070	Binds pbDT3' 207 bp downstream of mCherry	CACACATAAAATGGCTAGTATGAATAGCC
CVO119	1020-985 bp upstream of Pfs47 ATG	CATTCCTAACACATTATGTGTATAACATTTTATGC
CVO120	3' end of Pfs47 gene	CATATGCTAACATACATGTAAAAAATTACAATCAG
CVO505	*resa* promoter immediately upstream START	GGCTCCTAGGAATTATTTAGATATTTTCTTATTATAAATTATGTAAAAGTAAAAAATTAAAACC
CVO694	18pb upstream of pCAM, reads into Pfs47	TTAGCTAATTCGCTTGTAAGAGGTACTCTCGTTTATGC

C

Primer pairs

5': CVO600 + TMRO34

3': CVO545 + CVO560

WT: CVO545 + TMRO34

Name	Binding site	Primer sequence
CVO545	*resa* exon 2, 968bp upstream of STOP	GTGAACAAATGAATTCAATAACATACAATTTCG
CVO560	*apex* 3' end	ACGCGTTGCtTGtAGGGCATCAGCAAACCC
CVO600	Cam5' UTR 3' end	CAAAATGGTTAACAAAGAAGAAGCTCAGAG
TMRO34	*resa* gDNA 540 downstream of exon 2 STOP	GGGTGGAAAGAATTTTAATAAGAGACCATACTTAGAG

2.2.2 ***Plasmids***

2.2.2.1 *RESA-mNG (pTV002)*

In order to be able to track the formation of DGs using fluorescence microscopy, I produced a plasmid encoding a fusion of mNeonGreen (mNG) to the 3' region of the gene encoding RESA (PF3D7_0102200), followed by sequence encoding the T2A skip peptide and a neomycin resistance marker, to allow for selection of parasites with integrated plasmid using G418 (7). First, the gene encoding GFP was removed from the plasmid pRESA-GFP (8) by digestion with PstI and MluI and replaced with a 705 bp insert encoding mNG that was amplified using primers CVO550 and CVO551 (table 3) and digested with PstI and MluI for insertion into the pRESA-GFP backbone, producing plasmid pTV001. The genes encoding the T2A peptide and G418 resistance marker were added by amplification of a fusion of these two genes from JT02-01-31 (a kind gift of Dr James Thomas, LSHTM) using primers CVO576 and CVO577 (table 4) and inserted at the 3' end of the mNG fragment by digestion of pTV001 and the PCR fragment with MluI. The fragments were joined using In-Fusion (TaKaRa), producing plasmid pTV002, encoding a fusion of the 3' 821 bp of the gene encoding RESA, the open reading frame encoding the T2A peptide and G418 the resistance marker.

Table 3: Primers designed for the amplification of mNG.

Name	Binding site	Sequence	Restriction site
CVO550	mNeon Green 5' end	CTGCAGAAAAA GTTAGTAAAGGAGAAGAAGATAATATGGCAAG	PstI
CVO551	mNeon Green 3' end	ACGCGTTGC TTTATACAATTCATCCATTCCCATAACATCTGTAAATG	MluI

Table 4: Primers designed for the amplification of SLI.

Name	Binding site	Sequence	Restriction site
CVO576	T2A 5' end	ACGCGTGAAGGAAGAGGAAGTTTATTAACATGTGGAG	MluI
CVO577	neoR 3' end	ACGCGTTTAGAAGAACTCGTCAAGAAGGCG	MluI

2.2.2.2 *RESA-APEX-SLI (pTV003)*

To identify new proteins contained within the DG compartment the pTV002 plasmid was modified, replacing the mNG tag with the gene encoding APEX. The APEX fragment was amplified from the JT02-02-29 plasmid obtained from (James Thomas, LSHTM) using primers CVO559 and CVO560 (table 5). The mNG fragment was removed from the RESA-mNG fusion plasmid by digestion with Mlu1 and Pst1 and replaced with Mlu1/Pst1 digested APEX fragment followed by the Mlu1/Pst1 digested DNA fragment at the 3' end of the APEX to enable rapid selection of RESA-APEX integrants as described above. The resulting fusion plasmids were tested by diagnostic digest using HindIII and PstI, and DNA sequencing by Eurofins.

Table 5. Primers used in the amplification of APEX. Primers used in the amplification of APEX for generation of the RESA-APEX fusion construct used to biotinylate proteins within the DGs as described in Chapter 5.

Name	Binding site	Sequence	Restriction site
CVO559	APEX 5' end	CTGCAGAAAAAGGAAAGTCTTACCCAACTGTGAGTG	PstI
CVO560	APEX 3' end	ACGCGTTGCTTGTAGGGCATCAGCAAACCC	MluI

2.2.2.3 *RESA (pBLD722) and PTEX88 (Pbld724) – mCherry fusions*

To determine whether a DG targeting signal is present within DG proteins, RESA and PTEX88 truncation-mCherry fusion proteins were generated to allow tracking of truncated forms of RESA and PTEX88 in late-stage *Plasmodium* parasites. The plasmid encoding the RESA truncation-mCherry fusion, named pBLD722, was produced in two steps. First, a synthetic gene containing the first 336 bp of RESA (encoding the N-terminal 112 amino acids), followed by a BamHI site and the mCherry sequence, was fused by PCR, producing plasmid pBLD720. The RESA truncation-mCherry fusion was amplified using primers CVO701 and CVO702 and cloned using InFusion into AvrII and XhoI digested pBLD633 vector, that contains 1215 bp of the RESA promoter, to produce plasmid pBLD722.

To generate the PTEX88 truncation-mCherry fusion plasmid, the region between the AvrII and BamHI sites of pBLD722 was replaced with sequence encoding the signal sequence and 21 downstream base pairs of PTEX88. These fragments were amplified by PCR with the primers shown in table 6 and isolated using Monarch® PCR & DNA Cleanup Kit (NEB). The PTEX88 truncation was amplified using *Plasmodium falciparum* gDNA as a template with primers

CVO712 and CVO713 and ligated to pBLD722 that had been digested with AvrII and BamHI to generate plasmid pBLD724.

2.2.2.4 *AMA1 (Pbld725), KAHRP (pBLD723), an CAM (pBLD727) - mCherry fusions*

To investigate the effects of expression from the RESA promoter on protein localization, the locations of non-DG proteins fused to mCherry were tracked in late stage schizonts using fluorescent microscopy. To generate the AMA1 and KAHRP truncation-mCherry fusion plasmids the region between the AvrII and BamHI sites of pBLD722 was replaced with sequence encoding the signal sequence and several downstream amino acids of KAHRP and AMA1. The KHARP truncation also contained the PEXEL region. These fragments were amplified by PCR with the primers shown in table 6 and isolated using NEB Monarch® PCR & DNA Cleanup Kit. The AMA1 truncation was amplified using *P. falciparum* gDNA as template with primers CVO714 and CVO715 and ligated into pBLD722 that had been digested with AvrII and BamHI and dephosphorylated to generate plasmid pBLD725. The KAHRP truncation was amplified using *P. falciparum* gDNA as template with primers CVO708 and CVO709 and ligated to pBLD722 digested with AvrII and BamHI to generate plasmid pBLD723.

To place the RESA truncation-mCherry fusion under the control of the CAM promoter, the RESA truncation-mCherry fusion in pBLD720 was amplified by PCR using primers CVO707 and CVO702. The resulting PCR product was cleaned using NEB Monarch® PCR & DNA Cleanup Kit and cloned into pBLD650that had been digested with BamHI and XhoI using InFusion producing plasmid pBLD727.

Table 6: Primers used in the amplification of the N-terminal regions of RESA, KAHRP, PTEX88 and AMA1 for generation of the mCherry fusions described in Chapter 4. Red sequence indicates In-Fusion homology region overhangs.

Name	Binding site	Sequence	InFusion overhang
CVO701	RESA 5′ end	CTAAATAATTCCTAGGATGAGACCTTTTCATGCATATAGTTGGATTTTTTC	RESA promoter 3′ end with AvrII restriction site
CVO702	mCherry 3′ end	CGTTATGTTACTCGAGTTACTTGTACAGCTCGTCCATGC	PBLD633 backbone with XhoI restriction site
CVO707	RESA 5′ end	ATATCAGGATCCTAGATGAGACCTTTTCATGCATATAGTTGGATTTTTTC	Cam promoter 3′ end with BamHI restriction site
CVO708	KAHRP exon 1 5′ end	CTAAATAATTCCTAGGATGAAAAGTTTTAAGAACAAAAATACTTTGAGGAG	RESA promoter 3′ end with AvrII restriction site
CVO709	KAHRP 3′ end	CCTTGCTCACGGATCCATTATTGCAGTTATTAGAGCACTTCAAAACCCATAC	mCherry 5′ end with BamHI restriction site
CVO712	PtTEX88 signal 5′ end	CTAAATAATTCCTAGGATGATTTACCAATACATTTTTGTATTATGTATACTATTGGTG	RESA promoter 3′ end with AvrII restriction site
CVO713	PTEX88 signal 3′ end	CCTTGCTCACGGATCCTTTTATTTTATACATGCACTGACCCACATG	mCherry 5′ with BamHI restriction site
CVO714	AMA1 signal 5′ end	CTAAATAATTCCTAGGATGAGAAAATTATACTGCGTATTATTATTGAGCGC	RESA promoter 3′ end with AvrII restriction site
CVO715	AMA1 signal 3′ end	CCTTGCTCACGGATCCCCAATAATTCTGTCCTCTTCCAAAGTTTATC	mCherry 5′ end with BamHI restriction site

2.2.3 *DNA ligation*

DNA ligation reactions were set up to contain a 3:1 ratio of insert to vector DNA (considering the size of both insert and vector). A typical reaction volume of 5 µl contained 1 µl of 5 x quick ligation reaction buffer and 0.5 µl T4 DNA ligase enzyme (NEB), with water up to 5 µl if necessary.

2.2.4 *Bacterial transformation*

Competent *Escherichia coli* DH5α cells were removed from storage at -80°C and allowed to thaw on ice. 2.2 µl ligation product was added to 55 µl competent cells and kept on ice for 30 minutes. The reaction was heat shocked at 42°C for 45 seconds and placed on ice for a further 2 minutes. 450 µl LB was added and transformations were placed in a shaking incubator for 40 minutes at 37°C. Bacteria were pelleted and resuspended in 55 µl of LB and spread on LB agar plates containing the appropriate antibiotic using glass beads. The LB agar plates were incubated overnight at 37°C. Colonies were chosen at random for testing for the presence of the correct plasmid by colony PCR. A portion of each colony was retained at this step and in instances where colony PCR indicated the correct plasmid was present, the corresponding colony portions were used to inoculated 2 ml LB containing 50 ug ampicillin/ml and placed in a shaking incubator overnight. The plasmids were purified using the Monarch plasmid purification Miniprep kit (New England Biolabs) and tested by diagnostic digest and DNA sequencing.

2.3 **Co-expression network analysis**

In order to identify putative DG proteins, the online co-expression network analysis platform was used to identify proteins with expression patterns mirroring that of the known DG protein RESA. A RESA query of www.malaria.tools database provided a co-expression network dataset that was analysed using PlasmoDB.org (9). The output of the RESA query was a list of 59 proteins with expression patterns mirroring the late-stage expression peak of RESA. Proteins were considered to be potential DG proteins if they contained a TM domain or signal sequence, had previously described functions that could serve in host cell remodelling or protein transport. Proteins were eliminated from the list of potential DG proteins if they lacked a signal sequence or TM domain which would be necessary for targeting them to the secretory system, or if they had known functions relating to parasite metabolism of other functions unlikely to be performed by secreted proteins.

2.4 **Statistics**

For calculation of DG biogenesis timing relative to egress, box-and-whisker plot, interquartile interval and average of timing of DG formation to egress times were generated using GraphPad Prism 9.

2.5 **Protein and immunofluorescence techniques**

2.5.1 ***Immunoblot analysis***

Late-stage segmented schizonts were isolated from highly synchronised cultures by flotation on a 70% Percoll cushion and blocked with 25 nM ML10 until Giemsa smears showed only late-stage segmented schizonts. The schizonts were pelleted by centrifugation at 2,000 x g for five minutes, pellets were resuspended in SDS-PAGE loading dye and then heated to 98°C for 10 minutes (A 1x solution of SDS-PAGE loading dye comprises 50 mM Tris-Cl (pH 6.8), 2% SDS, 0.1% Bromophenol Blue, 10% glycerol and 100mM DTT).

Proteins were separated by SDS-PAGE on 12.5% gels at 200 V for 45 minutes and subsequently transferred to a nitrocellulose membrane at 0.1 A and 25 V for 50 minutes using a Bio Rad Transblot Turbo transfer system. The membranes were blocked with 5% milk powder (Waitrose LTD) dissolved in PBS-Tween (PBST) for one hour at room temperature before

incubation with primary antibodies in PBST for one hour. After multiple wash steps the membrane was incubated with HRP-linked secondary antibody at 1:5000 dilution (Bio Rad) diluted in PBST for one hour at room temperature. The blots were then washed with PBST and developed with Clarity ECL Western blotting substrate (Bio Rad). Slides were imaged on a Bio Rad ChemiDoc and the images were further cropped and sized using Abode Photoshop. Figures were produced using Adobe Illustrator. For immunoblotting antibodies were diluted in PBST as described in table 7.

Table 7: Antibody dilutions as used in immunoblotting experiments.

Primary antibody	**Dilution**
Anti-biotin (rabbit)	1:10,000
Anti-aldolase (HRP linked)	1:5000
Anti-mNG (rat)	1:1000
Anti-mCherry (rabbit)	1:2000
Anti-EXP2 (mouse)	1:1000
Anti-alpha tubulin (mouse)	1:1000
Anti-PV1 (rabbit)	1:1000
Secondary antibody	**Dilution**
Anti-rabbit HRP	1:5000
Anti-rat HRP	1:5000
Anti-mouse HRP	1:5000

2.5.2 *Indirect immunofluorescence assays*

Smears of late-stage segmented 3D7 *P. falciparum* schizonts purified on a 70% Percoll cushion were air dried and stored with desiccant beads at -20°C. Parasites were fixed with acetone for 30 minutes, circled using an immuno-pen and subsequently blocked with 3% BSA in PBS (blocking solution) for a further 30 minutes. Primary antibodies were diluted in blocking solution and applied to the smears which were incubated at room temperature for 1 hour. Anti-HSP40 (PF3D7_0501100) antibodies (a kind gift of Prof. Catherine Braun-Breton, University of Montpellier) anti-AMA1 and anti-Ron4 antibodies (kind gifts of Mike Blackman, Francis Crick Institute), anti-HSP70-x and ETRAMP2, 4, and 10.3 antibodies (a kind gift of Tobias Spielmann of the Bernhard Nocht Institute for tropical Medicine, Hamburg) and the anti-RESA monoclonal antibody 28/2 (obtained from the antibody facility at the Walter and Eliza Hall Institute of Medical Research) were diluted as shown in table 8. The slides were then washed three times with PBS before application of the appropriate fluorophore-linked secondary

antibodies and Hoechst 33342 nuclear stain at 15 µg/ml in blocking solution and incubation for a further 45 minutes at room temperature. Following three washes with PBS, the slides were covered with Vectashield antifade mounting medium and sealed with nail polish. Parasites were imaged on a Nikon Eclipse TE fluorescence microscope equipped with a Hamamatsu ORCA-flash 4.0 digital camera C11440. The images were deconvolved using the Richardson-Lucy algorithm with 15 iterations using Nikon NIS-Elements version 5.3 software. The images where then separated, cropped, coloured and overlaid using FIJI software. Images were further cropped and sized using Photoshop. Figures were produced using Illustrator. Pearson's coefficients were generated using the FIJI (ImageJ) Colocalize tool.

Table 8: **Antibodies and dilutions used in IFA imaging.** The dilutions of antibodies used in IFA imaging of HSP40 against markers of the dense granules (RESA), rhoptries (Ron4), and micronemes (AMA1) (Chapter 3), in imaging of HSP70x against mNG labelled RESA, and in imaging ETRAMPS 2. 4 and 10.1 against EXP2 (Chapter 4).

Antibody	Dilution
Anti-RESA (mouse)	1:500
Anti-HSP40 (rabbit)	1:250
Anti-AMA1 (mouse)	1:100
Anti-Ron4 (mouse)	1:250
Anti HSP70-X (rabbit)	1:1000
Anti-ETRAMP2 (rabbit)	1:200
Anti-ETRAMP4 (rabbit)	1:200
Amti-ETRAMP10.1 (rabbit)	1:200
Anti-mNG (mouse)	1:500
Anti-EXP2 (mouse)	1:1000

2.6 **Live microscopy**

Highly synchronous late stage schizonts were isolated on a 70% Percoll cushion. Serial dilutions of schizonts in cRPMI containing 100 µM resveratrol were transferred to Ibidi poly-L-lysine µ-Slide VI$^{0.4}$ channel slides (serial dilutions were prepared to ensure an optimal density of cells for imaging). The channel slide was then sealed with petroleum jelly to prevent evaporation of the medium. Parasites were maintained at 37°C during transport and transferred to a pre-heated Okolab Microscope Incubator Cage with Gas Micro-Environmental Chamber and Air Heater for live imaging. Imaging was carried out at 37°C in an atmosphere containing

5% CO_2 on a Nikon Eclipse TE fluorescence microscope equipped with a Hamamatsu ORCA-flash 4.0 digital camera C11440 controlled using Nikon NIS-Elements version 5.3 software.

2.6.1 *DG biogenesis timing assays*

Tightly synchronised late-stage (47 hpi) pTV002 schizonts expressing a RESA-mNG fusion were imaged every five minutes until egress had occurred in a majority of schizonts. Imaging conditions and equipment were as described in the live microscopy section above. To minimise fluorophore bleaching and oxidative stress, laser intensity was set to 5%. Image data were analysed using NIS-Elements AR Analysis Software v. 4.51.01. Three repeats of the experiments were performed. Schizonts were numbered and timing from granular fluorescent patterning formation to egress was measured individually.

2.6.2 *DG protein targeting assays*

Imaging conditions and equipment were as described in the live microscopy section above. For imaging rings and trophozoite stages of the mCherry-truncation parasites used in investigating DG targeting control in Chapter 4, DNA was stained using 0.5 µ Sir-Hoechst far-red DNA dye for live cell imaging (10), added to the cell suspension 30 minutes prior to imaging.

2.7 **APEX biotinylation assays**

Late-stage schizonts of the parasites expressing the RESA-APEX fusion were isolated from eight T-75 flasks by 70% Percoll density gradient as previously described and incubated with 25 nM ML10 at 37°C for 2 hours to maximise numbers of DG containing schizonts.

Schizonts were pelleted by centrifugation at 2,000 x g for 5 minutes and re-suspended in 6 ml warm cRPMI medium, with 25 nM ML10 and 0.5 mM phenol biotin and incubated for 30 minutes at 37°C. Schizonts were counted using a C-Chip disposable haemocytometer (Labtech). After 30 minutes 6 1 ml aliquots of the schizont suspension were transferred to microfuge tubes and hydrogen peroxide was added to 3 of the 6 tubes to a final concentration of 1 mM. After 90 seconds the schizonts were pelleted in a microcentrifuge at 12,000 x g for 70 seconds. Supernatant was removed and all schizont pellets were re-suspended in 1 ml quench solution. A 5 ml volume of quench solution is comprised of 100 µl 20 nM sodium ascorbate, 50 µl 5 mM Trolox, 50 µl 10 mM sodium azide and 4.35 ml PBS. This wash step

was repeated 6 times. Finally, schizont pellets were re-suspended in 500 µl stop solution per treatment group (500 µl for the schizonts treated with hydrogen peroxide catalyst, 500 µl for the negative control schizonts without catalyst). 5 ml of quench solution is comprised of 50 µl Trolox, 100 µl sodium ascorbate, 50 µl sodium azide and 4.8 ml RIPA with protease inhibitor (10 ml RIPA plus 1 cOmplete Mini EDTA-free protease inhibitor tablet (Sigma-Aldrich)). 500 ml RIPA buffer comprises 15 ml 5M sodium chloride, 25 ml 1 M Tris, 5 ml 10% SDS, 2.5 g sodium deoxycholate, 5 ml 1% triton x-100 and 450 ml sterile water. For each solution 10 µl was removed and mixed with equal volume 2X SDS-PAGE loading dye and boiled for 10 minutes for immunoblotting. Upon addition of stop solution samples were immediately frozen in an ethanol-dry ice bath and stored at -80°C.

2.7.1 ***Streptavidin-biotin affinity purification***

50 µl Pierce streptavidin-coated magnetic beads (Thermo Fisher) were aliquoted to each of 6 microcentrifuge tubes and washed in 1 ml PBST 3 times as per manufacturer instructions.

RIPA buffer with protease inhibitor was added to each of the samples from labelling experiments until they were no longer glutinous. Samples were mixed with the streptavidin-coated beads and incubated for one hour at RT with gentle mixing.

Beads were sequestered on a magnetic stand, supernatant was removed and saved for immunoblot analysis. Beads were washed with 1ml RIPA buffer with gentle mixing and beads were sequestered again, the supernatant was saved for immunoblot analysis. The wash step was repeated 7 times. After washing with RIPA the beads were washed with PBS to remove detergent and stored at -80°C until they were sent for analysis. 10 µl of bead solution was boiled in 4% SDS for 20 minutes for protein elution from the beads, the eluted protein solution was saved for immunoblot analysis.

Bibliography

1. Trager W, Jensen JB. Human Malaria Parasites in Continuous Culture. Science. 1976 Aug 20;193(4254):673–5.

2. Ressurreiçao M, Thomas Id JA, Nofal SD, Flueck C, Moon RW, Baker DA, *et al*. Use of a highly specific kinase inhibitor for rapid, simple and precise synchronization of *Plasmodium falciparum* and *Plasmodium knowlesi* asexual blood-stage parasites. Plos One. 2020;15(7).

3. Rivadeneira EM, Wasserman M, Espinal CT. Separation and Concentration of Schizonts of *Plasmodium falciparum* by Percoll Gradients. J Protozool. 1983;30(2):367–70.

4. Lambros C, Vanderberg JP. Synchronization of *Plasmodium falciparum* erythrocytic stages in culture. J Parasitol. 1979;65(3):418–20.

5. Collins CR, Das S, Wong EH, Andenmatten N, Stallmach R, Hackett F, *et al*. Robust inducible Cre recombinase activity in the human malaria parasite *Plasmodium falciparum* enables efficient gene deletion within a single asexual erythrocytic growth cycle. Mol Microbiol. 2013;88(4):687–701.

6. Knuepfer E, Napiorkowska M, Van Ooij C, Holder AA. Generating conditional gene knockouts in *Plasmodium* – a toolkit to produce stable DiCre recombinase-expressing parasite lines using CRISPR/Cas9. Sci Rep. 2017 Jun 20;7(1):3881.

7. Birnbaum J, Flemming S, Reichard N, Blancke Soares A, Mesén-Ramírez P, Jonscher E, *et al*. A genetic system to study *Plasmodium falciparum* protein function. Nat Methods. 2017;14(4):450–6.

8. de Azevedo MF, Gilson PR, Gabriel HB, Simões RF, Angrisano F, Baum J, *et al*. Systematic Analysis of FKBP Inducible Degradation Domain Tagging Strategies for the Human Malaria Parasite *Plasmodium falciparum*. Templeton TJ, editor. PLoS ONE. 2012 Jul 16;7(7):e40981.

9. Aurrecoechea C, Brestelli J, Brunk BP, Dommer J, Fischer S, Gajria B. PlasmoDB: a functional genomic database for malaria parasites. Nucleai Acids Res. 2009;37:D539–43.

10. Lukinavičius G, Blaukopf C, Pershagen E, Schena A, Reymond L, Derivery E, *et al*. SiR–Hoechst is a far-red DNA stain for live-cell nanoscopy. Nat Commun. 2015 Oct 1;6(1):8497.

RESEARCH PAPER COVER SHEET

Please note that a cover sheet must be completed <u>for each</u> research paper included within a thesis.

<u>SECTION A – Student Details</u>

Student ID Number	lsh1902773	**Title**	Miss
First Name(s)	Tansy		
Surname/Family Name	Vallintine		
Thesis Title	Shining a Light on Dense Granules – A Biochemical, Genetic and Cell Biological Investigation of an Essential but Understudied Compartment of the Malaria Parasite		
Primary Supervisor	Christiaan van Ooij		

If the Research Paper has previously been published please complete Section B, if not please move to Section C.

<u>SECTION B – Paper already published</u>

Where was the work published?	Microbiology		
When was the work published?	2023 Aug		
If the work was published prior to registration for your research degree, give a brief rationale for its inclusion			
Have you retained the copyright for the work?*	**Yes**	Was the work subject to academic peer review?	**Yes**

*If yes, please attach evidence of retention. If no, or if the work is being included in its published format, please attach evidence of permission from the copyright holder (publisher or other author) to include this work.

SECTION C – Prepared for publication, but not yet published

Where is the work intended to be published?	
Please list the paper's authors in the intended authorship order:	
Stage of publication	Choose an item.

SECTION D – Multi-authored work

For multi-authored work, give full details of your role in the research included in the paper and in the preparation of the paper. (Attach a further sheet if necessary)	

SECTION E

Student Signature	T Vallintine
Date	11/10/23

Supervisor Signature	Christiaan van Ooij
Date	11/10/23

MICROBIOLOGY

RESEARCH ARTICLE

Vallintine and van Ooij, *Microbiology* 2023;169:001389

DOI 10.1099/mic.0.001389

MICROBIOLOGY SOCIETY

OPEN ACCESS

Timing of dense granule biogenesis in asexual malaria parasites

Tansy Vallintine and Christiaan van Ooij*

Abstract

Malaria is an important infectious disease that continues to claim hundreds of thousands of lives annually. The disease is caused by infection of host erythrocytes by apicomplexan parasites of the genus *Plasmodium*. The parasite contains three different apical organelles – micronemes, rhoptries and dense granules (DGs) – whose contents are secreted to mediate binding to and invasion of the host cell and the extensive remodelling of the host cell that occurs following invasion. Whereas the roles of micronemes and rhoptries in binding and invasion of the host erythrocyte have been studied in detail, the roles of DGs in *Plasmodium* parasites are poorly understood. They have been proposed to control host cell remodelling through regulated protein secretion after invasion, but many basic aspects of the biology of DGs remain unknown. Here we describe DG biogenesis timing for the first time, using RESA localization as a proxy for the timing of DG formation. We show that DG formation commences approximately 37 min prior to schizont egress, as measured by the recruitment of the DG marker RESA. Furthermore, using a bioinformatics approach, we aimed to predict additional cargo of the DGs and identified the J-dot protein HSP40 as a DG protein, further supporting the very early role of these organelles in the interaction of the parasite with the host cell.

INTRODUCTION

Malaria is caused by invasion, remodelling and lysis of host red blood cells by parasites of the genus *Plasmodium*. Invasion of the host cell is controlled by the regulated secretion of proteins from three specialized secretory organelles: micronemes, rhoptries and dense granules (DGs) (Fig. 1). The presence of three distinct apical organelles allows for compartmentalization of proteins with specific functions and temporal regulation of protein discharge for rapid and efficient invasion and modification of the host cell [1–5]. Micronemes are the first to secrete their contents [2] and primarily control host cell recognition, attachment and invasion through release of proteins such as erythrocyte binding antigen 175 (EBA-175) [6–8] and apical membrane antigen-1 (AMA-1) [9–12]. The rhoptries are second to discharge their contents, which include lipid whorls in addition to proteins [2, 13]; based on the timing of discharge it was thought that a subset of rhoptry proteins and the lipids secreted from the rhoptries initiate and support parasitophorous vacuole (PV) formation and invasion [5, 14, 15]. This has been supported by the finding that the rhoptry-associated protein (RAP) complex facilitates parasite growth and survival within the host cell after invasion, with conditional knockdown of RAP components resulting in structural deformity of the PV membrane (PVM), delayed intra-erythrocytic development and decreased parasitaemia in mouse models [16]. Although the content of apical organelles appears to be segregated along functional lines, studies in *Plasmodium* parasites and *Toxoplasma* parasites have revealed that cooperation between microneme and rhoptry proteins occurs to allow parasite invasion of the host erythrocyte [17, 18]. Binding of the microneme protein AMA1 and the rhoptry neck protein RON2 triggers formation of the moving junction complex (MJ) [5, 19]. The MJ functions as an interface between the membranes of the invading parasite and the host cell through which the parasite passes into the host cell during invasion. Blockage of the AMA1 binding site of RON2 inhibits formation of the MJ and parasitophorous vacuole [5, 20].

Received 21 June 2023; Accepted 15 August 2023; Published 30 August 2023
Author affiliations: †Faculty of Infectious Diseases, London School of Hygiene & Tropical Medicine, London, UK.
***Correspondence:** Christiaan van Ooij, Christiaan.vanOoij@lshtm.ac.uk
Keywords: malaria; *Plasmodium*; apicomplexa; apical organelles; dense granules.
Abbreviations: DG, dense granule; DGPD, dense granule protein database; GIG, gametogenesis implicated protein; MJ, moving junction; mNG, mNeonGreen; PCC, Pearson's correlation coefficient; PEXEL, *Plasmodium* export element; PTEX, plasmodium translocon of exported proteins; PV, parasitophorous vacuole; PVM, parasitophorous vacuole membrane; SLI, selection-linked integration; TM, transmembrane.
Two supplementary tables are available with the online version of this article.

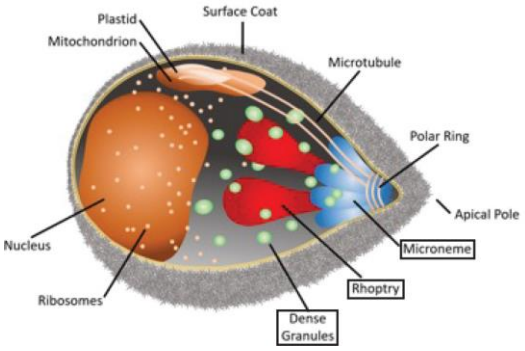

Fig. 1. A *Plasmodium falciparum* merozoite. Indicated are the different organelles inside the parasite, with the names of the apical organelles in boxes.

DGs are the last organelle to secrete their contents [21–23] and are speculated to be required for the remodelling of the host cell after invasion, thereby allowing parasite survival and replication through the asexual stages [1, 24]. However, little is known about DGs in *Plasmodium* parasites; only a few DG proteins have been identified in *Plasmodium falciparum*, whilst over 40 have been described in the related apicomplexan parasite *Toxoplasma gondii* [25, 26], in which DGs have been studied more extensively than in *Plasmodium* parasites. The few known *P. falciparum* DG proteins enable transport of parasite effector proteins into the erythrocyte [27–29] or are exported and subsequently mediate alterations of the biochemical and biophysical properties of the host cell [30]. The only known contents of *Plasmodium* DGs are the five core proteins of the *Plasmodium* translocon of exported proteins (PTEX) – EXP2, HSP101, PTEX150, PTEX88 and TRX2 – an essential protein complex that transports parasite effector proteins across the PVM into the host cell [28, 31–34]; PV1, which interacts with exported proteins and the PTEX [35, 36]; EXP1, a transmembrane protein in the parasitophorous vacuole membrane [37–39] that has an important role in nutrient uptake across the PVM through its effect on the localization of EXP2 [27, 29, 37, 40]; P113, a glycosylphosphatidylinositol (GPI)-linked protein that associates with the PTEX and with PVM and exported proteins [41, 42]; LSA3, the function of which is unknown [43]; and RESA (ring-infected erythrocyte surface antigen) [44], which binds to and stabilizes spectrin tetramers below the erythrocyte surface, thereby reducing host cell deformability [22, 30, 45–47] (Table 1). The recently published Dense Granule Protein Database (DGPD) (http://dgpd.tlds.cc/DGPD/index/), which provides information on identified and predicted DG proteins of apicomplexan parasites, lists an additional four PHIST proteins and a ClpB1 orthologue as putative DG proteins [48], although the ClpB1 orthologue has also been identified previously as an apicoplast protein [49] (Table 1). Hence, based on the function of the known DG proteins, this organelle appears to facilitate the modification of the host cell into a hospitable environment for parasite growth. For example, the increased cell rigidity caused by RESA allows infected cells to avoid filtration by the spleen by sequestering cells in the microvasculature whilst also increasing heat shock resistance, allowing parasites to survive the increased temperatures of febrile episodes and inhibit further invasion by other merozoites [45–47]. The timing of DG protein secretion immediately following invasion, the extensive nature of erythrocyte remodelling at that time and the greater number of DG proteins found in other apicomplexan parasites all suggest that DGs of *Plasmodium* parasites probably contain many more exported proteins than those currently identified [50]. This theory is further supported by the late-stage transcriptional profiles of 90 genes encoding putative exported proteins containing a *Plasmodium* Export Element (PEXEL) that are predicted to be exported into the host erythrocyte [51]. This demonstrates that in asexual *Plasmodium* parasites, a large proportion of exported proteins (although not all) are synthesized very late in the intra-erythrocytic life cycle [52, 53].

Despite the important role of DGs, many basic aspects of DG formation in *Plasmodium* parasites remain unknown, hampering the study of this important organelle. In this study we aimed to determine the timing of DG biogenesis and identify previously undescribed DG proteins. In order to investigate the timing of DG biogenesis, we generated parasites expressing RESA fused to mNeonGreen, allowing DG biogenesis to be observed by live video microscopy. RESA is the only currently known DG protein appropriate for use in DG formation imaging as the other known DG proteins are expressed earlier the intra-erythrocytic life cycle and localize to the PVM, where fluorescent signal would obscure signal from the forming DGs [54]. Using this knowledge of DG biogenesis, we applied a bioinformatics approach to identify additional DG proteins.

Table 1. Known and predicted *Plasmodium falciparum* dense granule proteins

Category	Gene ID	Name	Function	Comment
Known	PF3D7_0102200	RESA	Increases RBC rigidity	Also identified in the Dense Granule Protein Database (DGPD)
	PF3D7_1105600	PTEX88	PTEX core component	
	PF3D7_1436300	PTEX150	PTEX core component	
	PF3D7_1116800	HSP101	PTEX core component	Also in DGPD
	PF3D7_1345100	Trx2	PTEX core component	
	PF3D7_1471100	EXP2	PTEX core component, nutrient pore	Also in DGPD
	PF3D7_1129100	PV1	PTEX-associated PV protein	
	PF3D7_1420700	P113	PTEX-associated PV protein	
	PF3D7_1121600	EXP1	Integral PVM protein, regulates EXP2 pore activity	Also in DGPD
	PF3D7_0220000	LSA3	Exported protein of unknown function	
DGPD predictions	PF3D7_1149200	Ring-infected erythrocyte surface antigen (RESA 3)	Unknown, essential	Peak transcription mid-cycle
	PF3D7_1401600	PHISTb	MEC domain-containing protein	
	PF3D7_1252700	PHISTb	Unknown function	
	PF3D7_1201000	PHISTb	Unknown function	
	PF3D7_0532400	Lysine-rich membrane-associated PHISTb protein		
	PF3D7_0424600	PHISTb		Peak transcription mid-cycle
	PF3D7_0201700	DnaJ protein, putative		
	PF3D7_0816600	Chaperone ClpB1		Apicoplast protein

METHODS

Parasite culture

P. falciparum erythrocytic stage parasites of strain 3D7 were cultured in human erythrocytes (UK National Blood Transfusion Service and Cambridge Bioscience) at 3% haematocrit and 37 °C, 5% CO_2 in RPMI-1640 medium (Life Technologies) supplemented with 2.3 g l^{-1} sodium bicarbonate, 4 g l^{-1} dextrose, 5.957 g l^{-1} HEPES, 50 µM hypoxanthine, 0.5% AlbuMax type II (Gibco) and 2 mM L-glutamine [complete RPMI (cRPMI)] according to established procedures [55].

Transfection

Parasites were transfected using the schizont method [56]. For each transfection, 20 µg of plasmid in 100 µl buffer was precipitated using 10 µl sodium acetate and 250 µl 100% ethanol overnight at −80 °C. Precipitated DNA was washed with 70% ethanol and air dried in a sterile environment before re-suspension in 10 µl sterile TE buffer. The DNA for the transfections was resuspended in 10 µl TE and 100 µl AMAXA P3 buffer solution was added.

To prepare the parasites for transfection, two T-75 flasks of 3D7 parasite cultures containing predominantly late-stage schizonts were synchronized tightly using two rounds of density gradient centrifugation using 70% Percoll (GE Healthscience) and incubated at 37 °C with 25 nM of the parasite egress inhibitor ML10 for 1.5 h [57] to maximize numbers of late-stage segmented schizonts. The parasites were then washed with cRPMI to remove ML10 and resuspended in 5 ml cRPMI, which was distributed over five microcentrifuge tubes (one tube per transfection) and incubated at 37 °C for 18 min. The cells were pelleted, re-suspended in the DNA/AMAXA buffer solution and subsequently transferred to AMAXA transfection cuvettes and transfected using the LONZA Nucleofactor electroporation device using the P3 Primary Cell transfection reagent programme. The electroporated cell suspension was transferred to T-25 cell culture flasks containing 300 µl packed red blood cells (RBCs) in 2 ml cRPMI and the released merozoites were allowed to invade in a shaking incubator. After 30 min, 8 ml of medium was added to each flask and

the cultures were transferred to a non-shaking incubator. After 24 h, WR99210 [a kind gift of Prof. David Baker, London School of Hygiene & Tropical Medicine (LSHTM)] was added to 2.5 nM to the parasites to select for transfectants. Transfected parasites were generally recovered after approximately 3 weeks. Integrants were selected with treatment with G418 (Generon) at 600 µg ml^{-1}.

Plasmids

We aimed to produce a plasmid encoding a fusion of mNeonGreen (mNG) to the 3′ region of RESA (PF3D7_0102200), followed by sequence encoding the T2A skip peptide and a neomycin resistance marker, to allow for selection of parasites with integrated plasmid using G418 [58, 59]. First, the gene encoding GFP was removed from the plasmid pRESA-GFP [60] by digestion with *Pst*I and *Mlu*I and replaced with a 705 bp insert encoding mNG that was amplified using primers CVO550 and CVO551 (Table S1, available in the online version of this article) and digested with *Pst*I and *Mlu*I for insertion into the pRESA-GFP backbone, producing plasmid pTV001. The genes encoding the T2A peptide and G418 resistance marker were added by amplification of a fusion of these two genes from JT02-01-31 (a kind gift of James Thomas, LSHTM) using primers CVO576 and CVO577 (Table S1) and inserted at the 3′ end of the mNG fragment by digestion of pTV001 and the PCR fragment with *Mlu*I. The fragments were joined using In-Fusion (TaKaRa), producing plasmid pTV002, encoding a fusion of the 3′ 821 bp of the gene encoding RESA, the ORF encoding the T2A peptide and G418 the resistance marker.

Genomic DNA isolation

Erythrocytes were pelleted by centrifugation at 2000 ***g*** for 5 min and the resulting pellet was resuspended in an equal volume of 0.15% saponin in PBS to release the parasites from the erythrocytes. Parasites were pelleted by centrifugation at 13000 ***g*** for 5 min and the parasite DNA was isolated using the Monarch Genomic DNA Purification Kit (New England Biolabs).

Immunoblotting

Late-stage segmented schizonts were isolated from highly synchronized cultures by flotation on a 70% Percoll gradient [61] and blocked with 25 nM ML10 until Giemsa smears showed only late-stage segmented schizonts. The schizonts were pelleted by centrifugation at 2000 ***g*** for 5 min, pellets were resuspended in SDS-PAGE gel-loading buffer and then heated to 98 °C for 20 min.

Proteins were separated by SDS-PAGE on 12.5% gels at 200 V for 45 min and subsequently transferred to a nitrocellulose membrane at 0.1 A and 25 V for 50 min using a Bio Rad Transblot Turbo transfer system. The membranes were blocked with 5% milk powder (Waitrose) dissolved in PBS-Tween for 1 h at room temperature before incubation with either anti-mNG primary antibody diluted 1:1000 in PBS-Tween or horseradish peroxidase (HRP)-linked anti-aldolase antibody (Abcam) diluted 1:5000 in PBS-Tween for 1 h. After extensive washing, the blot probed with the anti-mNG antibody (ChromoTek) was incubated with HRP-linked secondary antibody (Bio-Rad) for 1 h at room temperature and after extensive washing with PBS both blots were developed with Clarity ECL Western blotting substrate (Bio-Rad). Both were imaged on a Bio-Rad ChemiDoc and the images were further cropped and sized using Adobe Photoshop. Figures were produced using Adobe Illustrator.

Video microscopy

Highly synchronous late-stage schizonts were isolated on a 70% Percoll gradient. Serial dilutions of schizonts in cRPMI containing 100 µM resveratrol were transferred to Ibidi poly-L-lysine µ-Slide VI$^{0.4}$ channel slides. Slide wells were then sealed with petroleum jelly to prevent sample dehydration. Parasites were maintained at 37 °C during transport and transferred to a pre-heated Okolab Microscope Incubator Cage with Gas Micro-Environmental Chamber and Air Heater for live imaging. Imaging was carried out at 37 °C and in an atmosphere containing 5% CO_2 on a Nikon Eclipse TE fluorescence microscope equipped with a Hamamatsu ORCA-flash 4.0 digital camera C11440 controlled using Nikon NIS-Elements version 5.3 software. Schizonts were imaged every 5 min until egress had occurred in a majority of schizonts. Image data were analysed using NIS-Elements AR Analysis Software v. 4.51.01. Three replicate experiments recording DG formation to egress provided timing data for 47, 14 and 30 schizonts, respectively. Schizonts were numbered and timing from granular fluorescence patterning formation to egress was measured individually.

Statistics

Box-and-whisker plots, interquartile intervals and average of timing of DG formation to egress times were generated using GraphPad Prism 9.

Co-expression network analysis

A query of the www.malaria.tools database using RESA (PF3D7_0102200) as input gave an initial co-expression neighbourhood dataset of 59 proteins (Table S2). The dataset was further analysed using PlasmoDB.org; proteins lacking a signal sequence or transmembrane (TM) domain or annotated as having a function unlikely to be performed by secreted proteins were removed. The final list of proteins for further investigation comprised 23 proteins (Table 1).

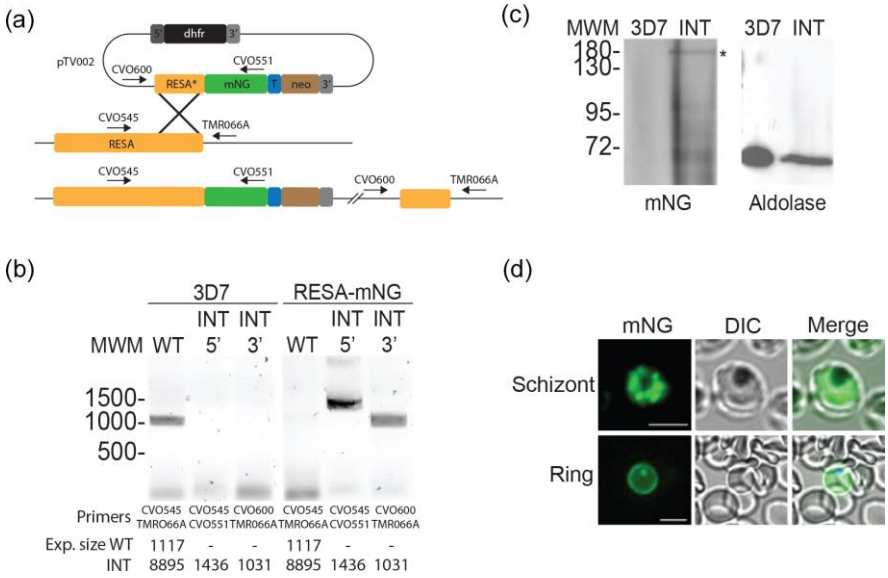

Fig. 2. Generation of an mNeonGreen-RESA-expressing parasite. (a) Integration strategy using selection-linked integration (SLI). mNG, mNeonGreen; T, T2A peptide; neo, amino 3′-glycosylphosphotransferase (neomycin resistance gene); 5′ and 3′, 5′ and 3′ regulatory regions, respectively. The plasmid pTV002, containing a fusion of the 3′ region of the RESA gene and the gene encoding mNG, was introduced into 3D7 parasites. Transfectants were selected with WR and integrants were subsequently selected with G418. (b) Integration PCR of genomic DNA from wild-type (3D7, left) and integrant (INT, right) parasites using the indicated primer pairs. See panel (a) for the binding sites of the primers. The expected sizes of the PCR products are indicated at the bottom. (c) Anti-mNeonGreen immunoblot of 3D7 (right) and RESA-mNG integrant parasite extracts (left). The band of the expected size is indicated (*). The same extracts were probed with anti-aldolase antibodies as loading control (right). (d) Live-cell fluorescence imaging of parasites expressing RESA-mNG. Top, schizont; bottom, ring. Bars, 5 µm.

Immunofluorescence assays

Smears of late-stage segmented 3D7 *P. falciparum* schizonts purified on a Percoll gradient were air dried and stored with desiccant beads at −20 °C. Parasites were fixed with acetone for 30 min, circled using an immuno-pen and subsequently blocked with 3% BSA in PBS (blocking solution) for a further 30 min. Primary antibodies were diluted in blocking solution and applied to the smears which were incubated at room temperature for 1 h. Anti-HSP40 (PF3D7_0501100) antibodies (a kind gift of Prof. Catherine Braun-Breton, University of Montpellier) were used at a dilution of 1:250; anti-AMA1 and anti-Ron4 antibodies (kind gifts of Mike Blackman, Francis Crick Institute) were used at a dilution of 1:100 and 1:250, respectively, and the anti-RESA mAb 28/2 (obtained from the antibody facility at the Walter and Eliza Hall Institute of Medical Research) was used at a dilution of 1:500. The slides were then washed three times with PBS before application of the appropriate fluorophore-linked secondary antibodies and Hoechst 33342 nuclear stain at 15 µg ml^{-1} in blocking solution and incubation for a further 45 min at room temperature. Following three washes with PBS, the slides were covered with Vectashield antifade mounting medium and sealed with nail polish. Parasites were imaged on a Nikon Eclipse TE fluorescence microscope equipped with a Hamamatsu ORCA-flash 4.0 digital camera C11440. The images were deconvolved using the Richardson–Lucy algorithm with 15 iterations using Nikon NIS-Elements version 5.3 software. The images where then separated, cropped, coloured and overlaid using FIJI software. Images were further cropped and sized using Photoshop. Figures were produced using Illustrator. Pearson's coefficients were generated using the FIJI (ImageJ) Colocalize tool.

RESULTS

Generation of a reporter strain for the study of DG formation

To study the biosynthesis of DGs and the movement of DG proteins through the secretory system, we fused the gene encoding the well-established DG marker RESA [22] with the gene encoding mNG. This fusion was introduced into 3D7 parasites and integration into the native *RESA* locus was selected for using selection-linked integration (SLI) [58] (Fig. 2a). Integration of the RESA-mNG gene fusion into the native RESA locus was verified using PCR and production of the expected mNG fusion protein

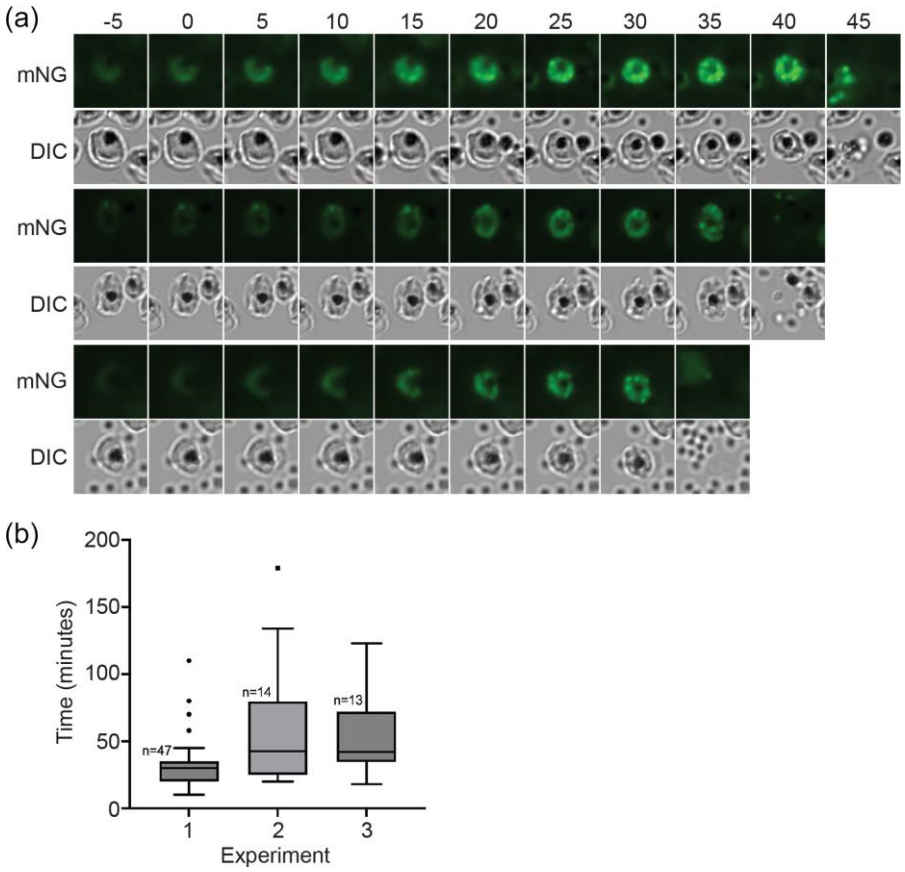

Fig. 3. Video microscopy of dense granule formation. (a) Highly synchronized RESA-mNG-expressing parasites were observed using live video microscopy at intervals of 5 min. Parasites were imaged on three separate occasions; each row is taken from a different experiment. The formation of punctate spots of fluorescence was designated as the start of dense granule formation (time point 0). mNG, mNeonGreen fluorescence; DIC, differential interference contrast. (b) Quantification of dense granule formation for the three different experiments. The boxes represent the interquartile range, where 50% of the data points are found. The horizontal line crossing the box represents the median. The *y*-axis represents the time (in minutes) from the first detection of clustering of RESA-mNG fluorescence in spots to egress of the parasites.

product was verified by immunoblotting (Fig. 2b, c). The transgenic parasites were brightly fluorescent in the schizont stage and displayed the expected fluorescence around the periphery of the infected erythrocyte after the parasites had invaded, as seen previously with RESA-GFP fusions [62] (Fig. 2d).

Timing of DG biogenesis

To determine the timing of DG biogenesis we observed the appearance of green fluorescence and the coalescence of the fluorescence into distinct organelles using live video microscopy imaging of the transgenic RESA-mNG-expressing parasites. As RESA expression initiates late in the erythrocytic cycle, as supported by our initial imaging experiments, we started imaging tightly synchronized late-stage schizonts from 46 to 47 h post-invasion at 5 min intervals. A 5 min interval was chosen to minimize the toxic effect of the laser exposure whilst providing an interval narrow enough to provide a reliable time frame. In three replicate experiments, schizonts were observed to undergo DG biogenesis, from the appearance of DG fluorescence to egress. The start of DG biosynthesis was set at the time of increasing fluorescence with the appearance of granular foci of fluorescence where one or more defined foci of fluorescence is visible (t=0) (Fig. 3a). The averaging of the times within the interquartile interval of each replicate revealed that DG formation occurs approximately 37 min prior to egress from the infected erythrocyte (Fig. 3b). Several

outliers were observed in which the period from DG formation to egress was far greater than the majority of the other events (five outliers out of 74 total events). These outliers, which fell outside of the interquartile intervals, were not included in the calculation of average DG formation to egress timing. In the outliers in which the timing of DG formation to egress greatly exceeded the average, the cells were observed to reach a point at which egress would be expected to occur based on appearance by both fluorescence and digital interference contrast (DIC) microscopy, but egress appeared blocked or delayed. In these instances, DG fluorescence grew progressively brighter than in other cells as the RESA-mNG fusion continued to be produced and transported to the DGs; no other difference in appearance was observed. We had previously observed inhibited egress and eventual parasite death when imaging without the antioxidant resveratrol.

As *P. falciparum* rhoptries are formed predominantly between the second and fourth round of nuclear division and merozoite formation begins at the end of the fourth round of nuclear division [63], these experiments indicate that DGs are unusual among the apical organelles in that they are formed well after the final round of nuclear division – on average only 37 min prior to egress – a tiny fraction (1.3%) of the entire 48 h intra-erythrocytic life cycle.

Co-expression network analysis to identify candidate DG proteins

As our results above revealed that DGs are formed very late in the intra-erythrocytic cycle, we inferred that expression network analysis to find proteins with a late-stage expression peak around the time of DG formation could identify potential additional DG proteins for further investigation. We therefore searched for proteins with expression profiles similar to that of RESA using the malaria.tools database [64] (Fig. 4a). This provided a co-expression neighbourhood dataset comprising 59 proteins (Table S2). A query of Plasmodb.org of the identified proteins provided data on protein features, including TM domains, signal sequences and predicted export signals, mutant phenotype and rodent genetic modifications where available [65, 66]. Of the proteins in the original malaria.tools output, 39 (66%) contained one TM domain or a signal sequence, indicating that they can enter the secretory pathway. The output also contained six RESA orthologues, which were included for further analysis. Proteins with an annotated function that indicates that they are not present in DGs were omitted.

Proteins were selected for further analysis on the criteria of having a previously described function with potential relevance to erythrocyte remodelling or protein transport and the presence of a signal sequence or TM domain capable of targeting the protein to the secretory pathway. Selection based on these criteria provided a list of 23 potential DG proteins (Table 2). Of the proteins that did not contain a TM domain or signal sequence, three were included in the final set based on their predicted function [v-SNARE, gametogenesis implicated protein (GIG) and DYN3/DrpC]. As v-SNAREs mediate fusion of vesicles and granules to target membranes [67–69], this v-SNARE was included to investigate a potential role in DG protein transport or fusion of DGs to the parasite membrane. GIG is implicated in gametocyte production and was included as it may point to gametocyte-specific alteration of the host cell [70]. The dynamin-like protein DrpC was included as tgDrpC is involved in vesicular transport and mitochondrial fission [71–73], and tgDrpB is required for formation of secretory organelles in *T. gondii* [74]. The role of DrpC in endocytosis has not been investigated. The final list of putative DG proteins comprised 23 proteins (Table 2). The previously identified DG proteins PTEX88 and LSA3 are present in the malaria.tools output, as well as several RESA N-terminal sequences, supporting the use of this technique as a tool for identifying DG proteins. However, as certain DG proteins, including EXP1 and EXP2, do not have this distinctive late-stage expression peak, they were not present in the output and it is likely that other DG proteins were not identified in this analysis for the same reason. Exported proteins are greatly overrepresented in the final list, and proteins for which mutant phenotypes have been described, for example PTP1 and PTP5, and members of the FIKK family, predominantly have roles in host cell remodelling and cytoprotection [75–77]. These characteristics are in keeping with the model that DGs are important mediators of host cell remodelling.

Localization of putative DG proteins

To verify whether proteins identified in the bioinformatics screen are transported to DGs, we determined the localization of one of the potential DG proteins for which an antibody was available, HSP40, using immunofluorescence assays. We first compared the expression profile of HSP40 with that of RESA using previously published tramscriptomic data [54], which confirmed that the expression pattern of HSP40 is indeed very similar to that of RESA (Fig. 4b). Co-staining of late-stage schizonts with anti-HSP40 antibodies and microneme, rhoptry and DG markers (AMA1, RON4 and RESA, respectively) revealed strong overlap of the RESA and HSP40 signals in all late-stage segmented schizonts, indicating co-localization of the two proteins (Fig. 4c). Indeed, almost no HSP40 staining distinct from RESA staining was detected in late-stage segmented schizonts. Staining using antibodies against the rhoptry neck marker Ron4 and the microneme marker AMA1 exhibit greatly lower levels of colocalization with anti-HSP40 antibodies. In these samples HSP40 staining was detected distinctly adjacent to AMA1 and RON4 staining. Strong overlap with DG marker staining compared to the distinct staining patterns seen with microneme and rhoptry markers indicate that HSP40 localizes to DGs and not to the micronemes and rhoptries. This was further supported by Pearson's correlation coefficient (PCC) for the antibody pairs HSP40–RESA (0.810), HSP40–AMA1 (0.370) and HSP40–RON4 (0.205) (Fig. 4d). This result identifies an additional DG protein and indicates that use of co-expression network analysis warrants further investigation as a tool for DG protein identification.

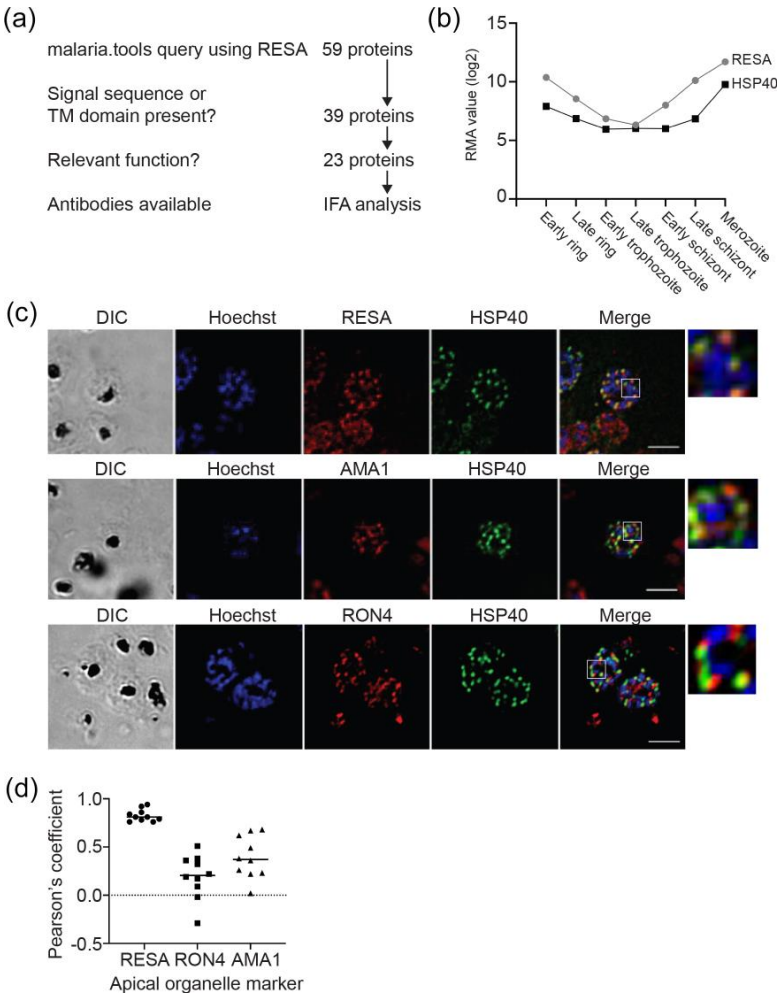

Fig. 4. Identification of additional dense granule proteins. (a) Outline of malaria.tools query using RESA (PF3D7_0102200). (b) Comparison of expression pattern of RESA and HSP40. Robust multi-array averaging (RMA) values of RESA (grey) and HSP40 (black) expression levels at different stages of the intra-erythrocytic life cycle are shown. Data were obtained from Le Roch *et al*. [54]. (c) Co-staining of *P. falciparum* parasites using anti-HSP40 and the dense granule marker RESA (top), the microneme marker AMA1 (middle) and the rhoptry neck marker RON4 (bottom). Samples were also stained with Hoechst 33342 to visualize DNA. Panels on the far right show an expanded view of the region indicated in the white boxes. Bar, 5 µm. (d) Pearson's correlation coefficient (PCC) of the colocalization of the anti-HSP40 staining and the staining using the indicated antibodies that recognize apical organelle markers. For each combination, the PCC was determined using ten clearly labelled merozoites in different schizonts.

DISCUSSION

Here we have shown that DGs in *P. falciparum* are formed extremely late in the erythrocytic life cycle – in our experiments DGs were detected on average 37 min prior to egress. However, as egress timing appears to be delayed by the oxidative stress induced by laser exposure and mNG fluorescence, this estimation of the start of DG biogenesis is likely to be an underestimation.

As DGs are formed very late in the intra-erythrocytic cycle and several known DG proteins, including RESA, consequently have a distinctive late-stage expression peak, we inferred that expression network analysis to find other proteins with a similarly distinctive late expression peak could identify potential DG proteins for further investigation. Through a search of the malaria.tools co-expression network platform using RESA as a query we identified genes with expression profiles similar to that of RESA,

Table 2. Putative *Plasmodium falciparum* dense granule proteins identified in malaria.tools using RESA as query

Name	Alias	Description	piggyBac mutagenesis	Rodent GM phenotype	Annotation (and putative PEXEL sequence)
PF3D7_0935600	GIG	Gametogenesis implicated protein	_	_	No transmembrane domain (TM), signal sequence or export signal
PF3D7_0220000	LSA3	Known DG protein	Dispensable	_	Recessed signal sequence, TM at C terminus, RSLGE
PF3D7_1201200	Plasmodium RESA N-terminal	Plasmodium exported protein (PHISTa-like), unknown function	Dispensable	_	TM domain, recessed signal sequence, exported, RKLAD
PF3D7_0702100	Plasmodium RESA N terminal	Plasmodium exported protein (PHISTb), unknown function, pseudogene	_	_	Exported, PEXEL-like sequences
PF3D7_1016700	Plasmodium RESA N-terminal	Unknown function	_	_	TM domains, exported protein
PF3D7_0424600	Plasmodium RESA N-terminal	Unknown function	Dispensable	_	Exported protein
PF3D7_1002100	PTP5	EMP1-trafficking protein	Dispensable	_	Recessed signal sequence, exported protein, RLLSE
PF3D7_0501100	HSP40	Heat shock protein 40, type II	Essential	_	Recessed signal sequence, exported, RSLAE
PF3D7_1218500	DYN3/DRPC	Putative dynamin-like protein	Essential	_	No signal sequence or TM
PF3D7_1016800	Plasmodium RESA N-terminal	Plasmodium exported protein (PHISTc), unknown function	Dispensable	_	TM domain, exported
PF3D7_1102800	ETRAMP11.2	Early transcribed membrane protein	Essential	_	Signal sequence and TM domain
PF3D7_1102700	ETRAMP11.1	Early transcribed membrane protein	Dispensable	_	Signal sequence and TM domain
PF3D7_1105600	PTEX88	Component of PTEX, known DG protein	Essential	Successful modification	Signal sequence
PF3D7_0424500	FIKK4.1	Serine threonine protein kinase	Dispensable	_	TM domain, exported
PF3D7_0902500	FIKK9.6	Serine threonine protein kinase	Dispensable	_	No signal sequence or
PF3D7_0202200	PTP1	EMP1 trafficking protein	_	_	TM domains, exported
PF3D7_0219700	GEXP20	Plasmodium exported protein (PHISTc), unknown function	Essential	_	Recessed signal sequence, exported
PF3D7_0402100	Plasmodium RESA N-terminal	Plasmodium exported protein (PHISTb), unknown function	Dispensable	_	Recessed signal sequence, exported
PF3D7_0202500	ETRAMP2	Early transcribed membrane protein 2	Dispensable	_	Signal sequence and TM domain
PF3D7_0523000	MDR1	Multidrug resistance protein 1	Essential	Non-successful modification	TM domains
PF3D7_0314100	v-SNARE	Vesicle transport, putative	Essential	_	TM domain
PF3D7_0425100	hyp6	Plasmodium exported protein, unknown function	Dispensable	_	Signal sequence, TM domain, predicted exported
PF3D7_1001900	PFJ23-hyp16	Unknown function	_	_	Recessed signal sequence, TM domains, exported

including heat shock protein HSP40 (Fig. 4b) [54]. We did indeed find that HSP40 co-localizes with RESA, indicating that HSP40 localizes to DGs in the late schizont stage [78]. This supports the use of co-expression network analysis as a method for DG protein prediction. As HSP40 is part of the J-dots, which are small parasite-derived structures found in the cytosol of infected erythrocytes that may be involved in the transport of parasite proteins through the host cell cytosol [79, 80], it indicates that at least some of the components of these structures are present in the DGs and exported to the host cell almost immediately after the parasite enters the host cell. Although the function of these structures remains unclear, it has been postulated that they may

have a function in the transport of parasite proteins through the erythrocyte cytosol [81]. Hence, by releasing the component protein of J-dots in DGs, the parasite may enhance its ability to target these proteins to their proper intra-erythrocytic location almost immediately after invasion. This finding therefore may also further support the hypothesis that DGs probably contain many more exported proteins that have yet to be identified. This aligns with the timing of DG discharge immediately following invasion and the hypothesized role of DGs in erythrocyte remodelling. Interestingly, one protein identified in the malaria.tools investigation, PTP1, is necessary for correct formation of Maurer's clefts and linking Maurer's clefts to the cytoskeleton [77]. This may well indicate that Maurer's clefts are formed very soon after invasion, using proteins that are exported immediately after DGs have been released.

Our bio-informatics approach identified the known DG proteins LSA3 and PTEX88 [34, 43]. However, several other DG proteins, including EXP1 and EXP2, were not included in the malaria.tools output, probably because they do not share the distinctive late-stage expression peak of RESA and instead are also expressed at other times throughout the life cycle. It is likely that other unidentified DG proteins will also be missing from the output owing to having expression profiles dissimilar to that of RESA. Combined, the listing of known and recently identified DG proteins, and the localization of the one protein that has been tested to date to the DGs, suggests that co-expression network analysis using malaria.tools works as a predictive method of identifying candidate proteins for further analysis. Further, exported proteins are over-represented within the dataset. As host cell effector proteins must be exported, the high number of exported proteins within the dataset accords with the understanding of the role of DGs as a secretory compartment containing proteins with roles in host cell modification that are released immediately after erythrocyte invasion. A recently developed database of predicted *Plasmodium* DG proteins also includes several PHIST proteins [48]. Whilst the function of many individual PHIST proteins remains unknown, the prediction of another family of exported proteins localizing to the DGs supports the theory of DG function in erythrocyte remodelling.

Three proteins with a transcriptional profile similar to that of RESA are of potential interest based on their putative function, despite lacking a signal sequence or TM domain: PF3D7_0314100, annotated as a v-SNARE, GIG and the dynamin-like protein DrpC. These proteins may serve important functions in the fusion of the DGs to the parasite plasma membrane, gametocyte-specific functions immediately after invasion and vesicular trafficking to the DGs, respectively [67–72, 82].

The endogenously tagged RESA line may be useful as a tool in future work aiming to identify factors that are involved in DG formation, sorting of proteins to the DGs and as a screen for drugs which act to inhibit DG formation or release.

This is the first description of the timing of DG biogenesis in *Plasmodium* parasites. This finding reveals that DGs are only present within the parasite for a very short portion (1.3%) of the 48 h asexual cycle. We also find that the exported protein HSP40 is present in DGs. As HSP40 interacts with HSP70x to form a chaperone complex within the infected host cell, this finding further supports the hypothesis that DGs have an important role in host cell modification, in this instance through the chaperoning of parasite effector proteins [78]. These results provide further insight into how the parasite prepares for modification of the host cell.

Funding information
This work was supported by an MRC-LID studentship to T.V. and a Medical Research Council Career Development Award (MR/R008485/1) to C.v.O.

Acknowledgements
We are grateful to Dr James Thomas (LSHTM) for providing the JT02-01-31 plasmid containing the SLI fragment and Dr Gerhard Wunderlich (Institute of Biomedical Sciences, University of Sao Paulo) for providing plasmid pRESA-HA. We thank Prof. Catherine Braun-Breton (University of Montpellier) for providing the anti-HSP40 antibody, and Mike Blackman (Francis Crick Institute) for the anti-AMA1 and anti-RON4 antibodies. We thank Prof. David Baker for sharing WR99210. The authors acknowledge the facilities and the scientific and technical assistance of the LSHTM Wolfson Cell Biology Facility, with specific thanks to Liz McCarthy.

Conflicts of interest
The authors declare that there is no conflict of interest.

References

1. Carruthers VB, Sibley LD. Sequential protein secretion from three distinct organelles of *Toxoplasma gondii* accompanies invasion of human fibroblasts. *Eur J Cell Biol* 1997;73:114–123.
2. Singh S, Alam MM, Pal-Bhowmick I, Brzostowski JA, Chitnis CE. Distinct external signals trigger sequential release of apical organelles during erythrocyte invasion by malaria parasites. *PLoS Pathog* 2010;6:e1000746.
3. Kats LM, Cooke BM, Coppel RL, Black CG. Protein trafficking to apical organelles of malaria parasites - building an invasion machine. *Traffic* 2008;9:176–186.
4. Gubbels MJ, Duraisingh MT. Evolution of apicomplexan secretory organelles. *Int J Parasitol* 2012;42:1071–1081.
5. Cao J, Kaneko O, Thongkukiatkul A, Tachibana M, Otsuki H, *et al*. Rhoptry neck protein RON2 forms a complex with microneme protein AMA1 in *Plasmodium falciparum* merozoites. *Parasitol Int* 2009;58:29–35.
6. Adams JH, Sim BKL, Dolan SA, Fang X, Kaslow DC, *et al*. A family of erythrocyte binding proteins of malaria parasites. *Proc Natl Acad Sci* 1992;89:7085–7089.
7. Camus D, Hadley TJ. A *Plasmodium falciparum* antigen that binds to host erythrocytes and merozoites. *Science* 1985;230:553–556.
8. Lee Sim BK, Toyoshima T, David Haynes J, Aikawa M. Localization of the 175-kilodalton erythrocyte binding antigen in micronemes of *Plasmodium falciparum* merozoites. *Mol Biochem Parasitol* 1992;51:157–159.

9. Peterson MG, Marshall VM, Smythe JA, Crewther PE, Lew A, *et al*. Integral membrane protein located in the apical complex of *Plasmodium falciparum*. *Mol Cell Biol* 1989;9:3151–3154.
10. Triglia T, Healer J, Caruana SR, Hodder AN, Anders RF, *et al*. Apical membrane antigen 1 plays a central role in erythrocyte invasion by *Plasmodium* species. *Mol Microbiol* 2000;38:706–718.
11. Bannister LH, Hopkins JM, Dluzewski AR, Margos G, Williams IT, *et al*. *Plasmodium falciparum* apical membrane antigen 1 (PfAMA-1) is translocated within micronemes along subpellicular microtubules during merozoite development. *J Cell Sci* 2003;116:3825–3834.
12. Mitchell GH, Thomas AW, Margos G, Dluzewski AR, Bannister LH. Apical membrane antigen 1, a major malaria vaccine candidate, mediates the close attachment of invasive merozoites to host red blood cells. *Infect Immun* 2004;72:154–158.
13. Stewart MJ, Schulman S, Vanderberg JP. Rhoptry secretion of membranous whorls by *Plasmodium falciparum* merozoites. *Am J Trop Med Hyg* 1986;35:37–44.
14. Bannister LH, Mitchell GH. The fine structure of secretion by *Plasmodium knowlesi* merozoites during red cell invasion. *J Protozool* 1989;36:362–367.
15. Ladda R, Aikawa M, Sprinz H. Penetration of erythrocytes by merozoites of mammalian and avian malarial parasites. 1969. *J Parasitol* 2001;87:470–478.
16. Ghosh S, Kennedy K, Sanders P, Matthews K, Ralph SA, *et al*. The *Plasmodium rhoptry* associated protein complex is important for parasitophorous vacuole membrane structure and intraerythrocytic parasite growth. *Cell Microbiol* 2017;19:12733.
17. Alexander DL, Mital J, Ward GE, Bradley P, Boothroyd JC. Identification of the moving junction complex of *Toxoplasma gondii*: a collaboration between distinct secretory organelles. *PLoS Pathog* 2005;1:e17.
18. Besteiro S, Michelin A, Poncet J, Dubremetz JF, Lebrun M. Export of a *Toxoplasma gondii* rhoptry neck protein complex at the host cell membrane to form the moving junction during invasion. *PLoS Pathog* 2009;5:e1000309.
19. Lamarque M, Besteiro S, Papoin J, Roques M, Vulliez-Le Normand B, *et al*. The RON2-AMA1 interaction is a critical step in moving junction-dependent invasion by apicomplexan parasites. *PLoS Pathog* 2011;7:e1001276.
20. Srinivasan P, Beatty WL, Diouf A, Herrera R, Ambroggio X, *et al*. Binding of *Plasmodium merozoite* proteins RON2 and AMA1 triggers commitment to invasion. *Proc Natl Acad Sci* 2011;108:13275–13280.
21. Torii M, Adams JH, Miller LH, Aikawa M. Release of merozoite dense granules during erythrocyte invasion by *Plasmodium knowlesi*. *Infect Immun* 1989;57:3230–3233.
22. Culvenor JG, Day KP, Anders RF. *Plasmodium falciparum* ring-infected erythrocyte surface antigen is released from merozoite dense granules after erythrocyte invasion. *Infect Immun* 1991;59:1183–1187.
23. Riglar DT, Richard D, Wilson DW, Boyle MJ, Dekiwadia C, *et al*. Super-resolution dissection of coordinated events during malaria parasite invasion of the human erythrocyte. *Cell Host Microbe* 2011;9:9–20.
24. de Koning-Ward TF, Dixon MWA, Tilley L, Gilson PR. *Plasmodium* species: master renovators of their host cells. *Nat Rev Microbiol* 2016;14:494–507.
25. Ming P, Mingjun L, Longjiao L, Yongle S, Lun H, *et al*. Identification of novel dense-granule proteins in *Toxoplasma gondii* by two proximity-based Biotinylation approaches. *J Proteome Res* 2018;18:319–330.
26. Griffith MB, Pearce CS, Heaslip AT. Dense granule biogenesis, secretion, and function in *Toxoplasma gondii*. *J Eukaryot Microbiol* 2022;69:e12904.
27. Ho C-M, Beck JR, Lai M, Cui Y, Goldberg DE, *et al*. Malaria parasite translocon structure and mechanism of effector export. *Nature* 2018;561:70–75.
28. Elsworth B, Matthews K, Nie CQ, Kalanon M, Charnaud SC, *et al*. PTEX is an essential nexus for protein export in malaria parasites. *Nature* 2014;511:587–591.
29. Garten M, Nasamu AS, Niles JC, Zimmerberg J, Goldberg DE, *et al*. EXP2 is a nutrient-permeable channel in the vacuolar membrane of *Plasmodium* and is essential for protein export via PTEX. *Nat Microbiol* 2018;3:1090–1098.
30. Pei X, Guo X, Coppel R, Bhattacharjee S, Haldar K, *et al*. The ring-infected erythrocyte surface antigen (RESA) of *Plasmodium falciparum* stabilizes spectrin tetramers and suppresses further invasion. *Blood* 2007;110:1036–1042.
31. Beck JR, Muralidharan V, Oksman A, Goldberg DE. PTEX component HSP101 mediates export of diverse malaria effectors into host erythrocytes. *Nature* 2014;511:592–595.
32. Charnaud SC, Kumarasingha R, Bullen HE, Crabb BS, Gilson PR. Knockdown of the translocon protein EXP2 in *Plasmodium falciparum* reduces growth and protein export. *PLoS One* 2018;13:e0204785.
33. de Koning-Ward TF, Gilson PR, Boddey JA, Rug M, Smith BJ, *et al*. A newly discovered protein export machine in malaria parasites. *Nature* 2009;459:945–949.
34. Bullen HE, Charnaud SC, Kalanon M, Riglar DT, Dekiwadia C, *et al*. Biosynthesis, localization, and macromolecular arrangement of the *Plasmodium falciparum* translocon of exported proteins (PTEX). *J Biol Chem* 2012;287:7871–7884.
35. Morita M, Nagaoka H, Ntege EH, Kanoi BN, Ito D, *et al*. PV1, a novel *Plasmodium falciparum* merozoite dense granule protein, interacts with exported protein in infected erythrocytes. *Sci Rep* 2018;8:3696.
36. Chu T, Lingelbach K, Przyborski JM. Genetic evidence strongly support an essential role for PfPV1 in intra-erythrocytic growth of *P. falciparum*. *PLoS One* 2011;6:e18396.
37. Günther K, Tümmler M, Arnold HH, Ridley R, Goman M, *et al*. An exported protein of *Plasmodium falciparum* is synthesized as an integral membrane protein. *Mol Biochem Parasitol* 1991;46:149–157.
38. Iriko H, Ishino T, Otsuki H, Ito D, Tachibana M, *et al*. *Plasmodium falciparum* exported protein 1 is localized to dense granules in merozoites. *Parasitol Int* 2018;67:637–639.
39. Simmons D, Woollett G, Bergin-Cartwright M, Kay D, Scaife J. A malaria protein exported into a new compartment within the host erythrocyte. *EMBO J* 1987;6:485–491.
40. Mesén-Ramírez P, Bergmann B, Tran TT, Garten M, Stäcker J, *et al*. EXP1 is critical for nutrient uptake across the parasitophorous vacuole membrane of malaria parasites. *PLoS Biol* 2019;17:e3000473.
41. Miyazaki S, Chitama B-YA, Kagaya W, Lucky AB, Zhu X, *et al*. *Plasmodium falciparum* SURFIN$_{4.1}$ forms an intermediate complex with PTEX components and Pf113 during export to the red blood cell. *Parasitol Int* 2021;83:102358.
42. Bullen HE, Sanders PR, Dans MG, Jonsdottir TK, Riglar DT, *et al*. The *Plasmodium falciparum* parasitophorous vacuole protein P113 interacts with the parasite protein export machinery and maintains normal vacuole architecture. *Mol Microbiol* 2022;117:1245–1262.
43. Morita M, Takashima E, Ito D, Miura K, Thongkukiatkul A, *et al*. Immunoscreening of *Plasmodium falciparum* proteins expressed in a wheat germ cell-free system reveals a novel malaria vaccine candidate. *Sci Rep* 2017;7:46086.
44. Aikawa M, Torii M, Sjölander A, Berzins K, Perlmann P, *et al*. Pf155/RESA antigen is localized in dense granules of *Plasmodium falciparum* merozoites. *Exp Parasitol* 1990;71:326–329.
45. Da Silva E, Foley M, Dluzewski AR, Murray LJ, Anders RF, *et al*. The *Plasmodium falciparum* protein RESA interacts with the erythrocyte cytoskeleton and modifies erythrocyte thermal stability. *Mol Biochem Parasitol* 1994;66:59–69.
46. Silva MD, Cooke BM, Guillotte M, Buckingham DW, Sauzet J-P, *et al*. A role for the *Plasmodium falciparum* RESA protein in resistance against heat shock demonstrated using gene disruption. *Mol Microbiol* 2005;56:990–1003.

47. Diez-Silva M, Park Y, Huang S, Bow H, Mercereau-Puijalon O, *et al*. Pf155/RESA protein influences the dynamic microcirculatory behavior of ring-stage *Plasmodium falciparum* infected red blood cells. *Sci Rep* 2012;2:614.
48. Hu H, Lu Z, Feng H, Chen G, Wang Y, *et al*. DGPD: a knowledge database of dense granule proteins of the Apicomplexa. *Database* 2022;2022:baac085.
49. El Bakkouri M, Pow A, Mulichak A, Cheung KLY, Artz JD, *et al*. The Clp chaperones and proteases of the human malaria parasite *Plasmodium falciparum*. *J Mol Biol* 2010;404:456–477.
50. Rezaei F, Sharif M, Sarvi S, Hejazi SH, Aghayan S, *et al*. A systematic review on the role of GRA proteins of *Toxoplasma gondii* in host immunization. *J Microbiol Methods* 2019;165:105696.
51. Marti M, Good RT, Rug M, Knuepfer E, Cowman AF. Targeting malaria virulence and remodeling proteins to the host erythrocyte. *Science* 2004;306:1930–1933.
52. Tomavo S. Evolutionary repurposing of endosomal systems for apical organelle biogenesis in *Toxoplasma gondii*. *Int J Parasitol* 2014;44:133–138.
53. Hallée S, Counihan NA, Matthews K, de Koning-Ward TF, Richard D. The malaria parasite *Plasmodium falciparum* Sortilin is essential for merozoite formation and apical complex biogenesis. *Cell Microbiol* 2018;20:e12844.
54. Le Roch KG, Zhou Y, Blair PL, Grainger M, Moch JK, *et al*. Discovery of gene function by expression profiling of the malaria parasite life cycle. *Science* 2003;301:1503–1508.
55. Crabb BS, Rug M, Gilberger TW, Thompson JK, Triglia T, *et al*. Transfection of the human malaria parasite *Plasmodium falciparum*. *Methods Mol Biol* 1999;270:267–276.
56. Collins CR, Hackett F, Strath M, Penzo M, Withers-Martinez C, *et al*. Malaria parasite cGMP-dependent protein kinase regulates blood stage merozoite secretory organelle discharge and egress. *PLoS Pathog* 2013;9:e1003344.
57. Ressurreição M, Thomas JA, Nofal SD, Flueck C, Moon RW, *et al*. Use of a highly specific kinase inhibitor for rapid, simple and precise synchronization of *Plasmodium falciparum* and *Plasmodium knowlesi* asexual blood-stage parasites. *PLoS One* 2020;15:e0235798.
58. Birnbaum J, Flemming S, Reichard N, Blancke Soares A, Mesén-Ramírez P, *et al*. Selection linked integration (SLI) for endogenous gene tagging and knock sideways in *Plasmodium falciparum* parasites. *Protoc Exch* 2017.
59. Birnbaum J, Flemming S, Reichard N, Soares AB, Mesén-Ramírez P, *et al*. A genetic system to study *Plasmodium falciparum* protein function. *Nat Methods* 2017;14:450–456.
60. de Azevedo MF, Gilson PR, Gabriel HB, Simões RF, Angrisano F, *et al*. Systematic analysis of FKBP inducible degradation domain tagging strategies for the human malaria parasite *Plasmodium falciparum*. *PLoS One* 2012;7:e40981.
61. Rivadeneira EM, Wasserman M, Espinal CT. Separation and concentration of schizonts of *Plasmodium falciparum* by Percoll gradients. *J Protozool* 1983;30:367–370.
62. Rug M, Wickham ME, Foley M, Cowman AF, Tilley L. Correct promoter control is needed for trafficking of the ring-infected erythrocyte surface antigen to the host cytosol in transfected malaria parasites. *Infect Immun* 2004;72:6095–6105.
63. Margos G, Bannister LH, Dluzewski AR, Hopkins J, Williams IT, *et al*. Correlation of structural development and differential expression of invasion-related molecules in schizonts of *Plasmodium falciparum* . *Parasitology* 2004;129:273–287.
64. Tan QW, Mutwil M. Malaria.tools-comparative genomic and transcriptomic database for *Plasmodium* species. *Nucleic Acids Res* 2020;48:D768–D775.
65. Amos B, Aurrecoechea C, Barba M, Barreto A, Basenko EY, *et al*. VEuPathDB: the eukaryotic pathogen, vector and host bioinformatics resource center. *Nucleic Acids Res* 2022;50:D898–D911.
66. David S. PlasmoDB: an integrative database of the *Plasmodium falciparum* genome. Tools for accessing and analyzing finished and unfinished sequence data. *Nucleic Acids Res* 2001;29:66–69.
67. Dhara M, Yarzagaray A, Makke M, Schindeldecker B, Schwarz Y, *et al*. V-SNARE transmembrane domains function as catalysts for vesicle fusion. *Elife* 2016;5:e17571.
68. Chen YA, Scheller RH. SNARE-mediated membrane fusion. *Nat Rev Mol Cell Biol* 2001;2:98–106.
69. Wang T, Li L, Hong W. SNARE proteins in membrane trafficking. *Traffic* 2017;18:767–775.
70. Gardiner DL, Dixon MWA, Spielmann T, Skinner-Adams TS, Hawthorne PL, *et al*. Implication of a *Plasmodium falciparum* gene in the switch between asexual reproduction and gametocytogenesis. *Mol Biochem Parasitol* 2005;140:153–160.
71. Heredero-Bermejo I, Varberg JM, Charvat R, Jacobs K, Garbuz T, *et al*. TgDrpC, an atypical dynamin-related protein in *Toxoplasma gondii*, is associated with vesicular transport factors and parasite division. *Mol Microbiol* 2019;111:46–64.
72. Melatti C, Pieperhoff M, Lemgruber L, Pohl E, Sheiner L, *et al*. A unique dynamin-related protein is essential for mitochondrial fission in *Toxoplasma gondii*. *PLoS Pathog* 2019;15:e1007512.
73. Breinich MS, Ferguson DJP, Foth BJ, van Dooren GG, Lebrun M, *et al*. A dynamin is required for the biogenesis of secretory organelles in *Toxoplasma gondii*. *Curr Biol* 2009;19:277–286.
74. Spielmann T, Gras S, Sabitzki R, Meissner M. Endocytosis in *Plasmodium* and *Toxoplasma* parasites. *Trends Parasitol* 2020;36:520–532.
75. Davies H, Belda H, Broncel M, Ye X, Bisson C, *et al*. An exported kinase family mediates species-specific erythrocyte remodelling and virulence in human malaria. *Nat Microbiol* 2020;5:848–863.
76. Maier AG, Rug M, O'Neill MT, Brown M, Chakravorty S, *et al*. Exported proteins required for virulence and rigidity of *Plasmodium falciparum*-infected human erythrocytes. *Cell* 2008;134:48–61.
77. Rug M, Cyrklaff M, Mikkonen A, Lemgruber L, Kuelzer S, *et al*. Export of virulence proteins by malaria-infected erythrocytes involves remodeling of host actin cytoskeleton. *Blood* 2014;124:3459–3468.
78. Liu Q, Liang C, Zhou L. Structural and functional analysis of the Hsp70/Hsp40 chaperone system. *Protein Sci* 2020;29:378–390.
79. Petersen W, Külzer S, Engels S, Zhang Q, Ingmundson A, *et al*. J-dot targeting of an exported HSP40 in *Plasmodium falciparum*-infected erythrocytes. *Int J Parasitol* 2016;46:519–525.
80. Külzer S, Rug M, Brinkmann K, Cannon P, Cowman A, *et al*. Parasite-encoded Hsp40 proteins define novel mobile structures in the cytosol of the *P. falciparum*-infected erythrocyte. *Cell Microbiol* 2010;12:1398–1420.
81. Behl A, Kumar V, Bisht A, Panda JJ, Hora R, *et al*. Cholesterol bound *Plasmodium falciparum* co-chaperone "PFA0660w" complexes with major virulence factor "PfEMP1" via chaperone "PfHsp70-x." *Sci Rep* 2019;9:2664.
82. Bai M-J, Wang J-L, Elsheikha HM, Liang Q-L, Chen K, *et al*. Functional characterization of dense granule proteins in *Toxoplasma gondii* RH strain using CRISPR-Cas9 system. *Front Cell Infect Microbiol* 2018;8:300.

Edited by: J. A Gralnick and M. Cayla

Chapter 4: Dense granule protein targeting: expression timing, target sequence, or both?

4.1 **Introduction**

The secretory pathway has been well described in the model organism *Saccharomyces cerevisiae*, predominantly thanks to the work of the Schekman laboratory for which he was awarded the 2013 Nobel Prize in Physiology and Medicine. However, the protein secretion effectors and pathways discovered in this organism effectors and pathways discovered in this organism have been found to be highly conserved among eukaryotes. In *S. cerevisiae* and other eukaryotes, proteins destined for the cell membrane or for secretion out of the cell are translated from messenger RNA by ribosomes within the rough ER (1,2). From the ER, proteins are transported to the Golgi apparatus for maturation and sorting for transport to their various cellular locations, including the plasma membrane, endosomal compartments (3–5) and in specialised cells such as the merozoites of *Plasmodium* parasites, other organelles such as the rhoptries, micronemes and DGs (6). After proteins enter the ER they are transported to the *cis* face of the Golgi network through vesicular transport (5). ER export is mediated by the COPII (coat protein complex II) coat mechanism (7), which functions with the microtubule and dynein/dynactin dependent transport machinery (8,9). Proteins then move between the different parts of the Golgi and exit the Golgi at the trans-Golgi network (TGN). Here, the proteins are concentrated into vesicles that are targeted to their respective organellar destinations. Broadly, the specificity of targeting of soluble proteins from the TGN relies on the presence of targeting signals within the proteins, which are recognised by specific membrane bound receptor proteins and recruited into budding vesicles along with transmembrane proteins by adaptor proteins. The specificity of transport is mediated by Rab (Ras-associated binding) proteins, small GTPases of the Ras (Rat sarcoma virus) superfamily that are key regulators in vesicular trafficking, and SNARE proteins (soluble N-ethylmaleimide-sensitive factor attachment protein receptors) that function in vesicle formation, transport and membrane fusion (10–12). *P. falciparum* encodes 11 Rab proteins, 10 of which are produced during the intraerythrocytic life cycle (13). In order to reach their intended destination, TGN-derived vesicles require a mechanism to allow them to fuse with the correct membrane or organelle. The specificity of membrane fusion is determined by SNARE proteins, which are membrane proteins that function as specificity determinants in vesicular fusion. The *P. falciparum* genome encodes 18 SNARE-like proteins (14). SNAREs are characterised by the presence of an N-terminal cytoplasmic sequence, a coiled-coil domain (15–19), a SNARE motif (a conserved sequence

of 60-70 amino acids), and a C-terminal transmembrane domain (15,18,20). Specific v-SNAREs (vesicular SNAREs) localise to specific compartments and interact selectively, the t-SNAREs (target membrane SNARE) that are localised to specific membranes, to form complexes termed SNAREpins that link the vesicular and target membranes (21). Interestingly, a putative v-SNARE (PF3D7_0314100) that is predicted to be essential (22) was identified as a potential DG-associated protein in the co-expression network analysis study described in Chapter 2. The distinctive late-stage expression peak of this putative v-SNARE indicates that it could function in protein transport and vesicular fusion of vesicles destined to the DG, thereby playing a vital role in DG biogenesis and targeting specificity or play a part in the secretion of DGs. In *Toxoplasma gondii*, the SNARE protein Stx12 has been identified as the SNARE protein required for correct transport of vesicles to apical organelles (micronemes and rhoptries) (23), but any role for SNARE function in the biogenesis of the apical organelles in *Plasmodium* parasites remains unknown.

Apical organelle biogenesis in *Plasmodium* parasites occurs via *de novo* synthesis during the last phase of division by a simplified regulated secretory pathway, not via a repurposed endosomal system as in *T. gondii* (24). In *P. falciparum* the apical organelles are formed during the last 10-12 hours of erythrocytic development (25). Rhoptry formation begins during the second round of nuclear division, and micronemes and DGs develop at the end of nuclear division, although the exact timing of the synthesis of the DGs has not been established (25,26). In accordance with this, most apical organelle proteins are expressed late in the erythrocytic cycle (24,27–30). Apical organelles in *Plasmodium* parasites are initially synthesised from vesicles derived directly from the TGN (25,26). Whilst some factors necessary for protein transport and subsequent organelle development have been identified (discussed below), the mechanisms underlying the original 'biogenesis' that create the initial structure to which protein transport vesicles can then be targeted, remain unknown. It should therefore be noted that authors commonly use the term biogenesis to refer to organelle development through correct protein cargo delivery, and this is how it is used in the section.

There are two steps involved in the transport of a protein to the correct organelle: recruitment of proteins to the correct secretory vesicles, followed by transport of these vesicles to the correct organelle. The first requires a recognition signal in the protein for recognition by sorting protein, the latter necessitates recognition of the sorting protein by transport machinery in the cytosol and the appropriate target membrane. Little is known about the mechanisms underlying rhoptry and microneme biogenesis and protein trafficking to these organelles in *Plasmodium*

parasites and even less is known about these factors in relation to DGs. Much of the current understanding of apical organelle development is founded on indirect evidence from co-localisation studies with conserved effectors of vesicular trafficking (13,31,32). For example, investigations in *T. gondii*, indicate that conserved protein trafficking factors have an essential role in apical secretory organelle biogenesis, including members of the small G-proteins Rab-GTPases TgRab5A and TgRab5C which function in the formation of rhoptries and a subpopulation of micronemes (30,33). Below I describe what is known about the biogenesis of the apical organelles in *Plasmodium* parasites.

4.1.1 ***Micronemes***

In *P. falciparum*, targeting of EBA-175 to micronemes requires a C-terminal cysteine-rich ectodomain, even when the transmembrane domain has been removed (34). Similarly, in *T. gondii* correct transport of the soluble microneme protein 3 (MIC3) depends on a cysteine-rich central region (amino acids 68-306) (35). It is possible that the cystine-rich regions are required for correct protein folding in the ER through the formation of disulphide bonds and/or that they function in receptor ligand interaction (36). This suggests a model in which the targeting signal is bound in the Golgi lumen by a TM protein that is recognised by microneme targeting machinery in the cytosol of the parasite. Further, knock down of the closest *Plasmodium* homolog of TRF1, pantothenate transporter (PAT) in *Plasmodium berghei* leads to a defect in microneme fusion to the plasma membrane in the sporozoite stage on (33). Similarly, conditional knock down of Transporter family 1 (TRF1), the closest orthologue of PAT in *T. gondii* causes a significant decrease in the number of micronemes, which take on an amorphic ovoid structure (37).

4.1.2 ***Rhoptries***

The majority of known rhoptry proteins lack a transmembrane domain, so by what mechanism do rhoptry cargo vesicles engage with the cytoplasmic trafficking machinery? *T. gondii,* the large dynamin-like protein B (DrpB) GTPase is required for the formation of the secretory vesicles necessary for microneme and rhoptry biogenesis (38). Conditional ablation of DrpB function in *T. gondii* produces daughter merozoites that lack micronemes and rhoptries and induces a lethal deficit in invasion (38), with secretory proteins mis-localising to the constitutive secretory pathway (38). The function of the *Plasmodium* ortholog of DrpB is currently unknown.

Investigation of transport of proteins to rhoptries in *Plasmodium* parasites have focused on Rhoptry Associated Membrane Antigen (RAMA). In parasites lacking RAMA, several rhoptry bulb and neck proteins become mislocalised and the rhoptry neck is deformed. Unexpectedly, these parasites also have a lethal invasion deficit (39). It is possible that RAMA generates clusters of soluble rhoptry proteins within vesicles destined for the rhoptries that exit the TGN (40). Immunoprecipitation and fluorescence resonance energy transfer (FRET) experiments have established that these RAMA-associated clusters contain members of the RAP complex, Rhoptry Associated Protein 1 (RAP1) and Rhoptry Associated Protein 2 (RAP2); it has been shown that the RAP1-RAP2 complex (the low molecular weight rhoptry complex) interacts with RAMA via the N-terminus of RAP1 (40). The escorter protein that interacts with RAMA and acts as a link to cytosolic sorting machinery is VPS10 (PfSortilin), which is sufficient for correct rhoptry targeting (41). Furthermore, knockdown of PfSortilin blocked protein transport to all apical organelles without affecting the constitutive secretory pathway (30). This suggests that PfSortilin has an essential role as the escorter of protein cargo targeted to the rhoptries, micronemes and DGs, and suggests a highly minimised regulatory secretory pathway in *Plasmodium* parasites. The question of how organelle specificity is achieved in the case of DGs remains to be addressed. Studies have shown that Sortilin also functions as an escorter in *T. gondii,* the Sortilin-like receptor (TgSORTLR) is essential for both microneme and rhoptry biogenesis in *T. gondii,* with parasites lacking TgSORTLR completely lacking these organelles (42). TgSORTLR localises to the Golgi compartment, where the luminal region of TgSORTLR interacts with the protein cargo whilst the cytoplasmic region interacts with vacuolar sorting factors including clathrin and AP adaptins (42). However, as TgSORTLR also interacts with protein cargo destined for the micronemes, a secondary level of control is required for correct protein targeting. This secondary level of control is currently unknown, possible factors involved in this process could include control of expression timing. It is important to note that *T. gondii* has no RAMA orthologue (41), so while the sorting mechanism may be equivalent in *T. gondii,* the mechanism of cargo sequestration into transport vesicles may differ.

Other factors necessary for correct protein transport to the rhoptries and micronemes in *T. gondii* include adaptor protein 1 (AP1), which is necessary for rhoptry biogenesis and correct sorting of proteins to the micronemes (43–45). The AP1 μ1 subunit interacts with tyrosine-based and di-leucine motifs in the cytoplasmic tails of TM proteins, such as the micronemal proteins MIC2 and MIC6, and is involved in targeting to the micronemes (45).

4.1.3 ***Dense granules***

But what do we know of protein transport to, and biogenesis of, the DGs? As described above, decreased expression of PfSortilin disrupts protein transport to the DGs, with the proteins instead aggregating in the endoplasmic reticulum and PV (30). This remains the only research that has been published about DG biogenesis or protein transport in *Plasmodium* parasites. Transport to the DGs has been studied more extensively in *T. gondii*, where it was discovered that the TM domain of the *T. gondii* DG protein GRA4 is necessary for correct sorting to the DGs (46). However, there are extensive differences between the DGs of the two apicomplexans. With the exception of GRA17 and GRA23, which are EXP2 orthologs that function in nutrient uptake in *T. gondii* but do not appear to function in protein transport (47), there are no *T. gondii* DG protein orthologues in *Plasmodium* parasites and *T. gondii* does not undergo schizogony (it retains its DGs throughout its life cycle), therefore, any finding in regards to targeting proteins to the DGs in *T. gondii* may not translate to *Plasmodium* parasites.

Interaction with PfSortilin is required for DG biogenesis, but the mechanism of PfSortilin recognition of DG proteins for transport is unknown (30,42). Further, as PfSortilin is also required for correct localisation of the other apical organelles, some additional control mechanism must be present to allow specified transport to the correct organelles. It is possible that PfSortilin is required for initial recognition and sorting of apical organelle proteins, but that recognition by another escorter is required downstream of this process for correct protein transport to the respective organelles. This process could require a more specific sorting signal or be controlled by expression timing. Early expression of RESA during the trophozoite stage has also been demonstrated to cause mis localisation to the PV, indicating that correct expression timing is also required for correct targeting (48). A search of malaria.tools (https://malaria.sbs.ntu.edu.sg/) indicates that PfSortilin is expressed at this stage, so an absence of this escorter protein is likely not the cause of mis localisation at this time.

The biogenesis of the apical organelles does not initiate simultaneously but rather at distinct rounds of nuclear division (49), with peak expression timing of many, but not all, apical organelle proteins mirroring the biogenesis timing of the organelle they are destined for (50). It is therefore possible that in some cases temporal regulation could be a factor in correct protein targeting. Indeed, alteration of expression timing can lead to mis-localisation of apical organelle proteins, as has been demonstrated for RESA. RESA localises to the PV when expressed under a heterologous early-stage trophozoite *Hsp86* promoter (48), and AMA-1, for

which altered expression timing leads to mistargeting to the parasite surface and cytoplasm (51). However, expression timing is only one factor involved in correct localisation, as concurrent expression timing of proteins destined to different compartments is common (43).

In summary, protein transport to apical organelles in *Plasmodium* parasites and other Apicomplexan parasites utilises diverse targeting mechanisms and involves interaction between proteins conserved among all eukaryotes and proteins specific to Apicomplexa.

Previous studies have determined the presence and location of targeting signal sequences through generation of fluorescently-tagged truncated protein chimeras, for example Richard *et al*. identified a bi-partite rhoptry targeting signal sequence in *P. falciparum* (40). Previous work had indicated that amino acids 1-344 of RAP1 are sufficient for rhoptry targeting (52), therefore initial fusions for testing the ability of GFP to be trafficked to rhoptries included a full length RAP1-GFP and a truncation consisting of amino acids 1-344 fused to GFP. Interestingly, whilst the full-length RAP1-GFP did localise to the rhoptry bulb as expected of native RAP1, the GFP-344 truncation localised to the rhoptry neck, co-localising with PfRON4. These results indicate that there is a bi-partite rhoptry signal sequence, with amino acids 1-344 containing a signal for targeting RAP1 to the rhoptry and the presence of an additional signal present in amino acids 344-782 for the correct localisation within the rhoptry. Richard *et al*. generated a series of N-terminal RAP1 truncations fused to GFP to identify the minimal region required for rhoptry targeting (40). Live fluorescence microscopy determined that a truncation including just the first 55 amino acids was correctly transported to the rhoptries, whereas a fusion containing the first 35 amino acids localised to the PV. Signal P analysis of RAP1 predicted cleavage between residues 21 and 22, indicating that the targeting signal required for transport to the rhoptries is contained in residues 22-55 (40).

My work aimed to address the question of DG biogenesis and protein targeting directly. We address two potential mechanisms concurrently, first, whether DG proteins contain a target sequence that is recognised by a targeting mechanism for transport to the DG, and second, whether protein transport to the DGs is passively regulated by timing of expression and is the default constitutive secretory pathway for soluble proteins, as seen in *T. gondii* (53), at the time the DGs are present in *Plasmodium* parasites. It is likely that correct protein localisation depends on both factors, where each is necessary, but alone not sufficient for transport to the DGs.

4.2 **Aims**

If a DG targeting signal sequence is present it can be identified by generating truncations of a known DG protein (e.g., RESA) tagged with a fluorescence protein and observing the movement and localisation of this fusion protein using fluorescence microscopy. Localisation can be observed by expression of the truncated protein using the RESA promoter in parasites that also expresses the native RESA protein (made distinguishable by tagging truncated RESA with a differently coloured tag, e.g., mNeonGreen). By observing whether truncations mis-localise (i.e. do not co-localise with native RESA), it will be possible to determine whether a section of sequence necessary for correct localisation to the DGs has been removed.

Alternatively, it is possible that DG protein targeting is controlled not by a target sequence but by late-stage expression timing. The effect of late-stage expression timing on protein localisation can be determined through generating a parasite line that express secreted non-DG proteins that are truncated to remove any conflicting targeting information and are fused to a fluorescent reporter, expressed under the RESA promoter. As no DG targeting sequence can be contained anywhere within this fusion, colocalization with a fluorescently-tagged version of the DG marker RESA will indicate that late-stage expression timing alone is sufficient for correct protein targeting to the DGs.

4.3 **Initial work**

To identify a possible DG targeting sequence, an initial strategy was developed for generation of progressively shorter truncations of the known DG protein RESA (figures 1 and 2). The truncations were to be fused to the red fluorescent protein TdTomato and introduced into parasites expressing the RESA-mNG fusion generated previously for studying DG biogenesis timing (Chapter 3). The truncations were to be integrated into the *pfs47* locus by Cas-9 mediated double crossover recombination and expressed under the *RESA* promoter to ensure correct expression timing. A series of primers were designed for amplification of the truncated regions (table 1). As a target sequence could be located nearer to either the C terminus or N terminus, portions of sequence were to be removed from each end of the protein in parallel, beginning with coarser truncations of about 65 amino acids. Four coarse truncations were to be generated with primers targeted sequentially further downstream from the N terminus of the protein, and five moving progressively upstream of the C terminus of the protein, including one containing only the signal sequence and PEXEL region as a control (figure 1). The recessed

signal sequence and PEXEL of RESA were to be amplified and included in all N-terminal truncations to retain correct targeting through the secretory pathway. A full-length RESA fusion was also to be generated to ensure that the TdTomato tag does not impede correct transport of the full protein to the DGs.

If any of the truncations were seen to mislocalise, finer truncations were to be produced until only the region necessary for targeting the fluorescence tag to the DGs remained, this being the target sequence. Once the target sequence had been isolated, it was to be fused to a fluorescent protein, in this case TdTomato and a signal sequence to promote entry into the secretory pathway, so that the intracellular localisation of the fusion protein could be tracked using fluorescence microscopy in parasites expressing a RESA-mNG fusion to determine DG localisation.

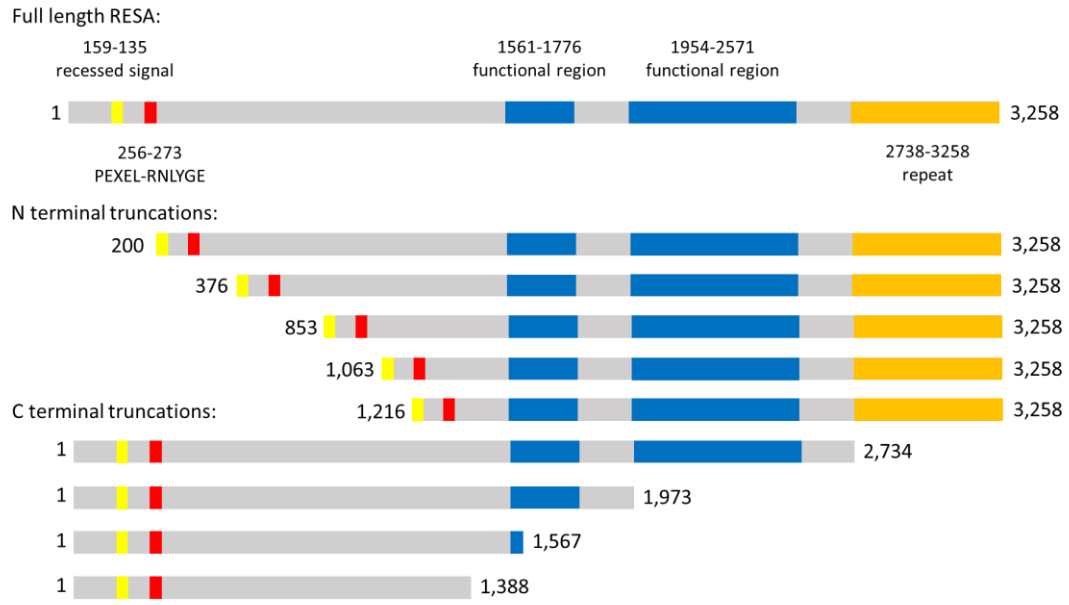

Figure 1. RESA truncations genes for target sequence identification. Diagram representing the planned RESA truncations to be produced, with nucleotides at the N and C-termini indicated. Functional regions (blue) are unlikely to contain a target sequence, these regions were not included in truncation design. The RESA recessed signal sequence (yellow) and PEXEL were included in all N-terminal truncations to allow targeting through the secretory pathway. A full-length RESA-TdTomato fusion was to be generated to ensure TdTomato tagging does not affect correct localisation to the DGs. Finally, an extreme C-terminal truncation comprising only a tagged signal/PEXEL region was planned, if this truncation was seen to localise to the DGs, temporal control of expression is likely the primary method of RESA targeting.

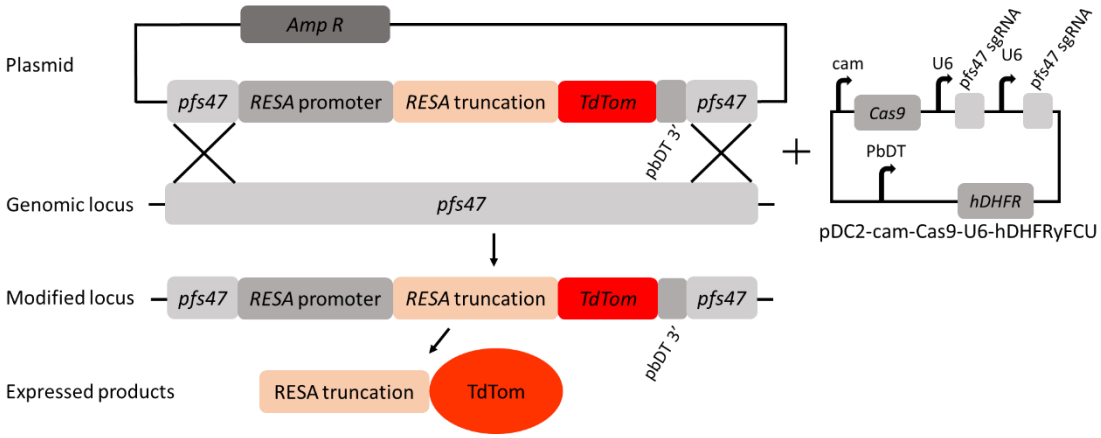

Figure 2. RESA truncation plasmid, integration into the *pfs47* locus and expressed product. A schematic of RESA truncation-TdTomato plasmid design, integration event into the *pfs47* locus via double crossover recombination, altered genomic locus, and expressed fusion product.

Table 1. RESA-truncation primers. Primers designed for amplification of N-terminal and C-terminal RESA and signal sequence fragments, TdTomato, and PEXEL region for inclusion in the N terminal truncations. 15 pb InFusion overhangs are shown in red.

RESA N terminal truncation primers

Name	Binding site	Sequence	InFusion overhang
TMR022	RESA 375 bp from START	CCAATAGTTGTAAGTCCTGATATTGATCATACAAATATTTTGGG	PEXEL and signal peptide
TMR023	RESA 852 bp from START	CCAATAGTTGTAAGTGCTTTATCCAACCAAATTCAATATTCATGC	PEXEL and signal peptide
TMR024	RESA 1,062 bp from START	CCAATAGTTGTAAGTCCACAACAAGAAGAACCAGTCCAAACC	PEXEL and signal peptide
TMR025	RESA 1,215 bp from START	CCAATAGTTGTAAGT GATGCTCTTTATACAGATGAAGATTTGTTATTTGATTTGG	PEXEL and signal peptide
TMR026	RESA 3' end	GCCCTTGCTCACCAT TTCATCATATTCTTCATTGTGTTCTTCAACATTTTC	TdTomato 5' end
TMR032	TdTom 3' end	CGTTATGTTACTCGACTACTTGTACAGCTCGTCCATGCC	plasmid backbone
TMR020	RESA 5' end with PEXEL	CTAAATAATTCCTAGATGAGACCTTTTCATGCATATAGTTGG	RESA promoter 3' end
TMR021	RESA PEXEL region	ACTTACAACTATTGGGTTTTCAGAATCAGC	Truncation

RESA C terminal truncation primers

Name	Binding site	Sequence	InFusion overhang
TMR027	531 bp upstream of STOP	GCCCTTGCTCACCATAGCATCATGTTCTACATTTTCTTCAGC	TdTomato 5' end
TMR028	1,224 bp upstream of STOP	GCCCTTGCTCACCATCCATTTTGAATCACCAGCTATACATGG	TdTomato 5' end
TMR029	1,595 bp upstream of STOP	GCCCTTGCTCACCATGGGGATTTCAATTGTTGGAGCTGCTTC	TdTomato 5' end
TMR030	1,887 bp upstream of STOP	GCCCTTGCTCACCAT GTCATCAGCAGTGTGTTCTTCTACATGTTC	TdTomato 5' end
TMR031	2,913 bp upstream of STOP	GCCCTTGCTCACCAT GGGTAAACCAAATACCTGACTTACAACTATTGG	TdTomato 5' end
TMR020	RESA 5' end	CTAAATAATTCCTAGATGAGACCTTTTCATGCATATAGTTGG	RESA promoter
TMR032	TdTom 3' end	CGTTATGTTACTCGACTACTTGTACAGCTCGTCCATGCC	plasmid backbone

If a target signal sequence is not identified (no truncation causes mis-localisation), it is possible that protein localisation to DGs is primarily dependent on expression timing, where proteins destined for the DGs need only to get into the secretory pathway at the correct time to locate to the DGs. This work will be facilitated by the results of the DG formation timing experiments described in chapter 3. As we have demonstrated that DGs are formed very late in the schizont stage, it is possible that all secretory proteins in the secretory pathway expressed after a certain point that do not have a target sequence sending them elsewhere go to the DGs as default.

We were unable to follow this initial approach due to difficulties in generating components of the planned plasmid constructs. Due to the highly repetitive and AT-rich sequence of *RESA*, we were unable to successfully amplify the regions of *RESA* which were required to generate the longer truncations, and the full-length *RESA* fusion required to investigate the potential effect of TdTomato on protein localisation. Additionally, despite attempts at re-codonising, we

were unable to successfully amplify *TdTomato*. Therefore, we adopted a simplified approach that was designed to address the core questions of this chapter: is a target sequence present within DG proteins or is expression timing alone the controlling factor in protein targeting to the DGs?

4.4 **Final approach**

Next, a simplified approach was developed to investigate the existence of a DG target sequence using only extreme C-terminal RESA truncations. The extreme C-terminal truncations contained just enough of the RESA signal sequence to target it to the secretory system and the PEXEL, with only minimal sequence remaining that could contain additional targeting information. These fusions were introduced into parasites expressing the RESA-mNG fusion designed for DG biogenesis imaging. These short truncations will allow us to quickly determine whether a sequence necessary for correct targeting was present while avoiding the need to generate multiple extended regions of *RESA*. Further work could then identify the location of the targeting sequence. These truncations were fused to the red fluorophore mCherry.

To determine whether the results were replicable between different DG proteins and not unique to RESA, this approach was repeated in a second DG protein, PTEX88, expressed from the RESA promoter to ensure late-stage expression (figure 3). It is possible to use RESA in truncation experiments as previous RESA-GFP studies have indicated that addition of a relatively large tag on RESA does not impede correct localisation (54). Following cleavage of the PEXEL sequence the RESA truncation measures 21 amino acids in length, fused to mCherry which is 237 amino acids in length this produces a RESA truncation-mCherry fusion of 30 kDa. Following cleavage of the signal sequence of PTEX88 the truncation measures 7 amino acids in length, producing a truncation of 28.5 kDa.

To investigate the role of expression timing on protein localisation to the DGs, mCherry fusion lines were generated in which truncations of the secreted non-DG proteins, KAHRP and AMA1, were fused to mCherry and expressed under the native RESA promoter to ensure late-stage expression timing (figure 4). Following cleavage of the signal sequence the AMA1 and KAHRP truncations measure 6 amino acids in length and produce a final mCherry fusion protein of 28.5 kDa. C-terminal truncation of these proteins ensured that any non-DG targeting signals which could influence protein localisation were removed. If these fusions are observed

to localise to the DGs it will demonstrate that DG protein targeting is controlled by late-stage expression timing due to expression under the RESA promoter. If the RESA truncations localise to the DGs, these non-DG fusion proteins will also address the possibility that some sequence within the remaining C-terminal region is controlling protein localisation, as this sequence will not be contained within a non-DG protein, indicating that expression timing must be the only contributing factor. Additionally, the role of early expression timing on DG protein trafficking was investigated by generating a RESA truncation-mCherry fusion expressed under the Cam promoter (peak expression occurs at the trophozoite stage, 28-30 hpi (50)), theorising that if correct localisation of DG proteins is controlled solely by late-stage expression timing then this fusion will not localise to the DGs (figure 5). However, to give reliable data the transgenic parasites would need to contain a full-length RESA-mCherry fusion expressed under *pCam* rather than a truncation, as truncation will have removed any targeting sequence present and it is therefore impossible to determine which factor, targeting sequence or expression timing, is influencing localisation.

If the RESA truncations do not localise to the DGs, this indicates that some sequence required for correct targeting of DG proteins to the DGs has been removed and therefore that DG proteins contain a targeting sequence. However, if the mCherry fusions expressed under the RESA promoter co-localised with the full-length RESA-mNG fusion it is likely that expression under the *RESA* promoter is the mechanism driving DG localisation.

It is possible that truncation of RESA could lead to misfolding and protein degradation in the ER. Western blot analysis can be used to verify that an mCherry-fusion of the expected size is produced using anti-mCherry antibody. Here a band the size of mCherry alone would indicate degradation of the RESA truncation. If misfolding is verified, similar truncations could be tried, or a model RESA structure can be generated for prediction of regions which can be kept intact to help retain structural stability.

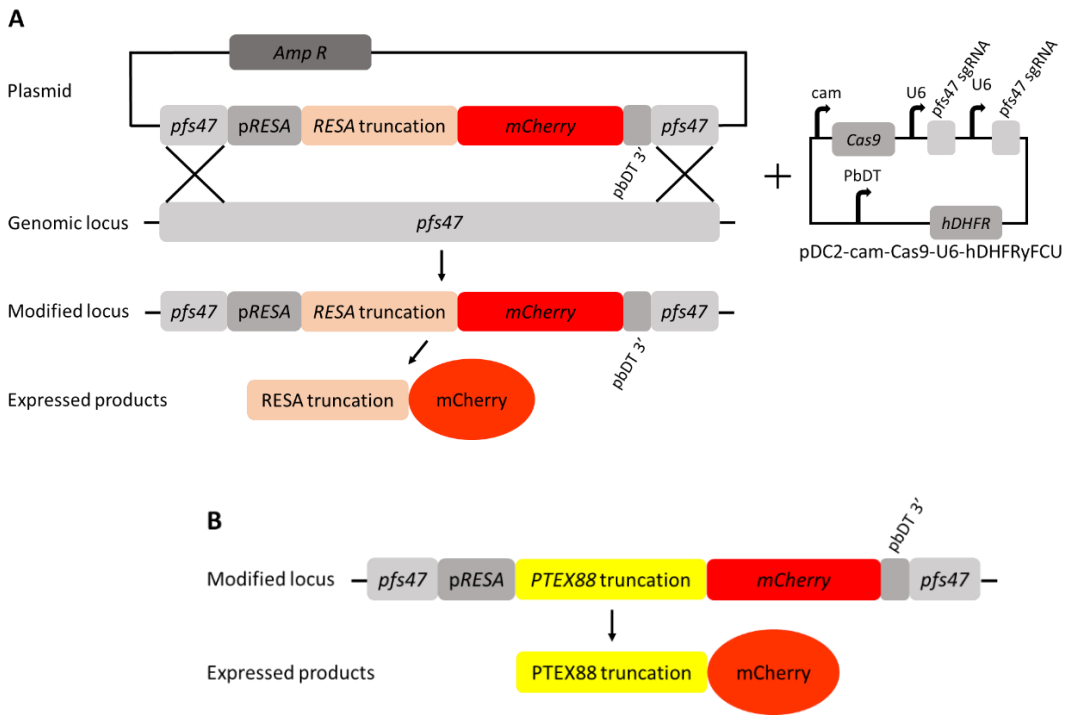

Figure 3. Strategy for production of parasites producing extreme C-terminal RESA truncation-mCherry fusion and extreme C-terminal PTEX88 truncation-mCherry fusion. (A) A schematic of the extreme C' RESA truncation-mCherry fusion, integration into the *pfs47* locus via double crossover recombination mediated by Cas9, and expression of fusion protein product under the RESA promoter. (B) PTEX88-mCherry fusion protein product.

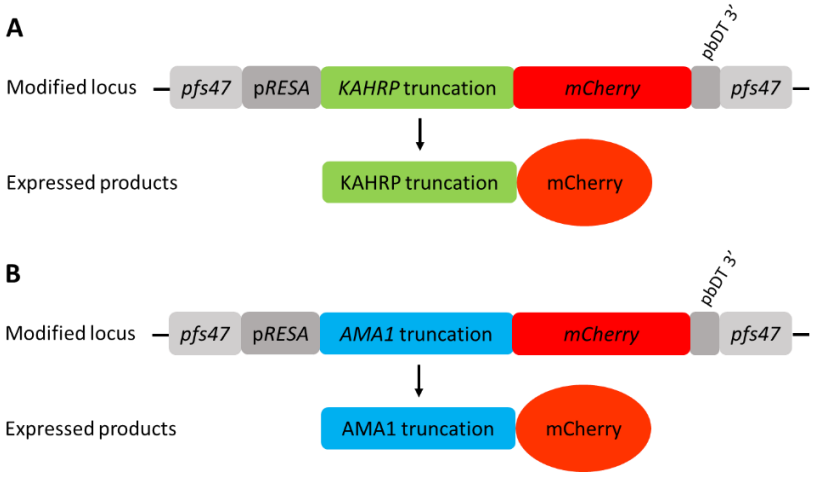

Figure 4. KAHRP and AMA1 truncation–mCherry integration and protein products. KAHRP-mCherry (A) and AMA1-mCherry (B) fusion protein product, plasmid design, promoter control, and integration strategy are the same as for RESA truncation-mCherry fusion as shown in figure 2.

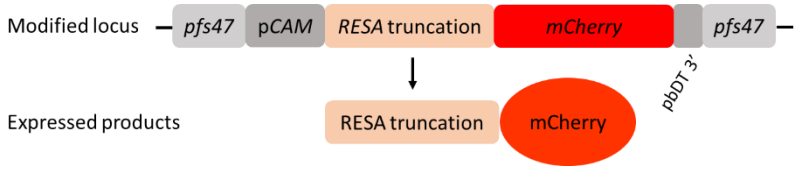

Figure 5. pCAM extreme C' RESA truncation–mCherry fusion integration and protein products. Extreme C' RESA truncation-mCherry fusion integration into the *pfs47* locus under the CAM promoter and protein product. With the exception of the presence of the CAM promoter expression in place of the RESA promoter, plasmid design and integration strategy are the same as for RESA truncation-mCherry fusion shown in figure 2.

4.5 **Results:**

4.5.1 ***Generation of reporter truncations for analysis of DG targeting control***

To determine whether DG proteins contain a targeting sequence necessary for correct localisation to the DGs, extreme C-terminal truncations of the well-documented DG markers RESA and PTEX88 were produced. To easily determine whether these truncated proteins are transported to the DGs, they were fused to mCherry and introduced into plasmids for integration at the *pfs47* locus through CRISPR-Cas9-mediated double-crossover recombination.

To determine whether late-stage expression timing is the primary factor controlling targeting to the DGs, truncations of the non-DG proteins AMA1 (which is a micronemal protein retained on the surface of the parasite (57)) and KAHRP (which is exported into the host erythrocyte (58)) were expressed under the RESA promoter and fused to mCherry for similar integration into the *pfs47* locus. Finally, to analyse the effect of early expression timing on DG protein localisation, the RESA truncation mCherry fusion was expressed under the Cam promoter and introduced that into the *pfs47* locus following the same double crossover integration strategy described above.

All of the truncation-mCherry plasmids were introduced into TV002 parasites that express the full length RESA-mNG fusion described in Chapter 3 (59,60). Integration into the *pfs47* locus was verified using PCR (figure 6A) using the primers indicated (figure 6B and C) and immunoblotting revealed that the expected protein products are produced (figure 6 D). Live parasite imaging revealed that the transgenic parasites displayed red fluorescence surrounding the parasite at the PV at the schizont stage, and within the parasites in egressed merozoites.

Table 2: The primer pairs used to verify integration of the mCherry fusions into the *pfs47* locus.

Primer pairs		Expected fragment size
5′ (pRESA): CVO120 + CVO505		2,355 bp
5′ (pCam): CVO120 + CVO694		1135 bp
3′: CV0119 + CVO070		1,942 bp
WT: CVO119 + CVO120		2179 bp
Name	Sequence	Binding site
CVO070	CACACATAAAATGGCTAGTATGAATAGCC	Binds pbDT3′ 207 bp downstream of *mCherry*
CVO119	CATTCCTAACACATTATGTGTATAACATTTTATGC	1020-985 bp upstream of *pfs47* ATG
CVO120	CATATGCTAACATACATGTAAAAAATTACAATCAG	3′ end of *pfs47* gene
CVO505	GGCTCCTAGGAATTATTTAGATATTTTCTTATTATAAATTATGTAAAAGTAAAAAATTAAAACC	*RESA* promoter immediately upstream of ATG
CVO694	TTAGCTAATTCGCTTGTAAGAGGTACTCTCGTTTATGC	Binds immediately upstream of pCam

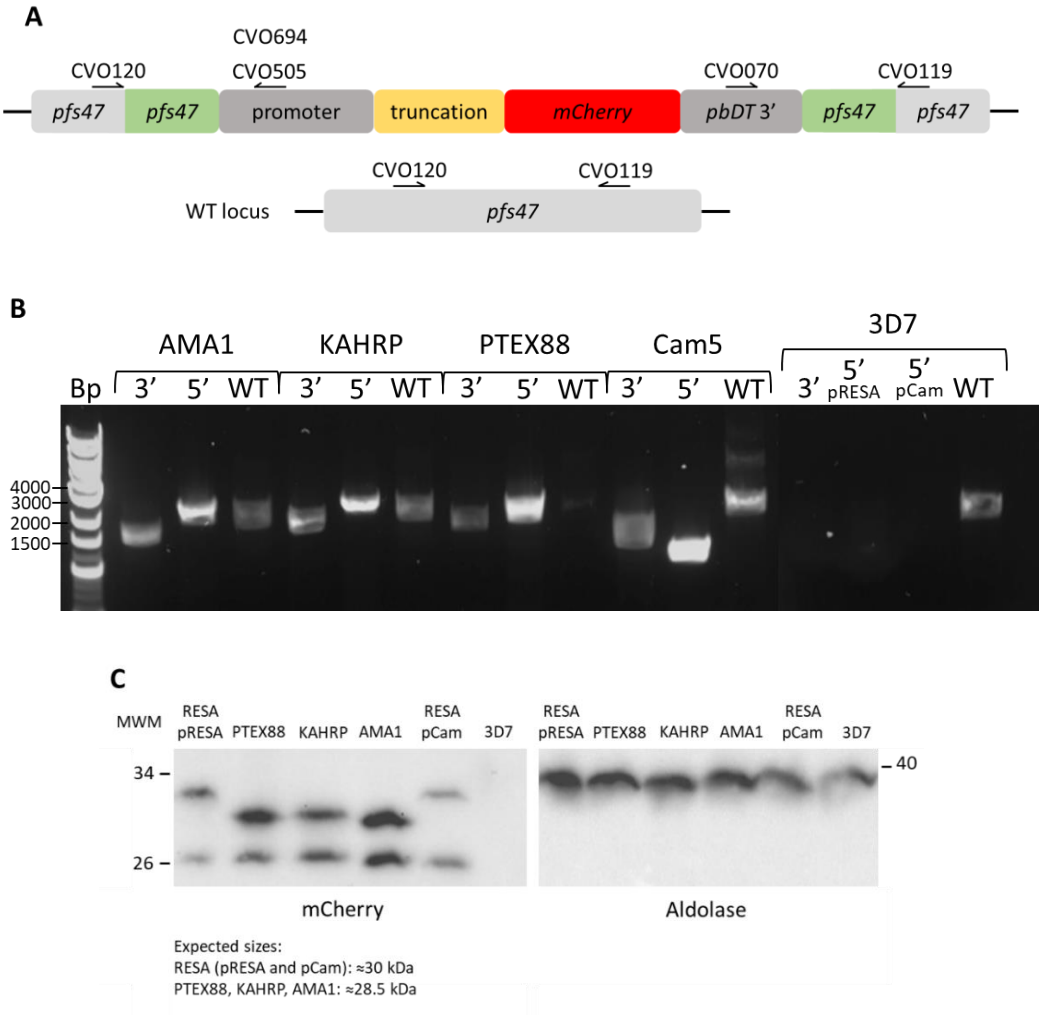

Figure 6. Verification of integration of the mCherry fusions into the *pfs47* locus. (A) A representation of the primer binding sites within the integration regions of the mCherry truncation fusions. Green indicates *pfs47* homology regions used for the integration, pale grey indicates genomic *pfs47* (primers CVO120 and CVO119 produce a WT band of 2339 bp), yellow indicates the gene fragment encoding the truncated secreted protein and red indicates the gene encoding mCherry, dark grey indicates promoter and untranslated 3' regions. (B) PCR verification of integration into the *pfs47*

locus by PCR using the primers indicated in table 2, that bind in positions shown in figure 6A. Note that some WT-specific PCR product was detected in each transfectant. 3' indicates the primer pair specific for the 3' end of the integrant, 5' indicates the primer pair specific for the 5' end of the integrant and WT indicates the primer pairs specific for the wild type *pfs47* locus. (C) Immunoblot using anti-mCherry antibodies verifying the production of the truncation-mCherry fusions. A second band is also present in each lane that corresponds to the size of digested mCherry. Anti-aldolase is used as loading control (right-hand panel).

4.5.2 *Fluorescence microscopy of mCherry fusions*

The localisation of the mCherry fusions in relation to the mNG-RESA DG marker was determined by live microscopy. As RESA expression initiates during the late schizont stage of the intraerythrocytic life cycle (61), for imaging of schizonts, tightly synchronised late-stage parasites were blocked from egress with ML10 (62) and imaged at around 47-48 hours post-invasion. For imaging of single merozoites parasites were similarly synchronised and blocked, but in this case ML10 was removed prior to imaging to allow egress and imaging of newly released merozoites.

Red mCherry fluorescence was not seen to co-localise with green mNeonGreen fluorescence of the native RESA DG marker at either stage for any of the mCherry truncation fusions generated. In comparison to the punctate foci of mNG fluorescence of the DG marker, mCherry signal appears to localise to the PV, surrounding the developing merozoites within late stage segmented schizonts (figures 7, 8, 9). In individual merozoites some mCherry signal is visible as a focus within the body of the merozoite that is distinct from and non-overlapping with the mNG fluorescence of the DG marker (figures 9, 10, 11). Interestingly, the RESA-mCherry truncation signal was visible in the host cell cytosol in early rings but becomes visible in the trophozoite stage (figure 12).

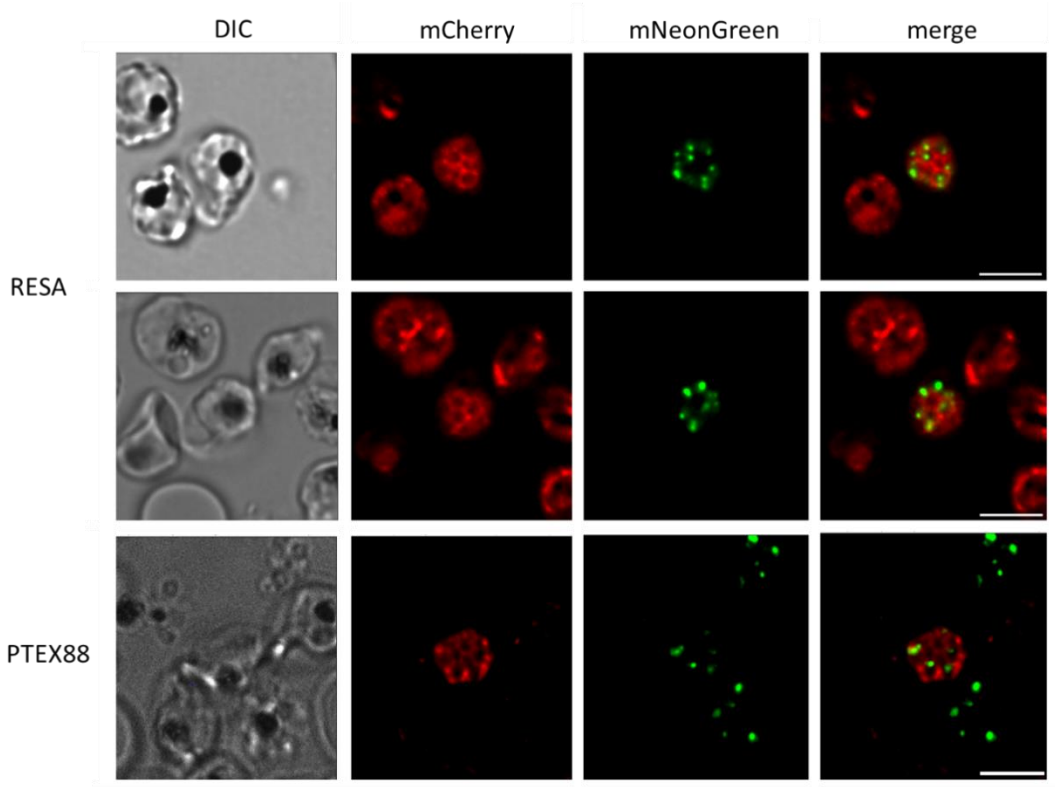

Figure 7. Late-stage segmented schizonts expressing RESA-mNG and either RESA truncation-mCherry or PTEX88-truncation mCherry. Fluorescence microscopy of late stage segmented schizonts of the line expressing RESA-mNG and RESA extreme C' truncation-mCherry fusion or PTEX88 truncation mCherry showing diffuse mCherry signal appearing to surround segmented daughter merozoites within the PV space, giving a honeycomb pattern appearance. mNG signal indicates DGs, appearing as punctate foci of fluorescence within the daughter merozoites. Size bars indicate 5 µm.

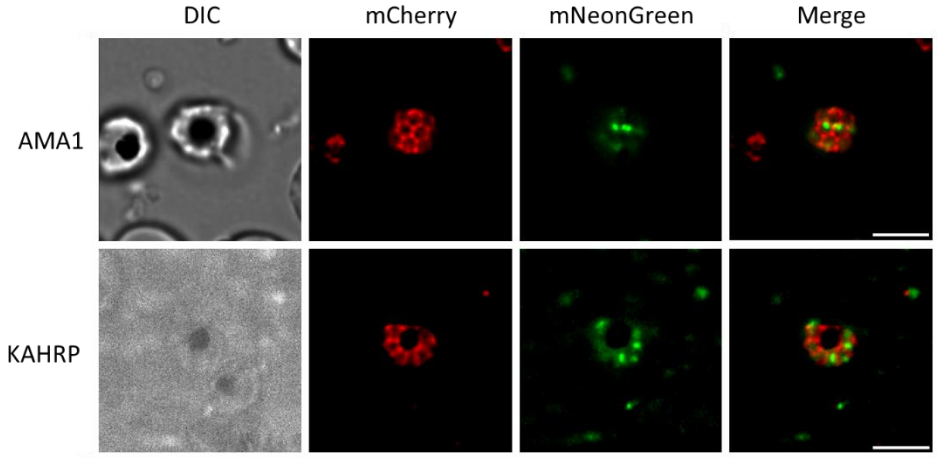

Figure 8. Late stage segmented schizonts expressing AMA1 and KAHRP-mCherry and RESA-mNG fusions. Fluorescence microscopy images showing mCherry signal of AMA1 and KAHRP-

mCherry fusions localising to the PV space between the segmented daughter merozoites and the PVM. mNG signal indicates DGs, localising to punctate foci within the daughter merozoites. Size bar indicates 5 µm.

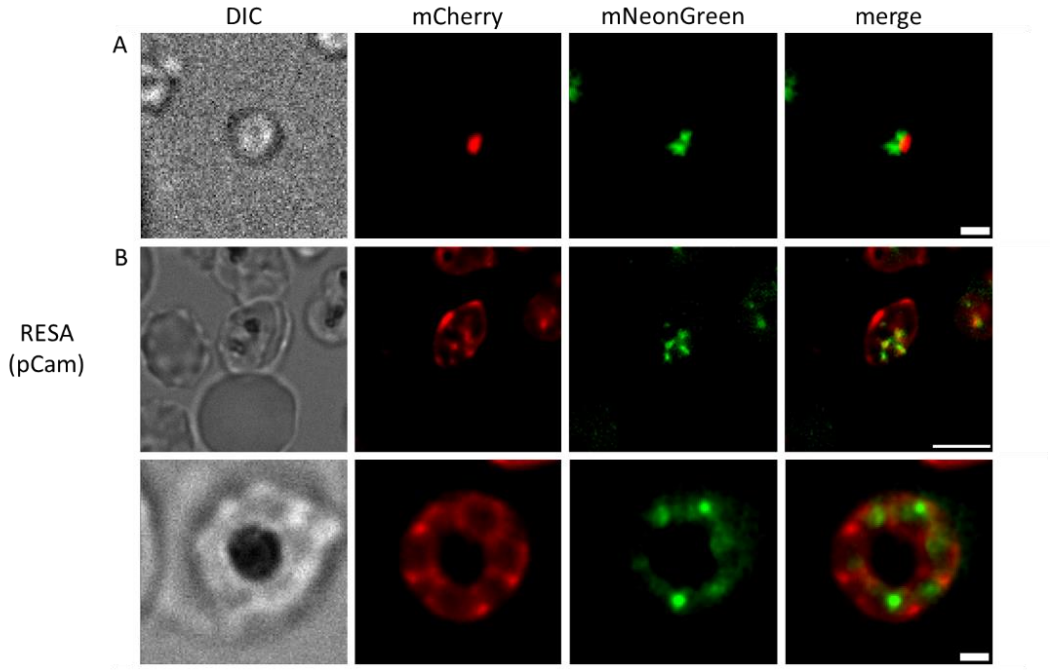

Figure 9. Fluorescence microscopy images of an individual merozoite and late stage segmented schizonts expressing RESA truncation-mCherry fusion expressed under the CAM promoter and RESA-mNG. (A) Fluorescence microscopy image of a single merozoite expressing RESA truncation-mCherry fusion under the Cam promoter. mNG and mCherry signal is visible at separate non-overlapping locations within the merozoite. Scale bar indicates 1 µm. (B) Fluorescence microscopy images of late stage segmented schizonts expressing RESA truncation-mCherry fusion under the Cam promoter. Diffuse mCherry signal appears to surround segmented daughter merozoites within the PV space, mNG signal indicates DGs, localising to punctate foci within the daughter merozoites. Size bar indicates 5 µm (top), and 1 µm (bottom).

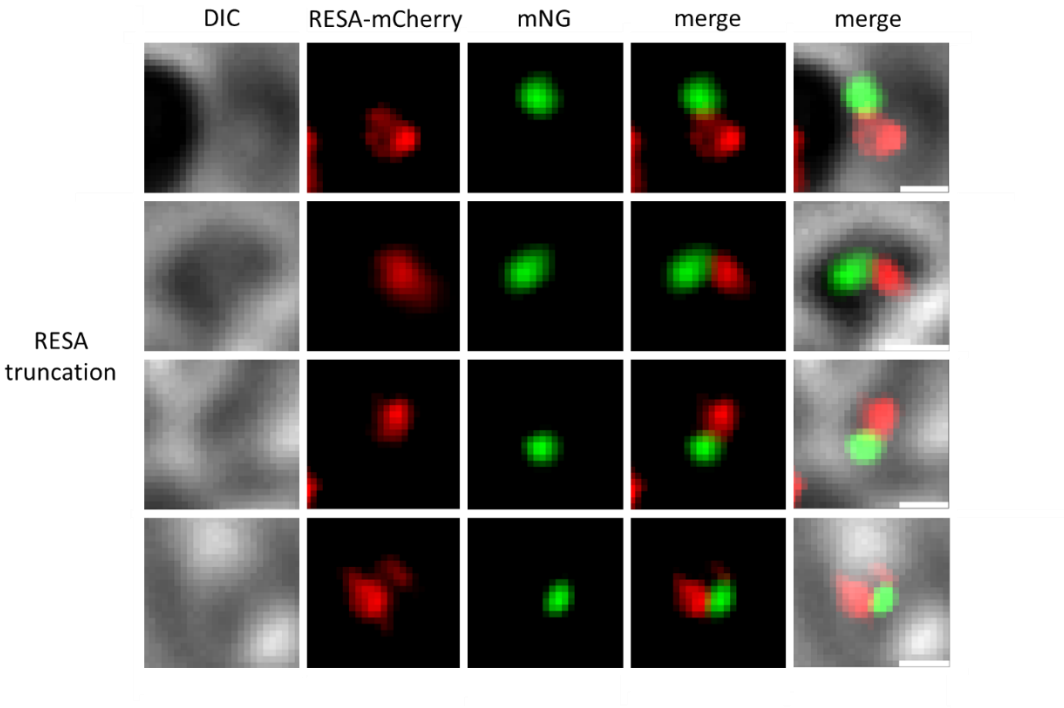

Figure 10. Individual merozoites expressing RESA truncation-mCherry and RESA-mNG. Fluorescence microscopy images of individual merozoites expressing RESA truncation-mCherry and RESA-mNG DG marker fusions. mCherry and mNG signal are visible as distinct and non-overlapping foci within the merozoite. Size bar indicates 0.5 µm. The DIC outline of merozoite is unclear due to high confluence of cells.

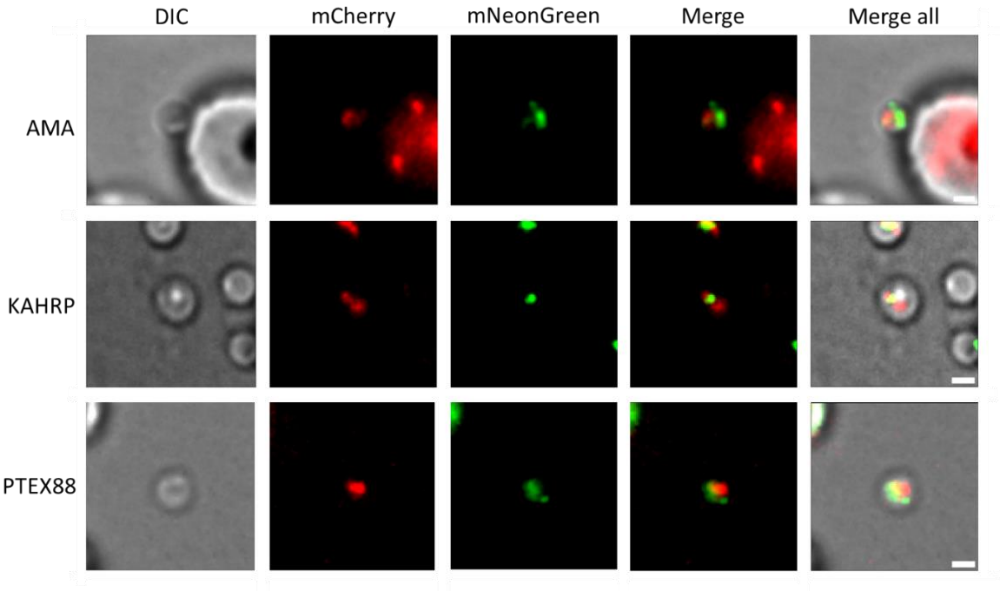

Figure 11. Individual merozoites expressing AMA1, KAHRP, and PTEX88 truncation-mCherry fusions and RESA-mNG. Fluorescence microscopy images of individual merozoites expressing

AMA1, HAHRP and PTEX88 truncation-mCherry and RESA-mNG DG marker fusions. mCherry and mNG signal are visible as distinct and non-overlapping foci within the merozoite. Scale bar 1 µm.

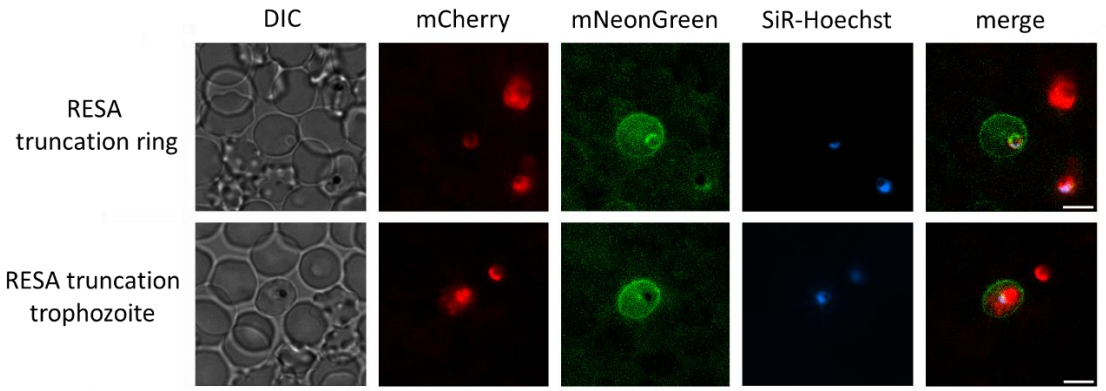

Figure 12. Newly invaded rings and trophozoites expressing RESA truncation-mCherry and RESA-mNG fusions. No mCherry signal is visible in the cytoplasm of erythrocyte containing newly invaded rings. RESA-mNG signal localises to the host cell periphery (above). mCherry signal is visible in cytoplasm of trophozoites. DNA is visualised with SiR-Hoechst far-red DNA dye. Size bar indicates 5 µm.

4.6 **Discussion**

The aim of these experiments was to determine whether DG proteins contain a targeting signal sequence that is required for their transport to the DGs or whether expression timing alone controls DG protein targeting. Fluorescence imaging of late stage segmented schizonts of the RESA and PTEX88 mCherry fusion lines showed that in contrast to mNG signal that localised to punctate foci within the daughter merozoites, mCherry signal is visible in a diffuse patterning that appears to surround the daughter merozoites which indicates accumulation in the PV, the default destination of the secretory pathway (63,64). This indicates that these proteins are not diverted into a pathway that transports them to the DGs, and therefore that DG proteins of *P. falciparum* may contain a targeting sequence that is necessary for correct localisation of proteins to the DGs, as neither of the extreme C-terminal truncated DG proteins co-localised with RESA-mNG DG marker. In merozoites, the mCherry signal is visible as a focus that does not co-localise with the full-length RESA-mNG DG marker. The observation that the mCherry fusion is present in merozoites indicates that it is produced at the time the merozoites are produced.

In newly invaded rings of parasites expressing the RESA truncation-mCherry fusion, mCherry signal does not localise to the erythrocyte periphery with full–length RESA-mNG signal and is not visible within the cytoplasm (figure 12). This is because, as the imaging results have shown, the RESA-mCherry truncation does not localise to the DGs for storage until invasion for timed release into the host cell, instead it is secreted into the PV where it is lost upon egress. Instead mCherry signal becomes visible with diffuse cytoplasmic staining in trophozoites as RESA expression continues through the ring and trophozoite stages, and the truncation lacks the regions necessary for recognition by the transport machinery required for transport to the host cell periphery and does not contain the regions required for binding to the host cell spectrin tetramers (figure 12).

In agreement with the results above, imaging of the AMA1 and KAHRP truncation-mCherry fusions indicates that late-stage expression timing under the RESA promoter is necessary but not sufficient for localisation of proteins to the DGs. Late-stage schizonts displayed diffuse mCherry signal within the PV. This indicates that the AMA1 and KAHRP truncation-mCherry fusions successfully entered the secretory system, but that expression under the RESA promoter was not sufficient to target them to the DGs, and without any additional targeting information the AMA1 and KAHRP truncation-mCherry fusions were instead secreted into the PV. In free merozoites, the mCherry signal was seen in foci which were distinct from and did not colocalise with mNG fluorescence.

The parasites in which RESA truncation-mCherry fusion expression is controlled by the Cam promoter displayed the same non-DG signal as above, with mCherry signal visible in the PV of schizonts and in a single focus within the body of free merozoites. However, we cannot draw conclusions about the effect of early DG protein expression from these data as the mCherry is fused to an extreme C-terminal truncation of RESA, meaning that the lack of mCherry punctate patterning within the parasite may be due to removal of a targeting sequence from the protein. Future work could address this by generating a full-length RESA-mCherry fusion under the Cam promoter, however during this project we have not been able to amplify full-length RESA by PCR, likely due to the highly repetitive and AT-rich nature of the gene. It may be possible to use a gene synthesising service to obtain the full-length RESA fragment for these purposes. It was not possible to use another DG protein in the place of RESA as all other *P. falciparum* DG proteins localise to the PV and PVM upon secretion during invasion with the exception of LSA3 which is exported, meaning that they are not appropriate for use as DG markers as the signal present in the PV or host cell obscures signal from within the parasite when imaging

DGs in the schizont stage. For this reason, there is a lack of DG markers in *P. falciparum* which can be used to verify protein localisation, and insertion of a full-length *RESA* fusion at the non-native locus is the only option currently available to verify the effect of expression under the Cam promoter on DG protein localisation. Additionally, it would be difficult to determine co-localisation as the RESA-mNG DG marker is under the native RESA promoter and therefore would not be expressed at earlier stages for comparison with the mCherry signal expressed under the Cam promoter. As many DG proteins are expressed earlier in the intraerythrocytic life cycle before DG organelles are present, localisation to regions such as the PVM further indicates that early expression of DG proteins does not lead to early DG formation.

Generation of a full-length RESA fusion would also be necessary to verify that target sequence removal, not the presence of the mCherry tag, is the cause on protein mis-localisation to the PV. However, the patterning seen is unlikely to be an effect of the mCherry tag as use of fluorescent reporters of similar size to mCherry is a well-established technique in studies of this kind, and RESA-GFP fusions have been shown to correctly localise to the DGs in previous work (48,54).

It is unclear what compartment the mCherry foci seen within free merozoites represent. It is possible that the truncations are localising to some intermediate compartment within the secretory system, or to a previously undescribed secretory organelle. There has been some indication of a novel secretory organelle termed the mononeme in the literature, identified through localisation of rhomboid-1 protease (65), therefore our finding is not the first indication that *Plasmodium* parasites may contain another as-yet undescribed secretory organelle. Alternatively, it is possible that some portion of the truncations remains in the ER, although this is unlikely as mCherry signal localising to the PV in schizonts demonstrated that secretion was not inhibited in the truncations.

Future work could aim to identify the transport machinery involved in recognition of DG proteins for specific trafficking to the DG organelles. One mechanism that could be explored to this end is immunoprecipitation, which could be used to purify DG proteins and associated transport machinery. The role of GPI-anchored RAMA in transport of RAP1 to the rhoptries was first identified by immunoprecipitation (40). Future work could also aim to locate the target signal sequence through purchasing commercially synthesised sequentially shorter C-terminal truncations. Once identified, the targeting signal can be verified by fusion to a non-DG

secretory protein expressed under the RESA promoter and imaging localisation in parasites expressing the RESA-mNG fusion.

4.7 **Conclusion**

When considered together, the results described in this study indicate for the first time that both the presence of an as yet undescribed DG targeting signal sequence and late-stage expression timing are necessary, but alone not sufficient, for correct localisation of DG proteins to DGs in *Plasmodium falciparum*.

Bibliography

1. Schwarz DS, Blower MD. The endoplasmic reticulum: structure, function and response to cellular signalling. Cell Mol Life Sci. 2016 Jan;73(1):79–94.

2. Bashan A, Yonath A. Correlating ribosome function with high-resolution structures. Trends Microbiol. 2008 Jul;16(7):326–35.

3. Novick P, Ferro S, Schekman R. Order of events in the yeast secretory pathway. Cell. 1981 Aug;25(2):461–9.

4. Hou J, Tyo KEJ, Liu Z, Petranovic D, Nielsen J. Metabolic engineering of recombinant protein secretion by *Saccharomyces cerevisiae*. FEMS Yeast Res. 2012 Aug;12(5):491–510.

5. Alberts B, Johnson A, Lewis J. Transport from the ER through the Golgi Apparatus. In: Molecular Biology of the Cell. 4th ed. New York: Garland Science; 2002.

6. Coffey MJ, Jennison C, Tonkin CJ, Boddey JA. Role of the ER and Golgi in protein export by Apicomplexa. Curr Opin Cell Biol. 2016 Aug;41:18–24.

7. D'Arcangelo JG, Stahmer KR, Miller EA. Vesicle-mediated export from the ER: COPII coat function and regulation. Biochim Biophys Acta BBA - Mol Cell Res. 2013;1833(11):2464–72.

8. Lord C, Ferro-Novick S, Miller EA. The Highly Conserved COPII Coat Complex Sorts Cargo from the Endoplasmic Reticulum and Targets It to the Golgi. Cold Spring Harb Perspect Biol. 2013 Feb 1;5(2):a013367–a013367.

9. Smirle J, Au CE, Jain M, Dejgaard K, Nilsson T, Bergeron J. Cell Biology of the Endoplasmic Reticulum and the Golgi Apparatus through Proteomics. Cold Spring Harb Perspect Biol. 2013 Jan 1;5(1):a015073–a015073.

10. Zerial M, McBride H. Rab proteins as membrane organizers. Nat Rev Mol Cell Biol. 2001 Feb;2(2):107–17.

11. McLauchlan H, Newell J, Morrice N, Osborne A, West M, Smythe E. A novel role for Rab5–GDI in ligand sequestration into clathrin-coated pits. Curr Biol. 1998 Jan;8(1):34–45.

12. Novick P, Zerial M. The diversity of Rab proteins in vesicle transport. Curr Opin Cell Bio. 1997;9(4):496–504.

13. Quevillon E, Spielmann T, Brahimi K, Chattopadhyay D, Yeramian E, Langsley G. The *Plasmodium falciparum* family of Rab GTPases. Gene. 2003 Mar;306:13–25.

14. Ayong L, Pagnotti G, Tobon AB, Chakrabarti D. Identification of *Plasmodium falciparum* family of SNAREs. Mol Biochem Parasitol. 2007 Apr;152(2):113–22.

15. Hong W. SNAREs and traffic. Biochim Biophys Acta. 2005 Jun 30;1744(3):493–517.

16. Mayer A. What drives membrane fusion in eukaryotes? Trends Biochem Sci. 2001 Dec;26(12):717–23.

17. Pelham H. SNAREs and the specificity of membrane fusion. Trends Cell Biol. 2001 Mar 1;11(3):99–101.

18. Jahn R, Scheller RH. SNAREs — engines for membrane fusion. Nat Rev Mol Cell Biol. 2006 Sep;7(9):631–43.

19. Leabu M. Membrane fusion in cells: molecular machinery and mechanisms. J Cell Mol Med. 2006 Apr;10(2):423–7.

20. Fasshauer D, Eliason WK, Brunger AT, Jahn R. Identification of a minimal core of the synaptic SNARE complex sufficient for reversible assembly and disassembly. Biochemistry. 1998;37(29):10354–62.

21. Parlati F, McNew JA, Fukuda R, Miller R, Söllner TH, Rothman JE. Topological restriction of SNARE-dependent membrane fusion. Nature. 2000 Sep;407(6801):194–8.

22. Aurrecoechea C, Brestelli J, Brunk BP, Dommer J, Fischer S, Gajria B. PlasmoDB: a functional genomic database for malaria parasites. Nucleai Acids Res. 2009;37:D539–43.

23. Bisio H, Ben Chaabene R, Sabitzki R, Maco B, Baptiste Marq J, Gilberger TW, *et al*. The zip code of vesicle trafficking in apicomplexa: Sec1/munc18 and snare proteins. mBio. 2020 Oct 20;11(5):1–21.

24. Krai P, Dalal S, Klemba M. Evidence for a Golgi-to-Endosome Protein Sorting Pathway in *Plasmodium falciparum*. Sinnis P, editor. PLoS ONE. 2014 Feb 25;9(2):e89771.

25. Margos G, Bannister LH, Dluzewski AR, Hopkins J, Williams IT, Mitchell GH. Correlation of structural development and differential expression of invasion-related molecules in schizonts of *Plasmodium falciparum*. Parasitology. 2004 Sep;129(3):273–87.

26. Kats LM, Cooke BM, Coppel RL, Black CG. Protein Trafficking to Apical Organelles of Malaria Parasites – Building an Invasion Machine. Traffic. 2008 Feb;9(2):176–86.

27. Agop-Nersesian C, Naissant B, Ben Rached F, Rauch M, Kretzschmar A, Thiberge S, *et al*. Rab11A-Controlled Assembly of the Inner Membrane Complex Is Required for Completion of Apicomplexan Cytokinesis. Sibley LD, editor. PLoS Pathog. 2009 Jan 23;5(1):e1000270.

28. Kaderi Kibria KM, Rawat K, Klinger CM, Datta G, Panchal M, Singh S, *et al*. A role for adaptor protein complex 1 in protein targeting to rhoptry organelles in *Plasmodium falciparum*. Biochim Biophys Acta - Mol Cell Res. 2015 Mar 1;1853(3):699–710.

29. Morse D, Webster W, Kalanon M, Langsley G, McFadden GI. *Plasmodium falciparum* Rab1A Localizes to Rhoptries in Schizonts. Tsuboi T, editor. PLOS ONE. 2016 Jun 27;11(6):e0158174.

30. Hallée S, Boddey JA, Cowman AF, Richard D. Evidence that the *Plasmodium falciparum* Protein Sortilin Potentially Acts as an Escorter for the Trafficking of the Rhoptry-Associated Membrane Antigen to the Rhoptries. mSphere. 2018 Jan 3;3(1).

31. Kremer K, Kamin D, Rittweger E, Wilkes J, Flammer H, Mahler S, *et al*. An Overexpression Screen of *Toxoplasma gondii* Rab-GTPases Reveals Distinct Transport Routes to the Micronemes. PLOS Pathog. 2013;9(3):e1003213.

32. Rached FB, Ndjembo-Ezougou C, Chandran S, Talabani H, Yera H, Dandavate V, *et al*. Construction of a *Plasmodium falciparum* Rab-interactome identifies CK1 and PKA as Rab-effector kinases in malaria parasites. Biol Cell. 2012 Jan;104(1):34–47.

33. Kehrer J, Singer M, Lemgruber L, Silva PAGC, Frischknecht F, Mair GR. A Putative Small Solute Transporter Is Responsible for the Secretion of G377 and TRAP-Containing Secretory Vesicles during *Plasmodium* Gamete Egress and Sporozoite Motility. PLoS Pathog. 2016;12(7):e1005734.

34. Treeck M, Struck NS, Haase S, Langer C, Herrmann S, Healer J, *et al*. A conserved region in the EBL proteins is implicated in microneme targeting of the malaria parasite *Plasmodium falciparum*. J Biol Chem. 2006 Oct 20;281(42):31995–2003.

35. Striepen B, Soldati D, Garcia-Reguet N, Dubremetz JF, Roos DS. Targeting of soluble proteins to the rhoptries and micronemes in *Toxoplasma gondii*. Mol Biochem Parasitol. 2001;113:45–53.

36. Feige MJ, Hendershot LM. Disulfide bonds in ER protein folding and homeostasis. Curr Opin Cell Biol. 2011 Apr;23(2):167–75.

37. Hammoudi PM, Maco B, Dogga SK, Frénal K, Soldati-Favre D. *Toxoplasma gondii* TFP1 is an essential transporter family protein critical for microneme maturation and exocytosis. Mol Microbiol. 2018 Jul 1;109(2):225–44.

38. Breinich MS, Ferguson DJP, Foth BJ, van Dooren GG, Lebrun M, Quon DV, *et al*. A Dynamin Is Required for the Biogenesis of Secretory Organelles in *Toxoplasma gondii*. Curr Biol. 2009 Feb 24;19(4):277–86.

39. Sherling ES, Perrin AJ, Knuepfer E, Russell MRG, Collinson LM, Miller LH, *et al*. The *Plasmodium falciparum* rhoptry bulb protein RAMA plays an essential role in rhoptry neck morphogenesis and host red blood cell invasion. Billker O, editor. PLOS Pathog. 2019 Sep 6;15(9):e1008049.

40. Richard D, Kats LM, Langer C, Black CG, Mitri K, Boddey JA, *et al*. Identification of Rhoptry Trafficking Determinants and Evidence for a Novel Sorting Mechanism in the Malaria Parasite *Plasmodium falciparum*. Striepen B, editor. PLoS Pathog. 2009 Mar 6;5(3):e1000328.

41. Sherling ES, Perrin AJ, Knuepfer E, Russell MRG, Collinson LM, Miller LH, *et al*. The *Plasmodium falciparum* rhoptry bulb protein RAMA plays an essential role in rhoptry neck morphogenesis and host red blood cell invasion. Billker O, editor. PLOS Pathog. 2019 Sep 6;15(9):e1008049.

42. Sloves PJ, Delhaye S, Mouveaux T, Werkmeister E, Slomianny C, Hovasse A, *et al*. *Toxoplasma sortilin*-like receptor regulates protein transport and is essential for apical secretory organelle biogenesis and host infection. Cell Host Microbe. 2012 May 17;11(5):515–27.

43. Ngô HM, Yang M, Paprotka K, Pypaert M, Hoppe H, Joiner KA. AP-1 in *Toxoplasma gondii* mediates biogenesis of the rhoptry secretory organelle from a post-Golgi compartment. J Biol Chem. 2003 Feb 14;278(7):5343–52.

44. Hoppe HC, Joiner KA. Cytoplasmic tail motifs mediate endoplasmic reticulum localization and export of transmembrane reporters in the protozoan parasite *Toxoplasma gondii*. Cell Microbiol. 2000;2(6):569–78.

45. Venugopal K, Marion S. Secretory organelle trafficking in *Toxoplasma gondii*: A long story for a short travel. Int J Med Microbiol. 2018 Oct 1;308(7):751–60.

46. Karsten V, Hegde RS, Sinai AP, Yang M, Joiner KA. Transmembrane Domain Modulates Sorting of Membrane Proteins in *Toxoplasma gondii*. J Biol Chem. 2004;279(25):26052–7.

47. Gold DA, Kaplan AD, Lis A, Cl Bett G, Rosowski EE, Cirelli KM, *et al*. The *Toxoplasma* dense granule proteins GRA17 and GRA23 mediate the movement of small molecules between the host and the parasitophorous vacuole HHS Public Access. Cell Host Microbe. 2015;17(5):642–52.

48. Rug M, Wickham ME, Foley M, Cowman AF, Tilley L. Correct promoter control is needed for trafficking of the ring-infected erythrocyte surface antigen to the host cytosol in transfected malaria parasites. Infect Immun. 2004 Oct;72(10):6095–105.

49. Liffner B, Diaz A, Blauwkamp J, Anaguano D, Frolich S, Muralidharan V, *et al*. Atlas of *Plasmodium falciparum* intraerythrocytic development using expansion microscopy. eLife. 2023;12.

50. Kucharski M, Tripathi J, Nayak S, Zhu L, Wirjanata G, Van Der Pluijm RW, *et al*. A comprehensive RNA handling and transcriptomics guide for high-throughput processing of *Plasmodium* blood-stage samples. Malar J. 2020 Dec;19(1):363.

51. Kocken CHM, Van Der Wel AM, Dubbeld MA, Narum DL, Van De Rijke FM, Van Gemert GJ, *et al*. Precise timing of expression of a *Plasmodium falciparum*-derived transgene in *Plasmodium berghei* is a critical determinant of subsequent subcellular localization. J Biol Chem. 1998 Jun 12;273(24):15119–24.

52. Baldi DL, Andrews KT, Waller RF, Roos DS, Howard RF, Crabb BS, *et al*. RAP1 controls rhoptry targeting of RAP2 in the malaria parasite *Plasmodium falciparum*. EMBO J. 2000;19(11):2435–43.

53. Griffith MB, Pearce CS, Heaslip AT. Dense granule biogenesis, secretion, and function in *Toxoplasma gondii*. J Eukaryot Microbiol. 2022 Apr; Available from: https://onlinelibrary.wiley.com/doi/10.1111/jeu.12904

54. Tarr SJ, Moon RW, Hardege I, Osborne AR. A conserved domain targets exported PHISTb family proteins to the periphery of *Plasmodium* infected erythrocytes. Mol Biochem Parasitol. 2014;196(1):29–40.

55. Aikawa M, Torii M, Sjolander A, Berzins K, Louis Millers AH. Pf155/RESA Antigen Is Localized in Dense Granules of *Plasmodium falciparum* Merozoites. Exp Parasitol. 1990;71(3):326–9.

56. Chisholm SA, Kalanon M, Nebl T, Sanders PR, Matthews KM, Dickerman BK, *et al*. The malaria PTEX component PTEX 88 interacts most closely with HSP 101 at the host–parasite interface. FEBS J. 2018 Jun;285(11):2037–55.

57. Bannister LH, Hopkins JM, Dluzewski AR, Margos G, Williams IT, Blackman MJ, *et al*. *Plasmodium falciparum* apical membrane antigen 1 (PfAMA-1) is translocated within micronemes along subpellicular microtubules during merozoite development. J Cell Sci. 2003 Sep 15;116(18):3825–34.

58. Rug M, Prescott SW, Fernandez KM, Cooke BM, Cowman AF. The role of KAHRP domains in knob formation and cytoadherence of *P. falciparum*-infected human erythrocytes. Blood. 2006 Jul 1;108(1):370–8.

59. Collins CR, Das S, Wong EH, Andenmatten N, Stallmach R, Hackett F, *et al*. Robust inducible Cre recombinase activity in the human malaria parasite *Plasmodium falciparum* enables efficient gene deletion within a single asexual erythrocytic growth cycle. Mol Microbiol. 2013;88(4):687–701.

60. Knuepfer E, Napiorkowska M, Van Ooij C, Holder AA. Generating conditional gene knockouts in *Plasmodium* – a toolkit to produce stable DiCre recombinase-expressing parasite lines using CRISPR/Cas9. Sci Rep. 2017 Jun 20;7(1):3881.

61. Tan QW, Mutwil M. Malaria.tools-comparative genomic and transcriptomic database for *Plasmodium species*. Nucleic Acids Res. 2020 Jan 1;48(D1):D768–75.

62. Ressurreiçao M, Thomas Id JA, Nofal SD, Flueck C, Moon RW, Baker DA, *et al*. Use of a highly specific kinase inhibitor for rapid, simple and precise synchronization of *Plasmodium falciparum* and *Plasmodium knowlesi* asexual blood-stage parasites. Plos One. 2020;15(7).

63. Waller RF, Reed MB, Cowman AF, McFadden GI. Protein trafficking to the plastid of *Plasmodium falciparum* is via the secretory pathway. EMBO J. 2000;19(8):1794–802.

64. Wickham ME, Rug M, Ralph SA, Klonis N, McFadden GI, Tilley L, *et al*. Trafficking and assembly of the cytoadherence complex in *Plasmodium falciparum*-infected human erythrocytes. EMBO J. 2001;20(20):5636–49.

65. Singh AP, Buscaglia CA, Wang Q, Levay A, Nussenzweig DR, Walker JR, *et al*. *Plasmodium* Circumsporozoite Protein Promotes the Development of the Liver Stages of the Parasite. Cell. 2007 Nov 2;131(3):492–504.

Chapter 5: Exploring the dense granule proteome, an APEX proximity biotinylation approach

5.1 **Background**

The maintenance of discreet, defined subcellular compartments containing proteins of specific function allows the existence of organelles with specific functions. Therefore, an understanding of the organellar function and complex cellular processes the organelle controls can be gained by determining the proteomes of such compartments. Historically, many approaches have been used to describe protein localisation at a subcellular level, in a field that is undergoing rapid development as new techniques become available. Subcellular localisation of proteins was originally investigated through targeted approaches for individual proteins, for example cell fractionation coupled with immunoblotting verification (1,2). As imaging-based techniques progressed, these were used to map subcellular protein localisation, however these antibody based and GFP-fusion based assays were only appropriate for use in localising a number of proteins of interest to a subcellular location, not for investigating the entire protein components of an organelle of interest (3). The event of sub-cellular fractionation coupled with mass spectrometry (MS) proteomics techniques has allowed researchers to better define organellar proteomes and on a wider scale. MS is used in characterisation and quantification of proteins in complex mixtures. For analysis of samples containing multiple proteins a 'bottom up' approach is commonly used in which the proteins are separated by molecular and isoelectric point, and enzymatically digested before being processed by the mass spectrometer and identified by peptide mass fingerprinting (4,5). The peptide 'fingerprint' outputs are computationally matched to protein sequence databases for protein identification (6).

More recently, the development of machine learning techniques has allowed researchers to predict cellular location based on protein quantification from multiple cellular fractionations by MS (7). Currently, proximity-based biotinylation (PBD) methods in combination with MS are potentially revolutionising the investigation of protein-protein interactions and organellar proteomics, allowing biotin labelling of proteins proximal to a bait protein of interest (to which the biotin enzyme is fused) in their native environment.

Co-immunoprecipitation can be used to identify interaction partners of a protein by isolating the protein of interest through immunoprecipitation and then identifying interacting proteins using immunoblotting techniques (8). This technique however is less suitable for mapping protein composition of entire organelles.

Cell fractionation involves the homogenisation of cells to form a suspension of cellular components. Homogenisation can occur in various ways, including osmotic shock, ultrasonic vibration, freeze thawing or pressure alterations. These techniques act to break the larger membranous structures of the cell including the plasma membrane and ER membranes, whilst leaving smaller membranous structures intact. Cellular components are then separated into fractions by differential centrifugation, whereby membranes, organelles and subcellular particles are separated by size and density. As components separate predictably based on known sedimentation rates, fractions containing the components of interest can then be isolated from the gradient for further analysis (1,9). Simple centrifugation in this manner only separates components based on large size differences. A greater degree of separation can be achieved by layering the homogenate onto a dilute salt solution. Upon centrifugation the homogenate components will progress through the salt solution at varying rates as a series of distinct bands, this process is called velocity sedimentation. For velocity sedimentation to work correctly, convective mixing, which occurs when a dense solution (such as the organelle containing homogenate) is layered above a less dense solution (such as the saline solution), must be avoided. This can be addressed by addition of a shallow sucrose gradient to the centrifuge tube. As the dense end of the gradient at the bottom of the centrifugation tube, this means that the salt solution is now progressively denser than the solution above it, allowing homogenate fractionation through the salt solution without convective mixing negatively impacting the fraction separation (9). Western blot analysis using antibodies against the target protein can then be used to determine which fraction contains the protein of interest, and as cell components fraction into predictable bands, the protein of interest can be assigned a subcellular location. Leriche and Dubremetz reported the first successful isolation of *Toxoplasma gondii* organelles using subcellular fractionation. Here subcellular fractionation on a Percoll gradient was used to isolate *T. gondii* tachyzoite rhoptries (although the fraction was contaminated with DGs), and monoclonal antibodies raised against these fractions were used to identify a number of rhoptry proteins by western blotting and immunoelectron microscopy. The identified rhoptry proteins included ROP1, ROP2, ROP3 and ROP 4 (previously described by Sadak *et al.*) (10), ROP7 (Previously described by Dubremetz *et al.*) (11) and the previously undescribed ROP5 (2).

More recently, MS has allowed researchers to identify all proteins within centrifugal fractions. Bell *et al.* (2001) used MS to identify 81 proteins within the Golgi apparatus of rat hepatic cells, including one novel Golgi-associated protein GPP34, which was later demonstrated to

help regulate Golgi membrane trafficking in eukaryotes (12). The work of Andersen *et al.* (2003) describes the use of sucrose gradient fractionation coupled with MS proteomic analysis to identify components of the human centrosome in the interphase of the cell cycle by quantitively characterising proteins contained within several centrifugal fractions (13). They identify and validate 23 previously undescribed components of the human centrosome and 41 likely candidates. This technique, often termed hyperLOPIT, has been used to describe a comprehensive subcellular proteomic atlas of *T. gondii.* Whole cell fractionation of *T. gondii* extracellular tachyzoites resulted in enrichment profiles for a wide range of organelle biomarkers. Of the 1,916 proteins that were assigned subcellular compartments, only 302 had described or hypothesised functions, and the subcellular localisation of the majority of these had not been previously experimentally verified. The use of hyperLOPIT in this instance represented a great advancement in the knowledge of the protein composition of subcellular compartments of *T. gondii* tachyzoites. For the apical organelles, this work identified 59 novel rhoptry proteins, 22 novel microneme proteins and 83 novel DG proteins, more than doubling the number of identified proteins for rhoptries and micronemes and tripling the number of described DG proteins (14).

Centrifugal fractioning can work well for isolation of many organelles, such as the mitochondrion, where the techniques was used to create MitoCarta, a map of the mitochondrial proteome (15). However, many organelles and other sites of interest such as the contact points between organelles do not purify well by centrifugation gradient. Fractionation of DGs has been attempted previously but to date has only been successful in the related Apicomplexan parasite *Sarcocystis tenella*, where fractionation on a sugar gradient was made possible by the drastically increased size and abundance of the DGs in relation to other Apicomplexan parasites (16).

Microscopy-based approaches can also be used in determining protein localisation, although these methods are more suited to investigating the localisation of single proteins, as described in Chapter 3 for localisation of HSP40, as opposed to investigating the proteome of a specific organelle or region. Kumar *et al*. reported the first proteome-scale analysis of protein localisation in a eukaryote, using plasmid-based over expression and epitope tagging of 60% of the *Saccharomyces cerevisiae* proteome. High-throughput immunolocalization of the epitope-tagged gene products allowed localisation of 2744 proteins (17). Some potential issues associated with this technique include that protein overexpression may cause abnormal subcellular locations due to saturation of intracellular transport pathways, and epitope tagging

of partial open reading frames could obscure localisation signals. Another approach at subcellular mapping through high throughput imaging technique employed by Huh *et al.* (2003) aimed to avoid these potential pitfalls by generating yeast strains in which full-length proteins expressed under their endogenous promoter were tagged at the C terminus with GFP by introducing the coding sequence for GFP directly preceding the stop codon, with the aim of maintaining WT levels of protein expression and expression timing whilst allowing live fluorescence microscopy. Hu *et al.* were able to classify 75% of the yeast proteome into 22 distinct subcellular locations and analyse the subcellular localisations of 70% of proteins for which localisations were previously unknown (3). Immunofluorescence imaging (IFA) can also be used to systematically map the spatial distribution of a cellular proteome. Thul *et al.* used this approach to map the human proteome in cultivated cell lines, a culmination of over 80,000 images targeting 12,003 proteins and utilising 13,993 antibodies, the resulting data describing the proteomes of 30 compartments and sub structures, and 13 major organelles in total. Although this technique can be very powerful, it requires access to vast numbers of reliable antibodies (18).

The emergence of proximity-labelling techniques over the last decade, coupled with MS has allowed the characterisation of the proteomes of specific organelles and other sub-cellular regions of interest as well as protein interactomes and complexes. Proximity labelling enzymes such as HRP and APEX function by generating reactive oxygen species that in the presence of biotin-phenol cause the covalent biotinylation of proteins that are proximal to the protein to which the labelling enzyme is fused. In the case of BioID the biotin ligase BirA* is fused to a protein of interest and can mediate the attachment of biotin to proximal proteins in the presence of biotin and ATP (19). Cells are then lysed, and the biotinylated proteins can then be isolated by biotin-streptavidin affinity purification for analysis by MS. In a semi-quantitative method, proteins with the highest abundance are usually selected for further analysis, although this excludes proteins of lower abundance that may have equal biological relevance. Quantitative MS can be used to generate a more complete list of high-confidence candidate proteins, which involves metabolic labelling such as stable isotope labelling by amino acid in cell culture (SILAC). Briefly, SILAC involves the cultivation of two cell lines in parallel, one if grown with normal medium, the other with medium containing amino acids labelled with non-radioactive heavy isotopes. Proteins from both cell lines are combined for MS analysis with chemically identical peptides can be distinguished by their differing isotope composition and therefore their differing mass. The ratio of peak intensities between identical peptide pairs

represents the abundance ration of the peptides (20–22). As cells remain intact during labelling, the potential incidence of false positives which may be caused by cell structural disruption or contaminants during sub-cellular fractionation is greatly limited.

There are three enzymes that have been most commonly used in protein proximity labelling to date: horseradish peroxidase (HRP), the *Escherichia coli* biotin ligase BirA and engineered ascorbate peroxidase (APEX). BioID utilises a mutated *E. coli* biotin ligase BirA (23–25), which in its endogenous environment functions to mediate the covalent attachment of biotin to target proteins in the presence of ATP by catalysing the conversion of biotin to a reactive biotinoyl 05'-AMP, which in turn labels a lysine residue of acetyl-CoA carboxylase with high specificity (26). BirA can be used to verify protein interaction through fusion of BirA to a bait peptide and expression in a line which also expresses a prey peptide-biotin acceptor peptide (BAP) fusion, where biotinylation verifies bait and prey interaction (27). To engineer more promiscuous labelling, the active site of BirA was mutated to allow labelling of proximal proteins which do not contain the BAP. This mutated form is termed BirA*, in which the mutated active site (R118G) has greatly reduced affinity for biotin-5'-AMP, which is freed from the active site and reacts non-specifically with the lysine residues of proximal proteins (25). BioID was first used in mammalian cells to investigate the interaction partners and proximal proteins of lamin-A (LaA), an intermediate filament protein that is a component of the nuclear lamina, a structural constituent of the nuclear envelope (25). This study identified many of the known interaction partners of LaA and a novel nuclear-envelope associated protein SLAP75, validating use of BioID in identifying both bait protein-protein interaction partners and neighbouring proteins in a native cellular environment (25). Schnider *et al*. used BioID to investigate the protein content of the PVM in *Plasmodium berghei*, a region for which investigations had historically been confounded by difficulties in separating the PVM from other membranous structures such as the PPM using traditional centrifugal fractioning (28). EXP1 is a DG protein that localises to the PV as part of the PTEX protein export machinery. The Burda lab generated a BirA*-EXP1 fusion to biotinylate proteins at the PVM, biotinylated proteins were then isolated by streptavidin-affinity purification and analysed by liquid chromatography-tandem mass spectrometry (LC-MS/MS) which identified 61 known and candidate PVM proteins. Validation by immunofluorescence microscopy led to the identification of three novel PVM proteins, serine/threonine protein phosphatase UIS2 and two conserved *Plasmodium* proteins of unknown function (PlasmoDB accession numbers PBANKA_0519300 and PBANKA_0509000) (28). In expanding the number of known *P.*

berghei PVM proteins, this work experimentally validated the use of BioID as a method for investigating the proteome of subcellular compartments of *Plasmodium* parasites.

HRP is a peroxidase that can also be used in proximity biotinylation experiments. HRP when activated by H_2O_2 converts biotin-phenol substrates into highly reactive radical oxygen species that covalently biotinylates the electron-rich amino acids of nearby proteins. The structure of the HRP enzyme is supported by two Ca^{2+} binding sites and four disulphide bonds. Consequently, the structure of HRP is disrupted in reducing conditions such as the cytosol, where HRP is inactive (29). HRP is however active in oxidising environments such as the Golgi and the extracellular cell surface. HRP can also be used for EM tagging, as in the presence H_2O_2 it catalyses the polymerisation of 3,3'diaminobenzamide, which precipitates to generate EM contrast upon fixation with OsO_4. There are two substrates that are commonly used in HRP proximity labelling, the enzyme mediated activation of radical source (EMARS) which utilises fluorescein aryl azide or biotin aryl azide (30–33), and selective proteomic proximity labelling assay using tyramide (SPPLAT) which uses biotin-tyramide, also known as biotin-phenol (34,35). Loh *et al.* 2016 used HRP to map the proteome of the synaptic cleft of living neurons by proximity biotinylation with biotin-phenol and H_2O_2, allowing assignment of many known synaptic proteins to specific cleft types, and identifying dozens of new synaptic cleft candidate proteins (36).

First introduced by Rhee *et al.* APEX is an engineered monomeric ascorbate peroxidase derived from soybean. In a similar chemistry to that described for HRP, upon exposure to H_2O_2 APEX catalyses the oxidation of biotin-phenol to transitory biotin-phenoxyl radicals (<1ms), which in turn biotinylate electron-rich amino acids (cysteine, histidine, and tyrosine) in proteins within a range of several nanometres (37,38). APEX is particularly well suited to proteomic profiling of organelles as biotin-phenoxyl radicals are not membrane permeable. Rhee *et al.* initially used APEX to describe the proteome of the human mitochondrial matrix, identifying 495 proteins, 31 of which had not been located to the mitochondria previously (37). The method allowed mapping with high specificity, distinguishing between the intermembrane space and proteins of the inner membrane that face the mitochondrial matrix. This specificity allowed reassignment of many protein localisations from the intermembrane space and the outer membrane to the matrix (37). Recent work that aimed to identify new transmission blocking vaccine candidates has used APEX to identify 50 novel ookinete microneme proteins in *P. berghei* (39). One of the identified proteins, akratin, was determined to be essential for microgametogenesis and ookinete migration through the mosquito midgut epithelium.

Some of the most significant differences between the peroxidase and biotin ligase techniques include the substrate used, the amino acid residues that are linked to biotin, the environments in which the enzymes are functional and the reaction kinetics. Whilst BioID uses biotin as its substrate, APEX uses biotin-phenol, and HRP can use biotin-phenol and biotin aryl azide. Some studies have indicated that biotin-phenol may not cross membranes as efficiently as biotin (34,35) which is actively transported across mammalian cell membranes (37). Additionally, the half-life of the biotin-5'-AMP radicals produced by BioID is in the range of minutes, which in contrast with the much shorter half-life of APEX-generated biotin-phenoxyl radicals (<1ms), indicates that APEX may have a smaller labelling radius than BioID. APEX has a labelling radius of 20 nm (40,41), BioID a radius of 10nm (42) and HRP a far larger one of 200-300 nm, however attempts to measure the labelling radius of these enzymes have occurred in different cellular environments using different approaches, meaning that they cannot be reliably compared. Like HRP, APEX polymerization and precipitation of DAB creates contrast for EM visualisation of APEX expression sites after fixation with OsO_4. Unlike HRP however, APEX is functional in a reducing environment and therefore can be used for labelling in the cell cytosol.

BioID has relatively slow kinetics compared to those of HRP (5-10 minutes) and APEX (≈1 minute), with an optimal labelling time of 15-24 hours. It has been suggested that such a prolonged labelling time limits the application of BioID in the investigation of dynamic processes such as cell signalling and could result in disrupted protein function. In response, TurboID was developed by the Ting Lab (43) to address the slow reaction kinetics of BioID, as whilst APEX labels proteins more rapidly with an optimal labelling time of around 1 minute, the reaction catalyst H_2O_2 can be toxic to living cells and an alternative fast acting proximity labelling method is therefore desirable. TurboID has two additional mutations to BioID (15 total from the original BirA) and a reaction time of 10 minutes, allowing investigation of interactions in transient and dynamic cellular processes whilst avoiding any oxidative stress toxicity which may arise from the use of H_2O_2. Additionally, BioID requires incubation at 37°C, whereas labelling by TurboID can be achieved at room temperature and APEX labelling has been demonstrated to take place at 25°C in *Drosophilla melanogaster,* at room temperature in yeast as well as at 37° (44,45). The variation in working temperatures of TurboID and APEX makes them suitable for use in varying model organisms.

When choosing the optimal method for investigating the DG proteome it was necessary to consider the varying capabilities of the described techniques. The object of this study was not

to produce a *P. falciparum* proteome wide imaging study as described by Kumar for *S. cerevisiae*, the technique chosen had to be appropriate for investigating protein content of a specific organelle (17). Traditional methods for organellar isolation would include centrifugal fractionation, however this has only been successfully performed for isolation of DGs in *Sarcocystis tenella* due to the increased size and number of the DGs (16), and this method is also prone to contamination with non-target membranous cellular components. HRP, BioID, and APEX proximity labelling techniques are appropriate for use in membrane bound organelles like the DGs, however, as the results of the DG biogenesis timing experiments detailed in chapter 3 indicated that DGs are present for an average of 37 minutes prior to egress a technique with a short reaction time was required. HRP and BioID have optimal reaction times of 5-10 minutes and 15-24 hours respectively, APEX was chosen for use in this study as it is the labelling technique with the fastest reaction time of ≈1 minute.

5.2 **Aims**

In order to identify new DG proteins I generated parasites that contain a fusion of the APEX protein to the DG protein RESA, initially in 3D7 and subsequently also in iGP parasites (which are parasites in which gametocytogenesis can be induced by addition of the Shield-1 reagent), which was engineered from *Plasmodium falciparum* NF54 by conditional overexpression of the sexual commitment factor GDV1 (46). This RESA- APEX fusion (figure 1, table 1) was developed to allow targeted expression of APEX to the DGs, where biotinylation would allow spatially distinct protein profiling to occur within the DG (figure 2). In addition to labelling proteins within the DG compartment this method may allow identification of proteins involved in DG protein trafficking and organelle biogenesis. Experiments were ultimately carried out in the modified iGP parasites as they would allow comparison of the DG proteome of asexual and sexually committed schizonts. Whilst asexual intraerythrocytic stages are sequestered in the host microvasculature, immature gametocytes are sequestered in the host bone marrow and spleen until they are released back into the circulation as mature gametocytes to be taken up by the mosquito vector in a blood meal (47,48). These differing maturation environments may necessitate different remodelling requirements for the host cell, which may lead to DGs of committed schizonts containing a different complement of erythrocyte remodelling proteins to those of non-committed schizonts. After performing the biotinylation reaction in these engineered parasites, biotinylated proteins can then be isolated via streptavidin affinity

purification protocols (37,38). In this case I used streptavidin magnetic beads (Pierce™, Thermo Fisher Scientific) to pull down biotinylated proteins. These isolated proteins can be identified in the MS/MS output and can then be compared to the list of candidate DG proteins predicted through expression network analysis in chapter 3.

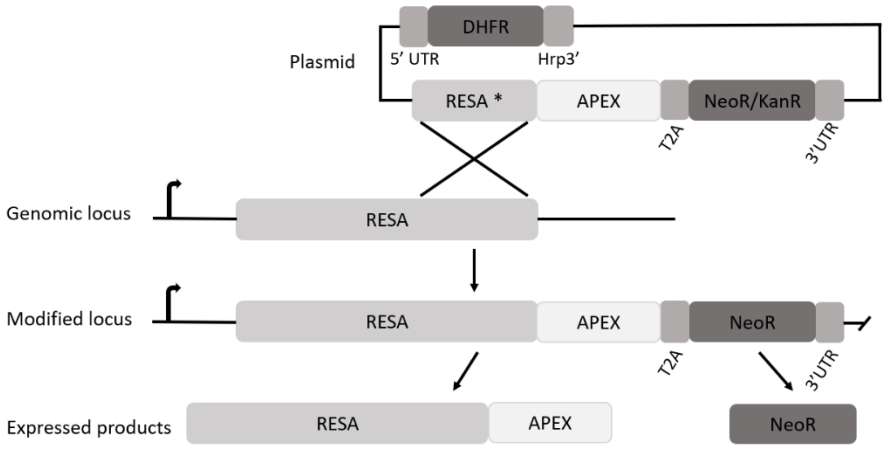

Figure 1. RESA-APEX construct, integration event and expressed protein product. A schematic of the RESA-APEX fusion plasmid design, integration event into the native RESA locus via single crossover recombination, altered genomic locus and final expressed protein product.

Table 1. Primers designed for the amplification of APEX by PCR.

SLI amplification primers

Name	Binding site	Sequence	Restriction site
CVO576	T2A 5' end	ACGCGTGAAGGAAGAGGAAGTTTATTAACATGTGGAG	MluI
CVO577	neoR 3' end	ACGCGTTTAGAAGAACTCGTCAAGAAGGCG	MluI

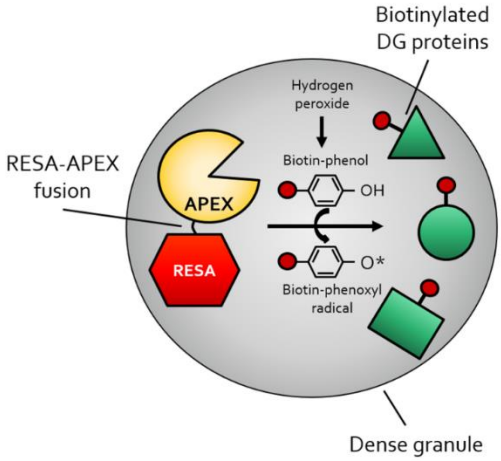

Figure 2. Diagram representing the proximity labelling approach developed for identification of novel DG proteins. A RESA-APEX fusion will be targeted to the DGs, where upon addition of biotin-phenol and H_2O_2, proteins in close proximity of the RESA-APEX fusion will become biotinylated.

5.3 **Results**

5.3.1. ***Generation of parasites expressing a RESA-APEX fusion***

Integration of the RESA-APEX construct into the native RESA locus was verified by PCR (figure 3, table 2). Bands of the expected size were seen for both the 5' and 3' integration regions amplified, indicating successful integration. A WT band present in the IGP-APEX sample indicated that some WT was present within the sample, drug selection was performed intermittently to minimise the effects of construct rejection.

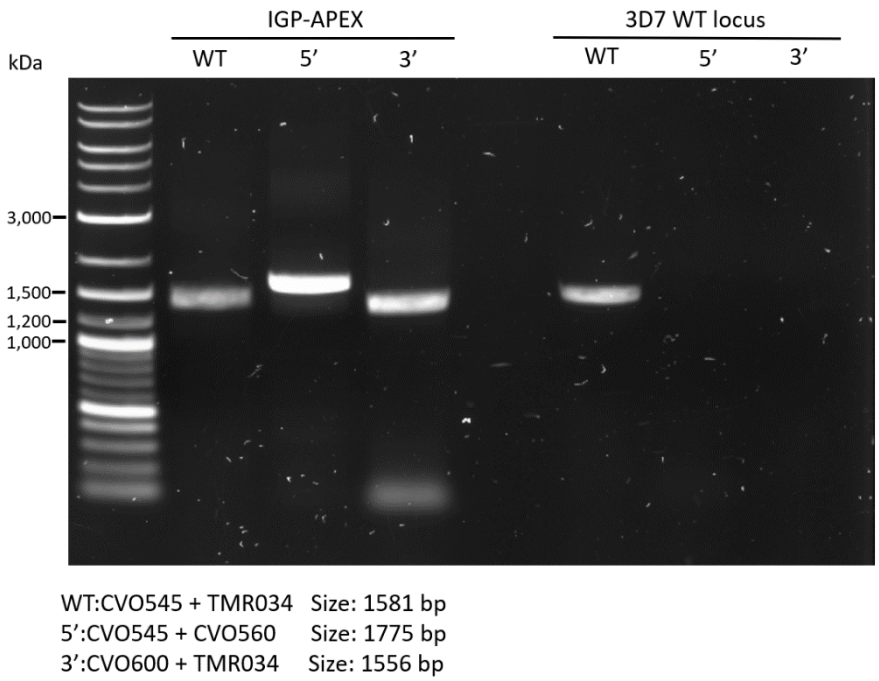

Figure 3. Integration PCR. PCR verification of integration of the RESA-APEX fusion sequence into the native RESA locus. Primer pairs used are shown below, and sequences given in table 2.

Table 2. Primers used in integration PCR. The names, sequences and binding sites of the primers used to verify integration of the RESA-APEX sequence into the native RESA locus.

Name	Binding site	Sequence
CVO545	RESA exon 2 968bp upstream of STOP	GTGAACAAATGAATTCAATAACATACAATTTCG
CVO560	APEX 3′ end	ACGCGTTGCTTGTAGGGCATCAGCAAACCC
CVO600	Cam5′ UTR 3′ end	CAAAATGGTTAACAAAGAAGAAGCTCAGAG
TMR034	RESA gDNA 1480 downstream of Cam 5′ UTR	GGGTGGAAAGAATTTTAATAAGAGACCATACTTAGAG

Several attempts were made to test integration by immunoblotting, however repeated attempts to visualise the RESA-APEX fusion by western blot analysis using anti-RESA antibodies were unsuccessful, and we conclude that the RESA epitope is likely obscured by the APEX tag. We subsequently obtained an anti-T2A skip peptide antibody (purchased from antibodies-online.com) to visualise the recombinant protein through labelling the skip peptide, however we were unable to visualise the RESA-APEX fusion of any other T2A-containing protein using this antibody and concluded that it was likely non-functional. I decided to determine whether the expected biotinylation could be detected in lysates from the transfected parasites, and to determine whether a band of the expected size of the RESA-APEX fusion is present simultaneously. To do this I set up the biotinylation reactions using highly synchronised

parasites and as a control H_2O_2 was omitted, which should prevent the biotinylation reaction from occurring. I then performed anti-biotin western blots using lysates from labelling experiments. This revealed that a protein of the expected size (around 180 kDa) of the RESA-APEX fusion could be detected. Interestingly, this protein was detected in lysates from parasites that had been incubated with and without hydrogen peroxide (figure 4).

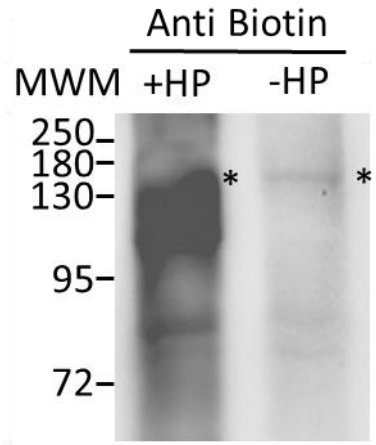

Figure 4. Anti-biotin immunoblot. An anti-biotin immunoblot showing a band of the predicted size of the RESA-APEX fusion at around 180 kDa (*) in samples incubated both with and without H_2O_2. HP-Hydrogen peroxide.

5.3.2 ***Initial biotinylating reactions and streptavidin-biotin affinity purification***

Whereas the anti-biotin signal was often present in both samples, the signal was always much stronger in the sample from the parasites treated with H_2O_2, indicating that biotinylation in the presence of the APEX enzyme was occurring on addition of the catalyst (figure. 4). The faint signal present in the lysate of the parasites that were not treated with H_2O_2 may indicate background levels of biotin or that a low level of biotinylation is occurring without addition of H_2O_2. Streptavidin-affinity purification of biotinylated proteins was tested in a similar manner, with samples taken at each stage of the pull-down to the binding of the protein to the breads and the success of elution (figure 5).

These blots indicated successful binding and elution of the biotinylated protein, with anti-biotin signal no longer or minimally visible in the sample following binding to the streptavidin beads, and the presence of biotin signal in the elution of the lysate of the parasites treated with H_2O_2. The signal in the elute was often fainter than the signal in the

starting lysate, this may be due to protein loss during stringent wash steps or incomplete elution due to the high strength of the streptavidin-biotin interaction.

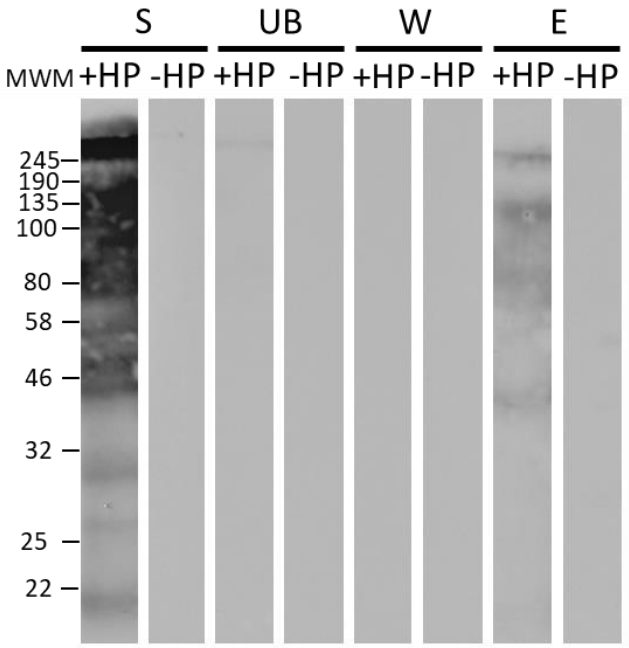

Figure 5. Anti-biotin immunoblots with samples from biotin-streptavidin affinity purification experiments. An anti-biotin immunoblot with samples taken at different stages of the biotin-streptavidin affinity purification pull-down experiments. Samples were taken at 4 stages, start (S), unbound (UB), wash (W), and elute (E). + and – HP indicate samples were incubated with and without H_2O_2.

The specificity of labelling for DG proteins was tested through immunoblotting with antibodies against the cytoplasmic marker alpha-tubulin and the DG markers PV1 and EXP2 at different stages of the pull-down. A band corresponding to the molecular weight of alpha tubulin was detected in the starting lysates from samples incubated in the presence or absence of H_2O_2 (as would be expected in a homogenised cell sample), and in the unbound fraction post-bead exposure, but was not detected in the elute of the lysate of the samples incubated with and without H_2O_2 conditions. These results indicate that alpha-tubulin does not bind the streptavidin beads and therefore is not biotinylated, and therefore is not positioned closely to the RESA-APEX fusion (figure 6A). In contrast, bands corresponding to the molecular weight of EXP2 and PV1 were present in the starting fraction, the unbound fraction for both + H_2O_2 and – H_2O_2 conditions and the elute fraction of the +H_2O_2 condition (figure 6B). The bands in the unbound fractions indicate that in these pull-downs not all biotinylated protein was bound to the beads, possibly due to a portion of the protein being unlabelled as a large fraction of EXP2 and PV1 are located in the PVM and PV, respectively, at the time of labelling. The

presence of bands corresponding to the molecular weight of PV1 and EXP2 in + H_2O_2 condition of the elute fraction confirms that biotinylation is occurring in the DG compartment in the presence of PV1 and EXP2 upon the addition of the H_2O_2 APEX reaction catalyst.

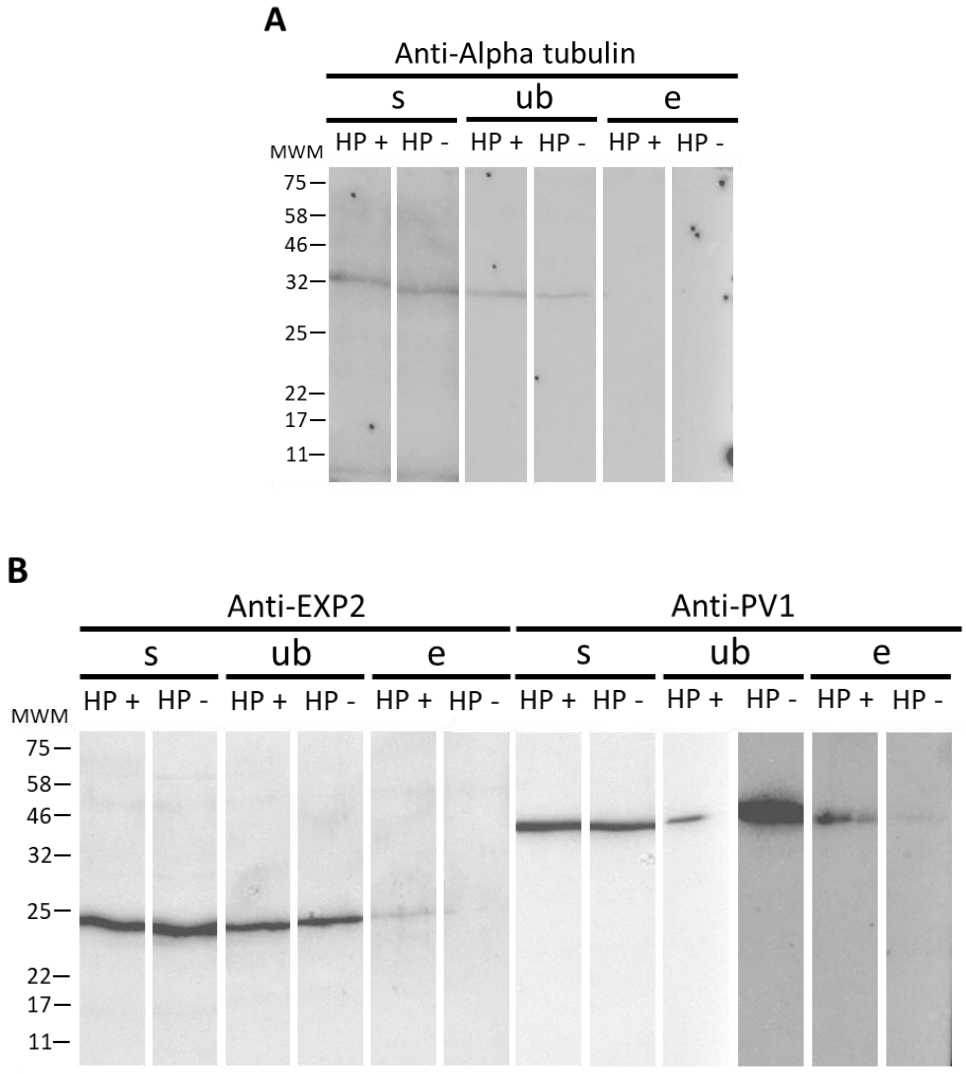

Figure 6. Immunoblots testing the specificity of labelling within the DGs. (A) Immunoblot using anti-Alpha-tubulin to test for pull-down of cytoplasmic proteins. (B) Immunoblots using anti-EXP2 and PV1to test for pull-down of known DG proteins. Samples were taken at 3 stages, start (S), unbound (UB), and elute (E).

5.3.3 *Proximity biotinylation experiments and mass spectrometry results*

In order to uncover the protein composition of the DG compartment, three replicate biotinylation and streptavidin purification experiments (A, B, and C) were carried out using

asexual stage iGP-RESA- APEX parasites. For each experiment, parasites were treated in the presence or absence of H_2O_2 (designated A+ and A-, B+ and B-, and C+ and C-). Pull-down experiments were performed by incubating parasite lysates with streptavidin beads for 1 hour, the streptavidin beads were then sequestered using a magnetic stand and the supernatant removed. The streptavidin beads were washed repeatedly with RIPA buffer and then PBS for detergent removal. Samples of lysate for immunoblot analysis were taken prior to bead incubation (start), and post bead incubation (un-bound). A sample of streptavidin beads was boiled with 4% SDS for 20 minutes to test levels of bound protein (eluate). Frozen pull-down samples from these experiments were sent bound to the streptavidin beads for mass spectrometric analysis by the BSRC Mass Spectrometry and Proteomics Facility at the University of St Andrews. Samples were analysed using liquid chromatography-mass spectrometry (LCMS), a combined approach that utilises the physical separation capabilities of liquid chromatography with the mass analysis abilities of mass spectrometry. The Mascot software search engine (www.matrixscience.com) was used to run the MS/MS output through the PlasmoDB NCBI *P. falciparum* database (PlasmoDB_Pfalciparum_NCBI_txid5833 230602 (191,192 sequences; 98,778,965 residues), and common contaminants databases cRAP 20190304 (116 sequences; 38,459 residues) and contaminants 20160129 (247 sequences; 128,130 residues) databases. The Mascot MS/MS report provides information on protein family, the database in which the peptide was matched, the NCBI accession, the protein score, the expected mass of the protein, the number of significant sequences, the number of significant matches and a basic description of the protein. The protein score reflects the combined scores of all observed mass spectra that are matched to peptide sequences for that protein and is a measure of confidence that a match between query and database entry are not random, with a higher score indicating increased confidence. Only statistically significant matches are listed in the output. The number of significant matches indicates the number of MS/MS spectra that are matched to the protein, with a confident identification usually requiring two or more matches. The number of significant sequences represents the number of significant distinct sequences matched for that protein.

The results yielded dataset sizes of: 581 hits (A+), 137 hits (A-), 426 hits (B +), 400 hits (B-), 818 hits (C+) and 806 hits (C–). Proteins of interest in datasets A, B and C are listed in tables 3, 4 and 5 respectively. Proteins from the MS output datasets were chosen for inclusion in tables A-C based on whether they are known DG proteins, predicted DG proteins (either by the malaria.tools co-expression network analysis in Chapter 3, or by DGPD), having functional or

spatial relationships to any of the known or predicted DG proteins, or localisation to other apical organelles as an indicator of non-DG labelling. Contaminants were highly represented in all 6 datasets, these were identified in the MS output through the contaminant and CRAPome databases and are easily differentiated as belonging to non-*Plasmodium* species. There was a great similarity in the proteins present in the lysates of parasites incubated in the presence and absence of H_2O_2 of replicates B and C, with sequences of known DG proteins (including the bait protein RESA), predicted DG proteins (identified in our malaria.tools dataset) and rhoptry proteins present in both conditions. The dataset of replicate B+ contains 5 known DG protein sequences (EXP1 (partial), EXP2, RESA, HSP101 and LSA3), while the dataset of replicate B- contains two known DG protein sequences (EXP1 (partial) and EXP2). The dataset of replicate C- contains 4 known DG proteins (EXP1 (partial), RESA (3D7), RESA (NF135), HSP101 and EXP2, whereas the dataset of replicate C+ contains 5 (EXP1 (PARTIAL), PTEX150, HSP101, and EXP2). In contrast, the two replicates for condition A contain quite different numbers of hits for DG proteins with the A+ dataset containing 6 known DG proteins (EXP1 (partial), PTEX150, RESA, RESA, HSP101, and EXP2), whereas the A- dataset contains none. In MS/MS datasets from proximity labelling experiments the bait protein typically has the most significant sequence hits with the highest protein score, in our datasets RESA is present in all +H_2O_2 conditions and the C- condition, where it does have a high score and number sequence hits relative to other DG sequences in all replicates, but it is not highly represented overall within the output. The sequences with the highest hits within all 6 outputs are contaminants like streptavidin and keratin, streptavidin is present within the samples from the streptavidin beads used in the pull-down experiments, and human keratin is a common contaminant of MS samples due to human skin cells present in the laboratory environment. Additionally, mature parasite-infected erythrocyte surface antigen (MESA/*P. falciparum* erythrocyte membrane protein 2 (PfEMP-2)) is present with high intensity in all replicates. Many rhoptry proteins are also represented within the datasets, with no determinable link between presence of H_2O_2 and the presence of rhoptry protein. The dataset of replicate A+ contains 7 rhoptry proteins; the dataset of replicates B+ and B- contain the same 4 rhoptry proteins, and the datasets of replicates C+ and C– have hits for the same 9 rhoptry proteins, and one microneme protein AMA1 (table 3). Many proteins from our list of predicted DG proteins developed from the malaria.tools co-expression neighbourhood of RESA (Chapter 3) were also present within the datasets, including Kelch13 in (datasets A+, B-, C+ and C-), MDR1 in (A-, B- and C+). RESA3 (PF3D7_1149200), a predicted DG protein in the Dense Granule Protein Database (DGPD) was also present in replicates A+, B-, and B+, and has a high protein score

close to that of RESA (2586 and 2920 respectively). HSP70x (PF3D7_0831700), which functions as a co-chaperone with the HSP40 (PF3D7_0501100) that was predicted as a potential DG protein in chapter 3 and was demonstrated to co-localise with RESA in IFA analysis, is present in datasets A+, B+ and C + and C-. While both our malaria.tools output and the DGPD contain several Plasmodium helical interspersed subtelomeric (PHIST) proteins, one of which PHISTb (PF3D7_0424600) is present in both, none of these proteins are present in the MS/MS results. However, several other PHIST proteins are present, with all three subgroups (a, b, and c) present in the datasets (see other, tables 3-5). Similarly, whilst the malaria.tools analysis of chapter 3 predicts MDR1 (PF3D7_0523000) and HSP40 (PF3D7_0501100) as DG proteins and the DGPD predicts DnaJ (PF3D7_0201700) as a DG protein, none of these proteins are present in the MS/MS datasets, however MDR2 (PF3D7_1447900), HSP40 (PF3D7_1437900), and DnaJ (Pf3D7_0823800) are present. Other proteins represented in multiple replicates include CLAG3.1, which is listed in the MS output for sample A+ and both conditions of replicates B and C, mature parasite-infected erythrocyte surface antigen (MESA) which is present in all MS/MS datasets with very high protein scores, and many conserved proteins of unknown function including PF3D7_0308700 (present in A+, A-, B+, and B-), and PF3D7_1455300 (present in A+, A-, B- and C+ and C-).

Table 3. Proteins from the MS/MS output of samples from replicate A. Accession number, protein score, number of significant matches and number of significant sequences are shown. Accession number is given as PlasmoDB id or NCBI protein ID where PlasmoDB id is not available.

A -H_2O_2					**A + H_2O_2**				
Malaria tools	**Accession**	**Score**	**Significant matches**	**Significant sequences**	**Malaria tools**	**Accession**	**Score**	**Significant matches**	**Significant sequences**
Kelch13					Kelch13	PF3D7_1343700	158	9	6
Kelch13 (partial)					Kelch13 (partial)	PF3D7_1343700	196	8	6
MDR1	PF3D7_0523000	24	1	1	MDR1				
DGPD					**DGPD**				
RESA3					RESA3	PF3D7_1149200	2586	78	32
Known					**Known**				
EXP1					EXP1 (partial)	PF3D7_1121600	110	3	2
PTEX150					PTEX150	PF3D7_1436300	869	25	16
RESA					RESA	PF3D7_0102200	2920	79	30
HSP101					HSP101	PF3D7_1116800	769	28	21
EXP2					EXP2	PF3D7_1471100	169	8	5
Other					**Other**				
HSP70x					HSP70x	PF3D7_0831700	686	22	13
MESA	Pf3D7_0500800	1026	45	31	MESA	Pf3D7_0500800	6347	189	74
PHIST a					PHIST a	PF3D7_0402000	714	22	11
PHIST a					PHIST a	PF3D7_1478000	47	2	2
Rhoptry					**Rhoptry**				
CLAG3.1					CLAG3.1	PF3D7_0302500	831	31	22
RAP1 (partial)					RAP1 (partial)	PF3D7_0105200	839	25	15
RhopH1/Clag8					RhopH1/Clag8	BAE16385.1	76	4	4
RON3					RON3	Pf3D7_1252100	809	31	27
RhopH3					RhopH3	PF3D7_0905400	363	13	12

RAP1					RAP1	PF3D7_0105200	839	25	15
RAP2					RAP2	PF3D7_0501600	358	12	8
RAP3 (partial)					RAP3 (partial)	PF3D7_0501500	97	3	2

Table 4. Proteins from the MS/MS output of samples from replicate B. Accession number, protein score, number of significant matches and number of significant sequences are shown. Accession number is given as PlasmoDB id or NCBI protein ID where PlasmoDB id is not available.

B - H_2O_2					**B + H_2O_2**				
Malaria tools	**NCBI Succession**	**Score**	**Significant matches**	**Significant sequences**	**Malaria tools**	**NCBI Succession**	**Score**	**Significant. matches**	**Significant sequences**
Kelch13	PF3D7_1343700	45	2	2	Kelch13				
MDR1	PF3D7_0523000	34	1	1	MDR1				
DGPD					**DGPD**				
RESA3	PF3D7_1149200	91	3	3	RESA3	PF3D7_1149200	493	20	15
Known					**Known**				
EXP1 (partial)	PF3D7_1121600	94	5	2	EXP1 (partial)	PF3D7_1121600	114	3	2
EXP2	PF3D7_1471100	29	2	2	EXP2	PF3D7_1471100	49	2	2
RESA					RESA	PF3D7_0102200	744	21	13
HSP101					HSP101	PF3D7_1116800	46	2	2
LSA1					LSA1	PF3D7_1036400	33	1	1
Other					**Other**				
HSP40	PF3D7_1437900	92	4	4	HSP40				
HSP70x					HSP70x	PF3D7_0831700	312	11	7
MESA	Pf3D7_0500800	1792	68	42	MESA	Pf3D7_0500800	2599	92	50
PHISTc	PF3D7_0801000	32	2	2	PHISTc				
Rhoptry					**Rhoptry**				
CLAG3.1	PF3D7_0302500	445	18	16	CLAG3.1	PF3D7_0302500	367	15	14
RhopH2	PF3D7_0929400	588	26	20	RhopH2	PF3D7_0929400	817	33	24

RAP1 (partial)	PF3D7_0105200	409	16	12	RAP1	PF3D7_0105200	325	12	12
RAP2	PF3D7_0501600	129	3	3	RAP2	PF3D7_0501600	267	7	5
RhopH3	PF3D7_0905400	137	5	4	RhopH3	PF3D7_0905400	246	7	6

Tables 5. Proteins from the MS/MS output of samples from replicate C. Accession number, protein score, number of significant matches and number of significant sequences are shown. Accession number is given as PlasmoDB id or NCBI protein ID where PlasmoDB id is not available.

C - H_2O_2					**C + H_2O_2**				
Malaria tools	**Accession**	**Score**	**Significant matches**	**Significant sequences**	**Malaria tools**	**Accession**	**Score**	**Significant matches**	**Significant sequences**
Kelch13	PF3D7_1343700	28	2	2	Kelch13	PF3D7_1343700	67	3	3
MDR1					MDR1	PF3D7_0523000	52	2	2
Known					**Known**				
EXP1 (partial)	PF3D7_1121600	53	2	1	EXP1 (partial)	PF3D7_1121600	48	2	1
PTEX150					PTEX150	PF3D7_1436300	36	2	2
RESA	PF3D7_0102200	538	22	15	RESA	PF3D7_0102200	685	22	14
HSP101	PF3D7_1116800	396	31	12	HSP101	PF3D7_1116800	377	18	14
EXP2					EXP2	PF3D7_1471100	28	1	1
Other					**Other**				
HSP40	PF3D7_1437900	454	16	11	HSP40	PF3D7_1437900	403	13	8
HSP70x	PF3D7_0831700	1423	42	19	HSP70x	PF3D7_0831700	1471	46	20
MDR2	PF3D7_1447900	199	4	3	MDR2	PF3D7_1447900	94	2	1
MESA	PF3D7_0500800	1304	38	27	MESA				
MESA	Pf3D7_0500800	1391	40	28	MESA	Pf3D7_0500800	1295	41	28
DnaJ	Pf3D7_0823800	365	11	9	DnaJ	Pf3D7_0823800	286	8	8
PHISTc					PHISTc	PF3D7_0801000	34	1	1
PHIST a					PHIST a	PF3D7_1478000	27	1	1
PHIST b	PF3D7_1476300	66	1	1	BHIST b				

Rhoptry					**Rhoptry**				
CLAG3.1	PF3D7_0302500	4408	153	64	CLAG3.1	PF3D7_0302500	4364	153	63
RhopH1/Clag8	BAE16385.1	370	19	12	RhopH1/Clag8				
RhopH1/Clag2	BAE16383.1 n/a	443	16	11	RhopH1/Clag2				
ROP14	PF3D7_0613300	60	2	2	ROP14				
RON2	PF3D7_1452000	386	16	15	RON2				
Ron3	Pf3D7_1252100	4103	137	74	Ron3				
PfRON5 (partial)	PF3D7_0817700	767	26	19	PfRON5 (partial)				
RAP1 (partial)	PF3D7_0105200	3234	102	31	RAP1 (partial)				
RAP2 (partial)	PF3D7_0501600	1929	55	19	RAP2 (partial)				
RAP3 (partial)	PF3D7_0501500	568	19	9	RAP3 (partial)				
Microneme					**Microneme**				
AMA1	PF3D7_1133400	42	1	1	AMA1				

5.4 **Discussion**

This study aimed to identify novel DG proteins through proximity based biotinylation assays using a fusion of the known DG protein RESA and the engineered ascorbate peroxidase APEX. Following labelling experiments, the biotinylated proteins were isolated by streptavidin-biotin affinity purification and identified by mass spectrometric analysis performed by the BSRC Mass Spectrometry and Proteomics Facility at The University of St Andrews. Although many known and predicted DG proteins are present within the MS/MS outputs, there is no clear difference in abundance of DG proteins between $+H_2O_2$ and $–H_2O_2$ conditions. A control without H_2O_2 was included to allow identification and subtraction of both endogenously biotinylated proteins and proteins that bind non-specifically to the streptavidin beads. However, the lack of consistency in protein content between the controls without H_2O_2 made this impossible. *Plasmodium* parasites are predicted to contain only one biotinylated protein, Acetyl-CoA carboxylase, which is expressed in both the liver and blood stages, but which is only thought to be biotinylated in the liver stages (49,50). It is possible that the APEX fusion promotes biotinylation also in the absence of the H_2O_2 catalyst, as indicated by the faint anti-biotin signal visible in the extracts of parasites that were not exposed to H_2O_2 in immunoblots of some of the labelling experiments. However, the similar numbers of DG protein hits, confidence score, and sequence matches obtained from the MS experiments between the samples from parasites incubated with and without H_2O_2 and does not align with the results of the anti-biotin immunoblotting experiments which consistently showed significantly stronger labelling signal in the $+H_2O_2$ than in the $-H_2O_2$ conditions. Additionally, many rhoptry proteins are present in each replicate, with abundance similarly seeming to bear no relation to the presence of H_2O_2 in the labelling reaction. RESA consistently has the highest protein score and number of significant sequence matches, as would be expected for the bait protein. EXP1, EXP2, PTEX150 and LSA3 have relatively low score and numbers of significant matches compared to other proteins in the MS output, we would expect these to be significantly higher if labelling occurred in the DGs.

One protein that is consistently present in the output is MESA; it consistently has high confidence scores, significant matches, and significance sequence scores relative to the other proteins across the datasets. MESA is an exported high molecular-weight phosphoprotein that binds to host cell ankyrin to increase rigidity of the host cell (51,52). Unlike RESA, which is detected predominantly in the ring stages, MESA is detected at later stages in trophozoites and

schizonts (51). Accordingly, the expression profile of MESA does not mirror that of most DG proteins (with the exception of EXP2), with peak intraerythrocytic expression occurring at 24 hpi (2198 transcripts per million (TPM)) and low levels of expression when DG proteins are expressed most highly (99.8 TMP at 48 hpi, compared to RESA at 27532.18 TPM) (53). The expression profile of EXP2 is unique among the known DG proteins in that it peaks at 24 hpi, however unlike MESA, EXP2 expression is still high at 48 hpi (1,400 TPM), likely due to its essential function as a PTEX translocon component, necessitating its storage in the DGs to allow immediate release upon invasion (53). Therefore, despite having a similar cellular localisation and function to RESA in binding host erythrocyte membrane cytoskeleton, MESA may not be a DG protein. It is unclear why MESA has such consistently high scores and numbers of significant sequence matches if it is not a DG protein, it is possible that biotinylation occurs at the host cell periphery. Clustal Omega alignment predicts only 23.10% similarity between RESA and MESA, therefore it is unlikely that RESA peptides are being mis-identified as MESA peptides.

The presence of RESA3, predicted to be a DG protein in DGPD, in sample A+ with a relatively high protein score of 2586 may result from peak expression levels occurring at the time of labelling (12242.88 TPM at 48 hpi) (53) which means that there is a high abundance of the protein in the cell at that time and it is therefore more likely to be present within the MS output as a contaminant. However, as the high-resolution time course transcriptome of the intraerythrocytic cycle by Kucharski *et al*. indicates that the transcription profile of RESA3 closely mirrors that of RESA, it is also possible that it is a DG protein and is present in the sample due as a result of labelling in DGs (53). However, if that were the case I would expect to see RESA3 in multiple replicates. Upon further investigation, it appears that RESA3 was not predicted as a potential DG protein in malaria.tools analysis as many transcription experiments (including those used by the malaria.tools platform) have an overall shorter time-course with the latest transcription level readings taken at 40 hpi and therefore do not cover the very late expression peak of some DG proteins. Indeed, only the beginning of the RESA expression peak is described by malaria.tools with a mean expression level of 10185 TPM for ‘schizont’ stage (no information about the time after invasion that samples were taken is provided) which is closest to the expression level of 10708.5 TPM at 44 hpi as described by Kucharski *et al*. and less than half of the peak expression level of 27532.18 TPM at 48 hpi (53). Based on the transcriptome of RESA3 described by Kucharski *et al*., I predict that RESA3 may be a DG protein (53).

P. falciparum proteins are prone to aggregate due to a high proportion of glutamine (Q), and asparagine (N) in the form of poly-N repeats (54–56), accordingly, molecular chaperones comprise a significant proportion of the genome (2%) and the parasite exportome (≈5%) (57). Of the ≈50 *P. falciparum* heat shock 40kDa family (HSP40/J domain proteins/DnaJ) documented in 3D7 and 6 of the cooperating heat shock protein 70kDa (HSP70), almost half of the HSP40s contain a PEXEL sequence and are therefore likely exported, whilst only one HSP70, HSP70x is known to be exported (58–61). HSP40 (DnaJ) proteins bind to and stimulate ATPase activity of HSP70 (DnaK), causing HSP70 to enter a state in which it can stably interact with the protein substrate (62–65). Of the 12 type IV HSP40 proteins encoded within the *P. falciparum* genome, 11 contain a PEXEL sequence targeting them for export, including RESA and MESA (52,58,66). The HSP40 listed in the B- and C+ and C- outputs (PF3D7_1437900) is unlikely to be a DG protein as its expression peaks at 22 hpi and it has low expression levels at 48 hpi at the time of DG biogenesis of 182.67 TPM. There are no transcription data available for the DnaJ listed in the MS output for the samples of replicate C (Pf3D7_0823800).

HSP70x is listed in the MS/MS output in the samples from conditions A+ (686), B+ (312), C+ (1471) and C– (1423), however, it is not particularly highly expressed at this time (583.66 TPM at 48 hpi), with peak expression of 2148.54 TPM occurring at 10 hpi (53). It is therefore unlikely that HSP70x is present in the samples as a contaminant due to very high levels of expression at the time the pull-down experiments were performed, as the high levels of HSP70x produced at 10 hpi will have been exported into the host cell by the time of the labelling experiments occurred. This protein was primarily considered of interest due to its function as a co-chaperone with the essential type II HSP40 listed in the malaria.tools output that was demonstrated to co-localise with RESA in DGs in previous experiments (PF3D7_0501100), indicating that this HSP40 is a DG protein (see chapter 3). HSP70x is also the only known exported HSP70, with studies indicating that it is exported despite lacking a PEXEL sequence and that it associates with the J-dots in the infected erythrocyte cytosol (60,67–69). Preliminary IFA data also indicated that HSP70x does not co-localise with RESA (see supplementary data figure 2).

Of the *P. falciparum* exportome, 89 proteins belong to the *Plasmodium* helical interspersed subtelomeric (PHIST) protein family (61,70,71). PHIST proteins are important in host-cell remodelling, with diverse functions in correct localisation of PfEMP1, gametocytogenesis, and host cell rigidification (52,70,72–76). RESA is also a PHIST protein, one of 7 proteins in the

PHISTb-DnaJ subgroup. Like RESA, many PHISTb proteins localise to the host cell cytoskeleton. Correct localisation of RESA to the host cell periphery is dependent on the presence of the PHIST domain and parts of the C-terminus (77). PHIST proteins represent 14% of all PEXEL containing proteins (61,70,78). PHISTa (PF3D7_0402000), which has the highest score and number of significant sequence matches of the PHIST proteins listed in the MS output (with the exception of RESA), interacts with human erythrocyte cytoskeleton protein band 4.1R which in turn binds to actin filaments and membrane proteins in a similar manner to MESA (which is not a PHIST protein) and co-localises with RESA at the host-cell periphery (79). However, the expression profile of PHISTa does not fit the expected profile of DG proteins, with peak expression at 22 hpi, and expression of only 13.74 TPM at 48 hpi, and therefore is unlikely to be a DG protein. PHISTa PF3D7_1478000 (GEXP17), a suggested surface protein (80), which is present in the MS output from condition A+, has an expression profile mirroring that of RESA, but has low expression levels overall (214.58 TMP at 4 hpi, 214.58 TMP at 48 hpi) (53). PHISTb (PF3D7_1476300) listed in the MS output for condition C- has a low protein score of 66, and low sequence match of 1, with peak expression at 40 hpi (162 TPM) and only 38.06 TPM at 48 hpi and is likely not a DG protein. Interestingly, the PHISTc listed in the MS output for conditions B- and C+ (PF3D7_0801000) localises to the J dots with HSP40 and HSP70x. The expression level of this PHIST protein does peak through late schizont to early ring stages (514.3 TMP at 52 hpi, 643.85 TMP at 4 hpi), therefore it is possible that this could be a DG protein, or that it could be being pulled down by co-immunoprecipitation through its interaction with HSP40.

Cytoadherence linked asexual protein 3.1 (CLAG3.1, PF3D7_0302500), is listed in all MS outputs, with the exception of A-, with very high protein scores and significant sequence matches. CLAG3.1 is a well-documented rhoptry bulb protein, part of the high molecular weight rhoptry complex, which localises to the erythrocyte periphery after invasion (81–84). CLAG3.1 could possibly be present in the datasets due to labelling by the RESA-APEX fusion at the cell periphery.

Several proteins linked to drug resistance were identified in the pull-downs. Plasmodium falciparum multidrug resistance protein 1 (PfMDR1) is an ATP-binding cassette transporter that causes antimalarial drug resistance (85,86). MDR1 was predicted as a candidate DG protein by the malaria.tools co-expression network analysis and is present in the MS output of conditions A-, B- and C+ with low sequence hits (1-2) and protein scores (highest score-52). Whilst MDR1 met the initial criterion to be included in the malaria.tools list of predicted DG

proteins, as it contains TM domains that allow it to enter the secretory pathway, it localises to the digestive vacuole and therefore is not exported and is unlikely to be a DG protein (87,88). Kelch13 is also linked to antimalarial drug resistance as artemisinins are activated by haemoglobin degradation products and the Kelch13-defined endocytosis pathway is necessary for endocytosis of haemoglobin from the host erythrocyte (89,90). Kelch13 is listed in MS outputs for conditions A+, B-, C+ and C-, however it has relatively low protein scores and numbers of significant sequences. Kelch13 was listed in the original malaria.tools RESA co-expression neighbourhood, at its expression profile mirrors that of RESA, peaking at 48 hours (191 TPM) (53). However, it does not contain a signal sequence or transmembrane domain and IFA experiments localise Kelch13 to regions proximal to the endosome-like compartment (91), therefore it is not a secreted protein and is therefore unlikely to be a DG protein.

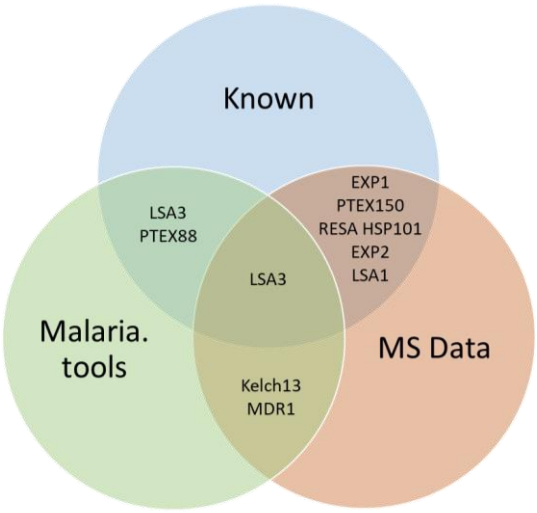

Figure 7: A comparison of the MS data output overlap with known and malaria.tools predicted DG proteins. The MS data contained 6 of the known DG proteins, one of which, LSA3, was also present in the malaria.tools list of predicted DG proteins. Kelch13 and MDR1 are both present in the malaria.tools list of predicted DG proteins and the MS data output, although they are not exported and are unlikely to be DG proteins.

Overall, molecular chaperones and proteins localising to the host cell periphery are highly represented in the datasets. It is possible that that this is due to labelling in the DGs, and that these proteins therefore contain many more chaperones and modifiers of host cell rigidity in addition to HSP40 and RESA. It is also possible that the labelling induced by the APEX-RESA fusion occurs at the host cell periphery as well as in the DGs. This non-DG labelling could explain the presence of some of the PHIST proteins within the MS outputs that localise to the

host cell periphery. Although MESA expression peaks at 24 hpi, when it has been indicated that levels of RESA at the host cell cytoskeleton begin to decrease (51,92), it is possible that RESA is still present at the host cell periphery at the time the labelling experiments were performed. Immunoprecipitation experiments indicated that RESA forms a cytoskeletal complex with MESA, PHISTb (PF3D7_1201000), and PHISTc (PF3D7_0936800) (neither PHIST is listed in the MS output) (93). We attempted to address the possibility of non-DG labelling at the infected red blood cell periphery by developing a protocol for removal of the host RBC membranes by saponin lysis prior to labelling by addition of H_2O_2, however during the pull-down experiments the magnetic streptavidin beads adhered to each other in a way that made washing for removal of detergent impossible, and we were advised by staff at the BSRC Mass spectrometry facility that these samples were unlikely to yield any usable results. It is possible that saponin lysis and removal of the host cell membranes was unsuccessful and instead lead to cell disruption and uninhibited labelling within the samples, as we had previously observed that beads from $+H_2O_2$ conditions often displayed increased adherence to each other during the pull-down experiments. We considered attempting labelling experiments in free merozoites, but it did not seem feasible to develop a protocol that would provide a sufficient number of merozoites isolated sufficiently from other membranous components within the remaining time of the project, we therefore decided to attempt the saponin protocol first and to follow this with merozoite labelling if the saponin protocol was unsuccessful. Ultimately, I was not able to develop a protocol for labelling of merozoites due to time constraints. If the modified protocols proved successful it would be possible to repeat the experiments using iGP-APEX parasites induced to enter gametocytogenesis to determine whether the differing destination of the gametocyte-infected erythrocyte requires alternate DG proteins. Initial induction experiments using anti-Pfs16 as a marker for gametocytogenesis indicated an average 80% conversion rate. In addition to developing modified protocols for APEX labelling, co-immunoprecipitation experiments using RESA could be performed to identify interacting proteins within the DGs.

It is also possible that the MS outputs contain a high number of chaperones due to the high number of molecular chaperones within the *P. falciparum* exportome that are expressed at this time (94). Possible labelling at the erythrocyte periphery was an unexpected outcome as the literature states RESA begins to dissociate from spectrin at 24 hpi, long before the labelling experiments were performed (95). However, as we see 'background' labelling without addition of H_2O_2, it is possible that labelling was occurring throughout the life cycle. We attempted to

test this possibility by performing labelling experiments in iGP parasites which did not contain the RESA-APEX fusion, but unfortunately the MS analysis of these samples was unsuccessful. In future work, I could attempt to repeat these experiments. Additionally, we attempted to visualise the subcellular localisation of labelling by staining samples from $+H_2O_2$ and $-H_2O_2$ conditions with fluorescently-labelled streptavidin. Initial attempts to perform these experiments were unsuccessful as it appeared that the streptavidin may not have been working, as only some background autofluorescence was detectable. In the future I could attempt to repeat these experiments with new fluorescently labelled streptavidin, repeat the IFAs with anti-biotin, or use APEX labelling in its imaging capacity to verify the fine subcellular localisation by EM.

Future experiments could be improved through use of quantitative mass spectrometry using isobaric tagging of peptides prior to HPLC separation (96). This technique could give a more accurate impression of the relative amounts of proteins being pulled down from the experiments performed in the presence and in absence of H_2O_2. This technique was used successfully by Barylyuk *et al.* (2020) in describing the *T. gondii* tachyzoite proteome (14).

Several reports have linked the poor membrane permeability of biotin phenol and the potential inhibitory effects of H_2O_2 on APEX function to decreased labelling activity in certain cell and tissue types (97–99). However, in our experiments membrane surface area exposure to biotin phenol is maximised, as the cells are labelled in suspension, and anti-biotin immunoblotting indicates strong labelling (figure 5). Tan *et al.* observed that the use of 6 mM of biotin phenol caused non-specific biotinylation in filter grown MDCK-II cells labelled with fluorescently tagged streptavidin, however we used only 0.5 mM biotin phenol as described by Kehrer *et al.* (2020) who used APEX to identify the microneme content of ookinetes in *Plasmodium berghei* (39,100). This indicates that the concentration of biotin phenol used in our labelling experiments was neither high enough to cause widespread non-specific labelling nor too low to label sufficiently.

5.5 **Conclusion**

Whilst the presence of many of the known and predicted DG proteins within the MS output was initially encouraging, the presence of these proteins in the control condition and the lack of consistency between replicates means that we cannot claim that this is due to labelling

occurring within the DGs. Further, the presence of proteins from other subcellular localisations including the rhoptries indicates that the streptavidin affinity purification procedure is not effectively isolating biotinylated proteins from other proteins within the parasite and the host cell, and that biotinylation may be occurring at locations other than within the DGs. We must conclude that at this time the system is not functioning sufficiently for any meaningful conclusions to be drawn. Future work can focus on developing a protocol for APEX labelling experiments on free merozoites to avoid labelling at the host cell periphery, and on developing more stringent wash steps to optimise removal of non-biotinylated proteins from the samples.

Bibliography

1. Blackman MJ, Bannister LH. Apical organelles of Apicomplexa: biology and isolation by subcellular fractionation. Vol. 117, Molecular & Biochemical Parasitology. 2001 p. 11–25.

2. Leriche MA, Dubremetz JF. Characterization of the protein contents of rhoptries and dense granules of *Toxoplasma gondii* tachyzoites by subcellular fractionation and monoclonal antibodies. Mol Biochem Parasitol. 1991 Apr;45(2):249–59.

3. Huh WK, Falvo JV, Gerke LC, Carroll AS, Howson RW, Weissman JS, *et al*. Global analysis of protein localization in budding yeast. Nature. 2003 Oct;425(6959):686–91.

4. Pappin D, Hojrupt P, Bleasbyl AJ. Rapid identification of proteins by peptide-mass fingerprinting. Curr Biol. 1993;3(6):327–32.

5. Thiede B, Höhenwarter W, Krah A, Mattow J, Schmid M, Schmidt F, *et al*. Peptide mass Fingerprinting. Methods. 2005;35:237–47.

6. de Azevedo MF, Gilson PR, Gabriel HB, Simões RF, Angrisano F, Baum J, *et al.* Systematic Analysis of FKBP Inducible Degradation Domain Tagging Strategies for the Human Malaria Parasite *Plasmodium falciparum*. Templeton TJ, editor. PLoS ONE. 2012 Jul 16;7(7):e40981.

7. Christoforou A, Mulvey CM, Breckels LM, Geladaki A, Hurrell T, Hayward PC, *et al*. A draft map of the mouse pluripotent stem cell spatial proteome. Nat Commun. 2016 Jan 12;7(1):9992.

8. Lin JS, Lai EM. Protein-Protein Interactions: Co-Immunoprecipitation. In: Methods in Molecular Biology. 2017. p. 211–9.

9. Alberts B, Johnson J, Lewis J, Raff M, Roberts K, Walter P. Molecular Biology of the Cell. 4th ed. New York: Garland Science; 2002.

10. Sadak A, Taghy Z, Fortier B, Dubremetz J F. Characterization of a family of rhoptry proteins of *Toxoplasma gondii*. Mol Biochem Parasitol. 1988;29(2–3):203–11.

11. Dubremetz J F, Sadak A, Taghy Z, Fortier B. Characterization of a 42 kDa Rhoptry Antigen of *Toxoplasma Gondii*. Host-Parasite Cell Mol Interact Protozoal Infect. 1987;11:365–9.

12. Bell AW, Ward MA, Blackstock WP, Freeman HNM, Choudhary JS, Lewis AP, *et al*. Proteomics Characterization of Abundant Golgi Membrane Proteins. J Biol Chem. 2001 Feb;276(7):5152–65.

13. Andersen JS, Wilkinson CJ, Mayor T, Mortensen P, Nigg EA, Mann M. Proteomic characterization of the human centrosome by protein correlation profiling. Nature. 2003 Dec;426(6966):570–4.

14. Barylyuk K, Koreny L, Ke H, Butterworth S, Crook OM, Lassadi I, *et al*. A Comprehensive Subcellular Atlas of the *Toxoplasma Proteome* via hyperLOPIT Provides Spatial Context for Protein Functions. Cell Host Microbe. 2020 Nov 11;28(5):752-766.e9.

15. Pagliarini DJ, Calvo SE, Chang B, Sheth SA, Vafai SB, Ong SE, *et al*. A Mitochondrial Protein Compendium Elucidates Complex I Disease Biology. Cell. 2008 Jul;134(1):112–23.

16. Dubremetz JF, Dissous C. Characteristic Proteins of Micronemes and Dense Granules from *Sarcocystis tenella* Zoites (Protozoa, Coccidia). Mol Biochem Parasitol. 1980;1(5):279–89.

17. Kumar A, Agarwal S, Heyman JA, Matson S, Heidtman M, Piccirillo S, *et al*. Subcellular localization of the yeast proteome. Genes Dev. 2002;16(6):707–19.

18. Thul PJ, Åkesson L, Wiking M, Mahdessian D, Geladaki A, Ait Blal H, *et al.* A subcellular map of the human proteome. Science. 2017 May 26;356(6340):eaal3321.

19. Chakravartty V, Cronan JE. Altered Regulation of *Escherichia coli* Biotin Biosynthesis in BirA Superrepressor Mutant Strains. J Bacteriol. 2012 Mar 1;194(5):1113–26.

20. Ong SE, Blagoev B, Kratchmarova I, Kristensen DB, Steen H, Pandey A, *et al.* Stable Isotope Labeling by Amino Acids in Cell Culture, SILAC, as a Simple and Accurate Approach to Expression Proteomics. Mol Cell Proteomics. 2002 May;1(5):376–86.

21. O'Meara TR, O'Meara MJ, Polvi EJ, Pourhaghighi MR, Liston SD, Lin ZY, *et al*. Global proteomic analyses define an environmentally contingent Hsp90 interactome and reveal chaperone-dependent regulation of stress granule proteins and the R2TP complex in a fungal pathogen. Leu JY, editor. PLOS Biol. 2019 Jul 8;17(7):e3000358.

22. Schoeters F, Van Dijck P. Protein-Protein Interactions in Candida albicans. Front Microbiol. 2019 Aug 7;10:1792.

23. Choi-Rhee E, Schulman H, Cronan JE. Promiscuous protein biotinylation by *Escherichia coli* biotin protein ligase. Protein Sci. 2008 Dec 29;13(11):3043–50.

24. Cronan JE. Targeted and proximity-dependent promiscuous protein biotinylation by a mutant *Escherichia coli* biotin protein ligase. J Nutr Biochem. 2005 Jul;16(7):416–8.

25. Roux KJ, Kim DI, Raida M, Burke B. A promiscuous biotin ligase fusion protein identifies proximal and interacting proteins in mammalian cells. J Cell Biol. 2012;196(6):801–10.

26. Beckett D, Kovaleva E, Schatz PJ. A minimal peptide substrate in biotin holoenzyme synthetase-catalyzed biotinylation. Protein Sci. 2008 Dec 31;8(4):921–9.

27. Fernandez-Saurez M, Chen T, Ting AY. Protein−Protein Interaction Detection in Vitro and in Cells by Proximity Biotinylation. J Am Chem Soc. 2008;130(29):9251–3.

28. Schnider CB, Bausch-Fluck D, Brühlmann F, Heussler VT, Burda PC. BioID Reveals Novel Proteins of the *Plasmodium* Parasitophorous Vacuole Membrane. Blader IJ, editor. mSphere. 2018 Feb 28;3(1):e00522-17.

29. Hopkins C, 'le Gibson A, Stinchcombe J, Futter C. Chimeric molecules employing horseradish peroxidase as reporter enzyme for protein localisation in the electron microscope. Methods Enzymol. 2004;327(2000):35–45.

30. Honke K, Kotani N. Identification of Cell-Surface Molecular Interactions under Living Conditions by Using the Enzyme-Mediated Activation of Radical Sources (EMARS) Method. Sensors. 2012 Nov 22;12(12):16037–45.

31. Miyagawa-Yamaguchi A, Kotani N, Honke K. Expressed Glycosylphosphatidylinositol-Anchored Horseradish Peroxidase Identifies Co-Clustering Molecules in Individual Lipid Raft Domains. Johannes L, editor. PLoS ONE. 2014 Mar 26;9(3):e93054.

32. Jiang S, Kotani N, Ohnishi T, Miyagawa-Yamgushi A, Tsuda M, Yamashita R, *et al*. A proteomics approach to the cell-surface interactome using the enzyme-mediated activation of radical sources reaction. Proteomics. 2012;12(1):54–62.

33. Yamashita R, Kotani N, Ishiura Y, Higashiyama S, Honke K. Spatiotemporally-regulated interaction between β1 integrin and ErbB4 that is involved in fibronectin-dependent cell migration. J Biol Chem. 2011;149(3):347–55.

34. Li XW, Rees JS, Xue P, Zhang H, Hamaia SW, Sanderson B, *et al*. New Insights into the DT40 B Cell Receptor Cluster Using a Proteomic Proximity Labeling Assay. J Biol Chem. 2014 May;289(21):14434–47.

35. Rees JS, Li XW, Perrett S, Lilley KS, Jackson AP. Selective Proteomic Proximity Labeling Assay Using Tyramide (SPPLAT): A Quantitative Method for the Proteomic Analysis of Localized Membrane-Bound Protein Clusters. Curr Protoc Protein Sci. 2015;80(1):1–19.

36. Loh KH, Stawski PS, Draycott AS, Udeshi ND, Lehrman EK, Wilton DK, *et al*. Proteomic Analysis of Unbounded Cellular Compartments: Synaptic Clefts. Cell. 2016 Aug;166(5):1295-1307.e21.

37. Rhee HW, Zou P, Udeshi ND, Martell JD, Mootha VK, Carr SA, *et al*. Proteomic Mapping of Mitochondria in Living Cells via Spatially-Restricted Enzymatic Tagging. Science. 2013;339(6125):1328–31.

38. Trinkle-Mulcahy L, Boisvert FM. Recent advances in proximity-based labeling methods for interactome mapping. F1000Research. 2019 [cited 2020 May 11];8. Available from: https://doi.org/10.12688/f1000research.16903.1

39. Kehrer J, Ricken D, Strauss L, Pietsch E, Heinze JM, Frischknecht F. APEX-based proximity labeling in *Plasmodium* identifies a membrane protein with dual functions during mosquito infection 2 3. bioRxiv;

40. Martell JD, Deerinck TJ, Sancak Y, Poulos TL, Mootha VK, Sosinsky GE, *et al*. Engineered ascorbate peroxidase as a genetically encoded reporter for electron microscopy. Nat Biotechnol. 2012 Nov;30(11):1143–8.

41. Uezu A, Kanak DJ, Bradshaw TWA, Soderblom EJ, Catavero CM, Burette AC, *et al*. Identification of an elaborate complex mediating postsynaptic inhibition. Science. 2016 Sep 9;353(6304):1123–9.

42. Kim DI, KC B, Zhu W, Motamedchaboki K, Doye V, Roux KJ. Probing nuclear pore complex architecture with proximity-dependent biotinylation. PNAS. 2014;111(24):E2453-61.

43. Branon TC, Bosch JA, Sanchez AD, Udeshi ND, Svinkina T, Carr SA, *et al*. Efficient proximity labeling in living cells and organisms with TurboID. Nat Biotechnol. 2018 Oct;36(9):880–7.

44. Bosch JA, Chen C, Perrimon N. Proximity-dependent labeling methods for proteomic profiling in living cells: An update. WIREs Dev Biol [Internet]. 2021 Jan [cited 2023 Jul 22];10(1). Available from: https://onlinelibrary.wiley.com/doi/10.1002/wdev.392

45. Yang X, Wen Z, Zhang D, Li Z, Li D, Nagalakshmi U, *et al.* Proximity labeling: an emerging tool for probing in planta molecular interactions. Plant Commun. 2021 Mar;2(2):100137.

46. Boltryk SD, Passecker A, Alder A, Carrington E, Van De Vegte-Bolmer M, Van Gemert GJ, *et al*. CRISPR/Cas9-engineered inducible gametocyte producer lines as a valuable tool for *Plasmodium falciparum* malaria transmission research. Nat Commun. 2021 Aug 10;12(1):4806.

47. Joice R, Nilsson SK, Montgomery J, Dankwa S, Egan E, Morahan B, *et al*. *Plasmodium falciparum* transmission stages accumulate in the human bone marrow. Sci Transl Med. 2014 Jul 9;6(244).

48. Obaldia N, Meibalan E, Sa JM, Ma S, Clark MA, Mejia P, *et al*. Bone Marrow Is a Major Parasite Reservoir in *Plasmodium vivax* Infection. Boyle JP, editor. mBio. 2018 Jul 5;9(3):e00625-18.

49. Dellibovi-Ragheb TA, Jhun H, Goodman CD, Walters MS, Ragheb DRT, Matthews KA, *et al.* Host biotin is required for liver stage development in malaria parasites. Proc Natl Acad Sci. 2018 Mar 13;115(11).

50. Müller S, Kappes B. Vitamin and cofactor biosynthesis pathways in *Plasmodium* and other apicomplexan parasites. Trends Parasitol. 2007 Mar;23(3):112–21.

51. Coppel R, Lustigman S, Murray L, Anders R. MESA is a *Plasmodium falciparum* phosphoprotein associated with the erythrocyte membrane skeleton. Mol Biochem Parasitol. 1988 Dec;31(3):223–31.

52. Da Silva E, Foley M, Dluzewski AR, Murray LJ, Anders RF, Tilley L. The *Plasmodium falciparum* protein RESA interacts with the erythrocyte cytoskeleton and modifies erythrocyte thermal stability. Mol Biochem Parasitol. 1994 Jul 1;66(1):59–69.

53. Kucharski M, Tripathi J, Nayak S, Zhu L, Wirjanata G, Van Der Pluijm RW, *et al.* A comprehensive RNA handling and transcriptomics guide for high-throughput processing of *Plasmodium* blood-stage samples. Malar J. 2020 Dec;19(1):363.

54. Singh GP, Chandra BR, Bhattacharya A, Akhouri RR, Singh SK, Sharma A. Hyper-expansion of asparagines correlates with an abundance of proteins with prion-like domains in *Plasmodium falciparum*. Mol Biochem Parasitol. 2004 Oct;137(2):307–19.

55. Pallarès I, De Groot NS, Iglesias V, Sant'Anna R, Biosca A, Fernàndez-Busquets X, *et al*. Discovering Putative Prion-Like Proteins in *Plasmodium falciparum*: A Computational and Experimental Analysis. Front Microbiol. 2018 Aug 7;9:1737.

56. Halfmann R, Alberti S, Krishnan R, Lyle N, O'Donnell CW, King OD, *et al*. Opposing Effects of Glutamine and Asparagine Govern Prion Formation by Intrinsically Disordered Proteins. Mol Cell. 2011 Jul;43(1):72–84.

57. Cortés GT, Wiser MF, Gómez-Alegría CJ. Identification of Plasmodium falciparum HSP70-2 as a resident of the *Plasmodium* export compartment. Heliyon. 2020 Jun;6(6):e04037.

58. Botha M, Pesce ER, Blatch GL. The Hsp40 proteins of *Plasmodium falciparum* and other apicomplexa: Regulating chaperone power in the parasite and the host. Int J Biochem Cell Biol. 2007;39(10):1781–803.

59. Njunge J, Ludewig M, Boshoff A, Pesce E, Blatch G. Hsp70s and J proteins of *Plasmodium* parasites infecting rodents and primates: structure, function, clinical relevance, and drug targets. Curr Pharm Des. 2013;19(3):387–403.

60. Hiller NL, Bhattacharjee S, Van Ooij C, Liolios K, Harrison T, Lopez-Estraño C, *et al*. A Host-Targeting Signal in Virulence Proteins Reveals a Secretome in Malarial Infection. Science. 2004 Dec 10;306(5703):1934–7.

61. Sargeant TJ, Marti M, Caler E, Carlton JM, Simpson K, Speed TP, *et al*. Lineage-specific expansion of proteins exported to erythrocytes in malaria parasites. Genome Biol. 2006 Feb 20;7(2).

62. Frydman J. Folding of Newly Translated Proteins In Vivo: The Role of Molecular Chaperones. Annu Rev Biochem. 2001 Jun;70(1):603–47.

63. Walsh P, Bursać D, Law YC, Cyr D, Lithgow T. The J-protein family: modulating protein assembly, disassembly and translocation. EMBO Rep. 2004 Jun;5(6):567–71.

64. Oakley MSM, Kumar S, Anantharaman V, Zheng H, Mahajan B, Haynes JD, *et al.* Molecular Factors and Biochemical Pathways Induced by Febrile Temperature in Intraerythrocytic *Plasmodium falciparum* Parasites. Infect Immun. 2007 Apr;75(4):2012–25.

65. Bork P, Sander C, Valencia, Bukau B. A module of the DnaJ heat shock proteins found in malaria parasites. Trends Biochem Sci. 1992;17(4):129.

66. Foley M, Tilley L, Sawyer WH, Anders RF. The ring-infected erythrocyte surface antigen of *Plasmodium falciparum* associates with spectrin in the erythrocyte membrane. Mol Biochem Parasitol. 1991 May;46(1):137–47.

67. Charnaud SC, Dixon MWA, Nie CQ, Chappell L, Sanders PR, Nebl T, *et al*. The exported chaperone Hsp70-x supports virulence functions for *Plasmodium falciparum* blood stage parasites. PLoS ONE. 2017 Jul 1;12(7).

68. Külzer S, Charnaud S, Dagan T, Riedel J, Mandal P, Pesce ER, *et al*. *Plasmodium falciparum* -encoded exported hsp70/hsp40 chaperone/co-chaperone complexes within the host erythrocyte: Chaperones in the *P. falciparum* -infected host cell. Cell Microbiol. 2012 Nov;14(11):1784–95.

69. Marti M, Good RT, Rug M, Knuepfer E, Cowman AF. Targeting Malaria Virulence and Remodeling Proteins to the Host Erythrocyte. Science. 2004 Dec 10;306(5703):1930–3.

70. Warncke JD, Vakonakis I, Beck HP. *Plasmodium* Helical Interspersed Subtelomeric (PHIST) Proteins, at the Center of Host Cell Remodeling. Microbiol Mol Biol Rev. 2016 Dec;80(4):905–27.

71. Frech C, Chen N. Variant surface antigens of malaria parasites: functional and evolutionary insights from comparative gene family classification and analysis. BMC Genomics. 2013;14(1):427.

72. Oberli A, Zurbrügg L, Rusch S, Brand F, Butler ME, Day JL, *et al*. *Plasmodium falciparum Plasmodium* helical interspersed subtelomeric proteins contribute to cytoadherence and anchor *P. falciparum* erythrocyte membrane protein 1 to the host cell cytoskeleton: PHIST proteins anchor PfEMP1 to the cytoskeleton. Cell Microbiol. 2016 Oct;18(10):1415–28.

73. Yang B, Wang X, Jiang N, Sang X, Feng Y, Chen R, *et al*. Interaction Analysis of a *Plasmodium falciparum* PHISTa-like Protein and PfEMP1 Proteins. Front Microbiol. 2020 Nov 13;11:611190.

74. Eksi S, Haile Y, Furuya T, Ma L, Su X, Williamson KC. Identification of a subtelomeric gene family expressed during the asexual–sexual stage transition in *Plasmodium falciparum*. Mol Biochem Parasitol. 2005 Sep;143(1):90–9.

75. Silvestrini F, Lasonder E, Olivieri A, Camarda G, Van Schaijk B, Sanchez M, *et al.* Protein export marks the early phase of gametocytogenesis of the human malaria parasite *Plasmodium falciparum*. Mol Cell Proteomics. 2010;9(7):1437–48.

76. LaCount DJ, Vignali M, Chettier R, Phansalkar A, Bell R, Hesselberth JR, *et al.* A protein interaction network of the malaria parasite *Plasmodium falciparum*. Nature. 2005 Nov;438(7064):103–7.

77. Tarr SJ, Moon RW, Hardege I, Osborne AR. A conserved domain targets exported PHISTb family proteins to the periphery of *Plasmodium* infected erythrocytes. Mol Biochem Parasitol. 2014;196(1):29–40.

78. Boddey JA, Carvalho TG, Hodder AN, Sargeant TJ, Sleebs BE, Marapana D, *et al*. Role of Plasmepsin V in Export of Diverse Protein Families from the *Plasmodium falciparum* Exportome. Traffic. 2013 May;14(5):532–50.

79. Parish LA, Mai DW, Jones ML, Kitson EL, Rayner JC. A member of the *Plasmodium falciparum* PHIST family binds to the erythrocyte cytoskeleton component band 4.1. Malar J. 2013 Dec;12(1):160.

80. Daily JP, Le Roch KG, Sarr O, Ndiaye D, Lukens A, Zhou Y, *et al*. In Vivo Transcriptome of *Plasmodium falciparum* Reveals Overexpression of Transcripts That Encode Surface Proteins. J Infect Dis. 2005 Apr;191(7):1196–203.

81. Kaneko O, Lim BYSY, Iriko H, Ling IT, Otsuki H, Grainger M, *et al*. Apical expression of three RhopH1/Clag proteins as components of the *Plasmodium falciparum* RhopH complex. Mol Biochem Parasitol. 2005 Sep;143(1):20–8.

82. Comeaux CA, Coleman BI, Bei AK, Whitehurst N, Duraisingh MT. Functional analysis of epigenetic regulation of tandem RhopH1/clag genes reveals a role in *Plasmodium falciparum* growth: P. falciparum RhopH1 paralogue expression. Mol Microbiol. 2011 Apr;80(2):378–90.

83. Nguitragool W, Bokhari AAB, Pillai AD, Rayavara K, Sharma P, Turpin B, *et al*. Malaria Parasite clag3 Genes Determine Channel-Mediated Nutrient Uptake by Infected Red Blood Cells. Cell. 2011 May;145(5):665–77.

84. Kaneko O, Tsuboi T, Ling IT, Howell S, Shirano M, Tachibana M, *et al.* The high molecular mass rhoptry protein, RhopH1, is encoded by members of the clag multigene family in *Plasmodium falciparum* and *Plasmodium yoelii*. Mol Biochem Parasitol. 2001 Dec;118(2):223–31.

85. Ferreira PE, Holmgren G, Veiga MI, Uhlén P, Kaneko A, Gil JP. PfMDR1: Mechanisms of Transport Modulation by Functional Polymorphisms. Costa FTM, editor. PLoS ONE. 2011 Sep 1;6(9):e23875.

86. Foote S, Thompson JK, Cowman AF, Kemp DJ. Amplification of the multidrug resistance gene in some chloroquine-resistant isolates of *P. falciparum*. Cell. 1989;57(6):921–30.

87. Reed MB, Saliba K, Caruana SR, Kirk K, Cowman AF. Pgh1 modulates sensitivity and resistance to multiple antimalarials in *Plasmodium falciparum*. Nature. 2000;403(6772):906–9.

88. Cowman AF, Karcz S, Galatis D, Culvenor JG. A P-glycoprotein homologue of *Plasmodium falciparum* is localized on the digestive vacuole. J Cell Biol. 1991 Jun 1;113(5):1033–42.

89. Birnbaum J, Scharf S, Schmidt S, Jonscher E, Hoeijmakers WAM, Flemming S, *et al*. A Kelch13-defined endocytosis pathway mediates artemisinin resistance in malaria parasites. Science. 2020 Jan 3;367(6473):51–9.

90. Wang J, Zhang CJ, Chia WN, Loh CCY, Li Z, Lee YM, *et al*. Haem-activated promiscuous targeting of artemisinin in *Plasmodium falciparum*. Nat Commun. 2015 Dec 22;6(1):10111.

91. Yang T, Yeoh LM, Tutor MV, Dixon MW, McMillan PJ, Xie SC, *et al.* Decreased K13 Abundance Reduces Hemoglobin Catabolism and Proteotoxic Stress, Underpinning Artemisinin Resistance. Cell Rep. 2019 Nov 26;29(9):2917-2928.e5.

92. Silva MD, Cooke BM, Guillotte M, Buckingham DW, Sauzet JP, Le Scanf C, *et al*. A role for the *Plasmodium falciparum* RESA protein in resistance against heat shock demonstrated using gene disruption. Mol Microbiol. 2005 May;56(4):990–1003.

93. Jonsdottir TK, Counihan NA, Modak JK, Kouskousis B, Sanders PR, Gabriela M, *et al.* Characterisation of complexes formed by parasite proteins exported into the host cell compartment of *Plasmodium falciparum* infected red blood cells. Cell Microbiol. 2021 Aug;23(8).

94. Shonhai A, Blatch GL. Heat Shock Proteins of Malaria: Highlights and Future Prospects. In: Heat Shock Proteins of Malaria. 2021. p. 237–46. (Advances in Experimental Medicine and Biology; vol. 1340).

95. Brown GV, Culvenor JG, Crewther PE, Bianco AE, Coppel RL, Saint RB, *et al*. Localization of the ring-infected erythrocyte surface antigen (RESA) of *Plasmodium falciparum* in merozoites and ring-infected erythrocytes. J Exp Med. 1985 Aug 1;162(2):774–9.

96. Chen X, Sun Y, Zhang T, Shu L, Roepstorff P, Yang F. Quantitative Proteomics Using Isobaric Labeling: A Practical Guide. Genomics Proteomics Bioinformatics. 2021 Oct;19(5):689–706.

97. Mannix KM, Starble RM, Kaufman RS, Cooley L. Proximity labeling reveals novel interactomes in live *Drosophila* tissue. Development. 2019 Jan 1;dev.176644.

98. Hwang J, Espenshade PJ. Proximity-dependent biotin labelling in yeast using the engineered ascorbate peroxidase APEX2. Biochem J. 2016 Aug 15;473(16):2463–9.

99. Chen CL, Hu Y, Udeshi ND, Lau TY, Wirtz-Peitz F, He L, *et al*. Proteomic mapping in live *Drosophila* tissues using an engineered ascorbate peroxidase. Proc Natl Acad Sci. 2015 Sep 29;112(39):12093–8.

100. Tan B, Peng S, Yatim SMJM, Gunaratne J, Hunziker W, Ludwig A. An Optimized Protocol for Proximity Biotinylation in Confluent Epithelial Cell Cultures Using the Peroxidase APEX2. STAR Protoc. 2020 Sep;1(2):100074.

Chapter 6: Discussion and conclusions

6.1 **Discussion**

The purpose of this study was to investigate an understudied compartment of the *P. falciparum* parasite that has a key function in parasite survival and propagation of infection, the dense granules. We aimed to determine the timing of DG biogenesis more precisely, to identify the factors controlling trafficking of DG proteins to the DG and to identify new DG proteins. Together, fulfilling these aims will provide further insight into the role of this organelle in the growth of the parasite and the mechanisms by which the parasite forms the organelle.

Using recruitment of RESA as a proxy for DG biogenesis timing, I have determined that DGs are formed around 37 minutes before parasite egress from the host erythrocyte, a tiny fraction (1.3%) of the 48-hour intraerythrocytic life cycle. This is possibly even an overestimation, as the imaging conditions may have slowed the forming of organelles compared to physiological conditions *in vivo* with a constant temperature and without the oxidative stress caused by laser exposure. The use of a fluorescent RESA fusion can only function as a proxy for DG biogenesis timing as it is possible that DG formation begins prior to RESA expression. However, DG biogenesis cannot be complete until RESA is recruited to the DGs, and this is the only method currently available as to date none of the transport machinery involved in DG formation has been identified. At the time of this experiment RESA was the only DG marker suitable for this experiment as other DG proteins are present within the PV at the time of DG biogenesis, meaning that the signal from fluorescent fusions of any of these other DG proteins at the PV would likely obscure the much weaker signal from the forming DGs within the parasite. However, as RESA is a well-documented DG protein, the recruitment of RESA does provide a framework for the timing of the formation of DGs.

As I verified HSP40 as a DG protein after it was identified as a possible DG protein in my expression network analysis (using RESA as query), it may be possible to repeat the experiment using a fluorescent HSP40 fusion as a DG marker. Interestingly, HSP40 has been demonstrated to localise to J-dots, where it works in conjunction with HSP70x in trafficking of the virulence factor PfEMP1 to the host cell surface, a function directly enabling the host cell remodelling process (1,2). HSP40 is therefore only the third DG protein described that is exported into the host erythrocyte cytoplasm, after RESA and LSA3 (3–5). As the expression timing of HSP40 mirrors that of RESA, HSP40 could be used to repeat the RESA-mNG video microscopy

experiments as a second estimation of DG biogenesis timing, or a HSP40-mCherry fusion and the RESA-mNG fusion could be introduced to the same line for comparison of DG localisation timing between the two proteins.

Although I identified HSP40 as a DG protein using the malaria.tools protein expression analysis, a database that is comprised of publicly available transcriptomic data from NCBI SRA (6) and the European Nucleotide Archive (ENA) (7,8), many other proteins may have been missed, as the latest timepoints described were taken at 40 hpi. For this reason, it is likely that potential DG proteins with expression peaks occurring after 40hpi would have been excluded from the RESA query co-expression network output, and that use of a high resolution intraerythrocytic time course in which samples are taken every two hours with the final measurement occurring at 52 hpi would result in a more comprehensive list of potential DG proteins.

I attempted to colocalise several other proteins identified by malaria.tools to have similar expression profiles to RESA and hence be potential DG proteins. We obtained antibodies against ETRAMP2 and HSP70x, which functions in conjunction with HSP40 in J dots in the cytosol of the host erythrocyte the host erythrocyte (9,10), as well as the related proteins ETRAMP4 (PF3D7_0423700, peak expression of 1205.65 TPM at 38 hpi, 684 TMP at 52 hpi), and ETRAMP10.1 (PF3D7_1001500, peak expression of 7123.85 TPM at 52 HPI) (11) (ETRAMP antibodies were a kind gift of Tobias Spielmann of the Bernard Nocht Institute for Tropical Medicine, Hamburg, and the anti-HSP70x antibody was a kind gift of Jude Przyborski), and used fluorescence microscopy to determine whether these proteins colocalise with DG markers. These experiments did not produce strong enough DG marker staining to produce many usable images, and therefore were not of publishable quality, however, initial results indicated that none of these proteins co-localised with the DG marker used (figures 1 and 2, supplementary data).

The list of potential DG proteins identified in the malaria.tools co-expression network analysis study included a v-SNARE (PF3D7_0314100) that was considered of interest as its function in vesicle fusion means that it could be involved in DG biogenesis. We attempted to generate a fluorescent fusion of the v-SNARE to be introduced into the RESA-mNG line pTV002 for subcellular localisation by fluorescence microscopy, however we were unable to generate the v-SNARE by PCR, and repeated attempts to have the gene synthesised commercially by ITD™

were also unsuccessful. Future work could instead visualise the subcellular localisation of this v-SNARE through production of an antibody for IFA analysis.

It has already been demonstrated that late-stage expression timing is necessary for correct targeting of DG proteins to the DGs (12). Given that the results of our DG biogenesis timing analysis indicated that DGs are made even later that previously anticipated, within the final 37 minutes of the *P. falciparum* intraerythrocytic life cycle, our initial hypothesis was that the late-stage expression of DG proteins (and the late formation of DGs) could be the factor controlling DG protein targeting, as they are formed so late in the life cycle that all secretory proteins expressed after ≈37 minutes prior to egress may form the DGs through a passive mechanism. Our DG targeting mechanism experiments indicated that this is not the case, and that DG proteins contain a target sequence that is required for correct localisation of proteins to the DGs and therefore both late-stage expression timing and the presence of a targeting sequence are likely required for correct protein trafficking to the DGs. Due to difficulties in generating a series of sequentially shorter truncations of RESA, we were unable to identify the DG targeting sequence, as was the initial aim of this study. Future work may be able to address this by having RESA or HSP40 truncations commercially synthesised. We were unable to verify the effect of expression timing ourselves, as this required generation of full-length RESA gene for expression under the Cam promoter and owing to the adenine AT- rich nature of *RESA* we were unable to generate the full-length gene by PCR. A full-length RESA fusion is also required to demonstrate that mislocalisation of the mCherry truncation fusions is not a result of the mCherry tag.

Fluorescence imaging of individual merozoites of the mCherry-truncation fusion lines demonstrated that mCherry fluorescence was present in merozoites in patterning distinct from the mNG fluorescence of the DG marker RESA-mNG. This has raised the question of where the mCherry-truncation fusions are located within the merozoite. All of the mCherry truncations are expressed under the RESA promoter, which drives peak expression 48 hpi, with expression nearly as high continuing into the merozoite stage at 52 hpi (11). As these truncations appear to be exported from the parasite through the secretory system, it is possible that continued expression in the merozoite stage is allowing visualisation of mCherry signal in the secretory pathway. Alternatively, it is possible that these truncations are localising to another secretory organelle such as the mononeme, first described by Singh at al. (2007), however the existence of the mononeme has yet to be verified (13).

To identify additional proteins in an unbiased manner, I set up a proximity biotinylation assay using a RESA-APEX fusion. Despite initially promising results indicating that biotinylation was occurring in the DGs and only in the presence of H_2O_2 (or in some cases in very low levels without H_2O_2), we were unable to draw any conclusions about DG protein content from the APEX-RESA proximity biotinylation experiments. The MS output indicates that biotinylation may be occurring without addition of H_2O_2, and therefore at multiple cellular localisations, for instance at the host erythrocyte surface where RESA localises, as well as within the parasite at the DGs. The labelling activity of APEX prior to addition of H_2O_2 also means that these experiments lack a negative control condition. To address this, experiments should be repeated in parasites that lack an APEX fusion. Additionally, a protocol for labelling experiments in free merozoites could address the issue of non-DG labelling within the host cell.

It is commonly believed that DGs contain proteins that function in host cell remodelling. However, of the 10 known *P. falciparum* DG proteins, only two, RESA and LSA3, have a direct role in host cell remodelling, with the others primarily having functions in protein export across the PVM as part of the PTEX or as PTEX accessory molecules. This study has identified an 11th DG protein, HSP40, which along with RESA and LSA3 is the third DG protein known to be exported across the PVM into the host erythrocyte. HSP40, however, does not function directly in host cell remodelling but instead is a chaperone involved in the transport of host effector proteins to the host cell surface (10). Taking this into account and evaluating what we already know of the *Plasmodium* parasite DG proteome it is possible that instead of host cell remodelling proteins the DGs instead predominantly contain proteins that are involved in protein export across the PVM and transport within the host cell. This hypothesis makes sense when considering that on a basic level the DGs exist to allow immediate secretion of a set of proteins upon invasion, as the first proteins that will be required before any others are the translocon components and chaperones that allow the remodelling proteins to fold properly and to reach their destinations within the host cell. Put another way, there is no point in exporting effector proteins immediately without a system of chaperones already in place to allow them to function.

6.2 **Conclusion**

In conclusion, through this project we have demonstrated that *P. falciparum* DGs are likely formed within the final 37 minutes of the intraerythrocytic life cycle, that DG proteins require

a targeting signal sequence that along with late-stage expression timing is required for correct transport to the DGs, and that HSP40 is a novel DG protein.

Bibliography

1. Chen Q, Barragan A, Fernandez V, Sundström A, Schlichtherle M, Sahlén A, *et al.* Identification of *Plasmodium falciparum* Erythrocyte Membrane Protein 1 (PfEMP1) as the Rosetting Ligand of the Malaria Parasite *P. falciparum*. J Exp Med. 1998 Jan 5;187(1):15–23.

2. Baruch DI, Pasloske L, Singh B, Ma XC, Taraschi F, Howard' J. Cloning the *P. falciparum* Gene Encoding PfEMPl, a Malarial Variant Antigen and Adherence Receptor on the Surface of Parasitized Human Erythrocytes. Cell. 1995;82(1):77–87.

3. Aikawa M, Torii M, Sjolander A, Berzins K, Louis Millers AH. Pf155/RESA Antigen Is Localized in Dense Granules of *Plasmodium falciparum* Merozoites. Exp Parasitol. 1990;71(3):326–9.

4. Da Silva E, Foley M, Dluzewski AR, Murray LJ, Anders RF, Tilley L. The *Plasmodium falciparum* protein RESA interacts with the erythrocyte cytoskeleton and modifies erythrocyte thermal stability. Mol Biochem Parasitol. 1994 Jul 1;66(1):59–69.

5. Morita M, Takashima E, Ito D, Miura K, Thongkukiatkul A, Diouf A, *et al*. Immunoscreening of *Plasmodium falciparum* proteins expressed in a wheat germ cell-free system reveals a novel malaria vaccine candidate. Sci Rep. 2017 Apr 5;7.

6. Leinonen R, Sugawara H, Shumway M, on behalf of the International Nucleotide Sequence Database Collaboration. The Sequence Read Archive. Nucleic Acids Res. 2011 Jan 1;39(Database):D19–21.

7. Silvester N, Alako B, Amid C, Cerdeño-Tarrága A, Clarke L, Cleland I, *et al.* The European Nucleotide Archive in 2017. Nucleic Acids Res. 2018 Jan 4;46(D1):D36–40.

8. Tan QW, Mutwil M. Malaria.tools—comparative genomic and transcriptomic database for *Plasmodium* species. Nucleic Acids Res. 2020 Jan 8;48(D1):D768–75.

9. Külzer S, Rug M, Brinkmann K, Cannon P, Cowman A, Lingelbach K, *et al.* Parasite-encoded Hsp40 proteins define novel mobile structures in the cytosol of the *P. falciparum*-infected erythrocyte. Cell Microbiol. 2010 Oct 1;12(10):1398–420.

10. Külzer S, Charnaud S, Dagan T, Riedel J, Mandal P, Pesce ER, *et al*. *Plasmodium falciparum* -encoded exported hsp70/hsp40 chaperone/co-chaperone complexes within the host erythrocyte: Chaperones in the *P. falciparum* -infected host cell. Cell Microbiol. 2012 Nov;14(11):1784–95.

11. Kucharski M, Tripathi J, Nayak S, Zhu L, Wirjanata G, Van Der Pluijm RW, *et al.* A comprehensive RNA handling and transcriptomics guide for high-throughput processing of *Plasmodium* blood-stage samples. Malar J. 2020 Dec;19(1):363.

12. Rug M, Wickham ME, Foley M, Cowman AF, Tilley L. Correct promoter control is needed for trafficking of the ring-infected erythrocyte surface antigen to the host cytosol in transfected malaria parasites. Infect Immun. 2004 Oct;72(10):6095–105.

13. Singh S, Plassmeyer M, Gaur D, Miller LH. Mononeme: A new secretory organelle in *Plasmodium falciparum* merozoites identified by localization of rhomboid-1 protease. Proc Natl Acad Sci. 2007;104(50):20043–8.

Supplementary data

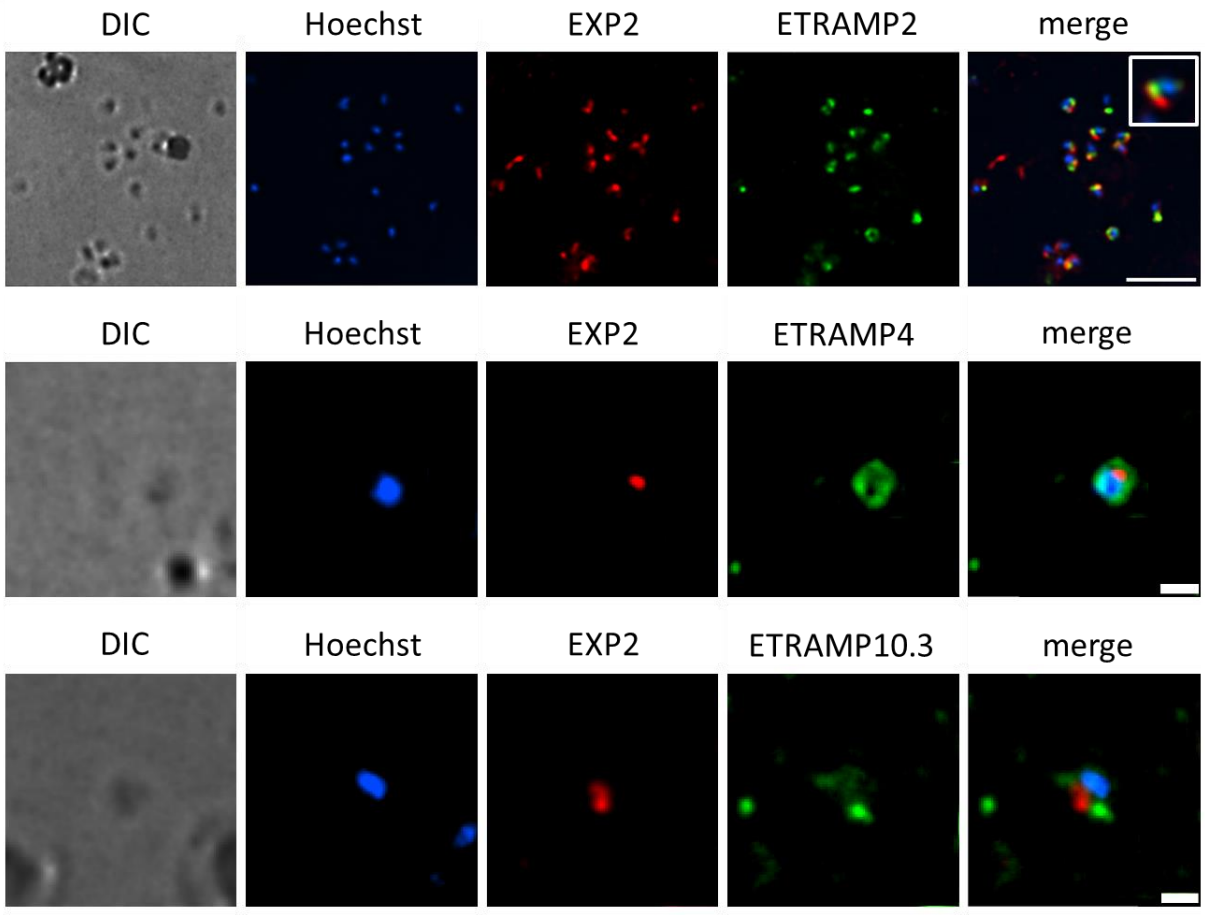

Figure 1. Preliminary IFA data indicating that staining against ETRAMPS 2, 4 and 10.1 does not co-localise with staining against the DG marker EXP2 in merozoites. At this time, we were unable to use anti-RESA as a DG marker and instead used EXP2 to label DGs in single merozoites Size bars indicate 5 µm, 1 µm and 1 µm (top town). Box in top right of ETRAMP2 series provides an enlarges image of an individual merozoite.

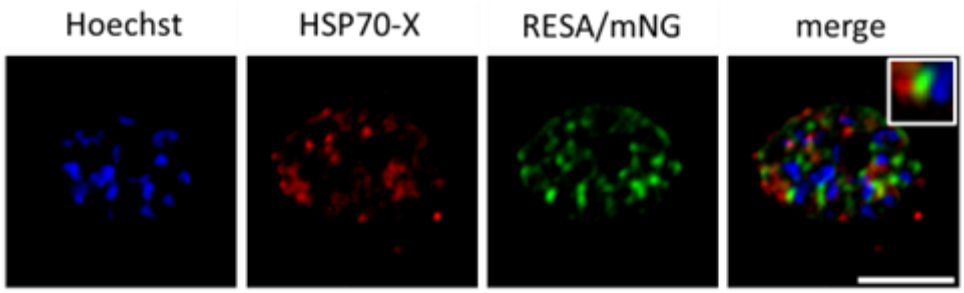

Figure 2. Preliminary IFA data indicating that HSP70x signal does not co-localise with mNG signal in late stage segmented schizonts of line pTV002 in which the DG marker RESA is fused to mNG. At this time, we were unable to use anti-RESA as a DG marker and instead used anti-

mNG to tag RESA-mNG in late stage schizonts of pTV002 to localise HSP70x in late stage segmented schizonts. Size bar indicates 5µm.